Characterisation of Lead-Free Solder Pastes and their Correlation with the Stencil Printing Process Performance

Antony Edward Marks

Electronics Manufacturing Engineering Research Group
School of Engineering
University of Greenwich, UK

A thesis submitted in partial fulfilment of the requirements of the University of Greenwich for the Degree of Doctor of Philosophy

2012

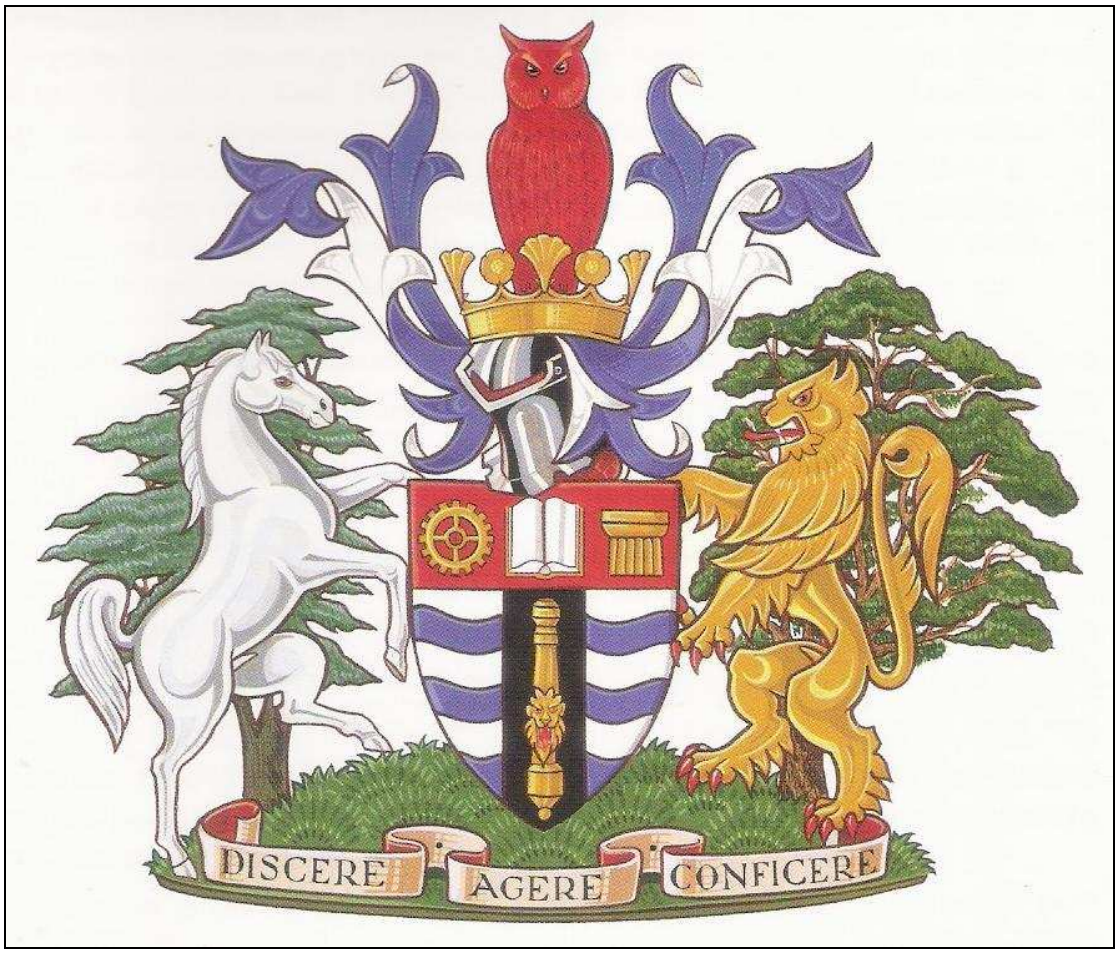

'Learn, Practise, Accomplish'

"Never, never, never give up!"
– Sir Winston Churchill

DECLARATION

I certify that this work has not been accepted in substance for any degree, and is not concurrently being submitted for any degree other than that of Doctor of Philosophy (PhD) being studied at the University of Greenwich. I also declare that this work is the result of my own investigations except where otherwise identified by references and that I have not plagiarised another's work

Signed by Student:

Date:

Signed by Supervisor:

Date:

ACKNOWLEDGEMENTS

I would firstly like to thank my project supervisor, Professor Ndy Ekere, who has provided me with guidance throughout the course of the study, presenting suggestions and opportunities to further the work and produce a result to be proud of. The vast understanding of the subject matter held by Professor Ekere was invaluable throughout the research and acted as the foundation for building my knowledge. My sincere gratitude is also given to my industrial supervisor, Dr Tim Lawrence, who has been a constant source of information, materials and support. His continued encouragement throughout the course of the study will not be forgotten, and his suggestions and input aided significantly in producing ideas for investigation.

I would also like to thank the members of the Electronics Manufacturing Engineering Research Group (EMERG), both past and current, for all their support, proofreading and company. Particular thanks must go to Dr. Sabuj Mallik who ensured that I stayed sane throughout the research, providing assistance with experiments when needed and a pleasant working environment. A great deal of thanks must also be given to the industrial collaborators: Henkel for its support with equipment, materials, information and knowledge base, and the EPSRC for funding the project.

I also express sincere thanks to my friends that have always provided me with encouragement and support, particularly Manjinder, Chris, Zena, Nicola and Sharon. I will always be grateful for all you have done for me. Last but by no means least; a special thank you is also given to my wonderful wife Georgina and my family, who have provided me with a great deal of support throughout the years. They have given me the courage to complete the PhD and provided me with motivation to progress with my studies to this level. I have learnt from them that anything is possible and never to give up on something you want to achieve. This thesis is dedicated to you.

ABSTRACT

Solder pastes are complex materials whose properties are governed by many factors. Variations exhibited in solder paste characteristics make it increasingly difficult to understand the correlations between solder paste properties and their printing process performance. The recent EU directives on RoHS (Restriction of Hazardous Substances – enacted by UK regulations) and WEEE (Waste from Electrical and Electronic Equipment) has led to the use of lead-free soldering in the SMA (surface mount assembly) process, and an urgent need for better understanding of the characteristics and printing performance of new solder paste formulations. Equally, as the miniaturisation of hand-held and consumer electronic products continues apace, the solder paste printing process remains a real challenge to the electronics assembly industry. This is because the successful assembly of electronic devices at the ultra-fine pitch and flip-chip geometry requires the deposition of small and consistent paste deposits from pad to pad and from board to board. The paste printing process at this chip-scale geometry depends on conditions such as good paste roll, complete aperture filling and paste release from the apertures onto the substrate pads. This means that the paste flow and deformation behaviour, i.e. the paste rheology, is very important in defining the printing performance of any solder paste. Rheological measurements can be used as a tool to study the deformation or flow experienced by the pastes during the stencil printing process. In addition, the rheological measurements can also be used as a quality control tool in the paste production process for identifying batch-to-batch variation, and to reduce the associated printing defects in the paste printing process.

The work reported here on the characterisation of lead-free solder pastes and their correlation with the stencil printing process is divided into five main parts. The first part concerns the study of the effect of variations in flux and particle size distribution (PSD) on the creep recovery performance of lead-free solder pastes used for flip-chip assembly.

For this study, a novel technique was calculating the extent of paste recovery and hence characterising the slumping tendency in solder pastes. The second part of the study concerns the influence of long-term ageing on the rheology and print quality of lead-free solder pastes used for flip-chip assembly, and the main focus of the work was to develop methodologies for benchmarking new formulations in terms of shelf life, rheological deterioration and print performance. The third part of the work deals with a rheological simulation study of the effect of variation in applied temperature on the slumping behaviour of lead-free solder pastes, and the fourth part considers the rheological correlation between print performance and abandon time for lead-free solder paste used for flip-chip assembly. The final part of the study concerns the influence of applied stress, application time and recurrence on the rheological creep recovery behaviour of lead-free solder pastes.

The research work was funded through the PRIME Faraday EPSRC CASE Studentship grant, and was carried out in collaboration with Henkel Technologies, Hemel Hempstead, UK. The extensive set of results from the experimental programme, in particular relating to the aspect of key paste performance indicators, has been adapted by the industrial partner for implementation as part of a quality assurance (QA) tool in its production plant, and the results have also been disseminated widely through journal publications and presentations at international conferences.

TABLE OF CONTENTS

CHAPTER 1
INTRODUCTION

CHAPTER 2
LITERATURE REVIEW

CHAPTER 3

THEORY AND BACKGROUND KNOWLEDGE

CHAPTER 4

EXPERIMENTAL DESIGN

CHAPTER 5

EFFECT OF FLUX COMPOSITION AND PSD ON THE CREEP RECOVERY PERFORMANCE OF LEAD-FREE SOLDER PASTES USED FOR FLIP-CHIP ASSEMBLY

CHAPTER 6

INFLUENCE OF LONG-TERM AGEING ON THE RHEOLOGY AND PRINT QUALITY OF LEAD-FREE SOLDER PASTES USED FOR FLIP-CHIP ASSEMBLY

CHAPTER 7

RHEOLOGICAL SIMULATION OF SLUMPING BEHAVIOUR FOR LEAD-FREE SOLDER PASTE AS AN EFFECT OF VARIATION IN APPLIED TEMPERATURE

CHAPTER 8

RHEOLOGICAL CORRELATION BETWEEN PRINT PERFORMANCE AND ABANDON TIME FOR LEAD-FREE SOLDER PASTE USED FOR FLIP-CHIP ASSEMBLY

CHAPTER 9
THE INFLUENCE OF APPLIED STRESS, APPLICATION TIME AND RECURRENCE ON THE RHEOLOGICAL CREEP RECOVERY BEHAVIOUR OF LEAD-FREE SOLDER PASTES

CHAPTER 10

CONCLUSIONS, AND RECOMMENDATIONS FOR FUTURE WORK

LIST OF FIGURES

LIST OF TABLES

GLOSSARY

3-D	three-dimensional
Ag	silver
BGA	ball grid array
Cd	cadmium
Cr VI	hexavalent chromium
Cu	copper
Hg	mercury
IPC	Institute for Interconnecting and Packaging Electronic Circuits
LVR	linear viscoelastic region
NC	No-clean
Pb	lead
PBB	polybrominated biphenyl
PBDE	polybrominated biphenyl ether
PCB	printed circuit board
PSD	particle size distribution
QA	quality assurance
RA	Rosin/Resin Activated
RoHS	Restriction of Hazardous Substances
RMA	Rosin/Resin Mildly Activated
RPM	revolutions per minute
SMA	surface mount assembly
SMT	surface mount technology
Sn	tin
TI	Thixotropic Index
WEEE	Waste from Electrical and Electronic Equipment
WS	Water Soluble

CHAPTER 1:
INTRODUCTION

This study concerns the characterisation of lead-free solder pastes and their correlation with stencil printing performance. The project was funded under the EPSRC, EPPIC-Faraday case studentship award as part of the EPPIC Leadout project, and was conducted in collaboration with Henkel Technologies (Hemel Hempstead). As can be seen from Figure 1.1, solder paste printing defects remains a big challenge in the assembly of electronic devices, reportedly accounting for some 60% of surface mount technology (SMT) assembly defects (Durairaj et al, 2002; Yang and Tsai, 2004; Jackson et al, 2005; Yang et al, 2005; Tsai, 2008) - approximated from the number of possible opportunities for defects on each board (Gastel, 2011). Furthermore; it is reported that up to 87% of defects observed during reflow originate from stencil printing defects (Okuru et al, 1993). For this reason, the characterisation of lead-free pastes and their correlation with stencil printing process performance remains an area of crucial importance to the electronics manufacturing industry, and especially to paste material suppliers such as Henkel Technologies.

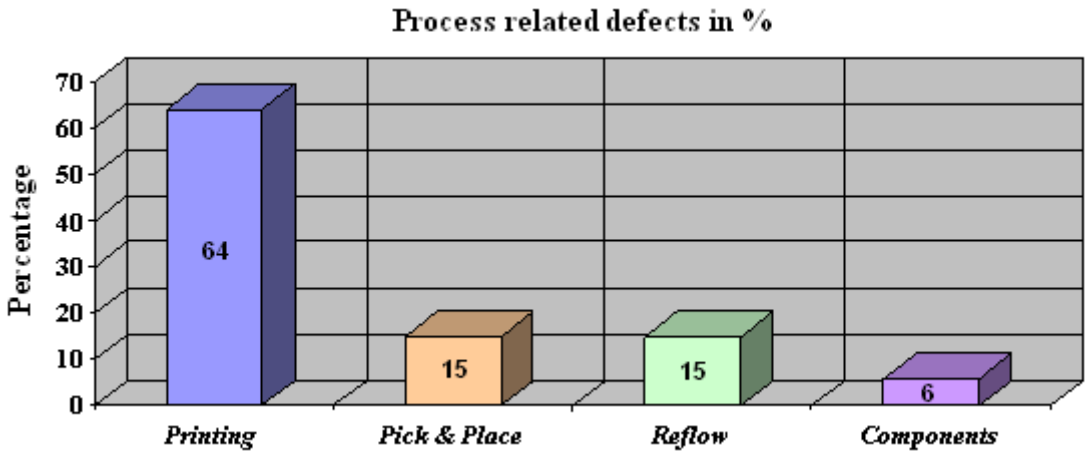

Figure 1.1: Contributions to SMT defects (Westerlaken, 2000)

In this study, different paste characterisation techniques have been investigated in order to correlate the flow characteristics of lead-free solder pastes to their printing

performance. These include viscometry as well as oscillatory and creep recovery tests, each of which are discussed in depth in Chapter 4. A better understanding of the correlation of various paste characteristics to printing performance is a key to achieving consistently good paste deposition and defect-free assembly processes.

1.1 The stencil printing process

The stencil printing process, shown in Figure 1.2, is the most widely used method of depositing solder paste onto circuit boards during surface mount assembly (SMA). During the stencilling process, the solder paste is 'rolled' along the surface of the stencil, entering the apertures as a result of hydrodynamic pressures generated by the squeegee (Mallik, 2009). As the squeegee continues in a forward motion over the filled apertures, the top of the solder paste is sheared off, preferably leaving a clean stencil surface behind the squeegee's direction of movement. The stencil is separated from the board once the limit for the print stroke has been reached, ideally leaving behind a 'brick'-shaped deposit of solder paste that demonstrates an elastic capability to resist slumping behaviour.

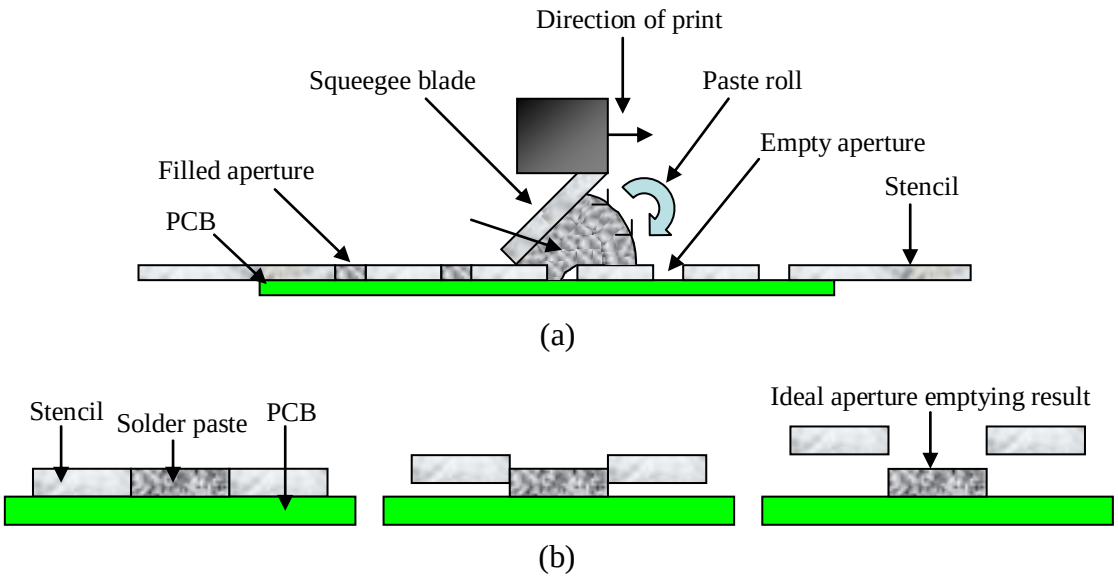

Figure 1.2: Illustration of (a) stencil printing process and (b) ideal aperture release

The printing process is said to revolve around five key physical sub-processes: 'pre-print' paste treatment; squeegee deformation; paste roll in front of the squeegee; aperture filling and emptying; and slumping (Durairaj, 2006). Each of these is interlinked as a result of the rheological properties and flow behaviour of the pastes.

However, it has additionally been shown that the printing process is controlled by a vast number of influences; as can be seen in Figure 1.3.

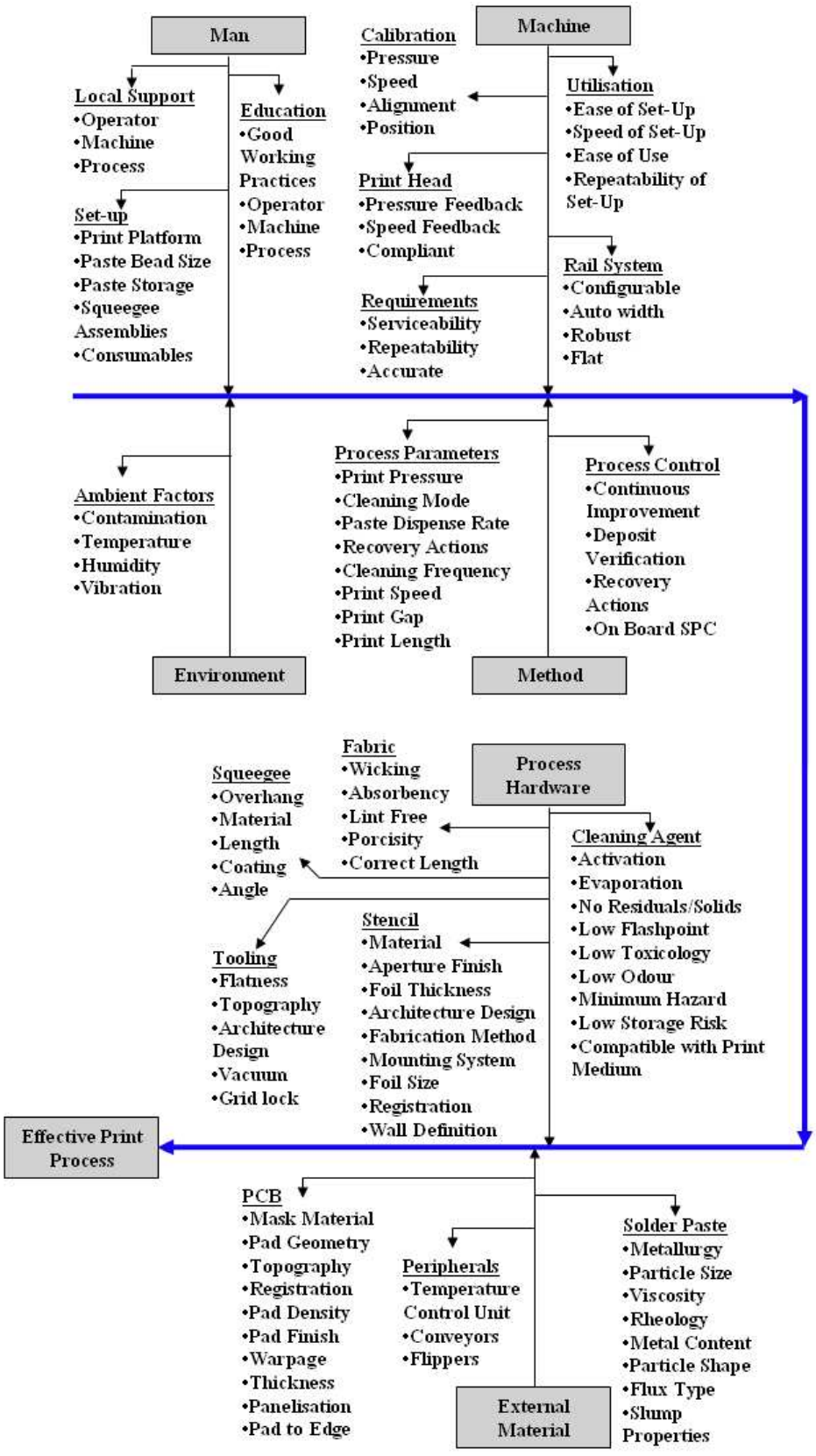

Figure 1.3: Factors that can affect the printing process (EM Asia, 2010)

Figure 1.3 demonstrates the immense number of factors that can dictate the effectiveness of the printing process. These can be divided into several categories including; (i) man, (ii) machine, (iii) environment, (iv) method, (v) process hardware and (vi) external material. Chapter 5 of this thesis addresses particle size distribution (PSD), flux and slumping properties; hence the key focus is on the external material. Chapter 6 relates to the influence of man, as this concentrates on paste storage. The influence of temperature is reported in Chapter 7, which is classified as an environmental factor. Finally, Chapter 8 focuses on the method, with investigations into abandon time capability.

With such a vast number of variables influencing the printing process, finding methods for limiting printing defects is essential. An important step in doing this is the relationship between solder paste rheology and print performance, which has been addressed in the investigations.

1.2 Lead-free solder paste

Solder paste consists of solder alloy powder suspended in a flux vehicle and is utilised as the primary joining medium within electronics manufacture. The general complexity of paste materials creates complications with predicting print performance. With a transition to lead-free soldering, these difficulties are further increased as Sn–Pb materials have continually been used as the primary bonding medium in SMA. With an extensive history of Sn–Pb paste application, tried-and-tested methods have been developed to ensure that efficiency of the printing process is maintained at a high standard. Although these methods address Sn–Pb pastes, a gap in knowledge still exists for lead-free materials.

On 1 July 2006, the RoHS and WEEE directives were enforced to safeguard both humans and the environment from hazardous materials; contributing to conservation thorough the recovery and disposal of both electrical and electronic equipment (ChemSec, 2010). As a result of these directives, the use of various materials has now been strictly limited to minor percentages by weight. These include: lead (Pb), mercury (Hg), cadmium (Cd), hexavalent chromium (Cr VI), polybrominated biphenyl (PBB) and polybrominated diphenyl ether (PBDE) flame retardants (DTI,

2006), all of which are restricted to 0.1% by weight in homogenous materials – with the exception of cadmium, which is limited to 0.01%. This significantly impacted the electronics industry as the common method of manufacturing products using Sn–Pb solder paste was from then on prohibited. Despite creating challenges with regard to finding a reliable alternative to Sn–Pb solders, the restrictions were also seen to affect the solderable coatings on both electronic components and printed circuit boards (PCB)s.

Figure 1.4 highlights the proposal for minimising the effect of hazardous materials resulting from the two directives, which emphasises the effort made prior to disposal (seen as the worst-case scenario). Following this hierarchy, attempts at minimising the environmental impact commence during design and manufacture, where reduction – or, ideally, elimination – of hazardous materials is most effective as a result of removing the need for specially treating waste. Assuming hazardous materials have been used, disposal is only seen as acceptable once reuse or recycling has been fully carried out in an attempt to minimise the environmental impact (Zeus Industrial Products, 2005).

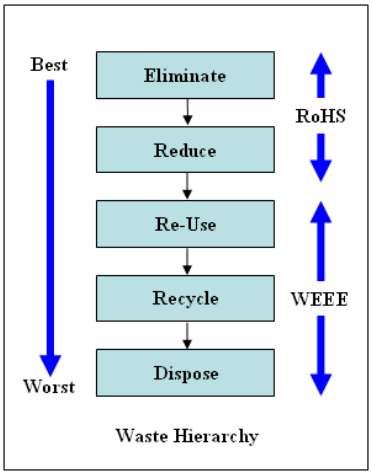

Figure 1.4: RoHS and WEEE waste hierarchy (Zeus Industrial Products, 2005)

With issues such as lead poisoning and the disposal of hazardous materials affecting both humanity and the environment, the RoHS and WEEE directives were clearly necessary. Consequently, the transition to Pb-free soldering was unavoidable. However, this evolution to Pb-free soldering has added significant pressure to other existing challenges within the electronics industry.

1.3 Unresolved issues and challenges

Correlating paste characteristics with stencil printing performance has long been an outstanding issue in the electronics manufacturing and assembly process. As the printing process is said to account for the majority of defects during PCB assembly, an understanding of such relationships will aid in the challenge of accurately predicting the outcome of the print. Prasad (1997) highlights this link between solder paste properties and print defects, stating that the viscosity of a solder paste is seen as critical in obtaining acceptable prints: for example, a high viscosity can lead to smearing, which is unacceptable as it causes solder bridges and/or solder balls, whereas an excessively high viscosity can lead to skipping, which creates insufficient solder joints. Frequent issues arise from the occurrence of slumping and bridging, which are two of the most frequent failures of the print cycle. However, these are only two examples from a range of defects that commonly occur; with others including skipping and irregular deposits (see Figure 1.5).

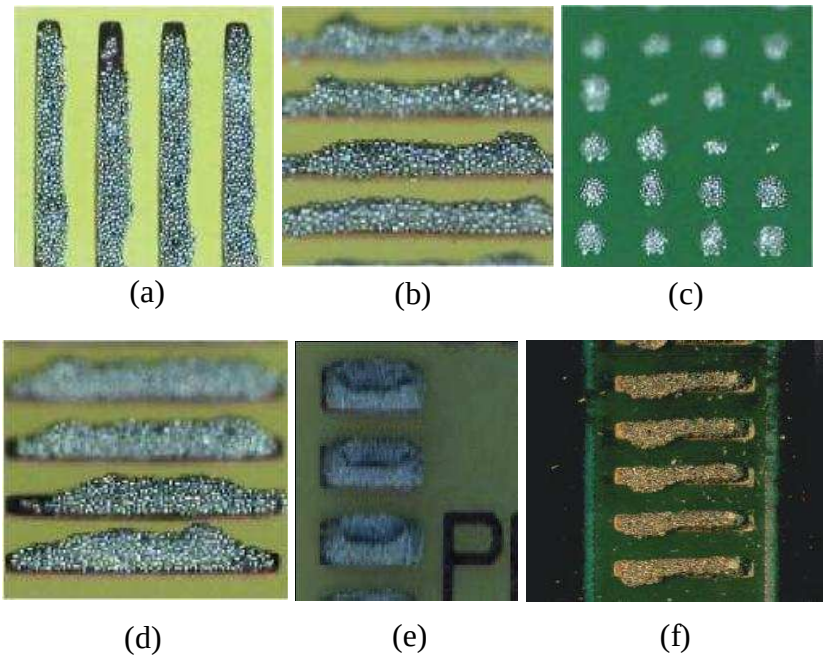

Figure 1.5: Examples of common print defects: (a) skipping (volume < 80%); (b) irregular deposits; (c) clogging; (d) slumping/onset of bridging; (e) scooping; (f) smudged deposits. (Images courtesy of Henkel Technologies)

Stencil printing is the most widely used method of depositing solder paste onto a substrate during PCB assembly and as such is an important process to understand (see Figure 1.2). By meticulously studying rheological properties, the printing process can be optimised, allowing for standard parameters to be discovered for new paste formulations. It is essential that the parameter settings, paste formulation and paste rheology are acknowledged as influencing factors for the desired print function in order to maximise the potential for acceptable prints. By way of illustration, in order to allow for flip-chip scale printing the paste must be formulated using particles which are smaller than the aperture, but pastes made with smaller particles are more likely to slump and hence bridging could become an issue; furthermore, if the pressure applied by the squeegee during the print cycle is insufficient, skipping could be observed. Studying the correlation between these influencing factors can present an opportunity to derive novel techniques and test methods for predicting the quality of the printing process.

With trends towards miniaturisation continuing, a drive exists for printing on smaller pitch sizes whilst ensuring that repeat printability and acceptability are maintained. This has further complicated the stencil printing process due to the reduction in aperture size required during the print. As a result, paste manufacturers consistently strive to reduce PSD to ensure demands for miniaturisation can be met (Table 1.1).

Type	90% (minimum) of all particles between	10% (maximum) of all particles less than
1	150–75µ	20 µ
2	75–45 µ	20 µ
3	45–25 µ	20 µ
4	38–20 µ	20 µ
5	25–15 µ	15 µ
6	15–5 µ	5 µ

Table 1.1: IPC standard PSD values for solder paste types 1–6 (Mallik, 2009)

The cellular and mobile phone industry is a prime example of continuing miniaturisation, with consumers demanding more functionality with reduced product size. This leads to the demand for increased board density and the requirement for printing solder paste on much smaller pitch sizes and through smaller apertures.

Depositing solder pastes at these fine-pitch and ultra-fine-pitch geometries has unfortunately led to an exponential increase in assembly defects associated with printing. Figures 1.6 and 1.7 demonstrate how the increase in board density – which has occurred with an increase in functionality and industrial demand for miniaturisation – has increased the challenges of depositing and placing components on the PCB for SMT assembly.

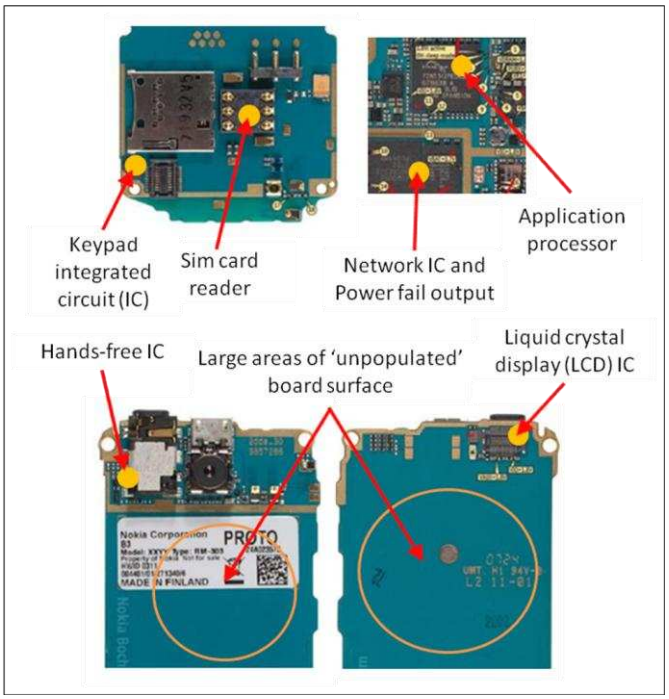

Figure 1.6: PCB example from 2007 (GSM Angel™ Nokia Solutions)

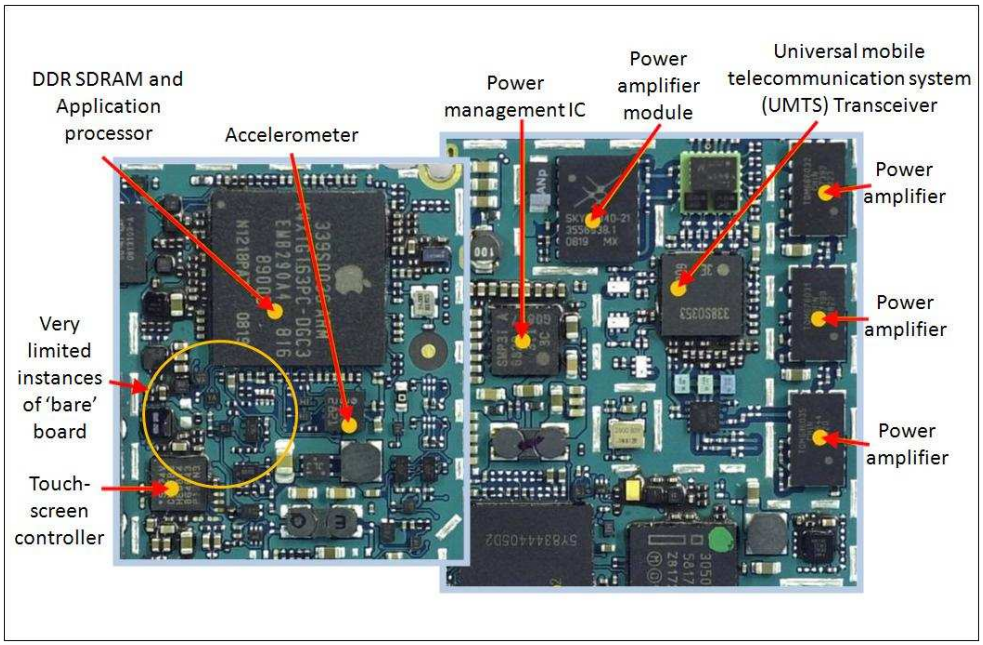

Figure 1.7: PCB example from 2008 with increased functionality (EE Times Asia)

With the RoHS and WEEE directives now fully in place, the need for formulating new Pb-free solder pastes has become paramount for the manufacturing process. With these new solder paste formulations replacing tried-and-tested methods of interconnection, it is essential that a full understanding of paste properties throughout processing is achieved. In doing this, joint reliability can be maximised whilst minimising the new challenges faced by the electronics industry. Electronics Yorkshire et al (2005) confirmed the need for understanding new paste materials, documenting (in a guide to Pb-free soldering) how the electronics industry could face many challenges, vis-à-vis the drive for lead-free assembly.

Due to the transition to Pb-free usage, the challenges of paste materials have become prominent in various areas, from formulation to reliability. One particular challenge that now faces the electronics industry is the net increase in the production cost as a result of using 'green' materials. Through comparing standard tin–lead alloys (Sn63% Pb37%) with the most popular lead-free alloy (Tin–Silver–Copper: Sn96% Ag0.5% Cu3%), an increase in base metal cost has been reported of 263% (Mallik, 2009). In his work, Mallik continues to discuss how the cost of Pb-free manufacturing is raised further through the necessity for monitoring and controlling the presence of lead contamination in materials. Electronics Yorkshire et al (2005) also highlight this cost increase, discussing how an alloy containing only 3% by weight of silver resulted in two times the cost of using a tin–lead formulation. Furthermore, as a result of raising the silver content to 4%, an additional increase in cost of 15% was observed.

A further challenge of the new RoHS and WEEE legislation is the increase in the processing temperature (Table 1.2). For example, while the melting point of Sn–Pb paste material is 183°C, that of the commonly opted-for Pb-free alternative, i.e. Sn–Ag–Cu, is 217°C, a 34°C difference in temperature. This increase in the melting point has created issues with the ability of PCB components to withstand the elevated temperatures experienced during the reflow process. In an attempt to combat this issue, manufacturers recommend that peak temperature ratings for components are raised. In order to address the rework and Pb-free assembly temperatures experienced by both large- and small-volume package components, it has been suggested that these 'peak temperatures' should be increased to 255°C and 265°C respectively.

Alloy composition	Melting point (°C)	Variation due to lead-free initiative (°C)
Tin–Lead	**183**	**–**
Tin–Bismuth	138	-45
Tin–Zinc	198.5	+15.5
Tin–Silver–Copper	217	+34
Tin–Silver	221	+38
Tin–Copper	227	+44
Tin–Antimony	232–240	+49 to +57

Table 1.2: Melting temperatures of alloys used in electronics assembly

Although these concerns have led to the development of materials that withstand higher processing temperatures, it is believed that this process will take time and may lead to an initial increase in component costs (Ganesan, 2006). Alternatives to Sn–Pb pastes exist that can actually reduce the melting point temperature (when compared with tin–lead); however, the Sn–Ag–Cu alloy is the most commonly selected for implementation in electronics assembly.

Literature findings highlight that the majority (if not all) of outstanding issues can be related to the reliability of the solder joint and to the presence of defects. In their work, Bradley et al (2007) examine the major challenges of Pb-free soldering, discussing how a considerable increase in voiding is observed when utilising Pb-free solders (compared with previous Sn–Pb materials), which may be a result of reduced wetting ability. In addition, the reduced wetting ability leads to an increased proneness towards so-called ‘tombstoning’ (where the components position themselves vertically due to wetting at one side before the other, which leads to surface tension erecting the component). With significant issues already existing with regard to slumping and bridging defects, the reliability of Pb-free soldering is a challenging concern for the electronics industry.

Therefore, it can be said that key challenges facing the electronics industry – which assisted with guiding the investigations of this project – can be related to but are not limited to:

- Further understanding Pb-free soldering
- Discovering correlations between paste rheology and the printing process
- Developing new methods of investigating paste rheology to assist with predicting the printing process
- Allowing repeat printability on fine pitch scales
- Reducing the cost of the manufacturing process.

1.4 Problem context and project objectives

The focus of this project is the rheological characterisation of Pb-free solder pastes and their influence on stencil printing performance. The project was therefore aimed at providing guidelines for industry and paste manufacturers (such as Henkel Technology, the project partner) relating to the paste stencilling process and the use of rheological measures for predicting performance. Through investigating the rheology of paste materials used for microsystems assembly applications, those issues and challenges discussed earlier in this chapter have been addressed, with novel techniques being reported for characterising new paste formulations.

To achieve this, a series of rheological experiments was devised to study key characteristics such as deformation and recovery, shear thinning nature and elastic/viscous properties, so that observations could be correlated to printing performance. Throughout the course of the project, various investigations were conducted to examine the influence of abandon time; ageing; temperature; creep recovery behaviour and formulation (such as flux) on the rheological properties of Pb-free solder paste. Through researching these particular aspects of paste rheology, a greater understanding of Pb-free solders was achieved. Consequently, methods have been reported that offer opportunities for predicting the performance of samples during the stencil printing process.

As the aim of the project was to develop new rheological techniques that could be used for predicting the printing performance of Pb-free paste materials, the project objectives can be summarised as follows:

1. To develop new techniques for characterising new paste formulations using the parallel-plate rheometer.
2. To investigate techniques for correlating specific paste material properties to print performance.
3. To develop a parallel-plate rheometry test for abandon time.
4. To develop a parallel-plate rheometry test for shelf life.
5. To assist with developing a greater understanding of Pb-free soldering and to investigate the possibility of reducing printing defects, identifying methods that could assist with this

From these objectives, the following research questions were answered throughout the studies:

- How does solder paste formulation influence slumping behaviour at increased temperatures?
- How does paste formulation influence creep/recovery behaviour?
- How does paste rheology affect abandon time?
- Can variations in storage increase the shelf life of a product?

1.5 Contributions from this research project

Results from the investigations into paste behaviour have demonstrated many significant findings. Furthermore, a number of methods have been offered for reducing the influence of defect occurrence at the stencil printing stage of SMA. From those results, several key contributions have been identified.

1. Work relating to the application of elevated temperatures offered a new technique for investigating paste behaviour at pre-heat reflow temperatures. Through utilising a rheometer during the study, it was possible to demonstrate a novel method for simulating the heating process rheologically.
2. From a printing process viewpoint, investigations into the ageing characteristics of solder pastes demonstrated that a six-month shelf life can be dramatically increased; a finding that has been conveyed to the project partner

(Henkel Technologies). By conducting further studies related to post-reflow acceptability, this could potentially be seen to be a definitive increase in shelf life rather than just from a stencil printing perspective. Furthermore, a significant finding from the study was that paste stored in freezer conditions demonstrated lesser variation in characteristics when compared with typical storage methods (despite many sources categorically dismissing paste storage at sub-zero temperatures – ADTOOL, 2002; Radio Electronics, 2007).

3. As with the ageing study, the abandon time investigation demonstrated that current abandon times can be increased considerably from a printing point of view when compared with those standards currently employed. This is of particular significance when considering the hazardous classification of solder pastes, and the strict guidelines that have now been applied with regard to disposal of such materials (as described by the WEEE directive).
4. A significant input to the field of paste rheology (and subsequently electronics manufacturing) was attained through deriving an equation for calculating the recoverability percentage of a paste. This equation relates to the ability of a paste deposit to recover structurally after removal of an applied stress (such as that generated during the printing process). This was seen as a significant contribution as it allows for an indication of paste behaviour upon stencil release to be rheologically simulated in terms of tendency towards slumping and, consequently, bridging.
5. By using the work conducted by Mezger (2006) relating to the Arrhenius equation, a novel single formula for predicting viscosity was developed during the project.

1.6 Overview of the thesis

Chapter 1 of this thesis provides an introduction to the project, presenting the importance of stencil printing and the significance of the transition to Pb-free soldering. Also discussed are those common problems faced within SMA. The chapter is concluded with information relating to the current challenges and issues within the electronics industry, the problem context for the course of the project, aims and objectives, and the contributions to knowledge.

Chapter 2 presents findings of the literature review, detailing information relating to work that has been previously undertaken in the field of electronics manufacture. Particular attention has been towards publications addressing the use of Pb-free solder pastes, and the stencil printing process. The chapter is concluded with details of outstanding issues and gaps in knowledge that appear to remain undocumented. In Chapter 3, fundamental rheometry is discussed, during which the importance of rheology is reported, with reference made to – and explanations given for – common terminology that is frequently related to the topic of rheology. The chapter also presents the various materials that exist (such as those that are non-Newtonian), and various classifications of solder paste and their formulations. Additionally, the chapter also addresses background theory for each of the experimental studies, including a discussion of various prediction methods that may potentially be utilised.

Chapter 4 illustrates the experimental design that was to be followed throughout the course of the project. This includes a discussion of the apparatus used and an overview of the solder paste materials used. Also included within this chapter is information relating to the pre-study investigations conducted (i.e. the speed step test and characterisation tests) that provide a fundamental understanding of the paste materials prior to the main study.

Chapters 5–9 contain the experimental results, where each chapter consists of an introduction, results, discussion and conclusion. In Chapter 5 the effect of flux and particle size distribution on the creep recovery behaviour of solder pastes is presented; Chapter 6 details the effect of long-term ageing on rheology and print quality; in Chapter 7, the rheological simulation of slumping behaviour is addressed; Chapter 8 examines the rheological correlation between print performance and abandon time; and Chapter 9 explores the effects of application time, applied stress and recurrence of application on the creep recovery behaviour of solder pastes.

Chapter 10 then provides conclusions and suggestions for further work. The chapter begins with a summary of important findings from this PhD project, comparing the results with existing results or methods. The initial aims and objectives of the project are then revisited, which is then followed by suggestions for future studies based on the work within the thesis.

CHAPTER 2:
LITERATURE REVIEW

2.1 Introduction

Despite the term only being conceived in 1929 (by Professor Bingham), the science of 'rheology' has long been employed within the field of materials science, with rheological measurements providing an important route to revealing the flow and deformation behaviours of materials that can considerably improve efficiency in processing (Herh et al, 1998). This importance of understanding the flow and deformation behaviour can be seen in works from Hooke (1678, on ideal elastic solids) and Newton (1687, on Newtonian materials); both examples highlight the significant contribution rheology has provided over a substantial period of time.

Existing literature demonstrates that the science of rheology has been (and can be) successfully applied to many fields to provide valuable information on the behaviour of materials and their processing in many applications such as electronics manufacturing, food technology and the pharmaceuticals industry. Furthermore, it can also be seen that rheological measurements are used in the study of differing materials in an attempt to improve their processing performance; examples include:

- **Printing inks:** Zettlemoyer and Lower (1955); Whitfield (1965); Prasad et al (2006)
- **Asphalt:** Romberg and Traxler (1947); Planche et al (1998); Polacco et al (2004)
- **Blood:** Dintenfass (1969); Van Acker et al (1989); Bremmell et al (2006)
- **Glass:** Navarrette (1969); Pandey and Saraf (1982); Di Cola et al (2009)
- **Food products:** Blair (1958); Ma and Barbosa-Cánovas (1995); Schantz and Rohm (2005)
- **Paints:** Fischer (1950); Dutt and Prasad (1993); Armelin et al (2006)

- **Geology:** Afrouz and Harvey (1974); Boitnott (1997); Bohloli and de Pater (2006)
- **Oils:** Jones and Tyson (1952); Matveenko et al (1995); Wan Nik et al (2005).

As was stated earlier (see section 1.3), the continuing miniaturisation of hand-held consumer electronic products has led to new challenges in the deposition of smaller paste deposits at fine-pitch and ultra-fine-pitch geometries used in SMT assembly. The deposition of consistent paste deposits from pad to pad and from batch to batch requires paste with good printability, which in turn calls for good paste formulation and a good understanding of paste rheology.

Flow behaviour is particularly important to the printing process and retaining deposit definition, as this can dictate both the quality and acceptability. Additionally, paste rheology is affected by both flow and elastic properties (i.e. viscoelasticity), which may consequently dictate the ability for dispensing and depositing. Therefore, controlling rheological properties is vital in ensuring paste materials can be adequately and reproducibly deposited during printing (Puttlitz and Stalter, 2004).

Furthermore, an understanding of paste rheology is necessary due to the long-term dependence of manufacturing on lead materials. Zou et al (2010) report how – for the electronics packaging industry – the Sn–Pb solder alloy has been the material of choice during interconnection, as alloys containing lead provide advantages regarding reliability whilst also being well tested and inexpensive. With such wide-scale use of lead products within manufacturing, the EU's implementation of the RoHS and WEEE directives necessitates a drive towards replacing these tried-and-tested methods of interconnection. Zou et al (2010) further report how identifying additional and appropriate substitutes for the Sn–Pb solder is seen as a matter of urgency. At present, the Sn–Ag–Cu alloy has been highlighted as the accepted 'green successor' to the Sn–Pb alloy (Suganuma, 2003; Price, 2005); but with the use of this alloy still in its infancy, rheological investigations remain essential.

Within electronics manufacturing, solder paste is typically processed through the use of stencil printing; this involves 'rolling' solder paste across the surface of a stencil to

shear the paste into apertures that align with required deposit locations on the board. The stencil printing process is therefore a fundamental aspect of SMA, and many faults that arise with SMT assembly can be sourced back to the paste printing process. Issues including poor deposit definition or shape, insufficient solder, and skips or voids within the printed solder paste account for up to 60% of all PCB assembly defects. Due to the number of challenges related to the printing process, the 'bottom line' cost of PCB assembly could be influenced significantly through elimination of some of these difficulties (National Electronics Manufacturing Centre of Excellence, 2000).

With SMT relying heavily on paste deposition onto circuit boards via stencil printing (Gilleo, 1996), it is very important that methods for reducing defects associated with stencil printing are discovered. It is for this reason that investigations into stencil printing are essential; in order to improve the efficiency of the print, consequently leading to (i) a reduction in observed defects, (ii) an improvement in the reliability of the end product and (iii) an enhanced long-term performance of the solder joint. Issues currently exist due to the vast number of variables present with stencil printing (such as squeegee pressure, squeegee speed, thickness of the stencil and paste formulation) and, consequently, specifying exact settings is highly complex – repeatable results can depend on subtle changes, particularly with regard to paste formulation. Despite these difficulties, investigating the stencil printing process and its variables offers the potential to discover methods for minimising the occurrence of defects.

As previously mentioned, solder paste rheology can be tailored to help improve solder paste printing performance and to help reduce the level of printing defects. Therefore, by determining correlations between the printing process and new Pb-free paste formulations, opportunities exist to develop methods of reducing print defects. The factors which can affect Pb-free paste rheology and the printing process include (but are not limited to) the following: alloy type, flux vehicle system, PSD and metal content. Therefore, understanding these new Pb-free materials is essential to the printing process (Marin and Simion-Zanescu, 2005).

2.2 Key issues and challenges

2.2.1 Correlating paste rheology with print performance

The correlation between solder paste properties and the printing process has long been an important subject of investigation (Bao et al, 1998). In one study, Bao and colleagues investigated the rheological properties of a series of solder pastes and fluxes, correlating those findings with process performance prior to reflow. In the aforementioned study, it was observed that the essence of conducting such an investigation was due to the knowledge that the flow and deformation behaviour of a solder paste could directly affect post-print behaviour and the quality of print. This could be seen through properties such as slump resistance. The correlation between rheological measurements and the printing process is therefore highly important for both the selection and formulation of a solder paste. Bao et al further stated that there was little evidence of the correlation between rheological properties of solder paste and the material's actual performance in the literature.

In order to bridge this gap in literature, oscillation, creep and flow tests were conducted on Sn solder pastes, using a rheometer with a parallel-plate geometry with diameter of 20 mm and a sample gap of 1 mm. During the course of the study, the temperature was maintained at a constant value of 25°C and frequency tests were conducted at 1 Hz, with an amplitude sweep from 1 Pa to 2000 Pa. Bao et al (1998) observed that the recovery behaviour of a solder paste is a characteristic that is primarily governed by the flux; creep tests highlighted that the print defects are proportional to the compliance for J_2 - the point at which recovery commences (a ratio of strain to applied stress); and solder pastes that exhibit a lower compliance will have less tendency to ooze underneath the stencil, thus reducing the possibility of smearing.

Bao et al (1998) also suggested that tests should be conducted in the linear viscoelastic region (LVR) in order to establish the best correlation between rheology and material micro-structural properties. Therefore, further work investigating the application of stress outside the LVR may be beneficial, in an attempt to replicate the conditions that would actually be observed during the print cycle. Additional work could also investigate the alternative viewpoints of those results achieved. In one

instance, Bao and colleagues discuss that a higher solid characteristic would reduce slumping, but they do not mention that this in itself could lead to further issues such as skipping. It is important to consider both aspects of these results, and this is part of the focus of the study reported in this thesis.

2.2.2 Effect of paste formulation on paste rheology

Work conducted by Nguty et al (1999) investigated the rheological profiles of different paste formulations, offering a more comprehensive understanding of the influence of composition on stencil printing performance. The key requirement for the study was the continuing miniaturisation trends within the electronics assembly industry. As trends towards miniaturisation continue, there is increased pressure for improved board density in a cost-effective manner. Furthermore, with such requirements, it is important to reduce particle size to correspond with miniaturisation of pad size for a consistent paste deposition (from board to board).

In their study, Nguty and colleagues (1999) considered a parallel-plate geometry of 40 mm and a sample paste height of 0.5 mm whilst conducting steady shear and oscillatory tests on Sn–Pb solder pastes. In the creep recovery testing, the sample thickness was increased to 2 mm with the temperature maintained at a constant 25°C. The study explored the influence of flux, PSD and metal content on paste creep recovery behaviour, with findings suggesting that a higher deformation index (J2/J1) would occur with an increase in the mean particle size. This signifies that the structural breakdown would be greater with an increased particle size. Furthermore, the authors observed that the PSD plays a role in the flow behaviour (into and out of the apertures), which could lead to issues of clogging. The deformation index (J2/J1) was also reported to be independent of the flux, assuming that all other variables (such as metal content) remained constant, with the slumping defect said to increase proportionally with a higher value for the creep recovery index (J3/J2).

One key issue that may have influenced the results negatively was the variation present with regard to paste height used within the creep tests (2 mm) and the oscillatory tests (0.5 mm). It is believed that introducing such variations within a study might pose some difficulty in making compare-and-contrast analysis of the

results. It was also noted that the ratio for recovery percentage was wrongly detailed as being J3/J1 because it fails to incorporate the value for J2, which is essential when discussing the recovery in terms of regaining structure after a period of breakdown. For this reason, equation [2.1] (Marks et al, 2011) has been derived during the course of this project for calculating recoverability as follows:

$$\text{Recovery percentage (\%)} = \frac{J_2 - J_3}{J_2 - J_1} \times 100 \qquad \textbf{[2.1]}$$

It was also noted that Nguty et al. (1999) failed to explain why they believed that deformation index was a constant with a change in the flux. Therefore, further investigation is needed to understand the influence of flux on the creep recovery properties of the solder paste, as the flux vehicle system of the paste has a major influence on its flow characteristic.

2.2.3 Effect of temperature on paste rheology

In another paper, Nguty and Ekere (2000[a]) studied the effect of temperature on the rheological properties of solder pastes and the flux vehicle system, because one of the key factors that instigate a change in solder paste viscosity is variation in temperature. Change in temperature can be due to environmental conditions or from the stencil printing process itself, and it is known to adversely impact the printing performance of the solder paste. Furthermore, subtle variations in solder paste formulation from batch to batch often mean that paste samples demonstrate a range of behavioural responses to changes in temperature.

Rheological measurements used in the study by Nguty and Ekere (2000[a]) were conducted on Sn–Pb paste using a parallel-plate geometry with diameter 40 mm and a sample thickness of 0.5 mm. The temperature was then incorporated as a variable, with a testing range detailed as 10–30°C. The flux and the PSD were also introduced as variables, and testing consisted of either a fixed shear rate or temperature as the viscosity is a function of both and therefore it was appropriate to investigate these individually.

From the tests, Nguty and Ekere (2000[a]) discovered that the flux introduces variations in the solder pastes sensitivity to temperature, and furthermore the viscosity of the solder paste decreases with an increase in temperature. They further asserted that this increase in temperature, leading to a decrease in viscosity, was an expected trend; nonetheless, it is important that this dependence, i.e. the influence of the flux on the properties and behaviour of the paste, be addressed. The authors further stated that despite using a limited range of temperatures, those values selected were sufficient to provide trends in rheological dependence on temperature. Although trends were highlighted, it might be beneficial to expand beyond the 30°C limit and discover the influence of high temperatures on the rheology of the solder paste. Furthermore, the study failed to discuss how the PSD affects the viscosity with a change in temperature, despite introducing this variable into the study.

2.2.4 Effect of storage on paste rheology

Owing to the dependence of a paste's rheological properties (such as viscosity) on its 'history' (paste storage), Nguty and Ekere (2000[b]) examined the effects of storage on the rheological properties of paste materials under two different sets of temperature and humidity conditions. During the study, an attempt was made to determine the shelf life of solder paste, whilst using rheological measurements to evaluate the effects that storage conditions have on the viscosity of solder paste.

Literature findings report that, during storage, sedimentation of the solder powder occurs, which results in the formation of a rich layer of flux at the top of the container (Ekere and Lo, 1991). This could then result in a loss of solvents, or a drying-up of the paste, which occurs at a slower rate with a decrease in temperature. To quantify such influences, Nguty and Ekere (2000[b]) employed a parallel-plate geometry with a 20 mm diameter and a 1 mm sample height. The solder paste investigated was Sn–Pb and was studied at temperatures of 4°C and an average temperature of 22°C. In order to monitor the effect of storage, the samples were checked after 30 days, 70 days, 121 days and 177 days, with experiments repeated to allow for an average measurement to be attained.

It was observed that viscosity measurements had increased by 60% over a period of five months for the solder paste that was allowed to sit at room temperature. Furthermore, there was a general trend of increasing viscosity with a prolonged period of storage. It should be noted that any future work relating to the shelf life of solder paste must be conducted with storage at stable temperatures, with constant parameters applied. In particular, the following should be noted:

- Nguty states that the room temperature was averaged at 22°C; yet as this was representative of a five-month period, seasonal temperature variations may have influenced observations significantly (particularly with the lack of climate control detailed). By excluding details of the observed temperature range, accuracy of results may become questionable because temperature is said to greatly affect the viscosity of the solder paste.
- Further to this, there appeared to be no consistent structure with regard to the storage period between observations (30 days, 70 days, 121 days and 177 days). Regular checks are important to enable trends to be observed and highlighted.
- Finally, it is believed that a single repeat of a testing phase is insufficient for detailing an accurate response, as anomalous results may pass unnoticed.

It is apparent that further work is needed relating to the effect of storage on solder paste properties, and guidelines have been highlighted relating to ways of improving the methodology undertaken and described above.

2.2.5 Lead-free solder paste development

The studies reported by Nguty et al (1999, 2000[a], 2000[b]) and Bao et al (1998) did not cover the use of Pb-free pastes. The EU directives on RoHS and WEEE in 2006 (enacted by the UK government) has led to a massive increase in the use of Pb-free solder pastes in SMT assembly, often in fine-pitch and ultra-fine-pitch geometries. This in turn has led to the urgent need for a better understanding of Pb-free solder paste printing performance and its rheology. Suganuma (2003) underlined the

importance of preparing for the prohibition of lead in solder alloys, and detailed an introduction to lead-free soldering technology.

The electronics manufacturing and assembly industry was very keen to find a replacement for the Sn–Pb alloy following the introduction of the RoHS and WEEE directives, and Suganuma (2003) highlighted the benefits of using the Sn–Ag–Cu alloy in new Pb-free solder paste formulations. The work of Suganuma (2003) showed that the Sn–Ag–Cu alloy has good stability and that it also meets the standard requirements for SMT assembly soldering, and it thus became the preferred alloy for Pb-free solder paste development.

To further support the work conducted by Suganuma, Price (2005) reported on the changes that the transition to Pb-free soldering would bring about. The work discussed the necessity of finding a new alternative for Sn–Pb pastes and, like Suganuma, assessed the acceptability of the Sn–Ag–Cu alloy. It also discussed the important challenges that were likely to arise from introducing new Pb-free pastes into the electronics industry, and the consequences for the assembly process.

One of the key issues discussed by Price (2005) was the need to allow for higher melting temperatures in the assembly process. From details of those Sn–Ag–Cu pastes selected for implementation within the project, the reason behind both Suganuma (2003) and Price (2005) stating the acceptance of the alloy becomes apparent. With a melting point of 217°C, the solder paste was within the desired range of 215–220°C; and with formulation of the alloy having 95.5% tin the pastes selected are a cost-effective means of replacing the Sn–Pb pastes.

Although Suganuma (2003) and Price (2005) both supported the switch to Pb-free soldering, along with the requirements of the EU directives pertaining to RoHS and WEEE, many studies were still published relating to Sn–Pb solders. One such study conducted by Billote et al (2006) focused on characterising rheological properties of a typical carrier fluid and its solder paste in relation to printing performance and spreading on circuit boards.

Billote et al (2006) stated that characterising paste materials in relation to their printing performance is essential due to the rheological complexity of solder pastes. Billote and colleagues (2006) also stated that this complexity is due to the composition of the carrier fluid, the properties required in the printing and soldering processes, and its shelf life. It is noted that one paste roll could typically be used for approximately 50 boards, and the material is therefore required to handle successive kneads without losing its viscoelastic properties. Billote et al (2006) also underlined that most studies tend to focus on the printing process and on suggesting improvements to the equipment; only a few authors have investigated the rheology of solder pastes in depth.

To explore this correlation, Billote et al (2006) employed a six-bladed vane-in-cup geometry with a gap of 8 mm. This geometry is of interest as it provides an alternative to the typical parallel-plate or cone-and-plate set-up utilised in most studies. Even so, this could create difficulties when attempting to compare and contrast with past work conducted using standard plate geometries.

The results of the work by Billote et al (2006) showed that problems of ageing were mostly due to the flux vehicle system, again emphasising the importance of understanding the influence this can have on the solder paste properties. Their results show that for flux samples older than four months the complex viscosity was found to be considerably reduced compared with that of freshly prepared flux. Consequently, Billote et al (2006) stressed the need for further study of solder flux samples that are less than three months old. As has been a common observation, the rheological complexity was found to be largely due to the flux vehicle system, and Billote et al suggested that paste formulations can be optimised by extrapolating the influence of adding solids and through studying the rheology of standalone flux vehicle systems.

Billote et al (2006) provided further evidence that investigating the influence of flux is essential; however, with the transition from Sn–Pb to Pb-free pastes, Billote and colleagues might have included Pb-free pastes in their investigations in order to ensure that future work could be correlated to those results obtained. In addition, the authors did not acknowledge the consequence of ‘optimal parameters’, stating that slumping can be avoided by using a highly elastic paste. Although slumping may be

reduced by using pastes with high elasticity, an overly elastic paste may lead to other printing challenges; hence, it is essential to explore all aspects of the solder paste properties.

2.2.6 Influence of PSD on paste rheology

The focus of the work conducted by Zhang et al (2010) was the effect of PSD on solder paste rheology – and, in particular, its effect on the viscosity of Pb-free solder pastes. In this study, Zhang and colleagues employed a rheometer with a parallel-plate geometry of 25 mm diameter and sample height of 0.5 mm, with the temperature maintained at 25°C. The effect of PSD was investigated by varying the PSD in the following ranges: 25–50, 20–40, 10–23, and 3–17 microns. The results showed that as the shear rate was increased during the tests, the hydrodynamic forces within the paste become more dominant, which results in the particles being forced into layers.

Results documented by Zhang et al (2010) emphasise the importance of the hydrodynamic forces acting as a catalyst for shear thinning behaviour. However, issues once again arise due to the inability to accurately replicate the tests. As opposed to utilising commercially available pastes (e.g. those from an industrial source), the authors describe how the pastes used were manufactured using two different PSD sizes, with the response then being studied. This makes the results difficult to understand fully because, rather than investigating (for example) the influence of a PSD of 25–50 microns, the authors were looking at the influence of a ratio between particle sizes of 25–50 and 3–17 microns. In addition, those PSD ranges used do not match any industrial standards, providing only a close comparison – for instance, a type-4 solder paste will typically have a particle size distribution of 20–38 microns, but in the Zhang study the PSD used was 20–40 microns.

2.3 Significant literature findings

Through researching available literature sources, it becomes apparent that there is a clear belief that the printing process is held accountable for the majority of defects in SMA. As 52–71% of surface mount defects – for fine and ultra-fine pitch assemblies – can be attributed to stencil printing, it is believed that a lack of understanding of this

process still remains (Pan and Tonkay, 1999). Rahn (2006) further addresses the issue of a lack of understanding of paste properties and their printing behaviour, and states that an analysis of SMA processes shows that the paste, paste handling and printing are the key sources of defects, with 40–70% of all faults accredited to these variables and merely 10–15% resulting from the placement and reflow stages of assembly. Additionally, defect occurrences within the printing process can have knock-on effects on the assembly process as a whole, leading to unreliable solder joints post-reflow, with the incidence of a single defect said to be more expensive to the assembly process than a 500g container of paste (Rahn, 2006). Rahn also states that the occurrence of defects may additionally result in reduced time efficiency, which may consequently outweigh the cost of a jar of solder paste by a factor of several hundred or possibly even several thousand, simply due to an hour-long downtime in the production line. Therefore, significant importance is placed on researching and understanding the printing process and the effect of the solder paste material.

2.3.1 The stencil printing process

As previously discussed in Chapter 1, the stencil printing process is commonly held accountable for the majority of defects in electronics manufacturing, including those encountered during reflow. Therefore, a better understanding of stencil printing is important for discovering methods of reducing surface mount defects. This was underlined by Ekere and Lo (1991), in which it was reported how the efficient and acceptable printing of solder paste onto a circuit board can dictate the success of reflow soldering in SMA.

Controlling the efficiency of the printing process can be a highly complicated process, which can be reliant on simply optimising the process to reduce rather than eliminate defects. Whilst discussing SMA, work by Tsai (2008) suggests that complex and non-linear behaviours exhibited during the stencil printing process – which might result in quality and production time losses due to soldering defects – may need to be addressed simply through maximising efficiency of printing procedures prior to component placement in order to reduce the cost of manufacture whilst increasing yields. Although the work by Tsai gives the impression of a ‘quick fix’ to the issues of stencil printing, this is unrealistic owing to the vast number of factors (such as

squeegee speed) that relate to the print alone (more than 40 factors have been identified by the National Electronics Manufacturing Centre of Excellence, 2000).

In work by Hwang (1994), the dependency of the stencil printing process on this wide range of variables is discussed further, with the five main factors that could contribute to print quality defined as:

1. Printing parameters, of which the three major parameters highlighted were: (i) squeegee speed, (ii) squeegee pressure, and (iii) snap-off distance
2. Stencil selection
3. Solder paste rheology
4. Solder paste viscosity
5. Solder powder size and size distribution.

With the complexity of controlling print quality and accounting for the influence of such a vast number of variables, several studies in the literature discuss the importance of understanding the correlations between variables and defects in order to optimise the print to attain a desired result such as paste volume or solder height:

- A strong connection exists between the volume of a paste deposit and the observed snap-off height (Owczarek and Howland, 1990[a] and 1990[b]).
- Printability, solderability and solder joint reliability are all factors that can be improved through an appropriate selection of solder paste and its composition (Ekere et al, 1994).
- The printing performance of a solder paste can be enhanced with variations of squeegee speed and squeegee pressure (Lofti and Howarth, 1998).

However, other studies appear to generate conflicting results regarding correlations between variables and the correct method for manipulating results of the print performance (Tsai, 2008). According to Mannan et al (1994), the height of a solder paste deposit can be seen as proportional to the squeegee speed, whereas in work by Pan et al (2004) it was discovered that the speed of the squeegee has an insignificant influence on the paste volume. Furthermore, Mannan et al (1994) and Pan et al (2000)

discuss how an appropriate and effective aperture design can significantly influence the volume of paste recorded, allowing for sought-after deposits to be achieved; Whitmore et al (1997) conversely describe how the volume of a solder paste deposit is uninfluenced by the stencil thickness and hence the design. Thus, despite a strong agreement that the quality can be improved through appropriately varying specific factors, it becomes apparent that a significant lack of understanding still remains. This is demonstrated through the conflicting opinions that exist throughout the literature as a result of the partial understanding of the non-linear behaviour and cause-and-effect relationships (Tsai, 2008).

In his work, Tsai (2008) also reported how an increase in first-pass yields of the stencil printing process can lead to a decrease in net manufacturing costs. Therefore, optimisation of solder paste printing can lead to improved efficiency and cost-effectiveness through identifying appropriate methods that increase the first-pass yields through preventing defect occurrence. However, much work and understanding is necessary in order to minimise the occurrence of defects. Furthermore, the occurrence of defects may be dependent upon the type of material used and developments in manufacturing (such as the switch to Pb-free paste, and miniaturisation). This becomes a notable concern because once methods have been developed to minimise the occurrence of defects, advancements in technology may render these strategies obsolete, forcing new techniques to be developed. This once again emphasises the challenges associated with the continued trends towards miniaturisation, as can be seen in work by Durairaj et al (2009[a]) in which it is reported that increased stencil clogging (and incomplete paste transfer to the PCB pads) commonly occurs with fine-pitch and ultra-fine-pitch applications.

Despite the continued complications that arise within SMA, it can be seen that many concepts exist that offer opportunities to apply defect-reducing methods to specific set-ups. One such example can be found in the work conducted by Morris and Wojcik (1991), where recommendations are made that during stencil printing the diameter of the largest particle within the solder paste should not exceed the value of one-half the smallest aperture dimension. Hwang (1989) reports how a ratio of one-third of the smallest dimension should typically be targeted to introduce a ‘safety factor’ during printing, where the largest particle should be no larger than one-third of the stencil

thickness. In this instance, it can be seen that the method of reducing the influence of clogged apertures need not be applied to specific materials (with a definite particle size). This hypothesis presented by Morris, Wojcik and Hwang, through reducing clogging, should allow for the solder paste height to become consistent, which is essential to the final quality of the assembly as paste deposit height is seen as an important measure of print quality. If the height of a solder paste deposit is too excessive, slumping tends to occur, which can result in bridging between leads during the reflow process. Conversely, a height that is too small will lead to an insufficient quantity of paste on the PCB to allow for an acceptable joint to be formed (Rajkumar et al, 2000).

Work conducted by Haslehurst and Ekere (1996) confirms the importance of the height of solder paste deposits (as detailed by Rajkumar et al, 2000) and attempts to highlight which parameters – such as squeegee speed and pressure – have a significant effect on the paste deposit height. The following conclusions were drawn from the study:

- Temperature and humidity need to be controlled during printing to improve yield from the production line.
- Solder paste on the stencil surface should be replaced on a regular basis in an attempt to maintain consistency.
- The quantity of solder paste used during the print cycle should be kept constant to facilitate consistent print deposits.
- Squeegee pressure, squeegee speed, direction of print stroke and separation speed are seen as the most significant printing parameters.

Although the work by Haslehurst and Ekere (1996) emphasised the importance of both the print direction and separation speed, particular significance is commonly seen to be placed on selecting an appropriate squeegee pressure and speed. In work conducted by Rajkumar et al (2000), it was stated that the optimum settings to employ included a low squeegee speed coupled with a high printing pressure. Results from the investigation highlighted this to be necessary because a decrease in the ratio between particle size and aperture width resulted in an increased level of skipping, which the

authors related to the tendency for increased particle jamming. Furthermore, the reasoning for attaining improved deposit height with increased squeegee pressure was suggested to be a result of the increased pressure restricting the influence of particle jamming. Rajkumar and colleagues also reported that a reduced squeegee speed allows for an increase in print time, which consequently improves aperture filling by allowing the squeegee an extended opportunity to compact paste into the aperture.

This observation was substantiated by Itoh (2002), who stated that a particularly high squeegee pressure will normally result in an excessive amount of solder paste being forced into the stencil apertures owing to the increase in downward force acting on the sample, possibly resulting in the presence of skipping defects. This increase in squeegee pressure initiates an elevated intensity of friction between the solder particles, which typically results in an unsuccessful paste release upon removal of the stencil (see Figure 2.1).

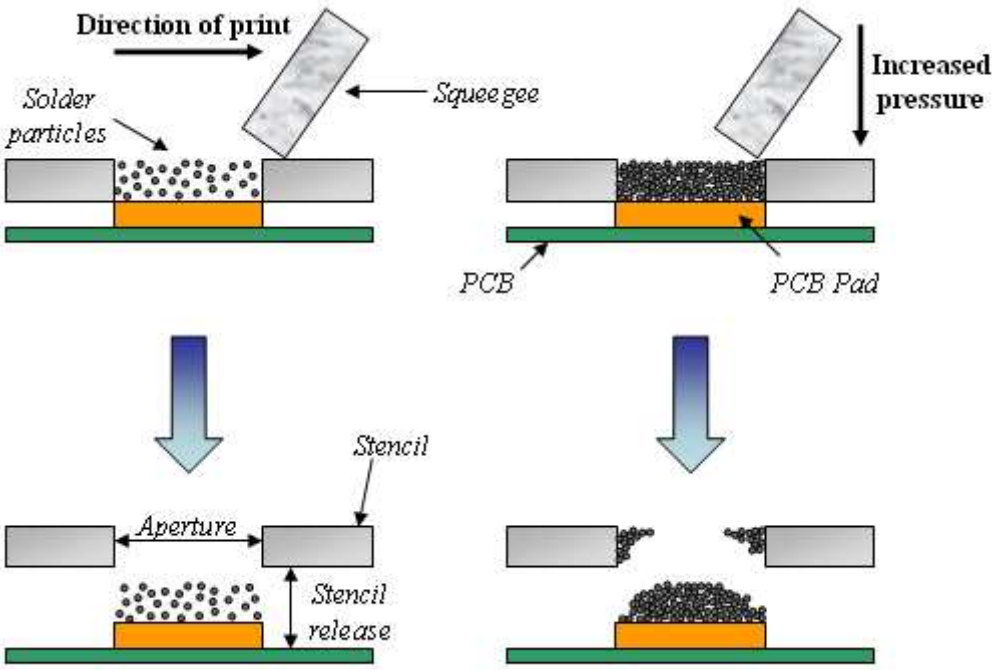

Figure 2.1: Influence of increased pressure during the stencil printing process (Itoh, 2002)

Danielsson (1995) provides a contrary argument to that presented by Rajkumar et al (2000), stating how a reduced paste height would be likely to be observed with an

increase in pressure applied – due to the tendency of the squeegee to scoop paste from the filled apertures. Furthermore, Freeman (1990) states that an excessive application of paste pressure can lead to bridging between paste deposits, with insufficient print speeds combined with a squeegee angle greater than 45° resulting in irregular aperture filling and consequently voids on the boards. Freeman's results do, however, corroborate the work by Rajkumar et al (2000), noting that with slower processing speeds, paste is allowed to flow more freely (and to a greater extent) into the stencil apertures prior to being sheared off by the squeegee, which can potentially improve print resolution significantly whilst also reducing the incidence of voids.

Several reports in the literature offer recommendations on the optimal settings for squeegee speed and pressure; however, contradictions can be seen between these recommended settings from one study to the other:

1. Morris and Wojcik (1991) reported that a consistent deposit height and cleanliness of stencil surface can be attained if the squeegee pressure is sustained at approximately 1 lb/in (0.454 kg/in length), whilst the speed is maintained below 1 in/s (25.4 mm/s).
2. Rajkumar et al (2000) noted that a pressure of 6 kg is required to achieve an acceptable print stroke.
3. Ekere and Lo (1991) suggested that the squeegee should be operated at a uniform speed that ranges between 40 and 60 mm/s.
4. Hillman et al (2005) reported that optimal settings for stencil printing were equal to 5.2 kg for the pressure and 20 mm/s for the squeegee speed.
5. Bentzen (2000) recommended that squeegee speed during the printing process should be maintained between 20 and 80 mm/s.

From these few studies, significant variations exist in the recommendations for both pressure and speed of the squeegee during printing cycles. However, one factor widely agreed upon is the method for determining the optimal pressure to be applied; where a low pressure is gradually increased until a clean sweep of the stencil is obtained (Hwang, 2004). This is also reported by Bentzen (2000), who recommends that the squeegee pressure should be as little as necessary to scrape the stencil clean of

solder paste particles. Importantly, both Hwang (2004) and Bentzen (2000) emphasise that the stencil must remain clean after completion of the print stroke.

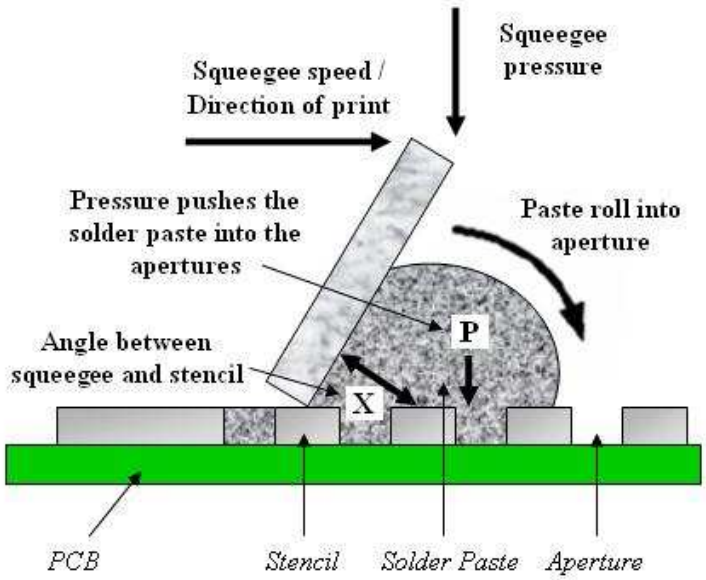

Figure 2.2: Illustration of the printing process emphasising the importance of paste roll (Durairaj et al, 2009[b])

As previously reported, the pressure and speed of the squeegee during the printing process are widely recognised to be the most important parameters associated with the occurrence of scooping and skipping defects. However, Mannan et al (1993) noted the role of the squeegee material. Results from the study report that a metal squeegee can assist in reducing the occurrence of scooping; however, a softer polyurethane squeegee was seen to decrease the influence of skipping. Further work relating to the squeegee material was then conducted by Mannan and colleagues (1994), in which paste deposit heights were monitored depending on paste viscosity, squeegee speed and aperture geometry. From that study, the authors reported how the pressure significantly influences paste height during printing, due to pressure variations between the apertures perpendicular to and parallel to the direction of the print stroke. Therefore, Mannan et al (1994) further emphasise the necessity for an appropriate application of squeegee pressure, and the influence that this parameter can have on defect occurrence. Mannan et al also concluded that the viscoelastic nature of solder pastes plays a significant role in creating pressure gradients during the stencil printing process.

Despite the observation by Mannan and colleagues regarding the viscoelastic behaviour of solder pastes, very limited work has been conducted in correlating printing performance with the viscoelastic nature of paste materials. This correlation is of importance because increasing production yield through minimising defect development is dependent on the relationship between rheological behaviour and printing performance of solder pastes (Durairaj et al, 2009[a]). One such instance where paste rheology has been correlated to print performance is that of Carpenter et al (1994). Results from those investigations showed that solder paste with a high viscosity did not slump but printed poorly, with skipping defects present. These results may possibly be linked to the work previously highlighted by Hwang (1989) and Morris and Wojcik (1991), where the particle size was observed to play a significant role in print quality. Carpenter et al (1994) also showed that a highly 'solid-like' solder paste requires application of higher printing pressures and will generally exhibit a poor aperture withdrawal characteristic.

2.3.2 Solder paste rheology

In work by Jirinec (1984), it was noted that temperature, paste composition, PSD and metal content can significantly impact the rheology of paste materials, contributing to substantial variations in observed viscosity. Hwang (2004) further expanded on the work by Jirinec, reporting how results of the paste printing process may be dependent upon a wide range of variables that address chemical, physical and rheological properties along with the quality of the solder paste itself; with major contributing factors including:

- Quality of the solder paste and its properties
- Solder powder characteristics
- Solder powder selection
- Stencil selection
- Stencil thickness versus aperture design
- Stencil aperture versus land pattern
- Operating parameters during printing
- Squeegee type.

Hwang (2004) further reports how the printing process can be influenced by a significant number of variables, all of which can shape the outcome of the process and acceptability of the print, with typical classification of these falling under one of five headings:

1. Printer operating parameters
2. Squeegee system
3. Stencil characteristics
4. Stencil aperture design
5. Substrate.

This means that the rheology of a solder paste is dependent on a vast number of variables.

Lapasin et al (1994) focused on one variable in particular, namely the flux vehicle used for the paste formulation process. From the study, Lapasin and colleagues reported that the rheological properties – in particular the viscoelastic behaviour – can be modified through adjusting the formulation of the flux vehicle. In a further work, Bao et al (1998) supplemented this result, once more emphasising the important role the flux vehicle plays on paste rheology and describing how the rheological properties of yield stress and paste recovery are two such characteristics that are primarily governed by the flux. Bao et al (like Lapasin et al) also examined the viscoelastic nature of solder pastes, noting that paste resistance to slumping can be increased with a higher storage modulus, due to the improved elastic behaviour and high viscosity that should result. Bao et al (1998) further reported how the recovery properties of solder paste (influenced by the viscoelasticity) allow for important trends to be validated:

1. The potential for minimising the occurrence of print defects can be increased through introducing:
    a. An increase in the yield stress
    b. Increased values for the elastic modulus and recoverability

   c. Reduced compliance values for J1 and J2, which relate to structural breakdown.
2. The tendency for solder pastes to exhibit smearing defects can be linked to higher compliance values and reduced yield stress due to the increased trend of paste flow underneath the stencil during the printing process.
3. Aperture clogging – and hence skipping – can be reduced through an increase in elastic behaviour due to the solder paste 'pulling together' during stencil release.
4. Slumping can be reduced through increasing the elastic properties and an increased solid behaviour.

In work conducted by Nguty and Ekere (2000[b]), it was stated that the viscosity (which according to Bao et al (1998) plays a significant role in reducing slump occurrence) and additional rheological properties are also dependent on the solder paste 'history' or method of paste storage. Results from the work showed that after a storage period of five months at room temperature, the viscosity of the paste samples was seen to increase by approximately 60%. The influence of storage (or ageing) is also confirmed in work conducted by Ekere and Lo (1991), in which it is noted that separation of the flux vehicle system may occur as a result of excessive periods of ageing or through inappropriate storage conditions. This natural separation process may consequently lead to an irreversible breakdown of the structure, which can impact the printing performance considerably. This significant influence of storage may also be directly linked to the effect that temperature may have on the rheology of solder pastes, as storage conditions can vary considerably between users of paste materials. In one example, Qualitek (2007) suggests that solder paste samples should typically be stored within a refrigeration system in which the temperature is maintained between 2°C and 10°C in an attempt to minimise the influence of chemical activity and the associated flux separation and solvent evaporation. In those instances where storage in this temperature range is not possible, Qualitek recommends that solder paste storage temperatures must not exceed 25°C.

Westerlaken (2000) further illustrates the important role that temperature can play on the rheological performance of paste materials, describing how the operating temperature of solder pastes should remain within the range of 22°C to 26°C. This

was illustrated through use of a temperature profile (see Figure 2.3), the results of which determined that below 22°C the temperature is perceived as too cold owing to the values recorded for G' and G" being too high, while beyond a temperature of 26°C these properties also tend towards unacceptable values.

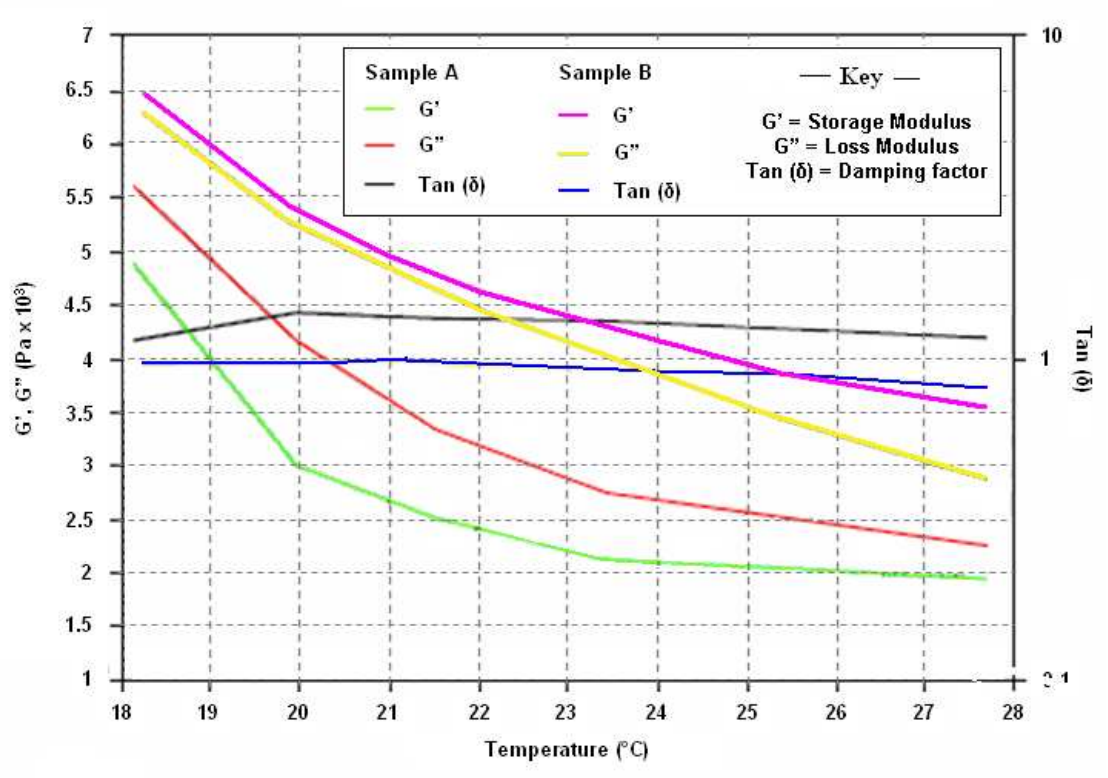

Figure 2.3: Illustration of an operating 'temperature window' (Westerlaken, 2000)

Evans and Beddow (1987) emphasise that the effect of temperature on paste viscosity is an important factor to understand, particularly as paste materials are frequently subjected to variations in temperature (such as those during storage and processing). As discussed further in Chapter 3, paste rheology is commonly said to be influenced by temperature variations generated by the stencil printing process (Barnes et al, 1989; Riedlin and Ekere, 1999). However, while investigating the effect of stencil printing on the rheological properties of solder paste, Mannan et al (1995) detailed how heat generated within the paste roll during printing does not allow for a noticeable temperature increase to occur.

In the study conducted by Mannan et al (1995), it was also noted that PSD can have a substantial influence on paste viscosity, with an increase in PSD leading to a reduction in viscosity and skipping – reiterated by Zhang et al (2010). Evans and

Beddow (1987) also reported that viscosity decreased with increasing PSD, but also linked this with a reduction in metal content. This was confirmed by Kim et al (2005), in which it was found that rheological properties can be significantly impacted by the solder particle content (see Figure 2.4).

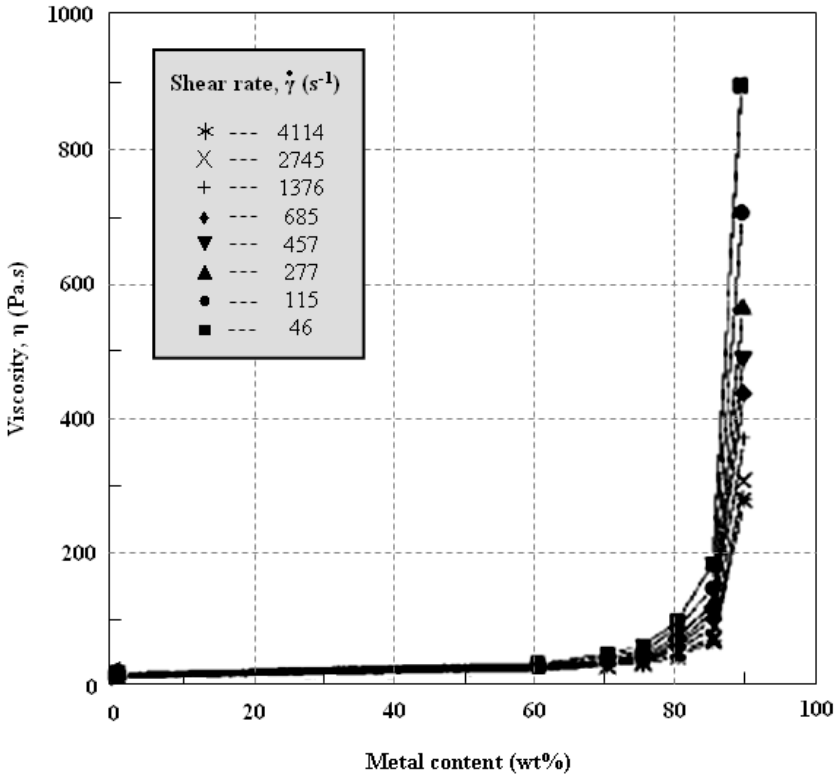

Figure 2.4: Influence of metal content on paste viscosity (Kim et al, 2005)

Complementing the works by Kim et al (2005), Evans and Beddow (1987), Mannan et al (1995) and Zhang et al (2010) (who detail the effect of PSD on viscosity), Aravamudhan et al (2002) reported on how the particle size can influence the manufacturing process as a whole. Results from this study highlighted that a switch in solder paste from type 3 to type 5 (i.e. decreasing the solder particle size – see table 1.1 of joint industry standards; J-STD) offers both advantages and drawbacks:

- Type 5 solder pastes – as opposed to type 3 – allow for improved transfer efficiency due to an increased number of particles occupying vacant spaces within the stencil apertures (as a result of the smaller particle sizes). Therefore, reducing the particle size results in an increase in paste volume deposited during the stencil printing process.

- When compared with the type 3 solder pastes, type 5 samples tend to exhibit a higher resistance towards the printing process – particularly regarding adherence to aperture walls – which may be attributed to the increased viscosity of the paste. Therefore, this increased viscosity may potentially account for subsequent issues relating to a reduction in release performance from the stencil apertures.

2.4 Conclusions

It becomes apparent that gaps still exist in the knowledge pertaining to the stencil printing process, the rheology of solder paste and, more importantly, the correlation between the two. EU directives restricting the use of lead-based materials have played a significant role in widening this gap further. Efforts are being made to improve understanding in these areas, in an attempt to minimise defect occurrence during stencil printing, which would consequently improve the efficiency and reliability of SMA. There is, however, considerable agreement that the stencil printing process can account for the vast majority of defects in the assembly process and, as such, methods must be developed to help reduce and alleviate the influence of these defects.

Although many studies have been conducted relating to the stencil printing process, one important conclusion drawn from reviewing the literature is that of the necessity of conducting printing trials prior to investigations so as to ensure optimum printing parameters are used throughout the experimental studies. This conclusion arises from the many conflicting recommendations relating to the optimum speed and pressure that should be applied during printing. As mentioned previously, Hillman et al (2005) discuss the use of a print speed of 20 mm/s whereas Ekere and Lo (1991) suggest 40–60 mm/s. With regard to the squeegee pressure, Morris and Wojcik (1991) state how this should be 0.454 kg/in length, whereas Rajkumar et al (2000) recommend a pressure of 6 kg. Due to these variations, the conclusion must be drawn that printer settings should be investigated to ensure that they are ‘material specific’ since the behaviour of solder paste materials is seen to vary considerably from product to product.

A further conclusion drawn from the literature review was the important role played by the flux, PSD, temperature and storage (possibly due to the range of temperatures experienced) on rheological behaviour of solder pastes and stencil printing performance. The flux and particle size in particular are frequently discussed as methods for controlling paste behaviour, and 'fashioning' desired characteristics. With the widespread opinion that there is a need for controlling the occurrence of printing defects, the flux and PSD could present great opportunities to address this issue by formulating solder pastes that avoid defects arising. Furthermore, temperature is a factor that needs consideration. This is due to the influences it presents within the storage process, during typical operating conditions or as those elevated temperatures experienced during the reflow process. As the temperature is said to dramatically influence paste viscosity (according to Maiso and Bauer (1990) a 1°C change in temperature can alter the viscosity of the solder paste by as much as 40 Pas), the significance of investigating this factor becomes obvious.

Thus it is clear from reviewing existing literature that many opportunities exist for minimising the influence of defects within the printing process. Consequently, significant strides can be made towards discovering methods of correlating paste rheology with the printing process in an effort to reduce defects, which in turn could improve the reliability of the manufacturing process as a whole.

CHAPTER 3:
THEORY AND BACKGROUND KNOWLEDGE

3.1 Introduction

'Rheology' is a term that was first conceived by Professor Eugene Bingham (Lafayette College, Pennsylvania, USA) in 1929, and is an amalgamation of the Greek word 'Rheos' meaning 'to flow' and 'ology' which relates to 'the study of'. The term was derived from the Greek expression 'παντα ρει', commonly denoted as 'panta rei', which loosely translated means 'everything flows' (Seman, 2010). The expression 'παντα ρει' is often attributed to the Greek philosopher Heraclitus of Ephesus (536–470 BC); however, Barnes (2002) reports how in actuality Simplicius (40 [c^6] M) has been recognised as having the earliest recorded occurrence of the phrase, with the actual theory of 'panta chôrei' (everything moves and nothing rests) accredited to Heraclitus.

Prior to Professor Bingham deriving the term rheology, a substantial measure of rheological work was undertaken on issues such as: i), Newtonian liquids ii) linear viscoelasticity and iii) non-linear viscoelasticity, with contributions to knowledge by renowned historical subjects such as Archimedes, Newton, Pascal and Einstein (see Table 3.1). Rheology (since being defined) has grown largely, with great strides being made in advancing knowledge of flow behaviour and attempting to identify reasoning behind such behaviours. One such development was the formulation of fundamental equations and models, with important examples including those by Cross and Carreau for modelling flow behaviour. Further developments include: insights into wall slip behaviour; the Cox–Merz rule for correlating linear viscoelastic properties with viscosity behaviour; further understanding of the thixotropic nature of some materials and flow instabilities of non-Newtonian materials (Doraiswamy, 2002).

Research Topic		Noteworthy Research	Period
Idealistic materials	Perfect rigid bodies	Archimedes (~250 BCE), Newton (1687)	Antiquity
	Ideal elastic solids	Boyle (1660), Hooke (1678), Young (1807), Cauchy (1827)	1600s
	Inviscid fluids	Pascal (1663), Bernoulli (1738), Euler (1755)	1700s
	Newtonian liquids	Newton (1687), Navier (1823), Stokes (1845), Hagen (1839), Poiseuille (1841), Weidemann (1856)	Early 1800s
Linear viscoelasticity		Weber (1835), Kohlrausch (1863), Wiechart (1893), Maxwell (1867), Boltzmann (1878), Poynting and Thomson (1902)	Mid 1800s
Generalised Newtonian liquids		Schwedoff (1890), Trouton and Andrews (1904), Hatchek (1913), Bingham (1922), Ostwald (1925) – de Waele (1923), Herschel and Bulkley (1926)	Late 1800s/ early 1900s
Non-linear viscoelasticity		Poynting (1913), Zaremba (1903), Jaumann (1905), Hencky (1929)	Early 1900s
Key material descriptions	Suspensions	Einstein (1906), Jeffrey (1922)	Early 1900s
	Polymers	Schonbein (1847), Baekeland (1909), Staudinger (1920), Carothers (1929)	
	Extensional viscosity	Barus (1893), Trouton (1906), Fano (1908), Tamman and Jenckel (1930)	
The origin of rheology		Bingham, Reiner and others	1929

Table 3.1: Significant rheological works prior to derivation of the term ‘rheology’ (Doraiswamy, 2002)

An important stride, since the 'inception of rheology', can be seen by the significant increase in investigations into solder paste rheology, including:

- Advancing existing knowledge such as yield stress, thixotropy and time-dependent behaviour
- Studying new materials, particularly new lead-free paste formulations
- Employing new techniques for investigation – for example, employing the use of an ultrasound method to record measurements [Seman, 2010].

Despite these advances in the field, gaps still exist in knowledge, particularly relating to the prediction of solder paste behaviour and the correlation of paste properties with the stencil printing process.

3.2 Fundamentals of rheology and its application

Rheology is commonly defined as the science of deformation and flow of materials (Barnes, 2000); however, this classification does not appropriately address the vast application of the subject. Questions such as 'Why does peanut butter demonstrate peaks?', 'What allows a person to run on the surface of custard?' and 'Why does chocolate melt?' can all be answered through utilising rheology to understand the reasoning for such behaviours. The application of rheology is extensively employed and is widely used on a day-to-day basis, commonly without recognition or realisation: Morrison (2004) reports how simply cooking, or having a bubble bath, allows for the influence of rheology to be experienced. Furthermore, to illustrate the extensive application, Morrison details how rheology is employed by geoscientists to study volcanism. Therefore, in order to more accurately define rheology, Johnson and Kevra (1989) discuss how the fundamental objective of rheology is to allow for the prediction of material behaviour upon the application of external forces.

Johnson further reports how (to assist with predicting behaviour) the motion for a deformable substance is derived from the fundamental equation:

$$\rho \left(\frac{dv}{dt} \right) = \rho g + \nabla \bullet T \qquad \textbf{[3.1]}$$

where ρ is the density, v is the velocity, t is time, g is acceleration due to gravity, and $\nabla \bullet T$ represents the internal stresses. For this equation, however, internal stresses must be defined, which is achieved through determining rheologically the relationship between stress and deformation or shear rate (rate of deformation):

$$\sigma = \eta \left(\frac{du}{dy} \right) \qquad \textbf{[3.2]}$$

where

$$\dot{\gamma} = \left(\frac{du}{dy} \right) \qquad \textbf{[3.3]}$$

In equations [3.2] and [3.3], σ is the shear stress, η is the viscosity and $\dot{\gamma}$ is equal to the shear rate, with equation [3.2] the fundamental equation developed by Newton.

Despite Newton's fundamental rheological equation for understanding the relationship between viscosity, shear stress and shear rate, the concept of rheology remains complex. This complexity exists due to the non-uniform behaviour of materials, particularly relating to the characteristic of viscoelasticity in which materials demonstrate properties of both a solid and liquid nature. Furthermore, such viscoelasticity is further complicated as the properties demonstrated by materials have the capacity to alter, depending on a range of influencing factors such as temperature and pressure applied. In order to assist with such difficulties, many equations and models have been developed (or simply applied to rheology in some instances) to facilitate the understanding of such behavioural trends, which include those set out next.

3.2.1 Hooke's Law

With Newton's work related to the behaviour of viscous fluids, it is important to identify methods for understanding the elasticity of materials. Hooke's Law [3.4] dictates that the stress applied to a material is linearly proportional to the strain, and demonstrates useful approximations for instances where relatively small deformations may be observed, i.e. where the measured deformation can be completely recovered. Thus we have

$$\sigma = E \gamma \qquad \textbf{[3.4]}$$

where σ is the stress, γ is the strain and E is the modulus of elasticity – which is a constant of proportionality (Gere and Goodno, 2009).

3.2.2 Maxwell, Kelvin–Voigt and Burger models

As Newton's and Hooke's equations address both elastic and viscous materials individually, a significant void within rheology, relating to the important viscoelastic materials, remains unfilled. This gap in knowledge was filled by models presented by Maxwell, Kelvin–Voigt and Burger, accounting for the behaviour of materials that exhibit both solid and liquid characteristics.

The model proposed by Maxwell uses a spring-and-dashpot system to describe the elastic and viscous aspects of materials, identifying these as two individual characteristics that are observed consecutively (the viscous characteristic following that of the elastic behaviour). Thus

$$\tau + \lambda \frac{d\tau}{dt} = \eta \dot{\gamma} \qquad \textbf{[3.5]}$$

where λ is the relaxation time, τ the shear stress, η is the viscosity and $\dot{\gamma}$ the shear rate (Macosko, 1994).

As an alternative, the Kelvin–Voigt model discusses the elastic and viscous characteristics functioning in parallel to one another (once again utilising the concept of the spring-and-dashpot system). As a result, the Kelvin–Voigt model assists with

addressing the viscoelasticity that is demonstrated by materials, as opposed to referring to elasticity and viscous behaviour as two individually operating characteristics. Here

$$\tau = G\gamma + \eta\dot{\gamma} \qquad \textbf{[3.6]}$$

where G is the spring modulus, γ the strain and $\dot{\gamma}$ the shear rate (and once more τ represents stress).

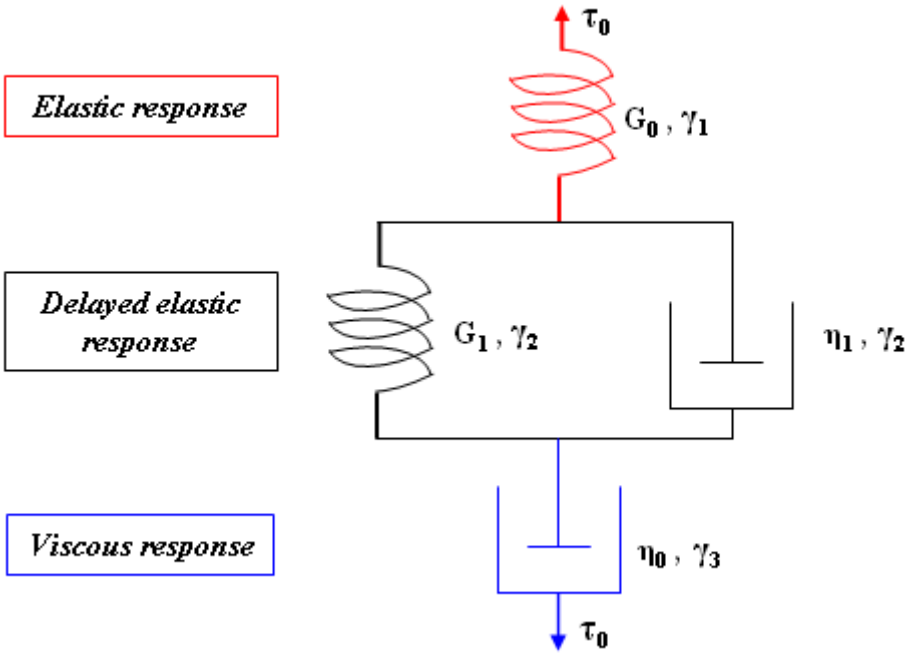

Figure 3.1: Representation of the Burger four-parameter model of viscoelasticity (Lee, 2006)

The Burger model – seen as a more complete model – combines the work by Kelvin–Voigt and Maxwell to emphasise how materials demonstrate instantaneous elastic behaviour, viscoelasticity and a continual viscous plateau (viscous response). This can be seen in the representative diagram as highlighted in Figure 3.1. Burger's formula is

$$\gamma(t) = \gamma_1 + \gamma_2 + \gamma_3 = \frac{\tau_0}{G_0} + \frac{\tau_0}{G_1}\left(1 - e^{\frac{-t}{\tau}}\right) + \frac{\tau_0}{\eta_0}t \qquad \textbf{[3.7]}$$

where the parameters in the equation (stated by Lee, 2006) are equal to those variables highlighted within Figure 3.1.

3.2.3 Cross model

The Cross model was developed to provide a valuable rheological tool for modelling the flow behaviour of materials, thereby contributing significantly to studies in the field. Those models previously discussed address both elastic and viscous materials and their viscoelastic response; it is therefore understandable that the Cross model is frequently used within rheological studies, as this concentrates on the importance of the flow behaviour (Cross, 1965).

$$\eta = \eta_{\infty} + \frac{\eta_0 - \eta_{\infty}}{1 + (K \dot{\gamma}^{n})} \qquad \textbf{[3.8]}$$

Where η_0 is the zero shear viscosity, η_{∞} is the infinite shear viscosity, $\dot{\gamma}$ is the shear rate, K is the Cross time constant and n is the Cross rate constant.

As seen from the four models discussed (Maxwell, Kelvin–Voigt, Burger and Cross), the science of rheology provides a valuable insight into the characteristic properties of materials. Consequently, rheology has become an invaluable tool within everyday life: from the study of solder paste rheology for mobile phone circuitry, to the study of ice cream rheology to ensure that the most pleasing texture is encountered; from understanding oil flowing through a car engine, to paint flowing after painting a bedroom. Typically, such materials are classified through the dependence of their viscosity response to an applied shear stress (σ) or shear rate ($\dot{\gamma}$) at both infinite and zero values. In order to understand such classifications, it is important to first gain an understanding of the basic terminology used in the field of rheology.

3.3 Common rheological terminology

3.3.1 Shear stress

Shear stress is commonly defined as the tortional force per unit area for the material, which is applied parallel to the surface (or face) and can be derived using the following equation:

$$\text{Shear stress } (\sigma) = \frac{\text{Force (F)}}{\text{Surface Area (A)}} \quad \textbf{[3.9]}$$

As the force is measured in newtons, and the surface area is measured in square metres, the unit of shear stress is the pascal (Pa).

3.3.2 Shear strain

The shear strain (often referred to simply as 'shear') is the ratio of resultant displacement to the sample height, identified when one face of the material is subjected to an applied stress that consequently results in either the top or bottom surface of the material sliding (or displacing) relative to the opposing surface. Due to this ratio involving two metrics of distance, the shear strain has no units. The shear strain can be calculated using the following equation:

$$\text{Shear strain } (\gamma) = \frac{\text{Deformation / Displacement } (\delta u)}{\text{Sample height (y)}} \quad \textbf{[3.10]}$$

3.3.3 Shear rate

Shear rate, as the name suggests, is defined as the rate of change in shear experienced by the sample. This can be obtained using equation [3.11] and is measured in reciprocal seconds (s^{-1}):

$$\text{Shear rate } (\dot{\gamma}) = \frac{\text{Shear strain } (\gamma)}{\text{Shear time (s)}} \quad \textbf{[3.11]}$$

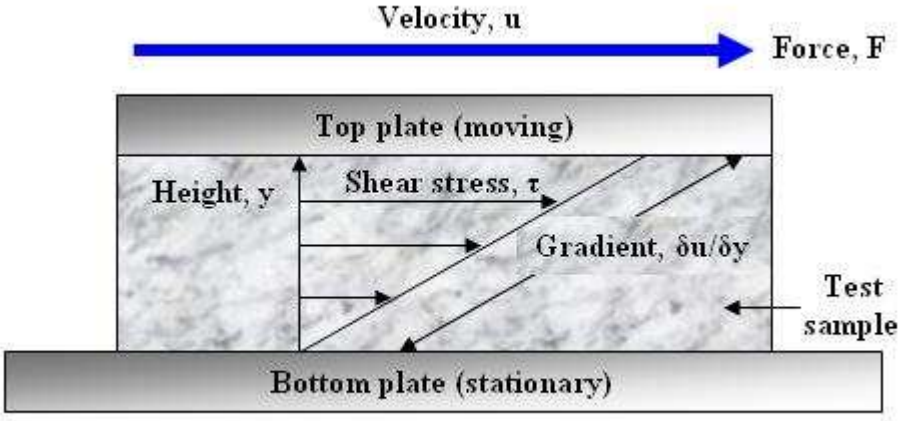

Figure 3.2: Illustration of typical flow behaviour (Mallik, 2009)

Sometimes, the shear rate is expressed as the ratio of the change in velocity (measured in metres per second) to the change in height (measured in metres) as shown in equation [3.12].

$$\text{Shear rate } (\dot{\gamma}) = \frac{\text{Change in velocity } (\delta u)}{\text{Change in height } (\delta y)} \qquad \textbf{[3.12]}$$

3.3.4 Viscosity

The viscosity of a material or fluid is defined as the internal resistance to flow exhibited upon application of a deforming force (such as an applied shear stress), and is often referred to as a measure of fluid friction. In the case of water; the viscosity is seen to be low, which indicates greater fluidity (that is, a considerable ease of movement). Furthermore, owing to the viscosity remaining constant regardless of the applied shear rate, water can be classified as a Newtonian fluid. Conversely, in the case of solder paste, the viscosity is seen to drop with increased shear rate, denoting a non-Newtonian fluid.

Typically, viscosity is calculated using equation [3.13]. As the shear stress operates with units of pascals (Pa) and shear rate with reciprocal seconds (s^{-1}), the viscosity of a material is measured using the units of the Pascal-second (Pa**.**s or simply Pas). And:

$$\text{Viscosity } (\eta) = \frac{\text{Shear stress } (\sigma)}{\text{Shear rate } (\dot{\gamma})} \quad \textbf{[3.13]}$$

Despite the common definition that viscosity is a material's resistance to flow; many variations of viscosity actually exist, where each has a specific definition of its own and, consequently, further equations exist to dictate the value of viscosity. Examples include:

- Apparent viscosity, which is the term given when the viscosity of a non-Newtonian material is calculated using the equations derived for Newtonian materials
- Dynamic viscosity, which is the ratio of the viscous modulus (G") with the angular frequency (ω)
- Kinematic viscosity, which is defined as the ratio of the dynamic viscosity (η') to the density of the fluid (ρ)
- Out-of-phase viscosity, which is calculated as the ratio of the elastic modulus (G') to the angular frequency (ω)
- Complex viscosity, which is calculated as the out-of-phase viscosity (η") subtracted from the dynamic viscosity (η').

3.3.5 Yield stress

Often cited as yield point, the yield stress is recognised as the applied stress required to initiate flow behaviour (or to allow the demonstration of viscous properties). Prior to reaching this yield stress, a material is said to behave with elastic deformation, where the removal of any stress will result in a return to its original structural properties – in other words, demonstrate a complete recovery from deformation. Once the yield point has been reached, however, the material is said to deform plastically, as some proportion of the deformation will become irreversible.

The derivation of yield stress is dependent on the method employed (as highlighted in Figure 3.3). In the case of a graphical plot of shear stress versus shear rate (graph

(A)), the yield stress is observed as the point at which the curve intersects the y-axis (shear stress). An alternative method, known as the stress growth method, is undertaken through applying a slow constant shear rate to the material and measuring the resultant stress as a function of time (graph **(B)**).

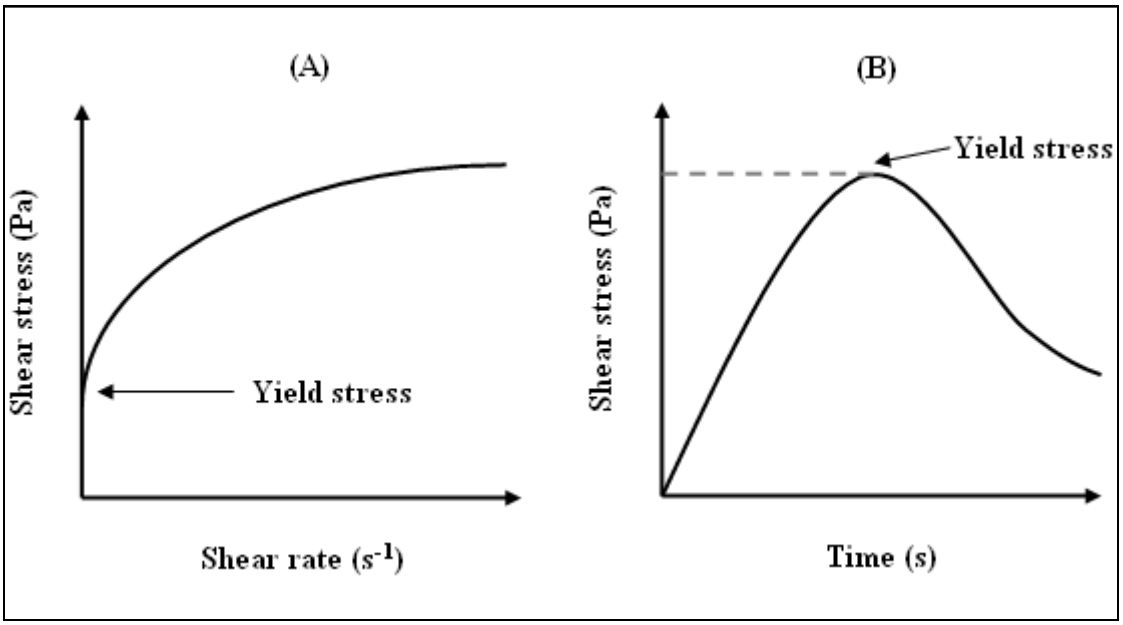

Figure 3.3: Representation of yield stress (Cunningham, 2010)

3.3.6 Storage and loss modulus

The storage modulus (also known as the elastic modulus or the modulus of elasticity) is a term that is used to describe the solid response of a material under an applied stress; similarly, the loss modulus (or viscous modulus, or modulus of viscosity) denotes the liquid response. Examining these properties therefore offers the possibility of identifying the stress at which the dominant solid characteristic is surpassed by the liquid characteristic (as is most frequently observed) – i.e. the point at which the material begins to exhibit a viscous nature. This can be observed in Figure 3.4, where G' initially displays the higher value, but G" exhibits a higher value once a specific value for applied stress is reached, consequently leading the material to demonstrate a tendency towards dominant viscous behaviour.

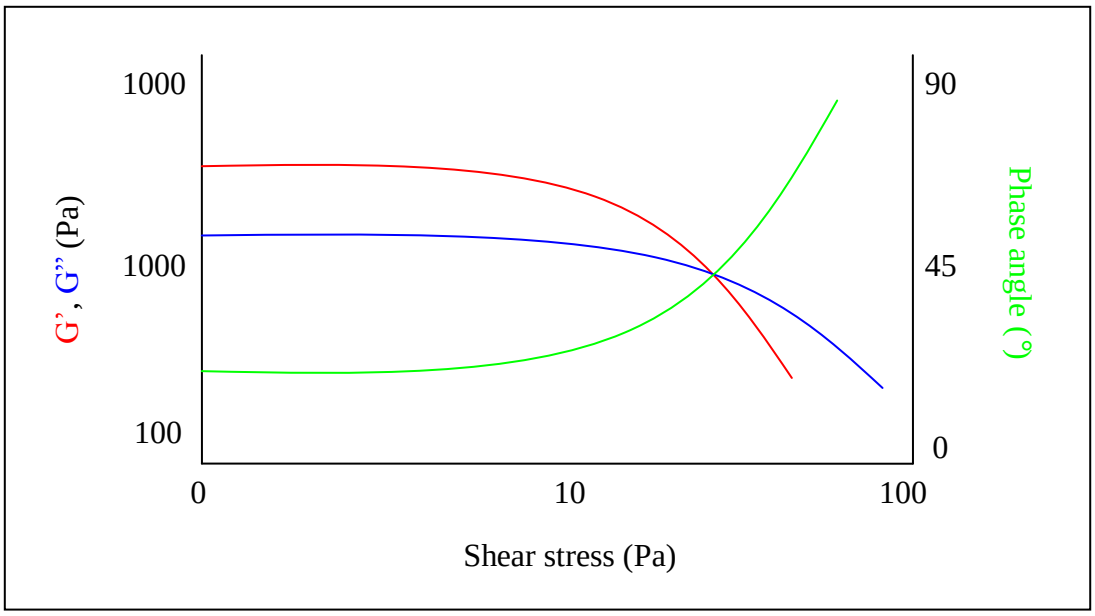

Figure 3.4: Representation of oscillatory amplitude sweep investigation into storage and loss modulus

From Figure 3.4 it is also possible to identify the phase angle of the material at a given stress. The phase angle (which is discussed in section 3.3.7) provides an indication as to the flow behaviour of the material, and can be seen to increase proportionally to the convergence of the storage modulus with the loss modulus.

Furthermore, through studying the storage and loss modulus of a material it is possible for a determination of the linear viscoelastic region (LVR) to be made. During oscillatory testing, this property can be identified as the point at which the linear plateau ceases and the value for the storage modulus begins to drop significantly (in Figure 3.4 this is approximately 10 Pa). Therefore, the storage modulus can indicate which values of stress can be applied to a sample to avoid permanent structural deformation. Additional investigations commonly performed – relating to the storage and loss modulus – involve frequency in an attempt to address the time-dependent behaviour of materials (see Figure 3.5). The importance of such an investigation lies with the ability to establish whether a material will behave elastically or viscously for both long and short timescales (where a stress is applied rapidly or over a long period of time as demonstrated within figure 3.11).

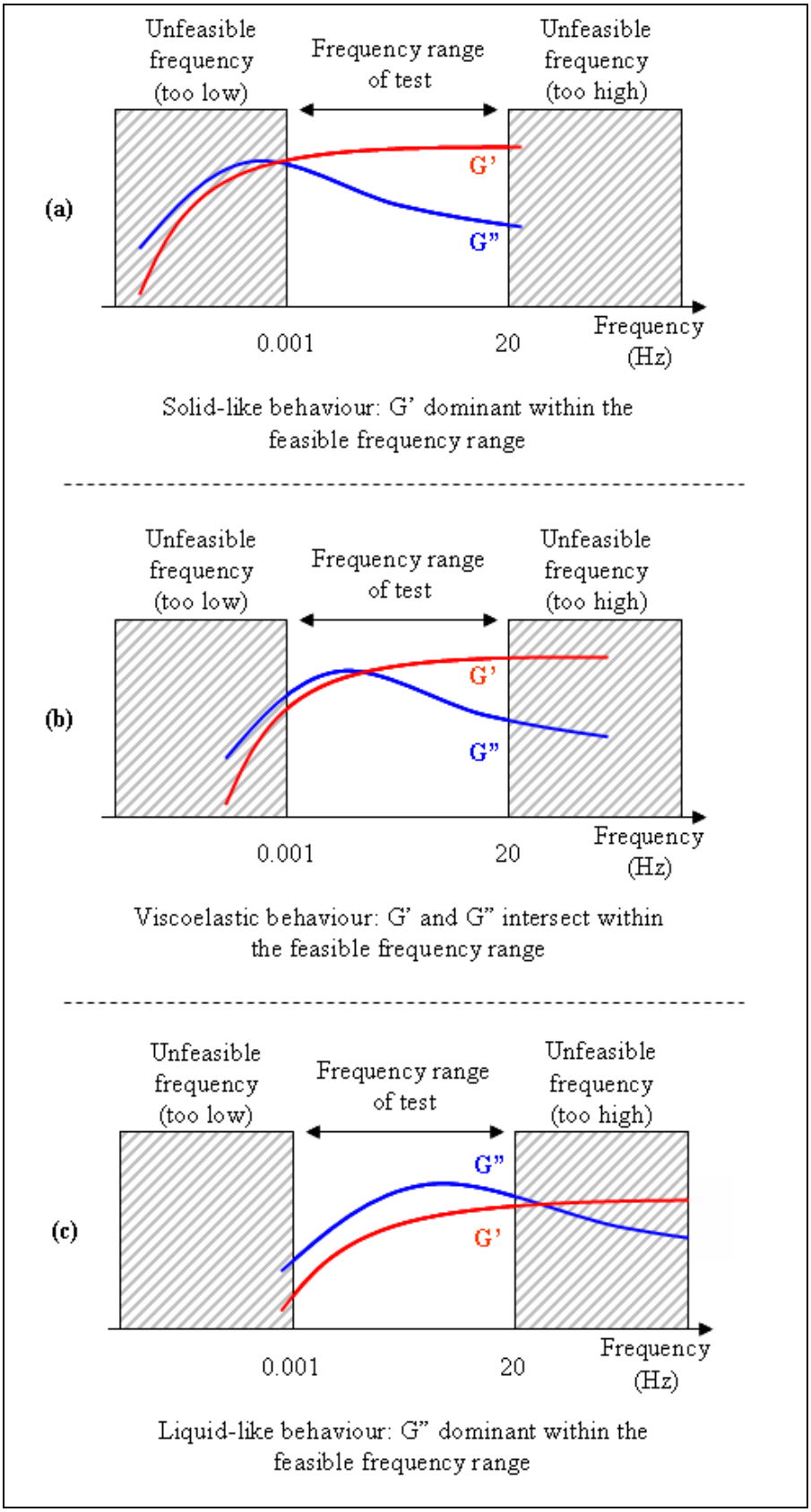

Figure 3.5: Examples of storage and loss modulus for various materials: (a) solid-like; (b) viscoelastic; (c) liquid-like. (Cunningham, 2007)

3.3.7 Phase angle

The phase angle is measured by applying to the sample a stress with a continuously changing value (following the equation of a sine wave), whilst recording the strain response to indicate the phase property. The phase shift of the sinusoidal wave indicates this nature of the material, with a value of 90° representing purely viscous flow and a value of 0° indicating purely elastic behaviour (see Figure 3.6).

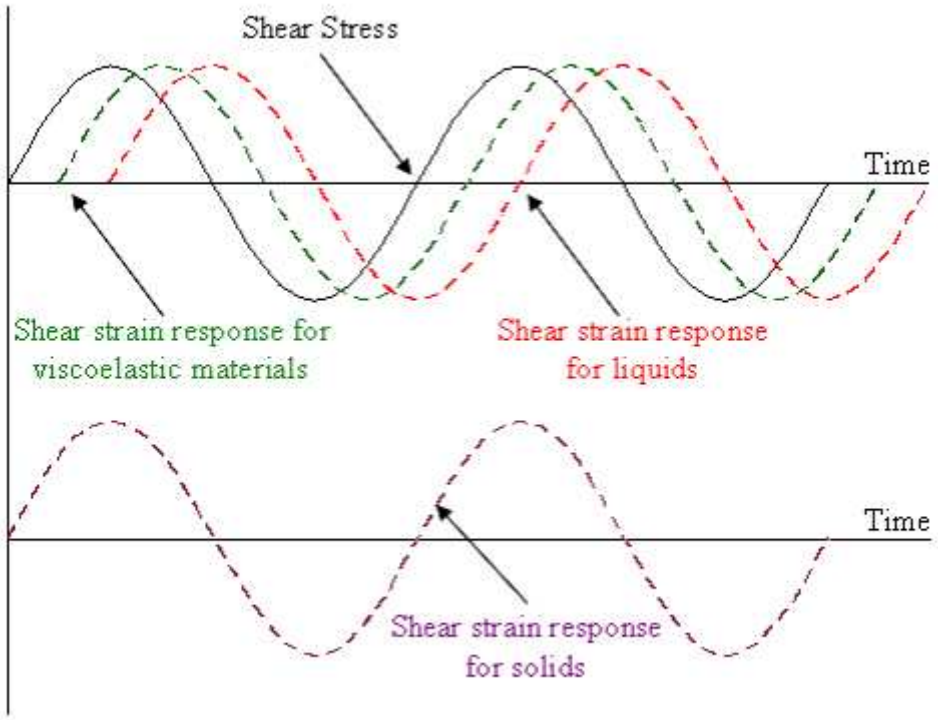

Figure 3.6: Graphical representation of phase angle measurements for varying materials

For those materials that demonstrate viscoelastic properties, determining the phase angle provides a valuable insight into flow behaviour for a given stress, because it highlights the relationship between applied stress and movement towards an elastic or viscous behaviour. In other words, determining whether a material is purely solid or liquid can be achieved with relative ease; in the case of viscoelastic materials, this is

not so simple but the phase angle nevertheless provides a numerical indication of which property of the material is the more dominant.

In order to derive the value of the phase angle (δ), equations [3.14] and [3.15] are commonly installed within rheometer software for calculation, with equation [3.16] providing an alternative to equation [3.15]. We have

$$\textit{tan}\ \delta\ \text{(Phase angle)} = \left(\frac{G''\ \text{(Loss modulus)}}{G'\ \text{(Storage modulus)}} \right) \qquad \textbf{[3.14]}$$

and

$$G'\ \text{(Storage modulus)} = G^*\ \text{(Complex modulus)}\ \textit{Cos}\ \delta\ \text{(Phase angle)} \qquad \textbf{[3.15]}$$

Alternatively:

$$G''\ \text{(Loss modulus)} = G^*\ \text{(Complex modulus)}\ \textit{Sin}\ \delta\ \text{(Phase angle)} \qquad \textbf{[3.16]}$$

where the complex modulus (G^*) is given by

$$G^*\ \text{(Complex modulus)} = \left(\frac{\sigma_0\ \text{(Shear stress)}}{\gamma_0\ \text{(Shear strain)}} \right) \qquad \textbf{[3.17]}$$

Through utilising equations [3.14] through [3.17], it can therefore be deduced that:

$$\textit{Cos}\ \delta\ \text{(Phase angle)} = G'\ \text{(Storage modulus)} \left(\frac{\gamma_0\ \text{(Shear strain)}}{\sigma_0\ \text{(Shear stress)}} \right) \qquad \textbf{[3.18]}$$

or, as an alternative to [3.18]:

$$\textit{Sin}\ \delta\ \text{(Phase angle)} = G''\ \text{(Loss modulus)} \left(\frac{\gamma_0\ \text{(Shear strain)}}{\sigma_0\ \text{(Shear stress)}} \right) \qquad \textbf{[3.19]}$$

3.4 Types of materials

The actual classification 'label' for materials can be said to be dependent on its flow behaviour, with common practices now existing where control of this characteristic is undertaken in order to fit the desired application. The importance of this element of control can be particularly seen with those materials where a high viscosity is required to resist flow generated by minor forces (such as those attributed to gravitational influences), whilst additionally exhibiting a reduced viscosity for instances where an excessive force is necessary for the function (such as brushing or pouring). Consequently, non-Newtonian properties are highly important, as these demonstrate a variation in viscosity that is dependent on the force applied to the material (Barnes, 2000). This manipulation of material properties presents valuable opportunities to maximise the efficiency of the application, for example by ensuring low viscosities whilst undertaking spraying processes (see Figure 3.7).

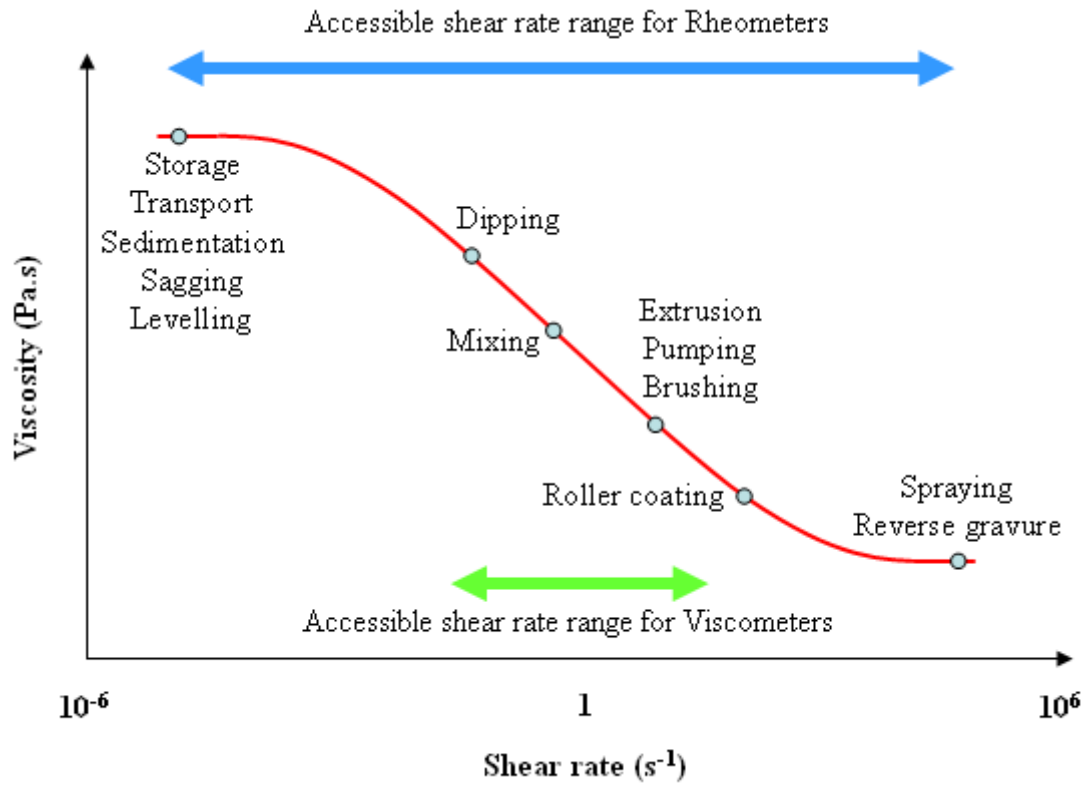

Figure 3.7: Example of viscosity requirements for varied applications (Malvern Instruments, 2004)

This necessity for controlling properties can also be seen to influence the field of solder paste rheology, with the print definition, paste life on the stencil, dispensing ability and consistency of coverage all properties that can be identified as dependent on rheological nature. Therefore, adaptation of paste materials must occur to ensure that processes are performed efficiently and to an optimal standard (Johnson and Kevra, 1989).

Malvern Instruments (2004) further emphasises the importance of controlling the properties of materials, demonstrating the contrast in behaviour of paint sample performance due to sensitivity of the materials to an applied stress (see Figure 3.8).

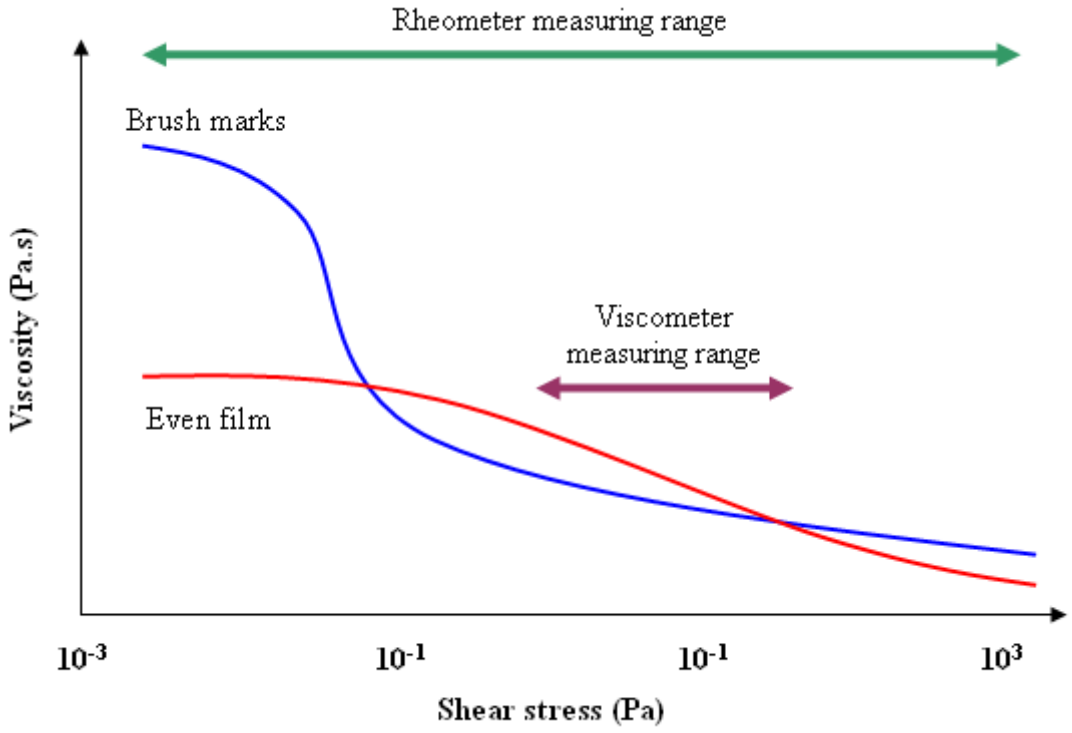

Figure 3.8: Example of variation in process performance with increased stress (Malvern Instruments, 2004)

Figures 3.7 and 3.8 clearly illustrate the importance of the relationship between viscosity and shear stress/shear rate, and as such it is essential to understand the aforementioned material classifications. Typically, materials fall into one of two categories, Newtonian and non-Newtonian, which can be further sub-categorised

depending on the nature of viscosity with increasing shear, and the yield stress (see Figures 3.9 and 3.10). The two main categories are further discussed below.

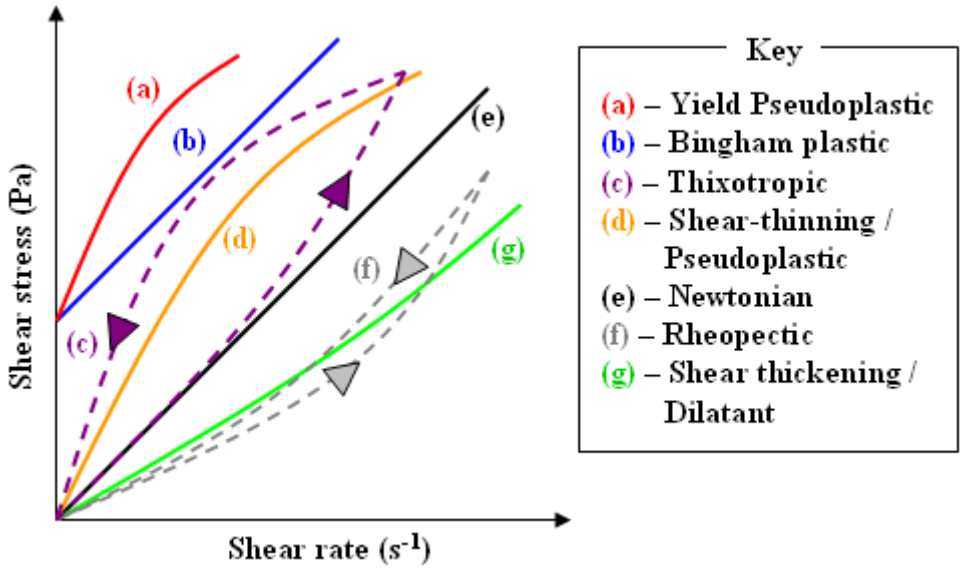

Figure 3.9: Variations in fluid flow behaviour (Lieberman and Lieberman, 2008)

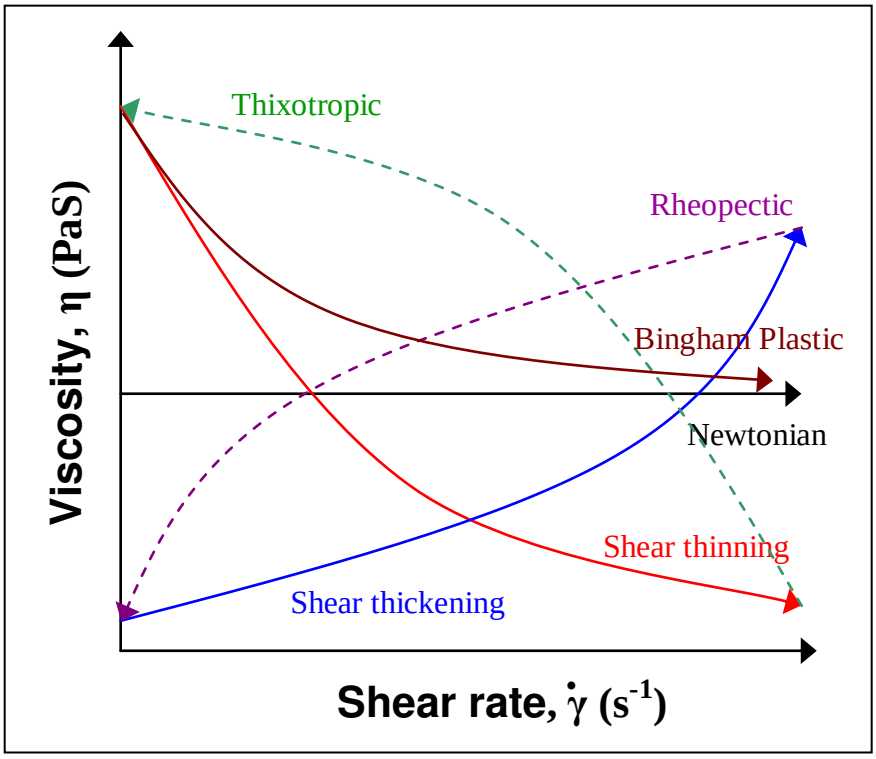

Figure 3.10: Viscosity behaviour of different materials

3.4.1 Newtonian materials

A Newtonian fluid can be described as a material that under a consistent temperature and pressure demonstrates both a constant viscosity and constant ratio of shear rate to shear stress regardless of flow behaviour (Lieberman and Lieberman, 2008). This is an important attribute, as the distinctive quality of Newtonian materials is that of demonstrating a constant viscosity regardless of shear rate applied (as can be seen within Figure 3.10), with commonplace examples being water and honey.

In order to understand Newtonian materials, equation [3.20] expresses the expected behaviour of such materials:

$$\tau = \mu \frac{du}{dy} \qquad \textbf{[3.20]}$$

where τ is equal to the stress (usually denoted σ), μ is the viscosity (usually denoted η) and du/dy is the velocity gradient, otherwise known as shear rate ($\dot{\gamma}$).

3.4.2 Non-Newtonian materials

Non-Newtonian materials are those that demonstrate a viscosity that is dependent on shear rate (regardless of maintaining a constant temperature and pressure), with commonplace examples including toothpaste and paints. In the case of toothpaste, the viscosity is required to drop on application of shear to ensure the paste can leave the tube; however, once this applied shear has been removed, the toothpaste is required to return to a state of high viscosity to ensure that it remains on the toothbrush without simply flowing away. In general, paints demonstrate an important response to shear, allowing a low viscosity at high shear rates to ensure the paint can be spread on surfaces. Conversely, at low shear rates the paint retains a high viscosity to avoid dripping (flowing) from the surface (see Figure 3.8).

Aside from this response to variation in shear, non-Newtonian materials may also exhibit time-dependent behaviour. Putty-like materials noticeably demonstrate this

characteristic of time-dependence, allowing for properties of both solid and liquid behaviour to be displayed: Upon putty being moulded into a spherical ball, the material demonstrates an apparent ability to retain this form permanently. However, upon allowing the material to remain in a state of rest it can be observed that sagging occurs over extended periods of time as a result of the weight of the putty. Furthermore, despite behaving like a highly viscous fluid over long time intervals, putty demonstrates viscoelastic behaviour with an applied stress over shorter timescales, allowing for the material to bounce; moreover, it behaves like a solid over particularly short timeframes, shattering upon the application of high stress (Cambridge Polymer Group, 2002).

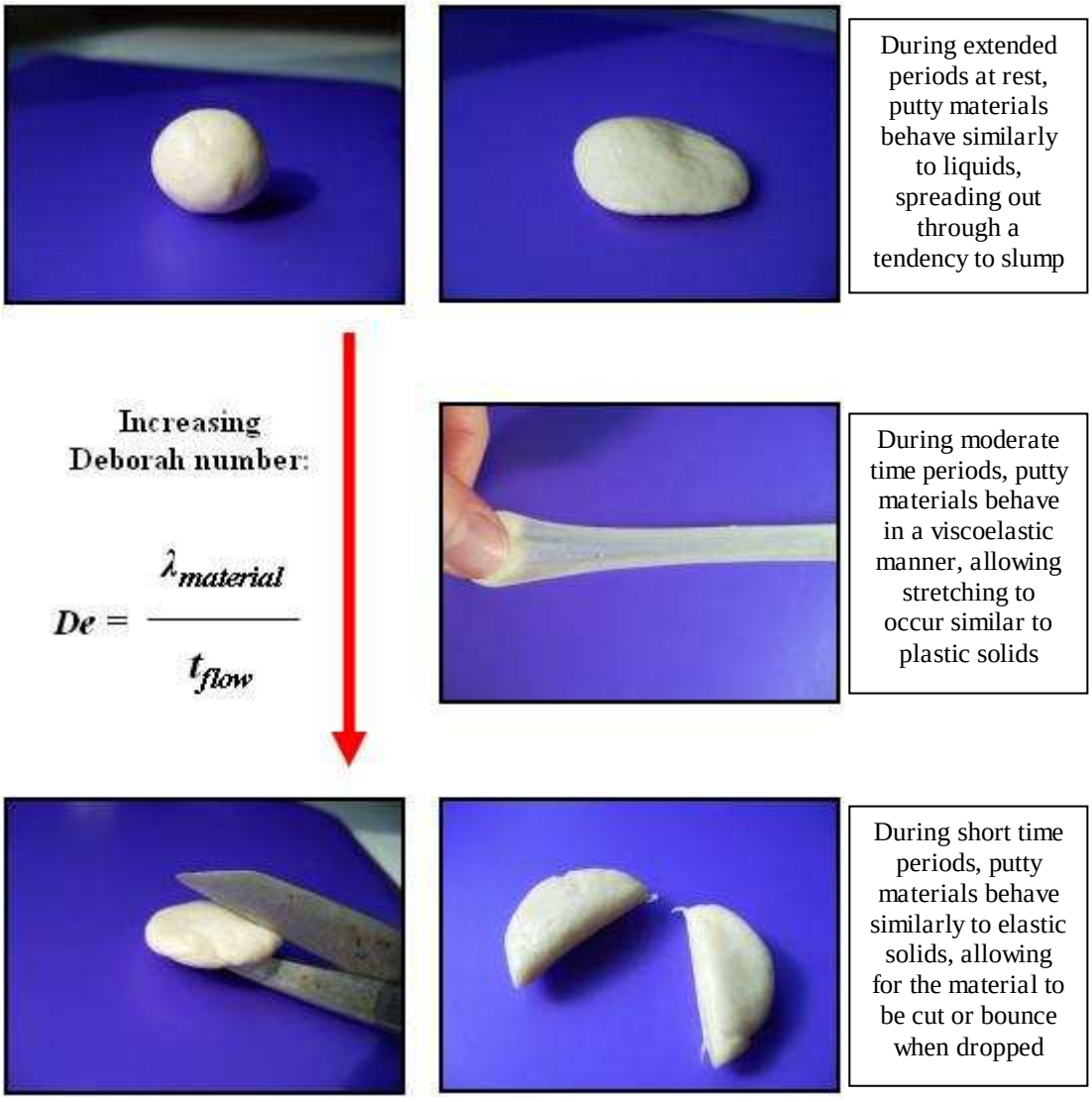

Figure 3.11: Non-Newtonian behaviour of putty (Cambridge Polymer Group, 2002)

Due to the possible influence of time-dependence and the many responses that can be exhibited upon increased shear rate/shear stress, it is often insufficient simply to classify a material as being non-Newtonian; consequently, several sub-category terms exist for such materials which assist with identification, and these are described next.

3.4.2.1 Bingham plastics

Bingham plastics (as highlighted in Figure 3.10) are defined by an infinite viscosity until a sufficient stress is applied to the material to initiate viscous behaviour. Once this stress is attained, the material demonstrates a linear flow curve, which signifies that the shear stress is directly proportional to the shear rate. Bingham plastics are typically denoted by the following equation:

$$\sigma = \sigma_y + \eta \dot{\gamma} \qquad \textbf{[3.21]}$$

where σ is the shear stress, σ_y is the limiting stress (or the yield stress), η is viscosity and $\dot{\gamma}$ is the shear rate. It follows from this equation that:

$$\dot{\gamma} = 0 \qquad \text{where } \sigma < \sigma_y \qquad \textbf{[3.22]}$$

and

$$\dot{\gamma} = \frac{(\sigma - \sigma_y)}{\eta} \qquad \text{where } \sigma \geq \sigma_y \qquad \textbf{[3.23]}$$

A typical example used to illustrate the concept of a Bingham plastic is that of toothpaste, where a particular stress is required to initiate flow and force the paste from the tube. Aside from the example of toothpaste, the suggestion of a Bingham plastic has been highly valuable in the approximation of fluids such as paints, slurries, plastics and solid–liquid dispersions (i.e. minute solids suspended in liquids) such as clay–water suspensions (Hughes and Brighton, 1999).

3.4.2.2 Yield pseudoplastics and yield dilatants

Yield pseudoplastics and yield dilatants (also termed non-linear viscoplastics) are those shear-thickening and shear-thinning materials that exhibit dependence on yield stresses (such as those associated with Bingham plastics). Despite both demonstrating a reliance on yield stress, the variation that exists between non-linear viscoplastics and Bingham materials is the lack of direct proportionality between the shear stress and shear rate on the resultant flow curve (for non-linear viscoplastics).

The Casson model (as seen in equations [3.24] and [3.25]) was developed as a method for theoretically estimating the shear-thinning behaviour and yield stress of fluid suspensions (Galdi et al, 2008); however, with yield pseudoplastics and yield dilatant materials the flow curves are generally described through the use of the Herschel–Bulkley model (shown in equation [3.26]). Thus we have

$$\sigma^{0.5} = \sigma_y^{0.5} + k(\dot{\gamma})^{0.5} \quad \textbf{[3.24]}$$

which is sometimes denoted as

$$\sqrt{\sigma} = \sqrt{\sigma_y} + k\sqrt{(\dot{\gamma})} \quad \textbf{[3.25]}$$

We also have

$$\sigma = \sigma_y + k(\dot{\gamma})^n \quad \textbf{[3.26]}$$

In these three equations, σ is the shear stress, σ_y is the limiting stress (or the yield stress), $\dot{\gamma}$ is the shear rate, k represents the slope of the flow curve for the plot of $\sqrt{\sigma}$ against $\sqrt{\dot{\gamma}}$, and n depicts the flow behaviour index, or the level of deviation from Newtonian behaviour (Rao, 2007; Mallik, 2009; Seman, 2010). Using the Herschel–Bulkley model, it is possible to gain an understanding as to the classification of the material; for instance, a value that is equal to 1 indicates that the material behaves as a Bingham plastic, while values less than 1 and greater than 1 point towards yield pseudoplastic and dilatant materials respectively.

3.4.2.3 Thixotropic and rheopectic materials

Thixotropy is the time-dependent behaviour associated with shear-thinning materials, whereas rheopexy is defined as the time-dependency connected with shear-thickening behaviour.

A material is said to behave in a shear-thinning manner when demonstrating a reduction in viscosity with an application of shear. However, in order to be classified as thixotropic, the material must demonstrate a recovery of viscosity to its original value after the conclusion of flow generated by a constant shear, therefore demonstrating a time-dependent viscosity. Boyes (2008) further elucidates this, reporting how thixotropy is demonstrated by materials that exhibit significant reductions in viscosity over time whilst subjected to a constant rate of shear. The material then continues to gradually return to the viscosity initially recorded following the conclusion of an applied shear. Thixotropic materials can be fairly commonplace, with typical examples including mayonnaise and solder paste.

Where thixotropic fluids demonstrate a decrease in viscosity with a constant shear applied, rheopectic materials display the reverse trend of increased viscosity with a constant shear applied. As with their counterpart, however, rheopectic fluids demonstrate a return towards the initial viscosity following the removal of shear, once more demonstrating the time-dependent behaviour that distinguishes between these materials and the dilatant classification. Rheopectic fluids are uncommon; even so, typical examples may include some printer inks and gypsum suspensions.

In order to characterise thixotropic or rheopectic behaviour, the hysteresis loop method is commonly employed (see Figure 3.12), where a plot of shear stress against shear rate is produced; the area inside the curve represents either a thixotropic breakdown or a rheopectic build-up of the material (Braun and Rosen, 2000). If the area within the curve is significantly large, a highly thixotropic/rheopectic material is represented. Alternatively, a seemingly absent area represents either non-thixotropic/rheopectic behaviour or an insufficient period for recovery, resulting in a failure to rebuild structure (Kelessidis, 2008).

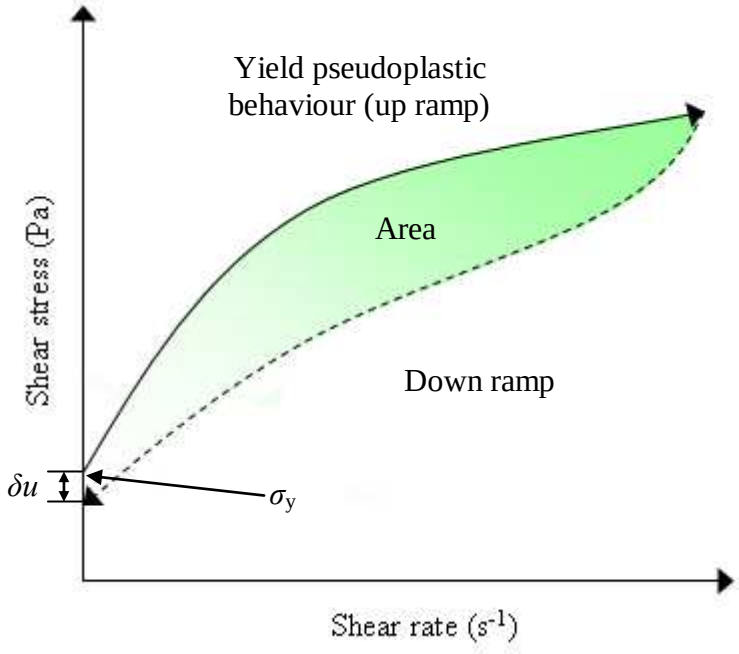

Figure 3.12: Example of a hysteresis loop for a thixotropic material

In Figure 3.12, δu represents the permanent deformation of the material, distinguished by an inability to return to the initial stress, and σ_y represents the yield stress required to initiate flow behaviour.

Further to assessment of thixotropy through the use of a hysteresis loop, the thixotropic index can be calculated, allowing for assessment of a material's properties to be made. Depending on the source, this can be conducted in various ways, with differing outcomes of analysis. Using equation [3.27], where stress is taken at a shear rate of $0.01s^{-1}$ (Braun and Rosen, 2000; Remington, 2005), the thixotropic index determines the level of breakdown observed, with a value of 1 indicating complete recovery and increased breakdown observed as the thixotropic index increases.

$$\textbf{Thixotropic index (TI)} = \frac{\sigma_{0.01}\ \textbf{(Stress before shearing)}}{\sigma_{0.01}\ \textbf{(Stress after shearing)}} \qquad \textbf{[3.27]}$$

A common alternative to this method states that the thixotropic index is calculated through equating a ratio of two viscosities that are measured at speeds with a relationship of 1:10 rpm (Licari and Swanson, 2005). Emerson and Cuming (2000) further discuss this technique, confirming the shear rates of 1 rpm and 10 rpm and reporting how dividing the viscosity value for the upper rpm by that for the lower rpm defines the thixotropic index. Standard values are measured between 1 and 5, which correspond to high flow and low flow respectively. However, the fundamental concern with this method – suggested by both sets of authors mentioned in this paragraph – is the measurement of time-independent non-Newtonian behaviour by the ratio. As discussed previously, thixotropy is time-dependent.

3.4.2.4 Shear-thickening (dilatant) materials

Shear-thickening (or dilatant) materials are, as the name suggests, those materials that demonstrate an increase in viscosity, or a thickening, with an increase in the applied shear rate. These types of materials tend to be classified as fairly uncommon, with examples being suspensions of cornflour in water, and china clay. The flow behaviour of dilatants may be represented by the power law model, known as the Ostwald and de Waale model (equation [3.28]), in which η_{app} is the apparent viscosity, K is the flow consistency index, the ratio of δu to δy is representative of shear rate, n is the flow behaviour index, and σ is the stress applied to the material. Thus:

$$\eta_{app} = K \left(\frac{\delta u}{\delta y} \right)^{n-1} \quad \textbf{[3.28]}$$

This is often related to the equation:

$$\sigma = K \left(\frac{\delta u}{\delta y} \right)^{n} \quad \textbf{[3.29]}$$

It should, however, be noted that these models are commonly applied to generalised Newtonian materials; but as dilatants are non-Newtonian, the equations are merely approximations of behaviour. Using the models, a value greater than 1 for the flow

behaviour index (n) represents shear-thickening behaviour (Chhabra and Richardson, 1999), a value less than 1 represents shear-thinning behaviour and a value of exactly 1 represents Newtonian behaviour.

A suspension of cornflour in water is a typical example of the nature of shear-thickening materials. At low shear rates, the water acts as a lubricating fluid for the suspension, which defines the relatively low viscosity. As the shear is increased, the water from the mixture begins to separate away from the cornflour molecules (seemingly being squeezed out), which allows for greater interaction between the molecules. This interaction consequently leads to an increase in frictional forces between the molecules, which increase the observed viscosity.

3.4.2.5 Shear–thinning (pseudoplastic) materials

Pseudoplastics, or shear-thinning materials, are the most commonly observed form of non-Newtonian fluids and are characterised by three identifiable stages: (1) a constant viscosity at very low or zero shear; (2) a seemingly constant viscosity at very high or infinite shear; and (3) decreasing viscosity with intermediate shear rates (Boger, 1977). This trend can be identified within Figure 3.13.

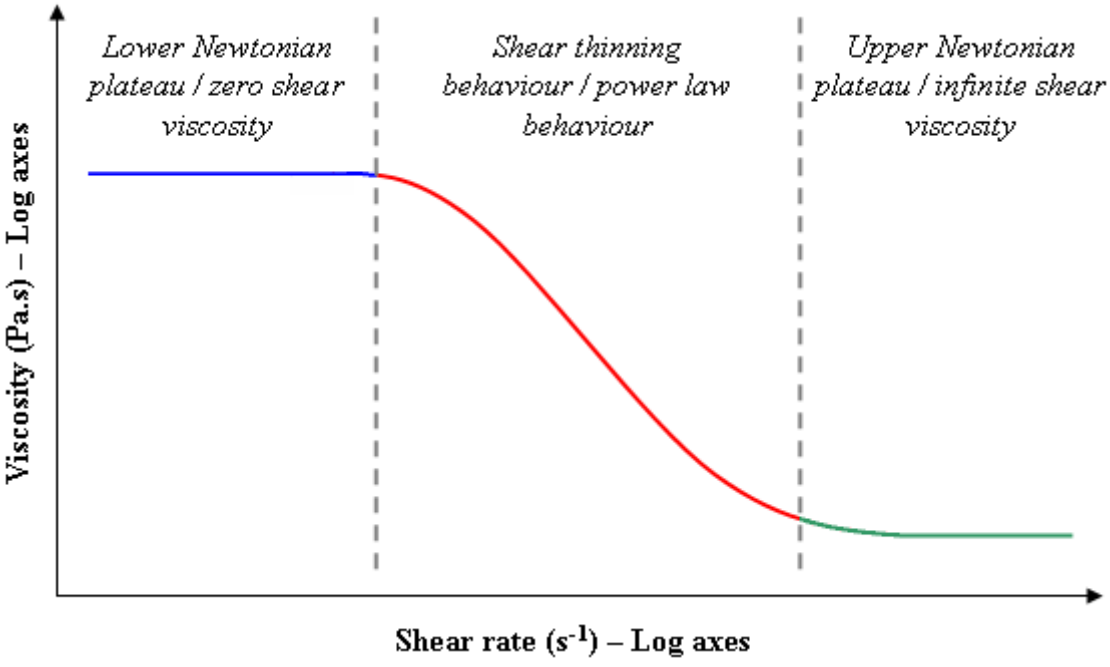

Figure 3.13: Ideal viscosity profile for pseudoplastic behaviour (Cunningham, 2007)

As with shear-thickening materials, the flow behaviour of pseudoplastics may be approximated through the use of the power law model proposed by Ostwald and de Waale (Osswald, 1998). Johnson and Kevra (1989) also confirm that the Ostwald and de Waale model may be used to approximate flow behaviour; however, those authors noted that pseudoplastics may also be modelled using the following:

- The Herschel–Bulkley model: (see equation [3.26])
- The Casson model (see equations [3.24] and [3.25])
- The Eyring model, given by:

$$\tau = \left(\frac{\dot{\gamma}}{B}\right) + C \sin\left(\frac{\tau}{A}\right) \qquad \textbf{[3.30]}$$

- The Williamson model, given by:

$$\tau = \left(\frac{A\dot{\gamma}}{B+\dot{\gamma}}\right) + \eta_{\infty}\dot{\gamma} \qquad \textbf{[3.31]}$$

In equations [3.30] and [3.31], τ represents the stress, $\dot{\gamma}$ the shear rate, η_{∞} the viscosity at infinite shear, and A, B, and C are all constants that are determined from a best fit of the data (Johnson and Kevra, 1989).

Shear thinning occurs as a result of the alignment process of the polymer chains in the solution reducing the material's resistance to flow. This occurrence has been reported by Remington (2005), where shear thinning is said to arise from alignment of the macromolecules and a reduction in the degree of entanglement between them. The applied shear causes these randomly coiled and entangled macromolecules to break free from each another, consequently leading to alignment with the direction of flow. Once a virtually uncoiled form is attained thereafter, less resistance is offered when compared with the initial entangled shape. As viscosity is a material's resistance to flow, it follows that this reduction in resistance therefore signifies a reduction in viscosity (see Figure 3.14).

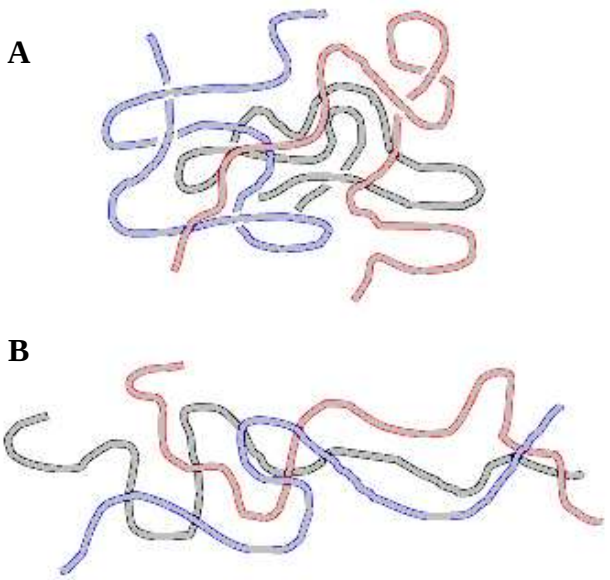

Figure 3.14: Example of three randomly coiled polymer chains during shear thinning: (A) at rest; (B) on applied shear. (Remington, 2005)

Blood, paint and ketchup are all commonplace examples of shear-thinning materials, as is solder paste. However, although the rheological properties of solder pastes demonstrate a shear-thinning nature, many influences (such as metal content) can significantly influence the level of shear thinning exhibited. As such, a greater level of complexity exists with pastes.

3.5 Solder pastes

Much of the complexity found with solder paste materials can be attributed to the flux composition, which is composed of several constituents such as activators, solvents and rheological additives (discussed further in section 3.9.1). Consequently, primary complexities arise from the formulation process, where the choice of activator is dependent on both the nature of contamination to be removed and the surface of the material to be soldered. Common examples include halides, organic acids and amines, which are effective for use against copper oxides, tin oxides and silver surfaces respectively (Pecht, 1993). As the role of the activators is to provide chemical fluxing in an attempt to remove oxides, this itself creates difficulties (with ensuring oxide removal); however, additional complexities are then highlighted as the formulation must (i) efficiently prevent re-oxidation (after oxide removal), (ii) remove any

residues and (iii) dictate the flow properties of the solder paste to ensure that the assembly process can be completed to an acceptable standard.

Flux, despite clearly influencing the complexity of solder paste, is but one variable that contributes to the intricate nature of paste rheology; thus in order to appropriately select a paste material, the other variables must be considered. In his work, Pecht (1993) noted those properties and parameters that must be considered to make an appropriate selection of paste material for the desired application. These include:

i) Alloy powder
ii) Flux
iii) Particle shape
iv) Particle size
v) Flow rate
vi) Apparent density
vii) Oxide content
viii) Activity
ix) Corrosivity
x) Cleanability
xi) Metal content
xii) Rheology
xiii) Viscosity
xiv) Solder slump
xv) Tackiness
xvi) Solvent volatility
xvii) Thermal stability

The work reported by Pecht (1993) underlines the complexity that exists with solder paste and, as such, appropriate selection of paste material requires significant research (particularly as the variables detailed by Pecht do not constitute a definitive list).

Many companies provide guidelines regarding how to select an appropriate solder paste for specific applications, and emphasise those considerations that are necessary beforehand. Nordson EFD (2007) is one such example, noting how the selection process plays an important role in determining the acceptability of the assembly and minimising those problems related to joint quality. The selection process is then detailed as a three-step procedure consisting of:

1. Alloy selection: including the metal content itself, the melting temperature of the alloy (Table 3.2) and the solder powder PSD as examples of subdivisions
2. Flux selection
3. Required flux characteristics.

	Alloy	Solidus (°C)	Liquidus (°C)	Tensile Strength (PSI)
Pb-Free Alloys	Sn42 Bi58	-E-	138	8000
	Sn96.3 Ag3.7	-E-	221	8900
	Sn100	MP	232	1800
	Sn86.5 Ag3.0 Cu0.5	217	219	8900
	Sn95 Ag5	221	245	10100
	Sn95 Sb5	232	240	5900
	Sn89 Sb10.5 Cu0.5	242	262	12000
Pb-Based Alloys	Sn63 Pb37	-E-	183	6700
	Sn43 Pb43 Bi14	144	163	6120
	Sn62 Pb36 Ag2	179	189	6700
	Sn60 Pb40	183	191	6200
	Sn10 Pb88 Ag2	268	290	4900
	Sn10 Pb90	275	302	4600
	Sn5 Pb92.5 Ag2.5	287	296	4210
	Sn5 Pb95	308	312	4190

Table 3.2: Example of various Pb-free and Pb-based solder alloys available (Nordson EFD, 2007)

The RoHS directive of 2006 made the selection process slightly easier by reducing the number of solder pastes available (as Pb alloy formulations became redundant). However, as previously mentioned, attempting to find an alternative to the Sn–Pb alloy has created its own problems. One such example, the Sn–Ag–Cu alloy, demonstrates a higher cost when compared with Sn–Cu; however, the superior performance in terms of wettability, dross formation and reliability under typical load conditions make it both more desirable and the closest matching alternative to Sn–Pb.

3.5.1 Variations between Pb and Pb-free pastes

The variations in density observed between the Sn–Pb and Pb-free alloys necessitate a differentiation in the metal loading of the solder paste (Shangguan, 2005). This is discussed in work by Bath (2007), in which it is explained that achieving good printability depends heavily on the metal-to-binder volume ratio, with the flux accounting for approximately 50% of the solder paste by volume. Bath (2007) also reported how the drop in density observed with a switch to Pb-free (in the region of 8.4 gm/cc) results in a slight reduction in metal content (from approximately 90% to 88%) in an attempt to maintain the metal-to-flux binder ratio.

With the reduction in metal content linked with a switch to Pb-free solders, it would be expected that a reduction in aperture clogging and an increase in slump should follow – due to the decrease in the concentration of solids during paste formulation. Puttlitz and Stalter (2004) underline this, reporting how the extent of slumping has been seen to be dependent on the percentage of metal content employed within a solder paste. However, work by Shangguan (2005) reported that there is no obvious or consistent variation between Pb and Pb-free in terms of printability, slumping, solder balling and tack, as the performance is not seen to be directly dependent on the solder alloy. This has been substantiated in the work by Puttlitz and Stalter (2004), who state that, in terms of printability (the ability of a paste to form well-defined deposits without slumping, spreading or bridging), Pb-free pastes behave similarly to eutectic Sn–Pb, with comparable deposition shape and volume, print quality and stencil release. Furthermore, paste roll was found to be visually identical between the two.

Additionally, work by AIM (2003) reports how differences in the printing of Pb and Pb-free pastes are negligible, and consequently factors such as paste stencil life, print definition, aperture release, high-speed printing capabilities and repeat printability should demonstrate a similar performance to Sn–Pb alloys. This is confirmed by Bath (2007), who identified that Sn–Ag–Cu pastes exhibit near-identical performance to Pb solders from the point-of-view of print definition, print consistency and stencil life.

Regardless of the similarity from a printing viewpoint, one significant variation between Pb and Pb-free pastes can be seen from the melting temperature of the alloy

(as highlighted in Table 3.2). The importance of this can be seen on two levels: first, the elevated soldering temperature needed for Pb-free pastes will require greater stability of the flux; and, secondly, the elevated temperature during reflow requires the threshold temperature for components to be raised.

The similarity in printing performance between Sn–Pb and Pb-free solders is clearly beneficial for the electronics manufacturing industry; however, the selection process continues to maintain its complexity. As previously mentioned, much of this complexity is due to the flux selection (which dictates the flow properties of the solder paste), with interactions between the flux and factors such as PSD influencing selection. It is therefore essential to gain an appropriate knowledge of the flux types available prior to selecting a paste.

3.6 Flux types

Typically, flux is divided into five groups:

1. **R** (Rosin): composed of rosin and solvent. These demonstrate low levels of chemical activity, and as such are primarily used for those instances where the surfaces are both clean and simple to solder.
2. **RMA** (Rosin or Resin mildly activated): like the rosin flux, this is composed of rosin and solvent; however, it also contains a small amount of activator.
3. **RA** (Rosin/Resin activated): this once more contains both rosin and solvent; however, rosin activated fluxes contain aggressive activators. Owing to these aggressive activators, it is possible to employ rosin activated flux with highly oxidised surfaces.
4. **NC** (No-clean): similar to the RMA flux containing rosin, solvent and a small amount of activator, but it provides the benefit of eliminating the necessity of cleaning the flux after reflow.
5. **WS** (Water soluble): composed of organic materials and a glycol base. The water soluble flux demonstrates the ability to be highly chemically active; however, it can also demonstrate lesser activity than simple rosin fluxes. As a result of this range of activity, WS fluxes are applied both to surfaces that are clean and easily soldered and to very difficult-to-solder surfaces.

One of the main functions of the flux is to make the joining process possible by chemically cleaning the surfaces to be soldered, which includes the removal of any surface oxides that may be present. With the importance of removing oxide layers, it follows that the surfaces to be soldered need to remain free of oxides; therefore, a second function of the flux is to prevent re-oxidation.

The flux vehicle functions as a carrier for the solder particles while also allowing for heat transfer between substrate and component, and it may comprise between five and 20 separate ingredients. These constituents of the flux vehicle provide the rheological properties of the paste material. Of those ingredients that are used to formulate the flux vehicle, it is commonly said that those of highest importance include solvents, activators and rheological additives (Mallik, 2009).

The solvents within the flux vehicle are used for dissolving solids, while the interaction between these solvents and the thickeners ensures that the paste rheology allows for effective dispensing and application of the material. By maintaining an effective rheology, the combination of solvents and thickeners therefore promotes a desired deposit volume and definition during SMA (Pecht, 1993). Many variations of solvents are used within solder paste technology, including alcohols and various glycols. The main role of the activator is the removal of the oxide layers, thus promoting a direct contact between the surfaces to be joined and the molten solder; examples of common activators used are acids, halogen and amines. The rheological additives ensure that the solder paste exhibits any required properties. This is achieved by altering the viscosity and rheology (such as flow behaviour and response to shear), and it is particularly important with the stencil printing process because the rheological properties dictate the ability to flow into the apertures. Common examples of the additives used may include synthetic polymers and waxes.

As mentioned previously, the activators are present in the flux formulation to enhance the removal of metal oxides from the surfaces to be soldered. In work by Shangguan (2005) it is reported that the activators are reactive at room temperature; however, with an elevated temperature (as seen during the pre-heat step of the reflow process), their activity is enhanced. Humpston (2004) confirms this, describing how acids

become progressively more active as temperature rises. Therefore, although activators can demonstrate corrosive properties at ambient room temperature, it is at substantially higher temperatures that they function effectively for the removal of oxides. This is shown in Figure 3.15, which presents an example of a typical reflow profile for solder paste (applied once the printing and component placement processes have been completed) and the corresponding transition to a solder joint.

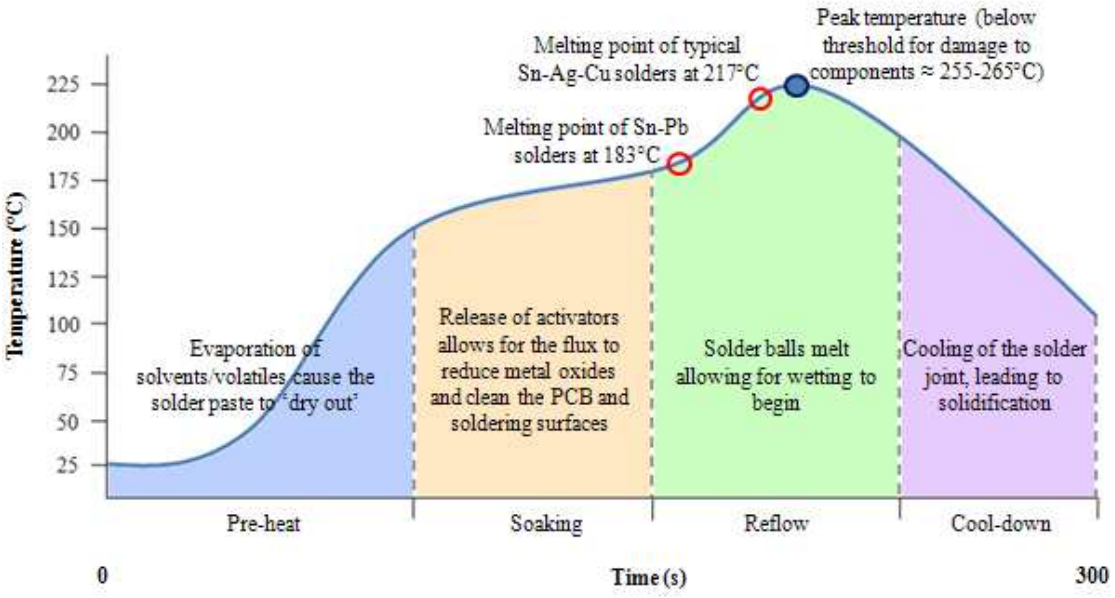

Figure 3.15: Typical reflow profile for paste materials (Tsai and Yang, 2005)

It is commonly found (as mentioned previously) that the necessity exists for 'manufacturing the behaviour' of solder paste through manipulating flow properties. Lee (2002) reports how the rheological properties of a paste must be adapted towards the particular application in an attempt to fulfil the process requirements (for example, manipulating behaviour to allow for fine-pitch printing free of slumping tendencies). Lee (2002) also suggests that success is typically achieved through introducing appropriate rheological additives into the flux system. Despite this common suggestion that simply using additives can allow for idealistic flow behaviour, prior knowledge as to the reasons for flow behaviour is essential. Understanding what causes viscosity may assist with meeting these flow requirements with minimal necessity for 'trial and error' periods of testing. A typical example of this can be highlighted by the concept of fluid friction; through minimising the fluid friction, the solder paste will flow easily.

3.7 Rheology of fluids (flow behaviour of materials)

Viscosity of a solder paste is quantified by the ratio between shear stress and shear rate, which originated from Newton's work that expressed viscosity using equation [3.32] (Brookfield Engineering Laboratories, 1985), where dv/dx is equal to the velocity gradient between the speed of the top plane and bottom plane of the fluid (dv being the variation in velocity and dx being the distance between parallel faces), F is the force required to maintain the speed difference (dv), A is the surface area and η is the viscosity. Thus:

$$\frac{F}{A} = \eta \frac{dv}{dx} \qquad \textbf{[3.32]}$$

From rearranging equation [3.32], we arrive at the relationship shown in equation [3.33]:

$$\textbf{Viscosity } (\eta) = \frac{\textbf{Shear stress } (\sigma)}{\textbf{Shear rate } (\dot{\gamma})} \qquad \textbf{[3.33]}$$

Using these equations, typical examples of (approximate) viscosity commonly recorded in literature are shown in Table 3.3.

Material	Viscosity (Pas)
Air	10^{-5}
Acetone	10^{-4}
Water	10^{-3}
Olive oil	10^{-1}
Motor oil	10
Glycerol	10
Bitumen	10^{8}
Glass	10^{18}

Table 3.3: Typical examples of material viscosities

With an increase in viscosity (such as glass at 10^{18} Pas), some materials have a tendency to appear naturally solid. However, it is often found that the viscosity is simply so high that observing flow behaviour becomes very difficult. One particular example can be seen in the measurement of pitch – a highly viscous material that appears solid, such as bitumen – in which an experiment at the University of Queensland (Australia) demonstrated that the viscosity was significantly high enough to limit observations of solitary 'drips' to once every 8–9 years on average (see Figure 3.16).

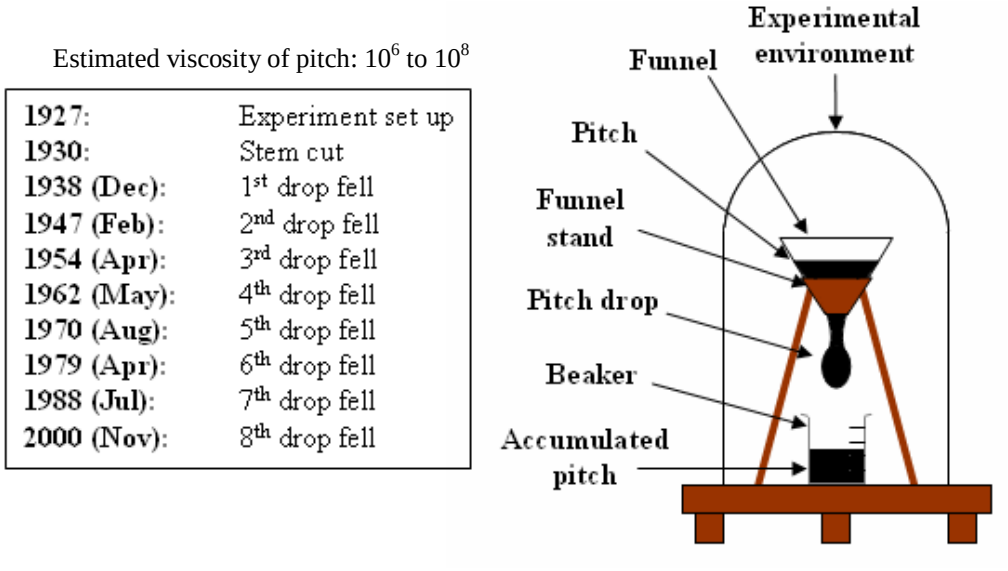

Figure 3.16: Example of an exceptionally high viscosity (Cunningham, 2007)

The equations previously mentioned allow for viscosity to be approximated with relative ease; however, it is also important to understand the internal behaviour of the fluid in creating this viscosity and therefore the relationship between flow behaviour and solid/liquid tendencies. When considering a fluid as being constructed of different 'layers', the explanation of viscosity can be understood to a greater extent. A force applied to the surface of a fluid (driving the 'top layer' to increase in velocity) is not necessarily applied uniformly throughout, and as such the adjacent layer will have a lesser velocity. This gradient throughout the fluid (see Figure 3.17) introduces an increased level of friction between particles, which results in resistance against the applied force, therefore demonstrating properties of viscosity.

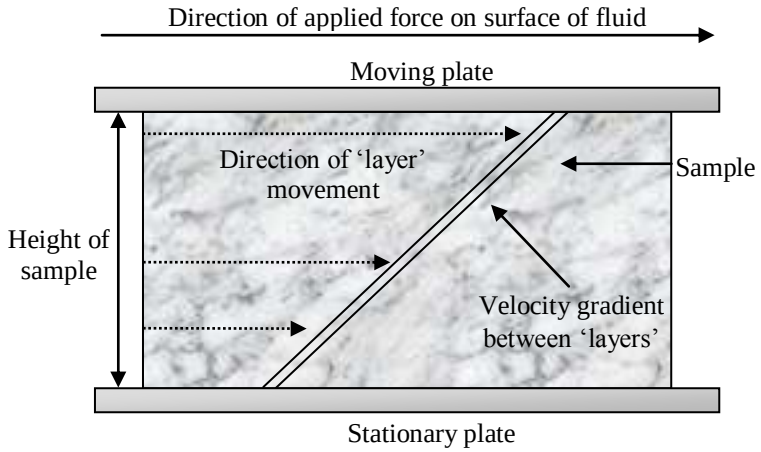

Figure 3.17: Illustration of the velocity gradient within a fluid

In addition to this fluid friction, viscosity can also depend on the general chemical formulation such as the interaction seen with molecular bonding. Therefore, the differences between fluids (as a result of internally occurring forces) may significantly influence viscosity. For example, oils exhibit the fairly weak van der Waals forces, and mercury demonstrates metallic interactions between fat molecules and atoms which are also fairly weak; water, on the other hand, consists of strong hydrogen bonding (SEED, 2009). When considering these bonds or interactions, a higher viscosity will be observed with an increase in the intermolecular forces. This is confirmed by Wang et al (2007), who stated that an increase in the cohesional inter-particle van der Waals force leads to an increase in the observed viscosity.

Material	**Nature of bond/force**	**Measured Viscosity (mPas)**
Water (H_2O)	Hydrogen bonds	0.890
Tetrachloromethane (CCl_4)	Van der Waals forces	0.908
Mercury (Hg)	Metallic interaction	1.526
Tetrachlorosilane ($SiCl_4$)	Polar forces	99.4

Table 3.4: Examples of different types of forces and viscosity in millipascal seconds (mPas) at 25°C (SEED, 2009)

With regard to the van der Waals force, the influence of this is dependent on the particle size observed within the fluid. Therefore, in relation to solder paste this could influence the viscosity with a variation in the PSD. A type 3 solder paste, for example, has a PSD of 20–45 microns (with a minimum of 80% of particles falling within this range) and an average particle size of 36 microns. Alternatively, a type 4 solder paste has a PSD of 20–38 microns, with an average particle size of 31 microns. Thus with this increase in particle size for a type 3 solder paste, an increase in the effect of the van der Waals force should be observed.

An additional factor that can significantly affect the viscosity is temperature. In work conducted by Nguty and Ekere (2000[a], 2000[b]) on Sn–Pb paste, it was reported that a rise in temperature of 1°C results in a 3–5% decrease in viscosity for solder paste. Furthermore, Maiso and Bauer (1990) observed that a 1°C change in temperature can alter the viscosity of the solder paste by as much as 40 Pas. Furthermore, the viscosity of a fluid can be influenced by the shear applied; consequently, the printing process itself may affect the viscosity of a solder paste. This increased shear may be seen from (i) the squeegee forcing the paste into a rolling motion along the surface of the stencil, (ii) the solder paste forced into the apertures or (iii) the squeegee 'shearing' the top of the deposit in the aperture. The National Electronics Manufacturing Centre of Excellence (2000) stated in one paper on the science of stencil printing that approximately 40 variables currently exist for the printing process. Although not all 40 variables will influence the viscosity, some – such as the squeegee speed, squeegee pressure and squeegee material – can play a role in the viscosity of the fluid and, as such, further complicate the issue of understanding viscosity.

3.8 Additional influences on viscosity

Aside from those factors previously highlighted, various other influences exist that contribute to the viscosity of materials. These may include (but are not limited to) those described next.

3.8.1 Metal content

Within paste rheology, materials are commonly stated as containing an approximate metal content of between 85% and 90%, with a common misconception being that this refers to the percentage volume of the paste. In actuality, this refers to the percentage weight of the solder paste, and is significantly different from the value applicable to volume ratios (as shown in Figure 3.18).

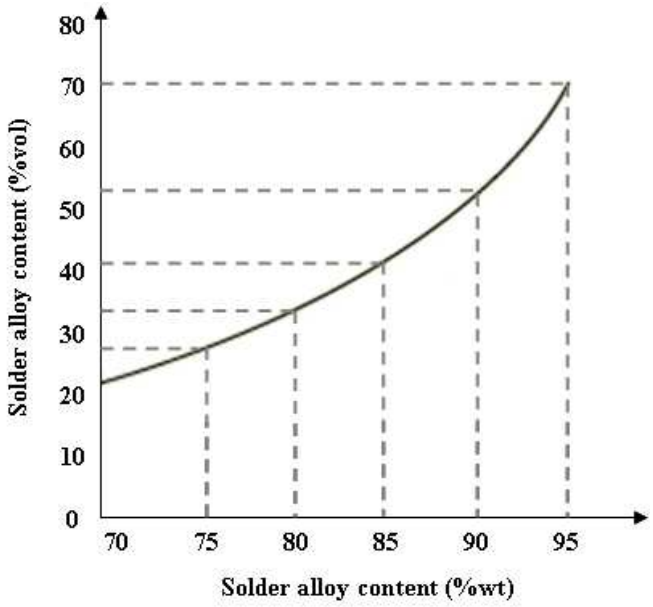

Figure 3.18: Relationship between metal content as a % wt and % vol (Tarr, 2007)

This relationship is significant as the viscosity of a material is ultimately determined by the volume of solder powder incorporated during formulation, while the percentage weight is simply viewed as convenient for certain purposes (Johnson and Kevra, 1989). By increasing the weight percentage of the metal content, an increase in viscosity is observed. This is a result of the displacement of viscous properties of the flux by the increase in solid particles, which essentially results in an increased solid characteristic of the paste.

Because of this increase in viscosity with increased metal content, paste manufacturers commonly attempt to reduce slump by formulating products using as high a metal content as possible. However, such increased paste viscosities are not necessarily recommended. An increase in the metal content may lead to jamming of

the apertures (which consequently leads to skipping defects); furthermore, research suggests that severe difficulties can be encountered with metal content exceeding 94% by weight, as the flux vehicle cannot absorb such elevated percentages and maintain a workable rheology (Tarr, 2007).

3.8.2 Particle shape

The shape of the alloy particles, despite seeming insignificant, can have an effect on the viscosity of the solder paste. This depends on how closely the particles resemble a spherical appearance and the quantity that can be classified as 'spheres' – because using spherical particles results in reduced paste viscosity. This is due to the ability of 'interlocking' exhibited by those particles with a random shape, which leads to increased viscosity. Furthermore, as spheres present the lowest surface-area-to-volume ratio, the influence of internal frictional forces is reduced, thereby leading to a decrease in viscosity (and the reduced surface area also provides benefits with a decrease in oxides). Additionally, during paste dispensing, spherical particles allow for improved transference through needles or printing masks, and thus are viewed as highly desirable (Manko, 2001). The decrease in viscosity observed with an increase in spherical particles can be computed from the Maron–Pierce equation:

$$\eta_r = \frac{1}{\left(1 - \frac{\phi}{\phi_{max}}\right)^2} \qquad \textbf{[3.34]}$$

where η_r is the relative viscosity, ϕ is a constant representing the solid volume fraction, and ϕ_{max} is the maximum packing value. Utilising this equation (assuming ϕ to be constant) it can be observed that as the maximum packing value increases (that is, as the particles move towards representing spherical shapes), the relative viscosity (η_r) decreases (Seman, 2010).

3.8.3 Volume fraction

The term 'volume fraction' in solder paste technology can loosely be defined as the amount of metal alloy content in the paste material (Mackie, 2009), and is calculated using equation [3.35]:

$$\phi = \frac{\left(\frac{M_{(metal)}}{\rho_{(metal)}}\right)}{\left(\frac{M_{(metal)}}{\rho_{(metal)}}\right) + \left(\frac{M_{(flux)}}{\rho_{(flux)}}\right)} \quad \textbf{[3.35]}$$

Where ϕ is the volume fraction, M represents mass and ρ represents the density.

Combining this equation for calculating volume fraction [3.35] with Einstein's equation for the viscosity of suspensions [3.36], it becomes apparent that solder paste viscosity is expected to increase with an increasing volume fraction. This assertion is confirmed in work conducted by Harper (2005), who states that a greater level of deviation from viscous flow is observed with an increase in volume fraction or an increase in the quantity of suspended particles occupying the material.

$$\eta = \eta_f \ (1 + 2.5\phi) \quad \textbf{[3.36]}$$

In equation [3.36], η represents the viscosity, η_f represents the viscosity of the flux medium and ϕ is the volume fraction as highlighted in equation [3.35].

This expected increase in viscosity (through combining Einstein's equation and that for volume fraction) is further substantiated by work conducted by Fletcher and Hill (2008). In this work, the authors reported that particles are forced tightly together with an increase in solid volume fraction, which consequently reduces the ability for unrestricted movement. Owing to the reduction in 'free space' for particle motion, the occurrence of particle-to-particle interactions and collisions increases and hence a rise

in viscosity is observed. This is highlighted in Figure 3.19, in which it can also be seen that a sharp rise in viscosity is observed as the volume fraction nears a maximum.

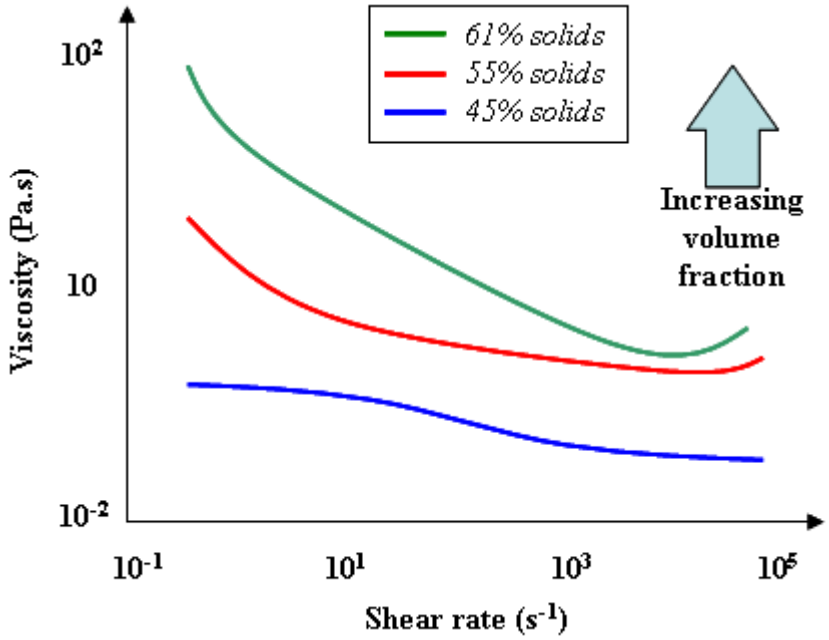

Figure 3.19: Example of flow behaviour with increasing volume fraction (Fletcher and Hill, 2008)

From the graph highlighted in Figure 3.19, Fletcher and Hill (2008) demonstrate how an increase in the volume fraction can play a significant role in increasing the viscosity of a material. However, it is also important to recognise that the increase in volume fraction leads to an increased shear-thinning nature, thereby indicating that the flow behaviour can also be influenced. This can be clearly observed by simply increasing the volume fraction from 45% (where, initially, approximate Newtonian behaviour can be observed) to 61% (where apparent shear-thinning behaviour is exhibited).

3.8.4 Inter-particle forces

The interactions between particles (or inter-particle forces) can significantly affect the viscosity of materials – as previously described by the discussion of van der Waals

forces, which refer to the attractive or repulsive forces between molecules. In addition, viscosity may be affected by electrostatic forces and steric forces.

Electrostatic forces can be seen as the attractive and repulsive interaction between electrically charged particles. As can be seen with common magnets, the attraction or repulsion is determined by the polarity of charge held by the particles – a positive charge is attracted to a negative charge but repelled by a similar positive charge. Ferguson and Kemblowski (1991) stressed the importance of these electrostatic forces, reporting how viscosity will increase in those instances where particles demonstrate an identical charge. This is due to the electrical repulsion leading to an increase in particle collisions, consequently increasing the viscosity of the suspension.

Steric forces are those that exist due to the presence of a polymer layer, which alters the reactivity of a molecule surface. Once a polymer layer has been established, the reactions between charged particles is restricted as a result of limiting the 'free' surface area. This consequently presents the possibility of a cessation in chemical reactions taking place, which leads to increased viscosity due to the suspension stability that is created (Seman, 2010).

3.9 Background theory on rheology and paste processing

3.9.1 Creep recovery behaviour

With regard to creep testing, a review of past literature shows that a number of studies have been undertaken in this area on the behavioural properties of asphalt/concrete mixtures (Naguib and Mirmiran, 2003; Zeghal 2008; Wang and Zhang, 2009). However, insufficient emphasis has been placed on the importance of this method for investigating solder paste materials and, furthermore, how this can provide an insight into acceptability during the printing process. As viscoelastic properties significantly influence rheological performance, studying the creep behaviour of materials becomes highly important.

As detailed previously, the Maxwell and Kelvin–Voigt models (see Figure 3.20) accentuate the presence of both elasticity and viscosity within materials using a

spring-dashpot schematic, a notion developed further by Burger's four-parameter model (Figure 3.21) to highlight the complexity of viscoelastic materials. A comparison of the three models demonstrates that, for viscoelastic materials such as solder paste, it is important to understand and consider each aspect of the creep curve in order to fully comprehend behavioural tendencies.

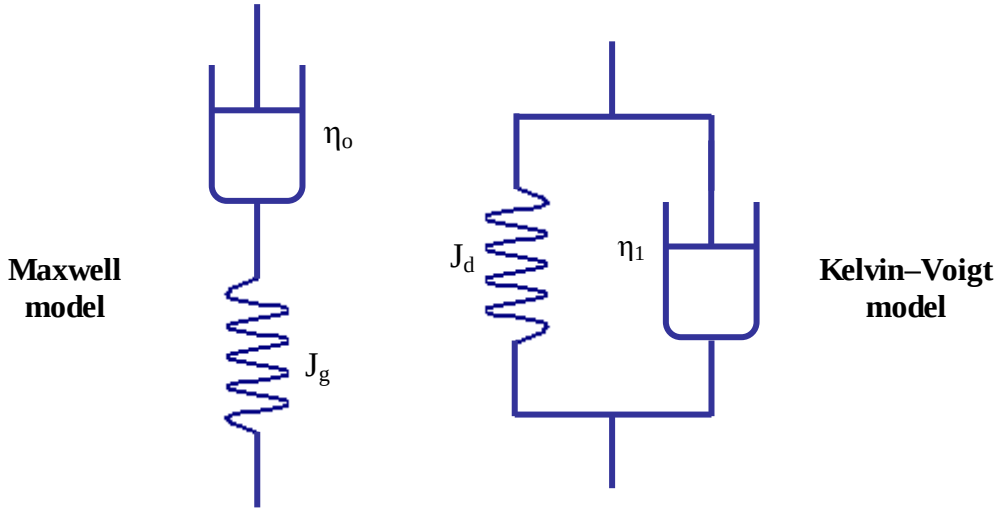

Figure 3.20: Maxwell and Kelvin–Voigt spring-dashpot models for viscoelasticity.

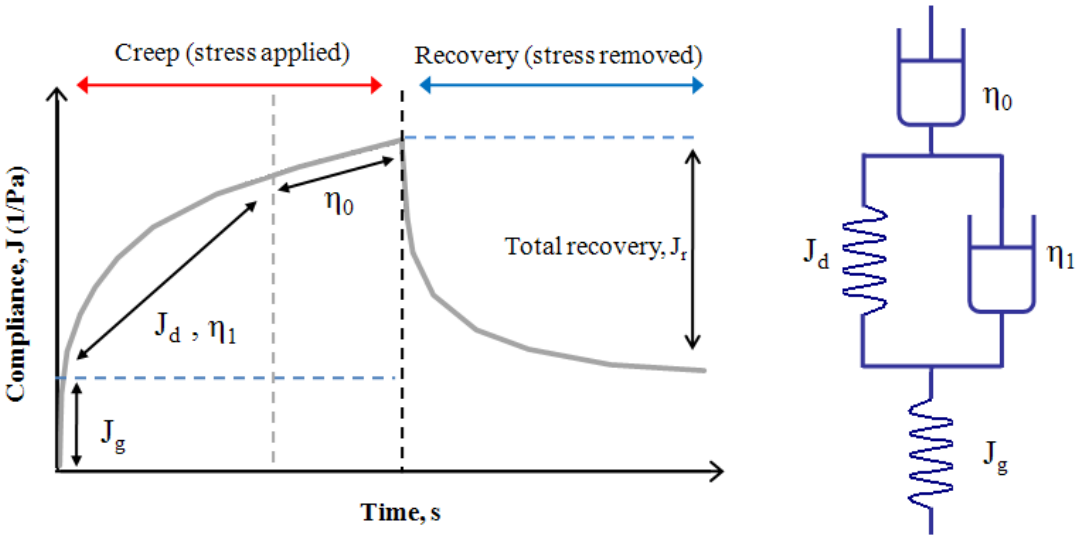

Figure 3.21: Burger's four-parameter model of viscoelastic behaviour (Malvern Instruments, 2004)

As can be seen from Figure 3.21 and as set out by Alger (1997), the creep compliance curve can typically be divided into three sections:

1. Instantaneous deformation (purely elastic response) on stress application (J_g)
2. Time-dependent deformation that arises from delayed elasticity (J_d, η_1)
3. Long-term viscous flow (η_o).

These sectors of a creep curve allow an overall understanding of behavioural properties to be gained for viscoelastic materials. However, with each of the models a further understanding of creep behaviour may be achieved from the corresponding equations. Despite the many equations available (Alger, 1997; Mezger, 2006; Lewandowski and Chorazyczewski, 2010), it is often believed that the Maxwell model is best suited for identifying relaxation behaviour of viscoelastic materials. This is highlighted within equation [3.37], where λ is the relaxation time, τ the shear stress, η is the viscosity and $\dot{\gamma}$ the shear rate (Macosko, 1994):

$$\tau + \lambda \frac{d\tau}{dt} = \eta \dot{\gamma} \qquad \textbf{[3.37]}$$

Whilst relaxation is an important attribute in terms of understanding the behaviour of viscoelastic materials, as a method of determining creep response the model is said to have limitations with respect to accurate prediction (McCrum et al, 1997). With the Kelvin–Voigt model allowing for an explanation of retarded elasticity behaviour, any attempt to understand creep properties becomes simpler. In work conducted by Lee and Kim (2009), it was reported that the theory of linear viscoelasticity dictates that the creep compliance J(t) is determined by the time-dependent relationship between the stress and strain of a viscoelastic material upon application of a constant uniaxial stress, σ. Following on from this, work conducted by Riande et al (1999) observed that simple equations can be derived to determine the creep compliance function for a material using the Kelvin–Voigt model [3.38].

$$J(t) = J \left[1 - \exp \left(\frac{-1}{\tau} \right) \right] \qquad \textbf{[3.38]}$$

where J is equal to the compliance and τ is equal to the shear stress – which Ferguson and Kemblowski (1991) explain can be derived from equation [3.39], in which G represents the spring modulus, γ the strain and $\dot{\gamma}$ the shear rate:

$$\tau = G\gamma + \eta\dot{\gamma} \qquad \textbf{[3.39]}$$

Riande et al (1999) also noted how, despite the simplicity of determining creep compliance from the Kelvin–Voigt model, complex models are needed to accurately measure a material's response to viscoelasticity since both the Kelvin–Voigt and Maxwell models are unable to effectively represent actual behaviour. As demonstrated in Figure 3.21, this is due to the complexity of viscoelastic materials. It therefore becomes necessary to amalgamate these two models to obtain a true representation of material behaviour. Upon combining them, it becomes possible to describe each section of a creep compliance curve, a method that can be achieved through use of the Burger model (Figure 3.21). Through utilising the corresponding equation [3.40], it is then possible to determine the creep response of a material:

$$J(t, \sigma_0) = \frac{1}{G_1} + \frac{t}{\eta_1} + \frac{1}{G_2}\left[1 - \exp\left(-t\,\frac{G_2}{\eta_2}\right)\right] \qquad \textbf{[3.40]}$$

where G_1, G_2, and η_1, η_2 are the moduli and viscosities of the Maxwell and Voigt–Kelvin elements respectively, and σ_0 represents the stress applied to the sample (Nguty and Ekere, 2000[c]).

Mezger (2006) underlines the opportunity presented by the Burger model for understanding viscoelastic behaviour under stress, but emphasises the complexity of analysing deformation behaviour through use of this model. This difficulty arises as differential equations must be solved as a function of time for both the first and second derivatives of shear stress and deformation. Therefore, as an alternative to the Burger model, the Bohlin model also exists, which attempts to minimise this complexity through integration within typical rheological software packages. This model is represented in equation [3.41]:

$$J(t, \sigma_0) = J_0 t^n \quad \textbf{[3.41]}$$

where J_0 is the initial compliance, t is the time, σ_c is the applied stress and n is the co-ordination number. By conducting appropriate mathematical calculations through the software, it is possible to eliminate human error and allow the focus to remain on the study as opposed to complex mathematical problems.

3.9.2 The influence of PSD and flux

Existing literature relating paste rheology to stencil printing performance places emphasis on selecting a suitable PSD and flux as determining factors in dictating paste behaviour and acceptability of the print. With the viscoelastic nature of pastes dictating creep-recovery behaviour, it is important to understand how these factors influence paste rheology when conducting creep tests.

Itoh (2002) reports how particle distribution can directly affect the rheology and printability of solder pastes, influencing such properties as slump resistance and rolling behaviour. Additionally, much emphasis has been placed on how the particle distribution can also affect the ability of the paste to separate from the stencil, and as such, particle sizes should be selected in accordance with the minimum pitch and population density of fine-pitch components.

The concept of paste separation from the stencil (based on particle size) has also been explored by Zou et al (2001), who underline the importance of this property. In their study, Zou and colleagues show how fractional print volume decreases with an increase in particle size, noting how a type 5 solder paste produced both the highest print volume and the highest wall angle while demonstrating the smallest particle size. This finding was attributed to the ratio of particle size to stencil thickness, an issue that had been previously raised by both Morris and Wojcik (1991) and Hwang (1989). Hwang discusses how an appropriate particle size selection is important, with consideration given to the stencil to be utilised, and states that the metal alloy particles should be no greater than one-third of the stencil thickness. Conversely,

Morris and Wojcik state that this ratio of particle size to stencil thickness need only be less than one-half to obtain high-quality prints.

An appropriate particle size selection also plays an important role in reducing the oxide content, and therefore the influence of oxides, on the SMA process. As can be seen from Figure 3.22, a direct correlation can be plotted relating oxide content to particle size.

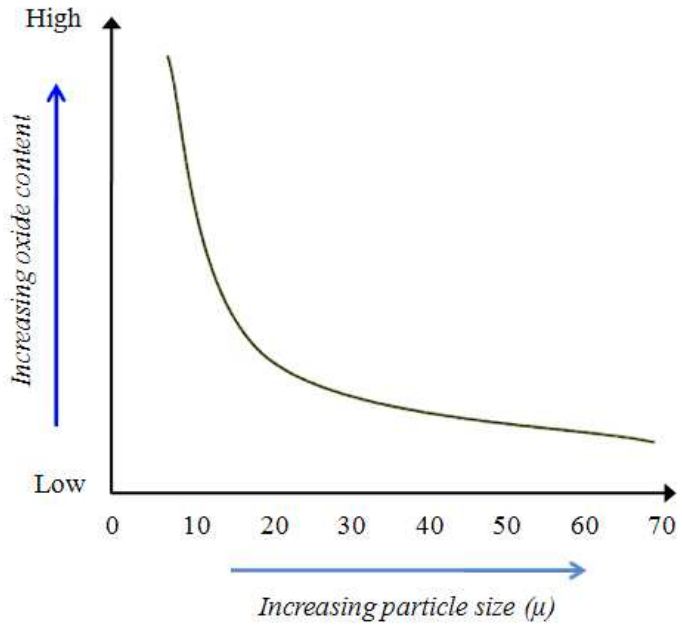

Figure 3.22: Relationship between particle size and oxidation level (Itoh, 2002)

The oxide content should be controlled in order to minimise the occurrence of micro solder balls during the reflow process; and in order to reduce this oxide content, the addition of those particles smaller than 20 μm must remain as few as possible during paste formulation. This is necessary due to the increase in relative surface area that can be observed with a reduction in particle size (Itoh, 2002). This is further enforced by Zou et al (2001), who reported that with fine metal particles an increase will be seen in relative surface area to volume, consequently leading to an increase in the amount of oxide in the paste. Therefore, despite offering superior printing characteristics, pastes formulated with fine particle sizes have an increased risk of solder balling – a direct result of increased oxides interfering with solder coalescence during reflow.

The difficulty of oxide minimisation, whilst being influenced by particle size, is also greatly affected by the flux. Instances of flux exhaustion increase the probability of oxides remaining as a solder alloy is solidified, leading to a greater tendency to produce solder balls (Zou et al, 2001). Although significantly influencing the possibility of oxide content, in general the flux has the capacity to control all the core properties of solder paste materials and is primarily responsible for dictating flow behaviour.

Figure 3.23: Typical constituents of a flux vehicle system (Hwang, 1989)

As can be seen in Figure 3.23, the flux vehicle system is a complex mixture of many ingredients, each of which plays a role in determining the nature of a solder paste. This may include thixotropic properties, shear-thinning behaviour or simply the viscosity under stable conditions. Table 3.5 highlights several characteristics and responsibilities of these components, further emphasising the important role that the flux vehicle system plays on solder paste characteristics.

	Component	Affects	Characteristics
Rosin	▪ Rosin hydride ▪ Disproportionated rosin ▪ Polymerised rosin ▪ Phenol denatured rosin ▪ Ester denatured rosin	▪ Soldering ability ▪ Printing ability ▪ Resistance to slump ▪ Tack properties ▪ ICT testability ▪ Colour of residue	Allows for control of slumping and additional properties through formulating 2 or 3 different rosins together. The rosins soften during the reflow pre-heat stage (≈ 80–130°C), spreading to the surface of the solder particles and substrate
Activator	▪ Organic acids ▪ Halides ▪ Amine hydrochloride	▪ Soldering ability ▪ Activation strength ▪ Reliability ▪ Shelf life	Significantly impacts the ability to remove oxides from the paste. Assists with the wetting of metal surfaces, and reacts with oxides to influence both chemical and electrical reliability
Thixotropic agent	▪ Caster oil hydride ▪ Honey wax ▪ Aliphatic amide	▪ Printing ability ▪ Viscosity ▪ Resistance to slump ▪ Thixotropic index ▪ Odour ▪ Cleanability	Introduces a resistance to shear stress within the paste during printing. Allows for the recovery of viscosity after conclusion of the printing process. Can dictate the quality of print through improving paste release from stencil apertures
Solvent	▪ Glycol ether ▪ Polyhydric alcohol	▪ Stencil life ▪ Resistance to slump ▪ Odour	Can significantly impact slump properties as a result of evaporation rate, which is dependent on the solvent's boiling point (commonly in excess of 200°C)

Table 3.5: Overview of flux components (Itoh, 2002)

A significant amount of literature exists relating the importance of the flux medium to solder paste behaviour, with Itoh (2002) listing the fundamental roles of the flux medium as being fourfold:

1. The elimination of oxide films on substrates, through chemically melting and removing the oxide film that forms on the surface of electrical components, substrates and solder

2. The prevention of re-oxidation, through allowing solids in the flux to become liquidous, covering the substrates, components and solder powder
3. The reduction of surface tension of the solder to enhance wetting, through increasing the contact area with the substrate and components
4. To provide rheology and viscosity in order to make the solder powder printable.

Durairaj et al (2009[b]) further underscore these points, describing how the flux system removes contaminants from the PCB surface, which helps to promote the formation of the metallic bond by providing a good wetting condition. Additionally, the flux vehicle is said to assist with providing the required rheological properties for processing and deposition of paste materials onto PCBs. Work by Lee (2002) further emphasises the extensive array of properties that the flux dictates; reporting how paste thickening on the stencil may be caused by high flux activity at ambient temperatures or, alternatively, by a 'drying out' of the sample because of volatile solvents within the flux.

It is clear from previous research that both PSD and flux are complex areas needing further research – particularly the influence of flux as this can dictate key properties of solder pastes. With issues such as the cohesive nature, vulnerability to structural breakdown and flow behaviour of solder pastes all dictated by the variables of flux and PSD, a potential exists to reduce the influence of print defects on the SMA process. Furthermore, the creep method presents many opportunities for gaining a valuable insight into the influence of these properties on the stencil printing process. With paste formulation significantly contributing towards process defects, understanding the impact of influences such as storage and temperature (where the flux vehicle tends to separate from the solder) can offer valuable insights into paste behaviour – and particularly the new Pb-free formulations, for which a void in knowledge still remains.

3.9.2.1 Storage and ageing

One of the key areas for study is the effect of long-term ageing on the rheological behaviour of solder pastes, as ageing will normally lead to changes in flow properties.

Of additional interest is the effect of ageing on printing performance: the changes associated with flow behaviour due to ageing also affect printing performance, as the paste rolling action and the aperture filling process are adversely affected. Furthermore, the storage method is seen to influence rheological behaviour, particularly the rate of change in these flow properties.

Assessment of the rheological properties and printing abilities of paste formulations allow paste manufacturers to derive a shelf life for their products, which can vary depending on the manufacturer or the paste itself. A current standard for paste materials is a shelf life of approximately six months, which is commonly seen between paste manufacturers (of which a few include):

- Almit: SRC Pb-free solder paste
- Ameritronics: 'zerolead' Pb-free solder paste
- Indium corporation: Indium 5.1 Pb-free solder paste
- Koki: S3X58 – M405 Pb-free solder paste
- Manncorp: PF - 606P Pb-free solder paste
- Qualitek: DSP 878 Pb-free solder paste
- Senju Manufacturing: M705-GRN360-KV Series Pb-free solder paste.

With each manufacturer listed, the technical data sheets for their product state that a six-month shelf life can only be achieved on the assumption that appropriate storage conditions are adhered to; this includes specific temperatures that should not be exceeded (and paste should typically be stored between 0°C and 10°C). ADTOOL (2002) attempted to emphasise the strictness of these storage temperatures/conditions, stating in their paste handling guidelines that:

A. Paste samples should never be returned to refrigerated environments once they have been removed.
B. A useful shelf life of one month is generally expected from a solder paste that has been allowed to return to an ambient temperature (≈ 25°C).
C. Solder paste must never be frozen.

D. The shelf-life of paste samples stored at 5°C to 10°C is six months from the date of manufacture.

These guidelines by ADTOOL (2002) and the industrial recommendation of a six-month lifespan for solder pastes raise many questions as to current levels of efficiency, particularly regarding storage conditions employed. Shelf life is typically advised because of the potential for reduced paste quality, which adversely affects print quality and increases defects during the SMA process. Some major causes for concern relating to long-term storage of solder paste include (but are not limited to): (i) an increase in print defect rate, (ii) flux separation, (iii) the formation of oxide layers, (iv) chemical deterioration of the flux, (v) a reduction in dispensing quality, and (vi) solder balling.

Manko (1995) indirectly underscores the necessity for investigating the shelf life of paste materials, reporting how the ageing process commonly leads to solder powder becoming tarnished and oxidised. As this oxide formation consumes flux, this becomes a major issue during production. The severity of flux consumption is addressed by Baluch and Minogue (2007), who report that the purpose of the flux is to ensure, at the time of joint formation, that the surfaces are free of oxides and consequently enable the formation. Once exposed to environmental conditions (temperature and humidity variation, for example), solder metals form oxides on their surface, which can result in weak solder joints on the PCB and reduced cohesiveness (the effect of which is minimised by the flux).

Prasad (1997) also addresses the issue of oxidation of solder powder particles, revealing how the process is accelerated by ‘improper’ storage, a variable that is commonly related to the ageing process. Coombs (2008) also notes this connection, stating how increased levels of oxidation are typically present in those instances of elevated storage temperatures. Furthermore, Prasad (1997) states that oxidation can instigate solder balling (depending on the capability of the flux and activators to remove oxide layers), where the inability of oxides to melt at soldering temperatures results in the oxide-free molten solder forcing the oxide-rich solder powder particles aside as a solder ball. Therefore, with the need for minimising the influence of oxidation (to promote strong and reliable solder joints), the accuracy of current paste

storage methods are questioned, with particular attention given to the reliability of those guidelines stating that solder paste materials must not be frozen (Radio Electronics, 2007; ADTOOL, 2002).

Improper storage, aside from accelerating oxidation, can also be related to the common issue of separation within paste materials, which can result in smearing, irregular deposit volume and slumping (possibly leading to bridging). In his work, Lee (2002) studies this issue of separation, linking the cause to paste materials remaining in storage for extended periods of time. This is substantiated by work by Nguty and Ekere (2000[b]) in which it is reported that excessive periods of ageing or storage typically result in either separation of the flux or gel formation. In addition, Nguty explains how separation of the material during storage can lead to the remaining acid and activators corroding the solder powder, which could decrease the reliability of joints formed with the paste sample.

The importance of reliable solder joints is self-evident within the field of electronics manufacturing; and with influences such as the formation of oxide layers, manufacturers justifiably adhere to the shelf life of a product. However, considering the cost of manufacture, cost of purchase and paste remnant disposal, it becomes important to question whether shelf life can feasibly be increased without losing print or paste quality.

Common paste retailers demonstrate a range of prices for paste materials. A comparison of Pb-free solder pastes with the Sn–Pb products previously available highlights that an increase in price has arisen due to the RoHS directive (see Table 3.6).

	Example of paste costs	
Paste supplier	**Pb paste**	**Pb-free paste**
Manncorp	SH-6309RMA: $49 (≈ £30.94)	PF-606P: $61.50 (≈ £38.84)
Indium	NC-SMQ92J: $105 (≈ £66.32)	8.9E: $120 (≈ £75.79)
Qualitek	818: £42.00	865A: £45.50
Multicore	MP200: £78.86	96SC: £125.70
Average cost	**£54.53**	**£71.46**

Table 3.6: Examples of comparative paste costs from major paste suppliers (All pastes detailed are classified as no-clean type 3 solder pastes and are retailed in 500g jars. Price conversions correct as of 1 October 2010)

Further to the costs for the paste itself, companies require payment for posting and packaging of the product. With the sensitivity and responsiveness of paste to minor environmental changes, this is invariably requested as next-day delivery, further elevating expenses. Once the paste becomes redundant, an additional expense occurs with regard to disposal. Despite paste materials offering Pb-free capabilities, solder pastes are still classified as hazardous and harmful, and as such require appropriate disposal. Keely (2000) states that waste from solder paste technology is a principal environmental concern and health risk within industrial manufacturing. Consequently, this classification forces electronics manufacturers to follow the requirements of local authorities relating to the disposal of waste and residues – primarily through use of a licensed contractor for metal recovery (BLT Circuit Services Ltd, 2009).

Therefore, from both a financial and environmental viewpoint, increasing the shelf life of solder paste products would be highly beneficial and it is therefore of great interest. Manko (2001) confirms this, suggesting that shelf life must be improved as it is a vital property of solder paste materials, and any increase in shelf life could improve efficiency, marketability, environmental effects and costs for the manufacturer.

3.9.2.2 Using the Cross model to predict flow behaviour

In order to assist with investigating the shelf life of solder paste materials, it is important to model and, if possible, predict paste behaviour. One method of interest for modelling flow behaviour is the Cross model, which offers an opportunity to identify the breaking down of structural relationships expected with ageing and prolonged storage.

Literature findings suggest that, prior to the Cross model, earlier works relating to the estimation of viscosity arose from efforts conducted by Einstein (1906, 1911) on dilute rigid sphere dispersions. Following on from this, Rao (2007) reported how the relative viscosity of dispersions (η_r) and volume fractions of suspended granules (Φ) form the basis for viscosity estimation of concentrated non-food dispersions, as shown in equations [3.42] and [3.43]:

$$\eta_r = \frac{\eta}{\eta_s} \qquad \textbf{[3.42]}$$

where η_r is the relative viscosity, η is the viscosity of the dispersion and η_s is the viscosity of the continuous phase (Jinescu, 1974; Metzner, 1985); and

$$\eta_r = 1 + 2.5\,\Phi \qquad \textbf{[3.43]}$$

where η_r is again the relative viscosity and Φ is the volume fractions of the suspended granules. Therefore, through combining the equations from the works by Einstein, Jinescu and Metzner, it should be possible to state that

if $$\eta_r = \frac{\eta}{\eta_s} \qquad \textbf{[3.44]}$$

then $$\eta = \eta_r \times \eta_s \qquad \textbf{[3.45]}$$

and therefore $$\eta = (1 + 2.5\,\Phi) \times \eta_s \qquad \textbf{[3.46]}$$

Although theoretically it should be possible to utilise this formula for modelling an estimation of viscosity, considerable work by Cross (1965) showed that exploiting such equations would be insufficient – due to the additional variables that could influence viscosity. This was further emphasised by Barnes et al (1989), who explained that a minimum of four parameters are required to form equations offering predictions as to the shape of general flow curves. The Cross model is one such example that operates a minimum of four parameters, as can be seen in equation [3.47]:

$$\frac{\eta - \eta_\infty}{\eta_0 - \eta_\infty} = \frac{1}{[\,1 + (K\,\dot{\gamma})^m\,]} \qquad \textbf{[3.47]}$$

Equation [3.48] highlights an equivalent form of the Cross model that is often described simultaneously with that in [3.47]:

$$\frac{\eta_0 - \eta}{\eta - \eta_\infty} = (K\,\dot{\gamma})^m \qquad \textbf{[3.48]}$$

where η_0 and η_∞ refer to the viscosity at zero-shear and infinite-shear rates respectively, $\dot{\gamma}$ is the shear rate, m is a dimensionless constant, and K is a constant with dimensions of time. Kay et al (2003) give further explanations and understanding of these variables, describing how K relates to the breaking down of structural relationships, whilst m – a dimensionless constant – dictates the degree of shear thinning. In this instance, a value of zero represents a Newtonian fluid, whereas a value tending towards unity implies the material is a shear-thinning liquid.

Despite Barnes et al (1989) identifying equations [3.47] and [3.48] as the Cross model for modelling estimated viscosity behaviour, subtle variations of that model exist. One such example can be seen in work by Rao (2007), who reports that both the Cross [3.49] or Carreau [3.50] models may be used to form correlations between the apparent viscosity of a solution (η_a) and the shear rate ($\dot{\gamma}$):

$$\eta_a = \eta_\infty + \frac{\eta_0 - \eta_\infty}{1 + (\alpha_c\,\dot{\gamma})^m} \qquad \textbf{[3.49]}$$

$$\eta_a = \eta_\infty + \frac{\eta_0 - \eta_\infty}{[\,1 + (\lambda_c \dot{\gamma})^2\,]^N} \qquad \textbf{[3.50]}$$

In this variation of the Cross model [3.49], α_c is a time constant that is related to the relaxation times of the polymer in solution (as is λ_c as seen in the Carreau model [3.50]). In both equations, the variables of m and N are dimensionless exponents. Rao (2007) continues to state that when utilising this equation, m – the Cross exponent – tends towards a value of (1 – n) for small values of infinite shear viscosity (η_∞), where n is defined as the power-law flow behaviour index. From acknowledging these additional variables, it becomes clear that the Cross model can be extended and then applied to the relevant requirements of this investigation.

Modelling the viscosity of pseudoplastic fluids has long been an area of interest, and Williamson (1929) derived an equation for correlating such fluids over a range of shear rates (see [3.51]). Due to the emphasis made in the equation relating to the two constants for the viscosity values (zero shear and infinite shear), a close relation to the Cross model exists. From Williamson we have

$$\eta = \eta_\infty + \frac{(\eta_0 - \eta_\infty)}{1 + \dfrac{|\,\tau\,|}{\tau_m}} \qquad \textbf{[3.51]}$$

where η_0 is equal to the zero shear viscosity, η_∞ is the infinite shear viscosity, $|\,\tau\,|$ is the absolute value of shear stress, and τ_m is the shear stress at which the apparent viscosity is the mean of viscosity limits η_0 and η_∞ (Braun and Rosen, 2000).

At $\tau = \tau_m$,
$$\eta = \frac{\eta_0 + \eta_\infty}{2} \qquad \textbf{[3.52]}$$

This equation [3.51] was then empirically extended by Cramer (1968) in which a variable of shear rate was introduced to assist with the prediction of flow behaviour, as shown in equation [3.53]:

$$\eta = \eta_\infty + \frac{(\eta_0 - \eta_\infty)}{\left(1 + \left(\frac{|\dot{\gamma}|}{\alpha_1}\right)^{\alpha_2}\right)} \quad \textbf{[3.53]}$$

where $|\dot{\gamma}|$ is equal to the absolute value of shear rate, and α_1 and α_2 are constants (once more, η_0 represents the zero-shear viscosity and η_∞ the infinite-shear viscosity).

As well as influencing the equation detailed in Cramer's (1968) work, it may be possible that Williamson influenced Cross in developing the Cross model: Braun and Rosen (2000) reported how Williamson assumed within his work that a shear-thinning fluid exhibits two separate regions of apparent constant viscosity, namely zero and infinite shear. Using simple kinetic theory as a basis, Cross derived a model that also incorporated this assumption by Williamson, which could be applied to any non-Newtonian fluid without a yield stress:

$$\eta = \eta_\infty + \left(\frac{(\eta_0 - \eta_\infty)}{1 + \alpha \dot{\gamma} N}\right) \quad \textbf{[3.54]}$$

where $\dot{\gamma}$ is equal to the shear rate, and α and N are constants. From this equation [3.54], the aforementioned presence of subtle variations in the Cross model can once again be observed – a trend that can be emphasised further through identifying the model (see equation [3.55]) used within the Bohlin rheometer software:

$$\eta = \eta_\infty + \frac{\eta_0 - \eta_\infty}{1 + (K \dot{\gamma}^n)} \quad \textbf{[3.55]}$$

where η_0 is the zero-shear viscosity (used to make assessments on suspension stability), η_∞ is the infinite-shear viscosity (indicating behaviour at very high shear conditions), K is the Cross time constant (signalling the shear rate at which shear

thinning commences), and n is the Cross rate constant, which is a dimensionless value where zero indicates Newtonian behaviour (Cunningham, 2009[a]).

Despite many equations existing that offer an ability to model the estimated viscosity of materials, common use is made of the Cross model, and this can be seen in many literature sources (Sybilski, 1993; Geraghty and Butler, 1999; Owens and Phillips, 2002; Koszkul and Nabialek, 2004). In their book entitled Computational Rheology, Owens and Phillips (2002) state that due to its capacity for predicting the two Newtonian plateaux, the Cross model is frequently applied to modelling the shear-thinning behaviour of non-Newtonian fluids. Despite this, Owens and Phillips continue to reiterate that the Carreau model is a popular alternative [3.56] (where both K_1 and m_1 are constants), due also to the model retaining an ability to predict the intermediate shear-thinning region and the two Newtonian plateaux. Thus we have:

$$\frac{\eta - \eta_\infty}{\eta_0 - \eta_\infty} = \frac{1}{\left(1 + (K_1 \dot{\gamma})^2\right)^{\frac{m_1}{2}}} \qquad \textbf{[3.56]}$$

With the confidence that has been gained regarding the accuracy of the Cross model, it is commonplace to find the equation as a pre-installed feature within rheometer software. This allows for a rapid comparison to be made between those results achieved through the use of the Cross model for predicting viscosity behaviour, and those actually obtained from rheometry tests. As such; it is believed that this could provide a significant input during the course of the study, particularly with regards to analysing those results attained.

3.9.3 The influence of temperature

Temperature effects on solder paste rheology are seen as a major concern and, with investigations into ageing addressing storage temperatures (from ambient to sub-zero), it is important to understand the role that elevated temperatures have on solder paste performance.

Literature readings show that the effect of temperature has long been an outstanding and important issue – for instance, Bursell (1960) studied the effect of temperature on the consumption of fat during pupal development, and Cha et al (2010) investigated the effect on glass lenses. These two publications not only highlight that temperature has been considered a concern for at least 50 years but also underline the significant effect of temperature on many materials. Other investigations include:

- Corrosion of low carbon steel – Khadom et al (2009)
- Algal growth – Goldman and Carpenter (1974)
- Grape ripening – Radler (1965)
- Elastic properties of carbon nanotubes – Chen et al (2009).

It therefore becomes apparent that temperature is considered to have a significant impact in numerous processes. This significance is further amplified in SMA, due to the continued exposure of the solder paste to variations in temperature, including the following:

1. **Storage conditions of the solder paste –** where the temperature could vary depending on whether the material is stored in a freezer (< 0°C), fridge (≈ 0°C to 10°C) or at room temperature (≈ 25°C). Nguty and Ekere (2000[b]) reported that paste stored at room temperature demonstrated an increase in viscosity of 60% when compared with a sample that was stored at 4°C over a given period of time.
2. **Removal of paste from storage –** where the solder paste is taken from the initial storage area and allowed to stand and naturally reach ambient temperature before use. LPKF Laser and Electronics USA (2010) states in its Pb-free paste guidelines that samples should be removed from storage a minimum of eight hours prior to use. Furthermore, Indium Corporation (2008) recommends that its paste be removed from storage a minimum of four hours before use, which allows a significant period of time for temperature variations to influence paste viscosity.
3. **Temperature variations during pre-shearing –** which could vary depending on the time allowed for the pre-shear and the level of shear applied. Barnes

et al (1989) details how heat within fluids is generated by the shearing process, which may cause sufficient change to result in a viscosity decrease.

4. **Temperature increases generated during the stencil printing process –** where a temperature gradient is demonstrated at the surface of the squeegee used in the printing. Riedlin and Ekere (1999) detail the necessity for controlling the heat generated in this way by the paste roll (as a result of viscous motion) in order to maintain consistent deposits.
5. **The significant temperature variations exhibited during the reflow process –** where the solder paste is heated initially to approximately 150°C, then further heated beyond the melting point of the paste (approximately 217°C). This temperature variation leads to what is known as 'heat slump' due to the reduction in paste viscosity that occurs through the reflow heating process (Itoh, 2002).

In an attempt to emphasise the significant impact that temperature could have on the performance of paste materials, Maiso and Bauer (1990) documented that a 1°C change in temperature can alter the viscosity of solder paste by as much as 40 Pas. Nguty and Ekere (2000[a], 2000[c]) further illustrated this point by reporting that a rise in temperature of 1°C would result in a 3–5% decrease in the viscosity of a Sn–Pb solder paste. As a result of those instances of temperature variations detailed previously (relating to the assembly process), this further emphasises the need to study the effect of temperature on solder paste.

Previous literature findings, despite suggesting how paste viscosity can be affected by printing and shearing, for example, do not fully address the need for investigating the high temperatures experienced during reflow, which remain a major cause for concern: Riedlin and Ekere (1999) reported that the stencil printing process merely raises the temperature by approximately 2°C, which is insignificant when compared with temperature increases that exceed 100°C during reflow. The standard test method for investigating slump behaviour[3.1] details that paste is heated to 150°C +/– 10°C to monitor how viscosity is affected. The paste is then allowed to cool to ambient temperature, where it is then examined for instances of slumping. This temperature is

[3.1] Standard test method for slump taken from the test methods manual of IPC (previously the Institute for Interconnecting and Packaging Electronic Circuits).

selected because it is commonly used for the pre-heat stage of the reflow process and is therefore applied to all paste samples during the manufacturing process (see Figure 3.24).

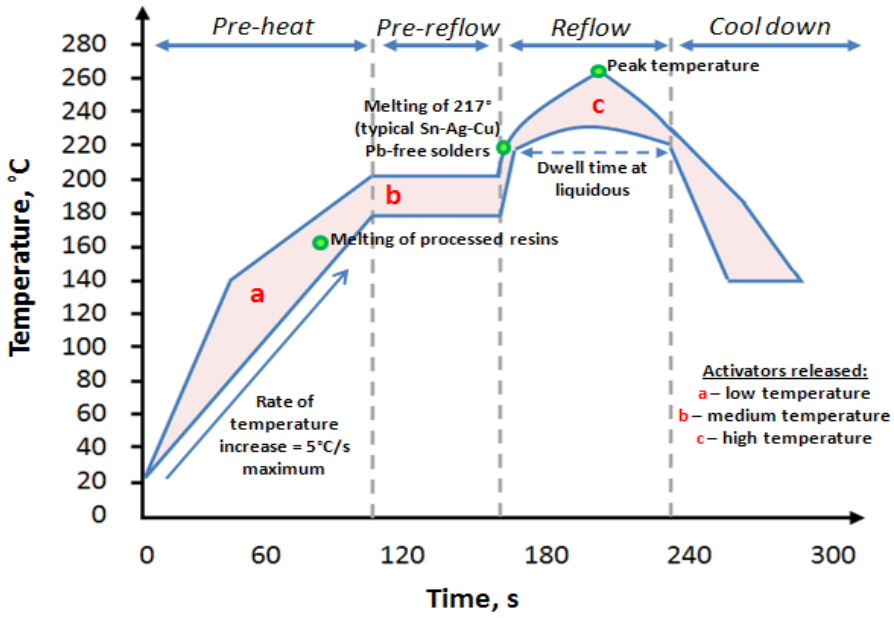

Figure 3.24: Illustration of a typical reflow process (Adams, 2009)

If the works by Maiso and Bauer (1990) and Nguty and Ekere (2000[a], 2000[c]) are assumed to accurately represent the effect of a 1°C increase in temperature; those temperatures presented in Figure 3.24 could drastically alter paste performance because of the substantial reduction in viscosity that would be expected. Therefore, with temperature variations commonly influencing paste samples, predicting paste behaviour at specific temperatures would be highly beneficial. If this were possible, the need for investigating paste behaviour at high temperatures could be removed – improving industrial efficiency as a result of the high number of solder paste samples that would no longer require extensive periods of testing.

3.9.4 Predicting the effects of temperature on solder paste behaviour

By investigating chemical reaction rates, it may be possible to predict viscosity and other properties of solder pastes. This is due to an increase in temperature instigating an amplified rate of chemical reaction, when a greater percentage of the reactant molecules retain energy that exceeds the reaction energy barrier (Connors, 1990). In

1889, Svante Arrhenius studied these chemical reaction rates and reported an empirical relationship for determining the effect that temperature has on chemical reactions:

$$k = A\, e^{-E_a / RT} \qquad \textbf{[3.57]}$$

where k is the rate constant for chemical reactions, T is the temperature (in kelvins), E_a is the activation energy, A is the pre-exponential factor and R is the gas constant. This relationship, known as the Arrhenius equation, is commonly represented using the linear form (Kotz et al, 2009), given by the relationship

$$\ln k = \ln A - \frac{E_a}{RT} \qquad \textbf{[3.58]}$$

These equations provide valuable insight into how applied temperature can influence the chemical reactions of materials; however, work conducted by Mezger (2006) provides the greatest opportunity for understanding the effect of temperature (on solder paste behaviour) from a rheological viewpoint. This is due to the modification of the Arrhenius equation in Mezger's work to allow for emphasis on predicting the viscosity variable. This prediction is possible as, in the form of a viscosity time function (η/T), the Arrhenius equation denotes the change in viscosity for increasing and decreasing temperatures (Mezger, 2006).

In order to allow for this prediction, an initial use of the shift factor equation is required, which is conducted using two known viscosities at two separate temperatures. The shift factor equation is:

$$\alpha_T = \frac{\eta\,(T)}{\eta\,(T_x)} \qquad \textbf{[3.59]}$$

where α_T is the shift factor for a temperature at which there is a known viscosity value, η (T) is the viscosity at the aforementioned temperature and η (T_x) is a second known viscosity value at an alternative temperature. When using the equation, it should be noted that the temperatures are taken with units of kelvins.

This is then followed by an equation to calculate the flow activation energy, where E_A is the flow activation energy, and R_G is the gas constant, which is equal to a value of 8.314×10^{-3} kJ / (mol • K):

$$\alpha_T = \exp\left[\frac{E_A}{R_G}\left(\frac{1}{T} - \frac{1}{T_x}\right)\right] \quad \textbf{[3.60]}$$

Using equation [3.60], the flow activation energy can be found via equation [3.61]:

$$E_A = \left(\frac{\left[R_G \bullet \ln(\alpha_T)\right]}{\left[(T)^{-1} - (T_x)^{-1}\right]}\right) \quad \textbf{[3.61]}$$

Based on these three equations described in Mezger's work (2006), equation [3.62] was derived during this study, allowing for predictions of viscosity dependence on temperature using a single step:

$$\eta_3(T_3) = \left[\exp\left[\frac{\left[R_G \bullet \ln\left[\frac{\eta_2(T_2)}{\eta_1(T_1)}\right]\right]}{\left[(T_2)^{-1} - (T_1)^{-1}\right]} \bullet \frac{1}{R_G}\right] \bullet \left[(T_3)^{-1} - (T_1)^{-1}\right]\right] \bullet \eta_1(T_1) \quad \textbf{[3.62]}$$

where R_G is the gas constant (8.314×10^{-3} kJ / [mol • K]), η_1 is the first known viscosity benchmark, T_1 is the temperature at this viscosity, η_2 is the second known viscosity benchmark, T_2 is the temperature at this viscosity, η_3 is the viscosity that is to be calculated, and T_3 is the applied temperature for which the calculated viscosity is related – and the temperature for each of these remains in units of kelvins.

However, due to the nature of the equation it becomes possible to remove the molar gas constant R_G from the formula, as the two instances where this is used cancel one another out, leaving the following novel equation:

$$\eta_3 (T_3) = \left(\exp \left(\frac{\left(\ln \left(\frac{\eta_2 (T_2)}{\eta_1 (T_1)} \right) \right)}{\left((T_2)^{-1} - (T_1)^{-1} \right)} \bullet \left((T_3)^{-1} - (T_1)^{-1} \right) \right) \bullet \eta_1 (T_1) \right) \quad \textbf{[3.63]}$$

To validate the accuracy of this novel equation for predicting viscosity, values from the work conducted by Mezger (2006) were input as variables; consequently, identical viscosity predictions were confirmed when compared with those values from Mezger's work.

Having derived this equation for calculating predicted viscosity for different temperatures, it was then possible to apply this to those paste samples being investigated. Initially it was decided that the predicted data would be calculated using benchmarked viscosities from the sample manufacturer (Henkel Technologies) within the equation. However, data sheets for the pastes provide information regarding viscosity measurements (at 25°C) recorded via use of Malcolm and Brookfield viscometers. With the Bohlin rheometer employed within this study, these measurements were set aside in an attempt to establish consistency. Furthermore, a comparison of results from the viscometers and initial results from the rheometer demonstrate that a substantial variation exists (Table 3.7).

Paste Sample	**Viscosity from measuring apparatus**		
	Brookfield viscometer	**Malcolm viscometer**	**Bohlin Gemini rheometer**
Sample A	765,000 cP (765 Pas)	1961 P (196 Pas)	2603 Pas
Sample B	526,000 cP (526 Pas)	953 P (95 Pas)	2443 Pas

Table 3.7: Benchmark viscosities from various apparatuses for paste samples

(Given that 100 cP = 1 Poise = 0.1 Pas)

Table 3.7 clearly identifies a substantial variation between the recorded viscosity from the Bohlin rheometer and those provided within the data sheet by the paste manufacturer. However, a comparison of those viscosities in Table 3.7 also demonstrates that a significant variation is present between those values given for the two viscometer measurements. For this reason, eight values were obtained for the viscosities at 25°C and 26°C using a rheometer, with the upper and lower values discarded and an average taken from the remaining data to attempt to find a reliable 'known' starting viscosity for calculations (Table 3.8).

Temperature (°C)	**Viscosity (Pas)**	
	Paste A	**Paste B**
25	2603	2443
	2651	**2535**
	2549	2485
	2869	2513
	2713	**2266**
	2239	2415
	3505	2496
	2743	2385
Average Viscosity	2688	2456.17
26	2520	2351
	2413	2401
	2595	2421
	2028	2316
	2501	**2009**
	3012	2342
	2486	**2510**
	2448	2363
Average Viscosity	2493.83	2365.67

Table 3.8: Measurements taken for benchmark values in predicting viscosity (discarded upper and lower values shown as italicised bold)

Incorporating these average values into equation [3.63] (as benchmark data for the paste samples) allowed for viscosity behaviour to be predicted for each of the pastes on temperature increase to 150°C (as highlighted in Table 3.9).

Temperature (°C)	Predicted Viscosity (Pas)	
	Paste A	Paste B
30	1856.806	2040.861
40	917.994	1434.279
50	474.085	1030.240
60	254.747	754.873
70	141.935	563.229
80	81.745	427.269
90	48.533	329.101
100	29.632	257.061
110	18.564	203.397
120	11.910	162.866
130	7.811	131.857
140	5.229	107.850
150	3.567	89.056

Table 3.9: Predicted paste viscosities at elevated temperatures (using equation [3.63]) all values correct to 3 decimal places – un-shaded values indicate the confidence level, after which estimations are prone to error

From Table 3.9 showing the predicted viscosities (assuming these to be accurate), the paste samples exhibit an expected trend of a severely reduced viscosity upon increase to 150°C (reflow pre-heat temperature). There is, however, a significant variation demonstrated between the two paste samples, with paste B maintaining a substantially greater viscosity. Using the data recorded in Table 3.9, theoretically the paste should behave similarly to that presented in Figure 3.25.

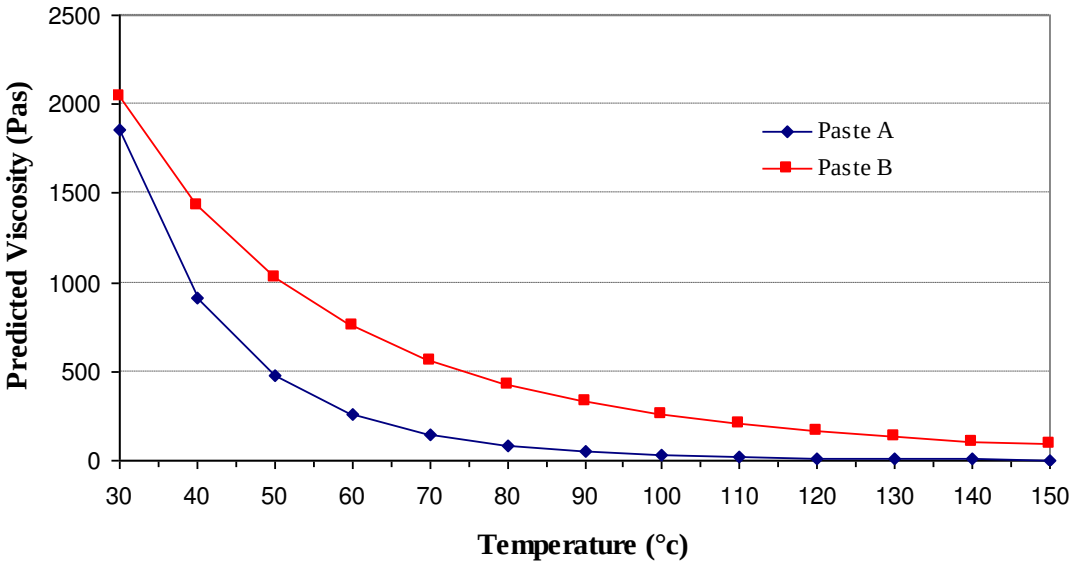

Figure 3.25: Graph of predicted trend of paste viscosity with increasing temperature

When comparing this predicted viscosity data with the statement made by Nguty and Ekere (2000[a], 2000[c]) – relating to the possibility of a 1°C increase leading to a 3–5% decrease in viscosity – it was found that a close correlation can be observed (Table 3.10). However, one observation of interest is how sample A follows the upper limit of this statement, whilst sample B follows the lower.

Temperature (°C)	Viscosity (Pas) Sample A		Viscosity (Pas) Sample B	
	Predicted Viscosity	After 5% reduction (50% actual due to increase by 10°C)	Predicted Viscosity	After 3% reduction (30% actual due to increase by 10°C)
30	1856.806		2040.861	
40	917.994	928.403	1434.275	1428.602
50	474.085	458.997	1030.241	1003.995
60	254.747	237.043	754.873	721.168

Table 3.10: Predicted viscosities compared with Nguty and Ekere statement (2000[a] and 2000[c])

3.9.5 Abandon time of solder pastes

Temperature variations and paste formulation have previously been described as significant influences on paste rheology and print performance (see sections 3.9.1–3.9.3). Consequently, abandon times observed during the manufacturing process can be detrimental to the quality of print achieved (as a result of the environmental influences such as fluctuating temperatures and the tendency for pastes to 'dry up' when exposed to atmospheric conditions). This is addressed by Gilbert (2001[b]), who reports that the majority of soldering defect occurrences are commonly said to be a result of the printing process, with environmental influences and printing delays severely affecting the quality of the print. These printing delays commonly fall under one of the following headings dependent on paste supplier – although each relates to the period of time (delay) between successive prints:

- Printer abandon time (Henkel Technologies)
- Printer downtime (Indium Corporation)
- Dwell time (ITW Kester)
- Response to pause (Indium Corporation)
- Idle time (Heraeus)
- Print after wait (Heraeus)
- Relax/Recovery (ITW Kester).

Regardless of the terminology, abandon time capability is universally agreed upon as being an important characteristic of any paste sample, because maintaining print acceptability is a critical step in reducing defects during production, particularly after a period of stencil 'down-time' (Gilbert, 2001[b]).

As mentioned previously, abandon time relates to the ability of maintaining acceptable prints following an idle period; however, the inability to deliver acceptable prints is commonly attributed to problems with placement or operator breaks (Harper, 2000). This is addressed by Jensen (2004), who reported that downtimes exceeding one hour are frequently encountered in a typical manufacturing environment as a result of equipment repair or the addition of components to machines. In addition to

relating to required downtimes, an extended abandon time can be highly important in reducing those defects commonly related to a 'drying-up' of the paste. Furthermore, an increased abandon time may also provide the opportunity to delay the reflow process for a period of up to 24 hours after conducting the print (Gilbert 2001[b]).

Current industrial standards typically suggest an abandon time limit of 60 minutes, after which undesirable and inadequate print results are observed. This can be seen throughout the major paste manufacturers – apparently regardless of formulation. Examples include the following:

- Qualitek DSP 798 Water soluble solder paste: Abandon time of 30–60 minutes
- Qualitek DSP 889 No-clean solder paste: Abandon time of 30–60 minutes
- Qualitek DSP XP799 Water Soluble (OA) solder paste: Abandon time of 30–60 minutes
- Heraeus F823 No-Clean solder paste: Minimum print after wait of 30 minutes
- Manncorp P/N PF610-PW Water soluble solder paste: If the printing is interrupted for more than one hour, the paste is to be removed from the stencil
- ITW Kester EnviroMark 919G No-clean solder paste: capable of a 60-minute 'relaxation' without causing any print-related problems.

In order to determine paste response to abandon time, it is essential to monitor the quality of the print on the first stroke after applying this period of downtime. Key issues to observe during this print stroke relate to:

1. The quality of the paste roll
2. The paste 'drop-off' from the stencil
3. The occurrence of bridging
4. The occurrence of skipping
5. The shape or definition of the deposit
6. The cleanliness of the stencil and apertures after the print.

However, Koorithodi (2010) describes abandon time as the ability of paste materials to print with consistent transfer efficiency following directly after a period of printer

idle time. As such, common industrial techniques for determining paste response to an abandon time revolve around the variation in paste height observed (Figure 3.26).

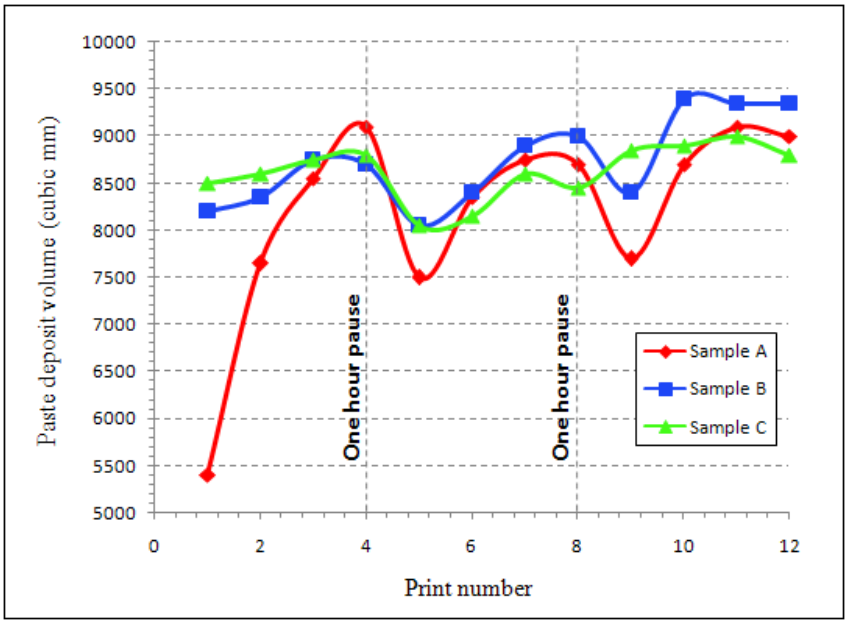

Figure 3.26: Comparison of paste volume after applying an hour-long abandon time (Jensen, 2004)

Koorithodi (2010) additionally noted how an acceptable paste would demonstrate minimal loss of transfer efficiency in response to a pause in the printing process, where the ratio for transfer efficiency is calculated utilising the following equation:

$$\text{Transfer Efficiency} = \frac{\text{Actual volume } (V_a)}{\text{Theoretical or Aperture volume } (V_t)} \quad \textbf{[3.64]}$$

Using equation [3.64], the closer the value of transfer efficiency is to unity, theoretically the more acceptable the quality of the print. Therefore, to facilitate calculating transfer efficiency as a percentage, it is possible to employ equation [3.65].

$$\text{Transfer Efficiency (\%)} = \frac{(V_a)}{(V_t)} \times 100 \quad \textbf{[3.65]}$$

Transfer efficiency is often evaluated alongside the actual reduction in paste volume as opposed to determining a 'theoretical volume' of the solder paste based on the volume of the aperture. Toleno (2005) states in one case study that the success of printing cycles was found to be determined through volumetric measurements and the absence of smearing or clogged apertures, with a requirement for consistent paste deposit volumes on each pad after abandon times of one, two and four hours.

Methods for conducting this investigation vary between companies, with one such example (Heraeus, 2005) recommending printing of five test boards followed by a stencil clean. Once the sixth board has been printed, an abandon time of 30, 45 or 60 minutes is introduced, with a seventh print following. The volume comparison between this sixth and seventh print (in this instance) dictates the acceptability of applying the abandon time. Heraeus also explains how a 15% or more reduction in the observed paste volume is generally considered as a failure.

Typically, the volume of an idealistic cuboid (i.e. the shape of a perfect print deposit) would be calculated using

$$\text{Volume} = \text{Width} \times \text{Length} \times \text{Height} \qquad \textbf{[3.66]}$$

However, as printed solder paste can vary in height between distances of microns, calculating the volume of a paste deposit is not as simple as equation [3.66] suggests. Therefore, to improve accuracy, it is necessary to introduce a significant number of reference point measurements, which allow for sudden height variations to be recognised. The VisionMaster solder paste height-measurement equipment computes the volume using the following equation:

$$\text{Volume measurement} = \Sigma\,(h_i) \qquad \textbf{[3.67]}$$

where h is equal to the height value at one pixel and i relates to the reference points and is calculated as:

$$i = N \times L_p,\quad N \times (L_p + 1),\quad N \times (L_p + 2),\ \ldots,\quad N \times U_p \qquad \textbf{[3.68]}$$

where N is the total number of height points in the measurement region, L_p is the lower sort cut-off percentage and U_p is the upper sort cut-off percentage. Therefore, if measuring 10,000 height points (N) in the measurement region, L_p and U_p provide a means of removing anomalous results. For example, the lower 5% and upper 5% of recorded measurements may be discarded; therefore, the values for i would range from 500 to 9,500 (as 10,000 × an L_p of 0.05 would equal 500 and, conversely; 10,000 × a U_p of 0.95 would equal 9,500).

Utilising previous knowledge, it is then possible to discover the actual volume percentage observed (due to the variation between the volume measurement and expected volume). This may be achieved through applying the following equation:

$$\text{Observed volume (\%)} = \frac{\Sigma\ (h_i)}{V_t} \times 100 \qquad \textbf{[3.69]}$$

where $\Sigma\ (h_i)$ is the volume measurement taken from the VisionMaster and V_t is the theoretical volume of the paste deposit (the expected volume given the aperture dimensions).

In work conducted by ITW Kester (2007), the observed volume percentage was used to provide guidance for the acceptability of the print after an abandon time. During the investigation, it was stated that the solder paste was subjected to temporary halts in the printing process of various lengths, with observations made after downtimes of 15 to 60 minutes. During the investigation, it was reported that a pass was applied to a paste deposition of at least 95%. Results from the investigation highlighted that applying a 60-minute abandon time was possible (for the EM919G paste) without resulting in any additional printing defects. In the ITW Kester study, the outcome of the pass was dependent on a successful ‘first print’ (without kneading) after the applied abandon time (see Figure 3.27).

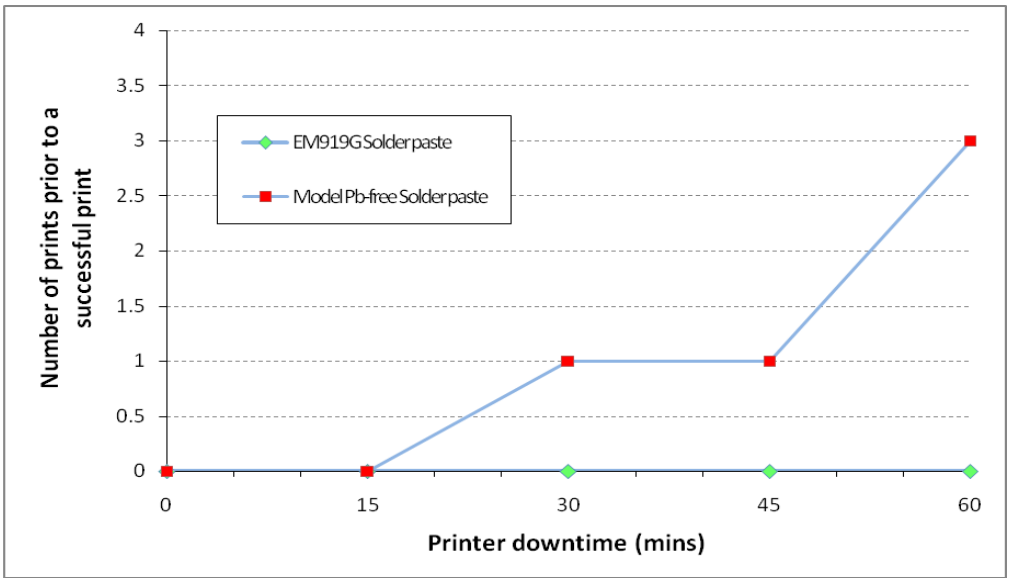

Figure 3.27: Comparison of successful 'first prints' after abandon times up to 1 hour (ITW Kester, 2007)

In addition to using volume measurement as a means of estimating quality, the average height of the deposit may be measured and compared with the expected height based on the thickness of the stencil. This may be calculated through use of the following equation:

$$\text{Average height measurement} = \frac{\Sigma\ (h_i)}{(N \times (U_p - L_p)} \qquad \textbf{[3.70]}$$

where $\Sigma\ (h_i)$ is equal to the volume measurement, N is once again the total number of height points in the measurement region, L_p is the lower sort cut-off percentage and U_p is the upper sort cut-off percentage.

Common trends within paste manufacturing incorporate quality checks on prints after applying an abandon time of one hour – as this is representative of severe customer requirements (Wiese et al, 2005). A few paste manufacturers (such as Henkel Technologies) increase this observation to four hours; however, this limit should be investigated to ensure maximum efficiency and prevent needless disposal of valuable paste.

The length of an acceptable abandon time, as mentioned previously, is commonly stated as 60 minutes (which usually dictates the maximum length of abandon time investigated by the manufacturer), with various failures being observed after periods of rest. However, from available literature it is clear that one key influence that appears to significantly impact the abandon time of solder paste is the 'thickening' behaviour observed with increasing idle time on the stencil. Lee (2002) reports how this characteristic of paste thickening on the stencil may be caused by several factors:

- An excessively high humidity
- An overly high ambient temperature
- Unexpected air drift over the top of the stencil
- Volatile solvents used during flux formulation causing paste to dry out rapidly
- Increased flux activity influenced by ambient temperatures, leading to paste crusting and cold-welding
- Insufficient paste consumption and replenishment rates.

Despite this occurrence of paste thickening (and the many additional influences that can affect abandon time acceptability), methods have been developed to assist with improving paste response to a pause, further increasing the need to investigate printer downtimes beyond even four hours. Gilbert (2001[b]) states that abandon time can be extended by means of the incorporation of solvents that optimise paste formulation. This method of 'developing' an extended abandon time can be achieved by using solvent systems that demonstrate boiling points above 250°C (as these reduce the rate of solvent evaporation, and corresponding changes in paste composition, at ambient temperatures). Therefore, it becomes apparent that the flux once again plays a significant role in dictating the behavioural characteristics of the paste material.

This flux dependency is confirmed by Lee (2002), who reports that increased exposure to low-humidity conditions typically leads to an increase in paste viscosity, as a result of heightened solvent loss. Furthermore, as a consequence of augmented chemical reactions between the flux and solder alloy – as demonstrated when subjected to moisture – paste viscosity can also increase with exposure to high humidity. However, Lee also suggests that viscosity of 'water washable' solder pastes

will decrease with extended periods of exposure (increased abandon times) and high humidity conditions, due to its hygroscopic nature promoting the ability to pick up moisture from the environment. This viscosity decrease occurs because any increase in viscosity – due to chemical reactions – is counteracted and surpassed by the rapid drop in viscosity that is associated with moisture absorption. The work by Lee (2002) indicates that, theoretically, observations from studying the abandon time should demonstrate an increase in paste viscosity with increased time on the stencil. This is due to using no-clean paste materials during the investigation as opposed to water-soluble ones, which according to the work by Lee demonstrate increased viscosity at both high and low relative humidity.

Using the information provided by ITW Kester (2007) regarding the number of prints necessary to accommodate abandon times up to 60 minutes (see Figure 3.27) the graph in Figure 3.28 was developed by identifying a linear trend to determine a theoretical number of cycles required to print successfully after an abandon time of four hours (and the data was also obtained from ITW Kester, 2009). From the results of Figure 3.28, theoretically (based on the findings from ITW Kester) after introducing an abandon time of four hours, approximately 11.3 printing cycles will be required before acceptable print results will once again be observed.

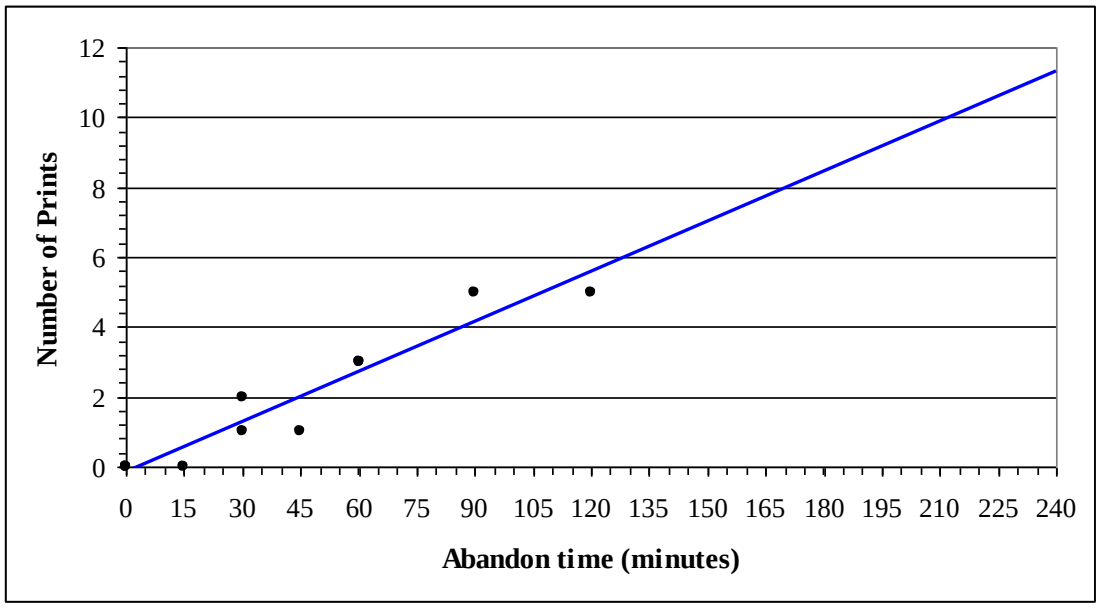

Figure 3.28: Linear prediction of number of prints required for acceptable prints after increased abandon times

3.9.6 Conclusions

3.9.6.1 Creep recovery behaviour

A review of available literature has highlighted that creep testing is an important step in determining the behaviour of asphalt/concrete mixtures (Naguib and Mirmiran, 2003; Zeghal, 2008; Wang and Zhang, 2009). However, despite its viscoelastic nature, creep recovery testing is not widely used for understanding paste rheology. This may be as a result of the complexity of viscoelastic behaviour (as noted by Riande et al, 1999) leading to limitations in predicting behaviour using common models. The Maxwell, Kelvin–Voigt and Burger models have been described as limited, inaccurate or highly complex (McCrum et al, 1997; Riande et al, 1999; Mezger, 2006) when determining creep recovery behaviour; however, with the Bohlin model said to eliminate these complexities (Nguty and Ekere, 2000[c]), this model was used to determine compliance values for creep recovery testing during the project. Creep recovery testing can offer valuable information on paste response to the printing process and viscoelastic behaviour, and as such should be more widely implemented during rheological characterisation. The studies reported in Chapters 5 and 9 demonstrate this importance of using the creep recovery test as a method for determining paste behaviour.

3.9.6.2 Storage and ageing

A review of solder paste manufacturers has illustrated a widespread agreement that paste materials have a typical shelf life of six months, with a few examples (including Almit, Manncorp and Qualitek) assuming storage between 0°C and 10°C but ADTOOL stating that paste must never be frozen. This limit of six months is said to be a maximum, as complications can occur beyond this – for instance an increase in print defects, flux separation and reduced dispensing quality as noted by Nguty and Ekere (2000[b]) and Lee (2002). With Pb-free pastes typically more expensive than Sn–Pb materials (both in terms of production and purchase) and with additional costs such as disposal (BLT Circuit Services Ltd, 2009), the RoHS and WEEE directives have led to an overall increase in paste processing costs. Chapter 6 addresses this

issue, investigating the flexibility of a six-month shelf life and of storage temperatures, and how changes in these variables can influence print performance.

3.9.6.3 The influence of temperature

Temperature has been reported to influence paste viscosity at each stage of the SMA process, from storage and pre-shear to printing and obviously reflow (Barnes et al, 1989; Riedlin and Ekere, 1999; Nguty and Ekere, 2000[b]; Itoh, 2002). In one study, Nguty and Ekere (2000[b]) noted that paste stored at room temperature demonstrated an increase in viscosity by 60% compared with a sample stored at 4°C. Additionally, Maiso and Bauer (1990) reported that a change in temperature of 1°C can alter viscosity by up to 40 Pas. Furthermore, Riedlin and Ekere (1999) suggested that stencil printing can raise the temperature of solder paste by 2°C. From these literature findings it was concluded that much work has been undertaken relating to the effects of temperature on paste materials; however, a void still remains relating to the influence of reflow temperatures. As the temperatures applied during reflow account for the most significant variation experienced during SMA, this has been investigated in Chapter 7.

Work by Mezger (2006) presented an opportunity to predict paste viscosity at specific temperatures by employing a series of equations. Using this as a basis, along with benchmark viscosities at 25°C and 26°C, predictions were made of viscosity measurements for the test materials. From these predictions, it was concluded that viscosity would demonstrate an exponential decay with an increase in temperature. Furthermore, assuming these predictions to be an accurate representation, the results of Nguty and Ekere (2000[a] and 2000[c]) in reporting a 3–5% reduction in viscosity with a 1°C increase in temperature were corroborated, as the two sets of results matched.

3.9.6.4 Abandon time

A review of available literature emphasises that delays in the printing process can severely influence the quality of the print attained (Gilbert, 2001[b]), with unacceptable prints commonly attributed to operator breaks (Harper, 2000). From conducting a review of paste manufacturers, it is commonly expressed that a maximum abandon

time of 60 minutes may be applied after which the paste must be replaced (Qualitek, Manncorp, ITW Kester). As with investigations into shelf life, this is an important factor to study because of the increase in costs associated with Pb-free materials and the environmental impacts from paste disposal.

In order to assess abandon-time capability, it was concluded that transfer efficiency plays an important role: Koorithodi (2010) reports abandon time as the ability of paste materials to print with consistent transfer efficiency after printer idle time. Using guidelines from Heraeus (a 15% reduction in observed paste volume is considered a failure) and ITW Kester (prints are classified as a 'pass' with a paste deposition of at least 95%), Chapter 8 investigates the abandon time capability of paste materials and assesses the possibility of increasing the maximum abandon time beyond one hour. To further assess this possibility, predictions were made regarding the effect of introducing a four-hour abandon time (using results from ITW Kester (2007) as a guideline), from which it was concluded that 11.3 print cycles would be required to achieve an acceptable print.

CHAPTER 4:
EXPERIMENTAL DESIGN

4.1 Introduction

Because of the complexity of solder paste materials, it is essential to select appropriate apparatus and methods to assist with the characterisation process and alleviate difficulty in understanding sample behaviour. As previously mentioned, solder paste materials are highly susceptible to slight changes in environmental conditions, paste formulation and applied stress (where variation in one of these areas can significantly alter flow properties and printing capabilities). Therefore, planning for any influences that could affect the samples, and predetermining experimental procedures, allows consistency and reliability to be improved and maintained throughout the research.

Considering the areas of investigation within the project, several pieces of equipment were paramount, particularly for rheological capabilities and stencil printing opportunities. Furthermore, with investigations conducted regarding slumping behaviour, paste measurement and heating equipment was essential. This chapter therefore addresses the equipment employed during the project, providing information about the solder paste samples used and the pre-study investigations conducted. The pre-study investigations relate to the speed step test and characterisation tests necessary for developing benchmark results to allow for comparisons with the individual studies.

4.2 Solder paste materials

4.2.1 Solder paste overview

With the introduction of new directives in July 2006 (RoHS and WEEE) that prohibit the use of lead in solder paste materials, the most commonly used constituent of paste

samples (to that date) was no longer permitted. As a result, Pb-free paste was developed, primarily consisting of a tin–silver–copper alloy, although various alternatives exist. With even further variations starting to appear, it has become apparent that an appropriate selection of materials is imperative. Those variations could include:

- PSD
- Metal content percentage by weight or volume
- Flux formulation
- Flux classification
- Percentage of each metal present.

Therefore, as a result of the various types of solder paste available (see Chapter 3, section 3.5), the complexity of the solder pastes themselves, and the vast range of paste suppliers, the selection of appropriate testing materials becomes even more significant. For this reason, in order to understand paste behaviour to a greater extent, efforts should be made to minimise sample variation. With such a vast number of variables having to be considered that could influence paste rheology, by restricting the number of variations between test samples the potential for understanding print behaviour and, moreover, its correlation to rheological behaviour may be significantly increased.

4.2.2 Solder paste samples studied

During the research, various new Pb-free paste formulations were utilised, which differed in both PSD and flux (see Table 4.1). This allowed for the possibility of stronger correlations and comparisons to be drawn between the results, as each solder paste could then be contrasted with others with deviations shown in just one variable. Therefore, it was possible to ensure that results were uninfluenced by minor variations (such as the quantity of one particular ingredient – additives or solvents being examples) during the manufacturing process.

Solder Paste	Solder Alloy	Flux Medium	PSD (µm)	Flux Classification	Metal Content (%wt)
Sample A	Sn 95.5% Ag 3.8% Cu 0.7%	F1	25–45	No-Clean	88.5
Sample B		F1	20–38		
Sample C		F2	25–45		
Sample D		F2	20–38		

Table 4.1: Details of solder pastes used within the study

As can be seen from Table 4.1, each of the solder pastes was formulated using a solder alloy consisting of tin, silver and copper, with a metal content of 88.5% by weight. The flux was seen to vary between samples, along with the particle size distribution, which varied from 25–45 microns (type 3 solder paste) to 20–38 microns (type 4 solder paste). These two variables (PSD and flux) allowed for a cross-reference to be made between results, in order to understand this effect on the behaviour of solder paste properties. Data sheets for the paste samples classify each as being halide-free, no-clean, Pb-free solder pastes, which have a broad process window for printing, reflow and humidity resistance, with a melting point of 217°C. Samples of each paste were stored at temperatures of –40°C, +4°C (as recommended by the paste supplier), and ambient room temperature, which is somewhat useful when determining the ageing properties of the samples. It should be noted that although it was not possible to control environmental conditions, these were monitored strictly for the duration of the experimental programme, with ambient conditions observed to fluctuate between 23°C and 26°C.

Prior to conducting each test, the samples were subjected to pre-shear and relaxation periods. This allowed for their structural integrity to be regained prior to investigation, removing (or at least minimising) the influence of the storage period. The initial pre-shear phase that was performed consisted of stirring the solder paste with a plastic spatula for a period of 30 seconds. The sample to be studied was then placed on the

rheometer for testing, where it was 'trimmed' to remove excess amounts of solder paste. An equilibrium period of 30 seconds was then applied before testing commenced, with each test being performed a minimum of six times.

During the investigation, the MasterSizer 2000 PSD measuring apparatus (Malvern Instruments) was used as a means of confirming that the PSD of each paste was as specified by the manufacturer. Results from the tests highlighted that for pastes A and C – with a PSD of 25–45 microns – the peak volume percentage for particles was between 34.67 and 39.81 microns (≈ 17% of all particles), with an approximate total of 85% of all particles between 25 and 45 microns in diameter. Regarding pastes B and D – with a declared PSD of 20–38 microns – the peak volume percentage was observed between 26.30 and 30.20 microns (≈ 11% of all particles), with approximately 80% of all particles between 20 and 38 microns in diameter.

4.3 Rheological measurements

In order to attain rheological measurements, it was possible to utilise either a viscometer or rheometer. As modern viscometers tend to employ a unidirectional rotating spindle for measuring viscosity, they are often labelled as simplistic (Carrington and Langridge, 2005). Rheometers, in contrast, offer a more extensive range of characterisation techniques, including the ability to measure viscoelastic properties, which is essential when working with solder paste materials.

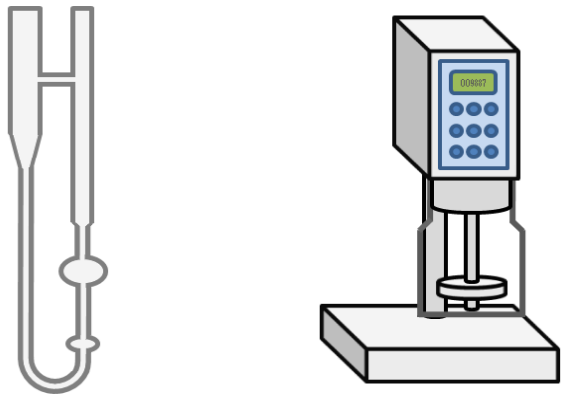

(a) (b)

Figure 4.1: Example types of viscometer: (a) U-tube viscometer; (b) Brookfield rotational viscometer

Despite the array of various types of viscometers available, a rheometer was selected for use within the research because of the following factors:

- The ability to measure viscosity across a much wider range – this helps in identifying properties such as yield stress
- The capability of controlling the temperature applied to the sample
- The oscillatory option that can be employed within the studies to identify further sample properties such as the viscoelastic behaviour
- The ability to apply rapid changes in speed, direction and applied stain.

4.3.1 Rheometer equipment

A Bohlin Gemini-150 controlled stress/strain rheometer from Malvern Instruments Ltd, Worcestershire, UK was utilised throughout the investigations (see Figure 4.2). This was connected to a computer allowing for automatic graphical representation, while also enabling the user to control the workings of the rheometer by raising and lowering the top plate as required and determining the gap between plates. Furthermore, a Peltier plate control unit allowed for management of the sample temperature (with an accuracy of ±0.1°C), along with an attached water-cooling system, and a continuous air supply ensured that the pressure input to the rheometer was substantial to ensure that the air bearing remained in working order by removing friction in the system.

Figure 4.2: Rheometer, computer, Peltier plate and air pressure configuration used during investigations

The Bohlin Gemini-150 rheometer offers a wide range of functionality to assist with the rheological characterisation of solder paste material, including:

- Good control on sample temperature ranging from –30°C to 200°C (Mallik, 2009)
- The convenience of using a wide range of measuring geometries (parallel-plate, cone-and-plate and cup-and-bob)
- Allowance for a wide shear-rate range (>10 orders of magnitude)
- Support for both controlled-stress and controlled-rate mode
- Allowance for both viscometric and oscillatory flow measurements
- Provision of high resolution and accuracy – particularly regarding torque settings, measurement of speed, temperature control and absolute position control (Ancey, 2005)
- Provision of software support and direct monitoring via a computer interface.

With this system, i.e. the Bohlin Gemini rheometer, it is possible to identify characteristics of fluids using a range of various investigations, which include viscometry, oscillatory, relaxation and creep recovery tests. From those tests offered by the Bohlin software, several offer great potential for sample characterisation prior to undertaking investigations. These pre-characterisation processes may then allow for analysis and understanding of variations in performance and properties. Furthermore, through taking advantage of the Bohlin Gemini, it was possible to ensure that the temperature was controlled at 25°C throughout all experiments (with the exception of the slump study, where temperature varied between 25°C and 150°C).

4.3.2 Types of measuring geometries

Typically, three variations in geometry are commonly utilised for characterising material properties, namely cup and bob (concentric cylinder), cone and plate, and parallel plate. With regard to the cup-and-bob geometry (see Figure 4.3), this is becoming less frequently selected due to:

- the requirement for using a large quantity of the sample to be measured
- the difficulties that arise with respect to cleaning the measuring system after use
- complications with measuring high-frequency data (due to large mass/inertia).

Furthermore, with continued development of rheometer capabilities, it can often be found that the cup-and-bob geometry is merely used for very low-viscosity fluids, or to minimise sample evaporation during temperature studies through reducing the exposed surface area (which can even be covered with a thin layer of oil to practically eradicate evaporation altogether).

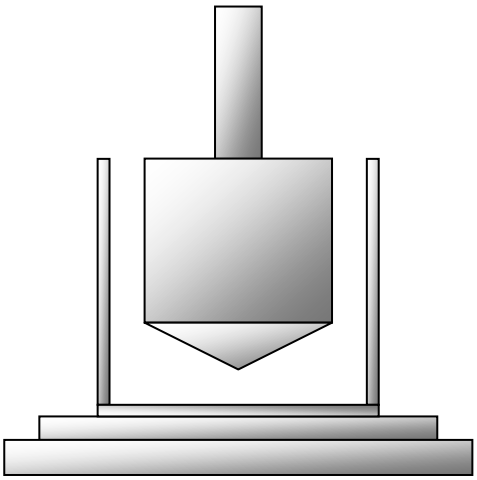

Figure 4.3: Cup-and-bob measuring geometry

Cone-and-plate geometry (Figure 4.4), along with parallel-plate geometry (Figure 4.5), are the two geometries most frequently used during rheological studies. The concept of introducing a cone shape into measuring geometries arose in an attempt to minimise variation in shear across the surface area of the test material, which is seen as the major advantage over alternative approaches. Despite presenting the opportunity for achieving a uniform shear across the sample, this consequently leads to the major disadvantage of the measuring geometry, namely that of particulates gathering at the apex of the cone, which can then result in unreliable test data.

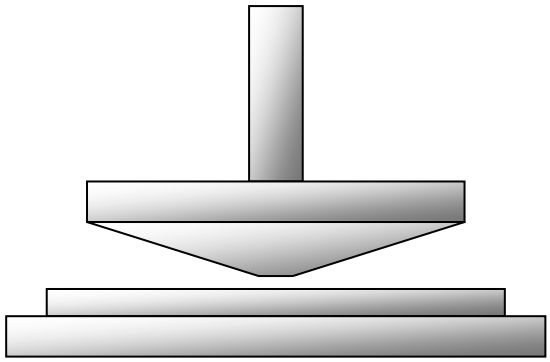

Figure 4.4: Cone-and-plate measuring geometry

With regard to the parallel-plate assembly (much like the cone and plate), benefits can be found from the ease of cleaning after use and, furthermore, the ability to conduct measurements through use of a relatively small sample size. Unlike the cone and plate, however, use of the parallel plate during testing allows for control over the gap between the plates during the testing phase – this becomes very beneficial when investigating materials with varying particle sizes. Furthermore, the ability to manipulate the gap setting allows for an improved opportunity to conduct temperature profile investigations. The only significant shortcoming of the parallel-plate geometry is that of the varied shear exhibited across the surface of the material; nevertheless, this influence is minimised by the rheometer through obtaining an average value from across the sample. Figure 4.5 illustrates the parallel-plate geometry employed throughout the research.

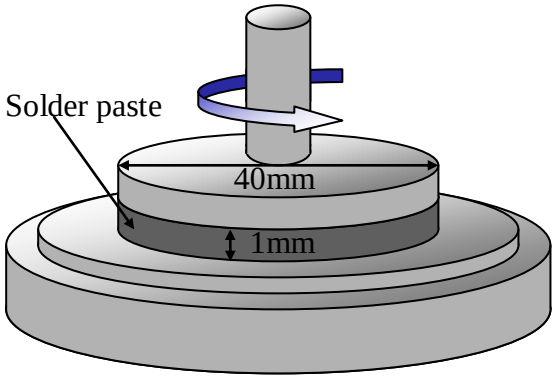

Figure 4.5: Parallel-plate measuring geometry used during the study

One variation of the parallel plate that has been introduced into rheometry is that of the serrated plate (Figure 4.6), which is said to assist with minimising the influence of wall slip. The serrated-plate geometry has been widely used across a variety of fields as an alternative to parallel plate arrangements. Examples of such work include:

- Han et al (1996): viscoelastic properties of hydrogels
- Pal (2000): slippage during the flow of emulsions
- Franco et al (2005): manufacture of lubricating greases
- Navarro et al (2005): rheological behaviour of modified bitumen
- Mallik et al (2008): rheological properties of Pb-free solder pastes.

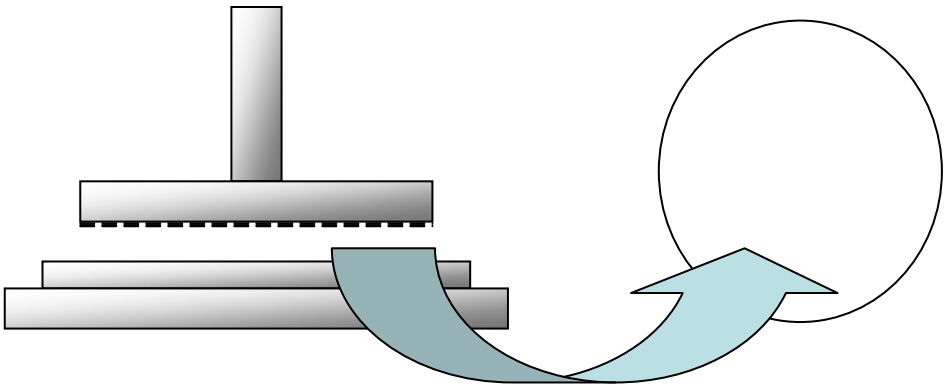

Figure 4.6: Serrated-plate measuring geometry

Even so, as mentioned above, the selected geometry for use in the studies was the parallel-plate arrangement, and one was chosen with a diameter of 40 mm and a solder paste gap height of 1 mm (Figure 4.5). This format was selected because of the benefits that were offered, particularly its ability to control the gap settings and the opportunity to undertake temperature profile investigations reliably. Furthermore, it was possible to utilise past experimental work as benchmark references for confirming the validity of results. One final influence was that of the inability to accurately ensure that the serrations on the serrated plate were of an exact consistency. With the issue of discrepancies arising due to a varied shear across the surface of the test material (as the serrated plate behaves in the same manner as a parallel plate), it was believed that any further possible inconsistencies should be avoided.

4.4 Printing trials

4.4.1 Stencil printers used during the study

In this aspect of the research, two separate stencil printers were used. The DEK 260 stencil printer was employed as the main component and was used in order to attain results from printing trial experiments. The secondary printer used was that of the DEK Europa, which was employed in an attempt to confirm the validity of observed results.

4.4.1.1 DEK 260 stencil printer

The DEK 260 stencil printer allows the user to conduct print cycles using a semi-automatic approach, where the only required input is that of the removal/replacement of boards and initiating the cycle itself (once predetermined values have been established by the user). With regard to the variables that may be specified by the user, these are numerous and allow for a high level of control over the printing process to be gained. These user-determined variables include (DEK, 2005):

- **Print mode:** Identifies the actual print mode, such as print/print and double squeegee. Print/print mode relates to the operation type for use with a single squeegee, where a hop-over is programmed.
- **Forward and reverse speeds:** Dictates the speed (in mm/s) at which the squeegee moves across the stencil.
- **Print gap:** Defines the distance from the upper face of the board to the underside of the stencil.
- **Front and rear limits:** Restricts the distance that the squeegee can travel during a print stroke.
- **Separation speed:** Defines the speed at which the board is separated from the underside of the stencil.
- **Pressure setting:** Dictates the pressure that is applied by the squeegee on the solder paste during the print.

- **Table in delay:** Creates a delay between activating the apparatus and the movement of the table.
- **Squeegee delay:** Creates a delay between the completion of the print and the removal of the squeegee.
- **Screen frame:** Details the thickness of the stencil frame that is used during the print.
- **Hop-over distance:** Allows multiple print cycles using a single squeegee blade.
- **Hop-over delay:** Creates a pause during the hop-over to allow for any accumulated paste to fall from the squeegee blade.

Figure 4.7: DEK 260 semi-automatic stencil printer

4.4.1.2 DEK Europa stencil printer

The DEK Europa is classified as a mass-imaging platform stencil printer that incorporates micron-class high accuracy to offer next-generation capabilities to the SMT industry (DEK, 2004). The Europa stencil printer was essential to employ for reliability testing, due to the precision and accuracy that it offered to enable successful Pb-free manufacturing. Key features of the DEK Europa include (DEK, 2007):

- A high throughput conveyor that allows for a superior cycle time of 6 seconds
- Flexible process handling due to the wide range of board handling options that are offered

- Improved accuracy and repeatability of processes due to an optimised printer frame
- An integrated squeegee drip tray within the print carriage
- Reliable paste-on-pad repeatability of 2 cpk at ± 20 µm
- Web-based support services (DEK Interactiv)
- Error recovery and on-board help (DEK Instinctiv^{TM})
- A remote solvent tank that allows for rapid replenishment.

4.4.2 Squeegee selection for printing

With the research being undertaken using a DEK 260 stencil printer, it was necessary to select an appropriate squeegee design for use with the apparatus in order to carry out printing trials (as the printer allows for interchangeable squeegees and does not employ a fixed system). The two commonly used variations of squeegee are metal and rubber/polyurethane, with further differences existing between these, such as length and contact angle.

Rowland (2006) details how, despite metal squeegee blades tending to allow for a more controlled (and, importantly, consistent) print height, acceptable results may be obtained even using urethane blades assuming that a minimal number of large pads are present on the board. This opportunity exists because hard urethane – or alternatively high-density polyethylene – blades reduce the defect of scooping on small pads, therefore encouraging consistent deposit heights. From this statement, it appears that the use of metal squeegees offers a more beneficial approach to that of a urethane selection, which is further supported in work by Prasad (1997). Prasad highlights that, with fine-pitch applications, the required pressure to print the solder paste tends to be high, which can lead to scooping and bleeding underneath the stencil. Metal squeegees can be used at lower pressures and have therefore become popular for use with fine-pitch components. Furthermore, polyurethane blades can be worn easily when compared with the metal squeegees, and thus need to be sharpened.

With the ability to produce a consistent paste height during the printing cycles, and due to the preferred selection during fine-pitch applications, it was decided that the

appropriate selection of squeegee was that of a metal variety. While undertaking the investigations, two squeegees were used: one to enable a forward printing cycle, and the second to enable the reverse printing cycle. The squeegees used (Figure 4.8) were designed with a contact angle of 30° with the stencil surface and a length of blade of 300 mm.

Figure 4.8: Squeegee design used throughout the printing trials

4.4.3 Stencils integrated into the printer

Two key stencils were identified for use during the printing trials. Initially it was believed that the Benchmarker II stencil (Figure 4.9) would provide the greatest contribution, due to the common use of the stencil within industrial settings for quality assurance approaches (such as the occurrence of solder balling, IPC slump, x-ray voiding, and wetting). However, as the slump issue itself is one of the greatest concerns within PCB assembly (particularly as this leads to the bridging defect), it was concluded that the main stencil for use should be that of the IPC-A-21 slump stencil (Figure 4.10) that has been purposely designed in order to allow for the influence of slump to be monitored. For this reason, the Benchmarker II stencil was solely used as a secondary stencil to ensure no other major defects were observed during the print.

Figure 4.9: Benchmarker II stencil

Figure 4.10: IPC slump stencil IPC-A-21

Although the Benchmarker II stencil allows for an investigation into the slumping behaviour of solder pastes (Figure 4.11), it was concluded that this should be set aside in favour of the IPC stencil. This was because of the latter's ability to contrast and compare slumping behaviour between numerous collections of paste deposits (Figure 4.12) as opposed to the single opportunity provided by the Benchmarker II stencil.

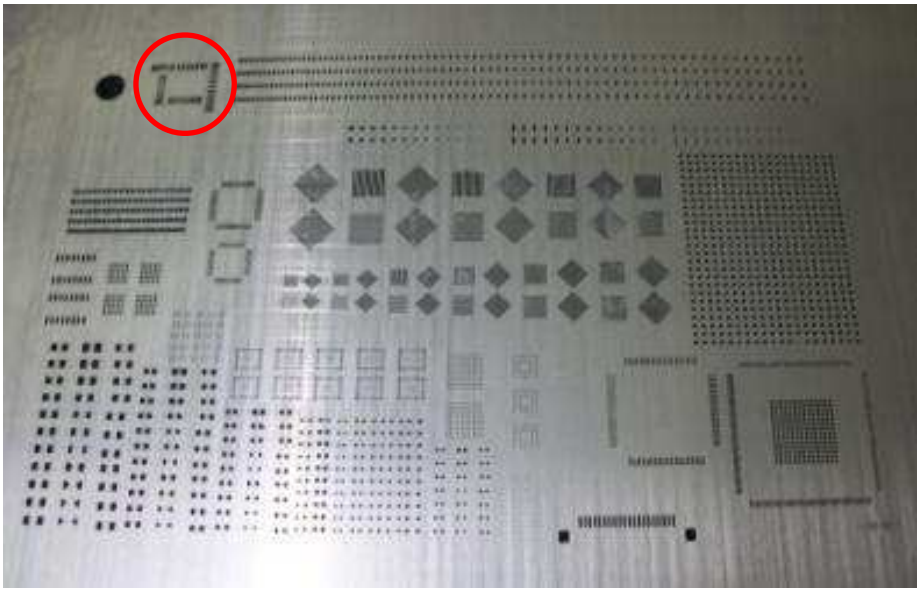

Figure 4.11: Benchmarker II aperture design (IPC slump test circled)

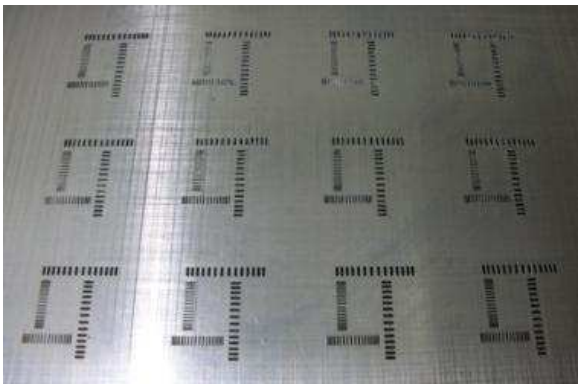

Figure 4.12: IPC laser cut slump stencil IPC-A-21 design
(Stencil thickness of 0.1mm)

Upon comparing those images highlighted in Figures 4.11 and 4.12, it can be seen that when investigating the slumping behaviour of solder pastes using the Benchmarker stencil, an additional 11 print cycles would be required to allow for the same level of result comparison to take place. Moreover, the IPC slump stencil is also able to present valuable results with regard to the repeatability of printing on pitch sizes as small as 0.06 mm (Figure 4.13) while also allowing for an identification of common defects such as skipping or irregular deposits.

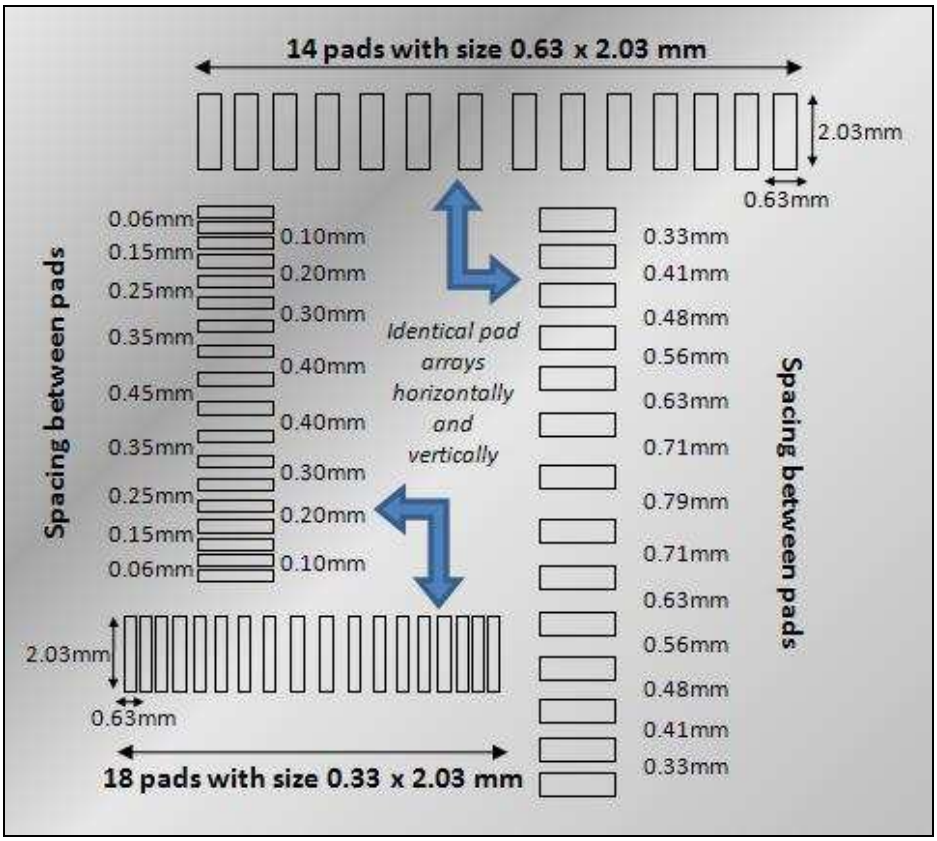

Figure 4.13: Schematic diagram of the IPC-A-21 slump stencil (IPC, 1995)

4.4.4 Test boards

In order to successfully carry out printing trials, it was important to select the appropriate boards for use during the printing process. With secondary printing observations undertaken after having used the Benchmarker II stencil, it was evident that the Benchmarker II test boards were required to ensure that all observations could be accurately understood – for example, the solder balling aperture should correlate to the solder balling pad on the board.

As a result of the trials conducted using the IPC slump stencil, it was decided that the appropriate selection was of bare copper boards (Figure 4.14). This selection ensured that all prints remained clear for observations, while also offering confidence that the measuring equipment would be able to distinguish between print deposits. Furthermore, this selection ensured that the materials used could be maintained throughout all experimental procedures – this could have become a concern,

particularly during periods of heating, if, for example, ceramics had been used for printing on.

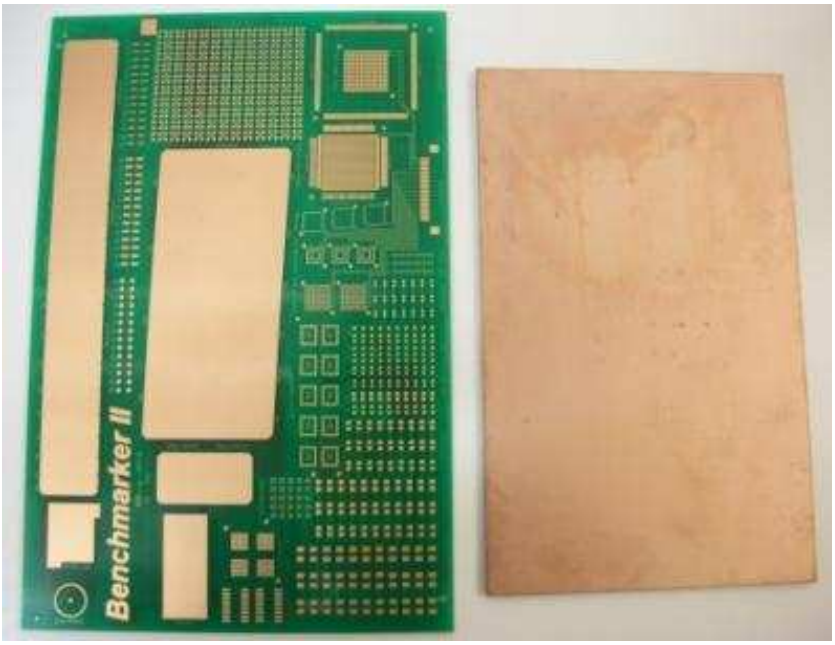

Figure 4.14: Test boards used during the printing cycles

4.4.5 VisionMaster solder paste height measurement equipment

The VisionMaster apparatus (Figure 4.15) was seen to offer significant opportunities in analysing results from the investigations. The rheological software (linked to the rheometer) allows for users to gain a graphical representation of results, along with tabulated data that can then be interpreted. The VisionMaster equipment complements these results through contributing a visual identification of actual results. The equipment is considered as a solder paste inspection system and allows for 3-D imaging of solder paste deposits, which can offer significant results particularly during slump investigations, where the height of the solder paste can be monitored. The apparatus is equipped with a streaming camera link to a computer, which allows for analysis of specific paste deposits, offering accurate and repeatable 3-D measurements (with an accuracy of reading given as ±0.3 microns or ±0.01 mils/0.00001 inches) of many PCB features including pads and ball grid arrays (BGAs; Laser Vision Technologies, 2005).

Figure 4.15: VisionMaster solder paste height measuring apparatus

4.4.6 Vision Engineering Mantis apparatus

For general inspection of the boards (to look for signs of print defects), Vision Engineering's Mantis apparatus was used (Figure 4.16). The advantage of this lies in its ability to conduct small-scale magnification rapidly in a straightforward manner, with the possibility of amplifying paste deposits up to an enlargement of 10 times the standard during the inspection process. Vision engineering states that the Mantis is commonly applied in three fields of engineering: (i) PCB and component assembly, (ii) inspection (quality control), and (iii) rework and soldering. Since the research is focused on the quality of solder prints during the PCB assembly process, it is essential that each of these three fields is addressed. Hence the choice of equipment made.

Figure 4.16: Vision Engineering Mantis inspection apparatus

4.4.7 Batch oven used for slump investigation

With the necessity for investigating slumping behaviour of solder paste during the research, the Reddish Electronics 'Batch' forced convection reflow oven (Model SM500 CXE) was selected for use, as accurate temperature control was possible while retaining the opportunity to actually 'view' the heated sample – the glass cover allows the entire duration of the temperature profile to be observed (Figure 4.17).

Figure 4.17: Reddish Electronics 'Batch' forced convection reflow oven

The oven allows for users to programme the heating elements to operate four different cycles, which run in a consecutive manner allowing for the temperature (which can be programmed to reach 300°C) and application time of the temperature to be varied throughout the investigation period. In order to clarify the accuracy of the temperature being applied to the sample, Reddish Electronics recommends incorporating a thermocouple into experiments. During heating, the apparatus allows for the two heating elements (rear and front) to be operated individually at separate temperatures; however, in order to avoid inconsistent results, this facility is often disregarded in order to ensure desired temperatures are reached.

4.5 Preliminary investigation

4.5.1 Speed step test

The aim of the speed step test is to determine optimum settings for implementation in the solder paste printing process, relating to the speed and pressure of the squeegee

during the print. By identifying these settings, it is possible to apply those parameters that would be most likely to allow for the highest quality of print to be attained. From this investigation, it is then possible to achieve a level of confidence that the parameters applied in the studies are appropriate.

When conducting printing trials, it should be noted that the squeegee pressure should be as little as necessary to scrape the stencil clean of solder paste particles, and that the printing speed must be set so the solder paste rolls perfectly on top of the stencil – typically between 20 and 80 mm per second (Bentzen, 2000). While investigating jamming and skipping during solder paste printing, Hillman et al (2005) corroborated the work by Bentzen from an experimental viewpoint, noting that optimal settings for squeegee speed and down force were set at 20 mm/s and 5.2 kg respectively.

Despite this work by Hillman et al (2005), it was found that a pressure of 5 kg was insufficient to clean the stencil of Pb-free solder paste used during the project. As a result, residual paste was observed, which could have been the reason for incomplete deposits during the printing process. From further investigation, it was discovered that a squeegee pressure of 7 kg was the minimum applicable to ensure a clean stencil after printing. However, because optimal print settings change from sample to sample (paste A may demonstrate a clean stencil with 7 kg of force, whereas paste B may require 8 kg), it is necessary to appropriately plan the investigation since variables may not be changed dependent on the material used, as this removes consistency from the study.

4.5.1.1 Design of experiments

'Design of experiments' comprises a formal method of collecting information from an experiment where more than one variable exists. To assist with conducting such an investigation, several concepts were developed by Ronald A. Fisher in his book of the same name (1935):

- First is blocking design, where experimental factors or variables are grouped into blocks depending on similarity, in order to remove or minimise the presence of unnecessary values.

- Second is that of a comparative design, which attempts to use standard or existing results as a benchmark to compare against, in order to assess reliability of results.
- Third is that of factorial experiments, which highlight interactions between variables by measuring two or more values simultaneously.
- Finally is replication design, which requires the repetition of measurements within an experiment in order to identify any variations and in turn estimate these differences.

The factorial method of experimental design (see the third bullet point above) is one that is applied to an investigation that consists of two or more factors for which there are several possible values. This is conducted in an attempt to identify all possible combinations between the factors and values, and the interaction between them. One of the key arguments in favour of using the factorial design was postulated by Fisher (1926), who stated that it was more efficient to employ methods such as full factorial experiments as opposed to studying one factor at a time.

As it was necessary to determine appropriate settings for both the speed of the print stroke and the pressure exerted by the squeegee, the factorial design method was seen to offer an insight into the interaction of these individual properties and thus their impact on performance. Successfully acknowledging and comparing these interactions between properties allowed for the identification of appropriate parameters to apply throughout the testing period. Table 4.2 highlights the method undertaken for the speed step test that was selected following a factorial experiment design.

Speed (mm/s)	**Pressure (kg)**		
	7	**8**	**9**
20	Test A	Test B	Test C
30	Test D	Test E	Test F
40	Test G	Test H	Test I
50	Test J	Test K	Test L

Table 4.2: Sequence of speed step tests undertaken

For the speed step test, investigations were conducted using the DEK 260 stencil printer, with an initial speed of 20 mm/s and pressure of 7 kg. The speed was then increased in steps of 10 mm/s, while the pressure for each speed setting was incremented by 1 kg.

4.5.1.2 Results

Investigations into the optimal parameters to apply during the stencil printing process identified values of 20 mm/s for squeegee speed and 8 kg for squeegee pressure (Test B in Table 4.2) as providing the highest quality of print (Table 4.3).

	Paste 1		**Paste 2**	
Test	**Bridging (0.33 pads)**	**Drop off (sec)**	**Bridging (0.33 pads)**	**Drop off (sec)**
A	0.15 mm pitch	15–20	0.2 mm pitch	25–30
B	**0.15 mm pitch**	**15–20**	**0.1 mm pitch**	**15–20**
C	0.2 mm pitch	25–30	0.15 mm pitch	15–20
D	0.2 mm pitch	15–20	0.15 mm pitch	15–20
E	0.2 mm pitch	15–20	0.2 mm pitch	15–20
F	0.2 mm pitch	25–30	0.2 mm pitch	15–20
G	0.2 mm pitch	25–30	0.2 mm pitch	10–15
H	0.2 mm pitch	15–20	0.2 mm pitch	0–5
I	0.2 mm pitch	15–20	0.2 mm pitch	5–10
J	0.2 mm pitch	15–20	0.2 mm pitch	10–15
K	0.2 mm pitch	15–20	0.2 mm pitch	10–15
L	0.2 mm pitch	15–20	0.2 mm pitch	10–15

Table 4.3: Results of the speed step test for two representative pastes.

Further observations were made relating to the deposit shape, presence of skipping, cleanliness of the apertures after print, cleanliness of the stencil after print, and quality of paste roll for the tests. During the testing period, it was evident that some of the trials led to issues of skipping, an unclean stencil, clogged apertures and poor deposit definition, but a further issue observed was the inability of the paste in some cases to actually roll. In these instances, the paste was simply being pushed along the surface of the stencil; and since one of the prerequisites of an acceptable print cycle is good paste roll, this was invariably seen as unacceptable.

With the exception of two instances of a faster drop-off speed, those quality inspection characteristics required for an acceptable print were best achieved with squeegee speed and pressure at 20 mm/s and 8 kg respectively. The standard test method pertaining to the abandon time capability of solder paste products during the printing process states that the test requirement is for the solder paste to show a good paste roll, drop off, deposit definition and resistance to bridging (Gregoire, 2003). Therefore, values within Table 4.3 and those observations made, suggest that the aforementioned parameters best fit the requirements for a print of acceptable quality.

4.5.2 Characterisation tests

In addition to the speed step investigation, pre-study experiments were conducted in order to understand the standard behaviour of the solder pastes. This was undertaken in the form of characterisation tests, which allowed for an insight into the properties of the solder paste samples prior to commencing individual studies – that is, before working or applying a stress/shear to the pastes. By conducting a series of rheological tests that highlighted viscometry, oscillatory and creep-recovery behaviour, it was then possible to understand properties such as:

- Shear thinning behaviour
- The linear viscoelastic region (LVR)
- Elastic/Viscous behaviour (storage/loss modulus)
- Response to time
- Response to an applied stress

- Response to removal of an applied stress.

As a result of successfully understanding these properties prior to commencing research, it was then possible to gain a better understanding as to the reasoning behind results from the studies. This was due to the results from the characterisation tests acting as a benchmark for comparisons to be drawn.

Work conducted by Dusek et al (2002) identified that the most commonly used and practical methods for characterising the paste flow behaviour were those of: (i) viscometry testing, (ii) creep recovery testing, and (iii) oscillatory testing. Initial investigations into the characterisation of the paste samples therefore included a viscometry shear rate sweep, an oscillatory amplitude sweep and an oscillatory frequency sweep – each described next below. These characterisation tests allowed results to be obtained pertaining to the LVR, storage/loss modulus and shear-thinning behaviour of the pastes. During the testing period, each test was conducted several times in an attempt to ensure that each result obtained could be identified as a true representative of the characteristics of the pastes.

4.5.2.1 Shear rate sweep

The shear rate sweep may be viewed as the most important of the characterisation tests, as it allows for a perception to be gained of a sample's response to an applied shear. Through analysis and understanding of the results obtained, it is then possible to identify how a material will behave in operational situations. With regard to the SMA process, the importance can be seen because of the method presenting an opportunity to highlight a sample's response to the printing process, where a high shear rate is applied due to the squeegee pressure, and a low shear is seen upon removal of the stencil. Typically, viscosity of a material due to shear behaviour can be divided into three categories: shear thinning, shear thickening and Newtonian (Figure 4.18) – where shear thinning and shear thickening are examples of non-Newtonian behaviour of materials.

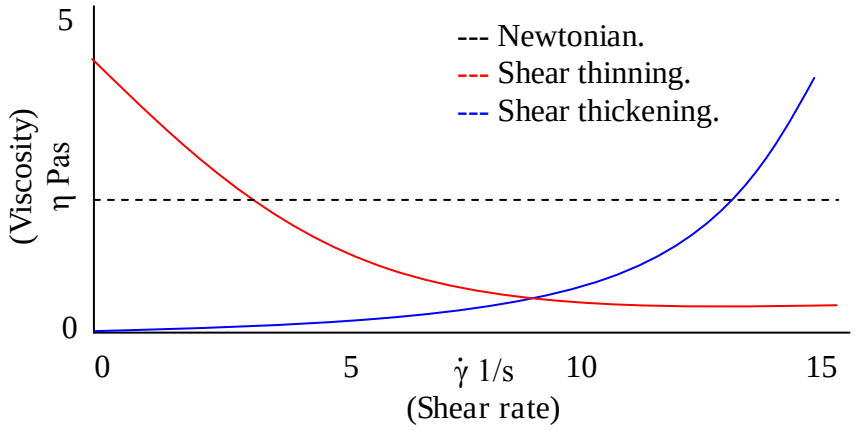

Figure 4.18: Example graph of the shear behaviour of materials.

4.5.2.2 Amplitude sweep

The oscillatory amplitude sweep is commonly used as a method within the characterisation of solder paste materials, as it allows for the determination of the linear viscoelastic region (LVR). This is an important property of solder paste to identify, as it provides an indication as to the range of stress values that can be confidently applied to a sample before a breakdown of paste structure is exhibited. This is indicated by the conclusion of the plateau stage of the test, and thus the onset of reduced viscosity (Figure 4.19). Also, through application of the amplitude sweep test, an indication of the elastic (storage) modulus and viscous (loss) modulus may be gained, which details the nature of the paste with regard to its solid-like behaviour.

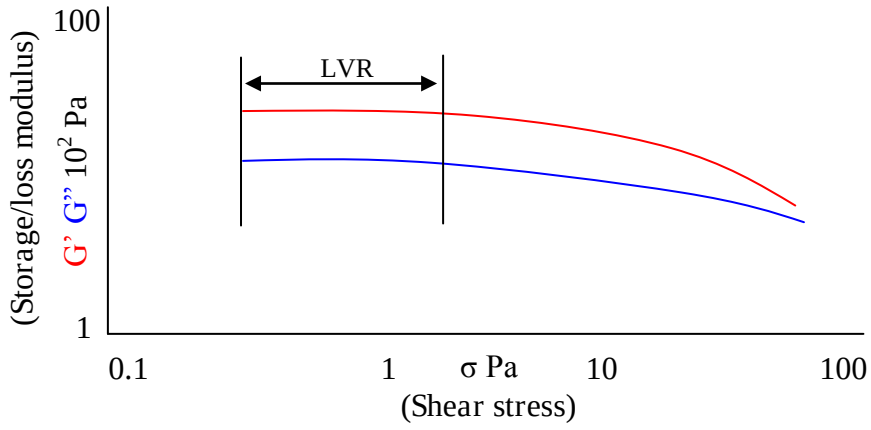

Figure 4.19: Graphical representation of a typical amplitude sweep

4.5.2.3 Frequency sweep

The oscillatory frequency sweep once again helps with characterising solder paste behaviour, providing an understanding of the storage (G') and loss (G") modulus – which denote the elastic and viscous components of the sample respectively – as a function of time. Using this method, it is possible to understand whether the paste will demonstrate a predominantly solid behaviour or liquid tendencies. Furthermore, the ability to identify the phase angle property of the material is highly beneficial during characterisation (Figure 4.20), as this indicates the flow behaviour of the solder paste, with a value of 90° signifying a purely viscous flow and 0° indicating pure elasticity.

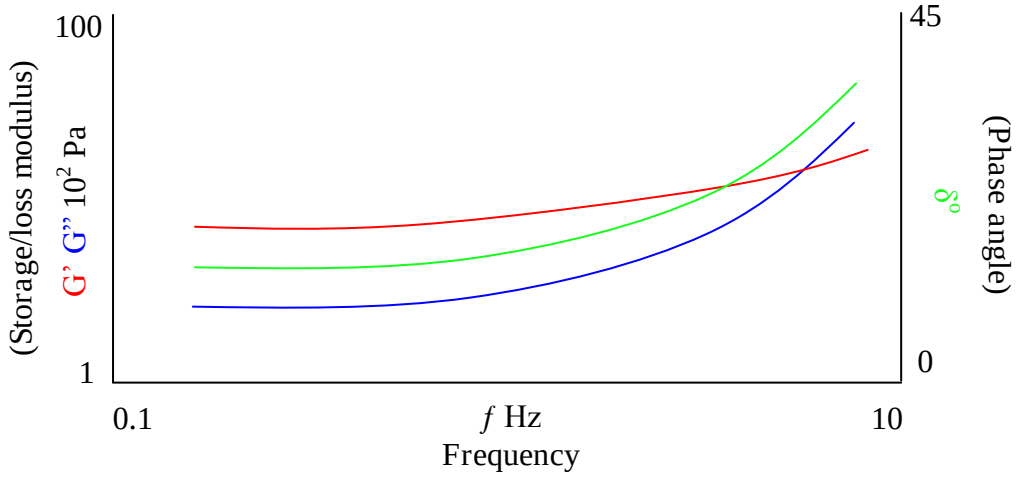

Figure 4.20: Graphical representation of a typical frequency sweep

4.5.2.4 Parameters used in the characterisation tests

With respect to the amplitude sweep, a shear stress range of 0.5 Pa to 50 Pa was investigated with a constant frequency of 1 Hz. During the frequency sweep, a constant stress of 2 Pa was applied, as this was identified to be within the LVR for the pastes, while for the frequency a range of 0.1 Hz to 10 Hz was used. Regarding the shear rate sweep, a range of $0.001s^{-1}$ to $15s^{-1}$ was considered (see Table 4.4). It should be noted that during each of the characterisation tests, a parallel-plate geometry with a diameter of 40 mm and a sample thickness of 1 mm was employed, with a constant ambient temperature of 25°C.

Characterisation Test	σ – shear stress (Pa)	f – frequency (Hz)	$\dot{\gamma}$ – shear rate (s^{-1})	Temperature (°C)
Amplitude sweep	0.5 to 50	1	-	25
Frequency sweep	2	0.1 to 10	-	25
Shear rate sweep	-	-	0.001 to 15	25

Table 4.4: Parameters used in the rheological characterisation tests

4.5.2.5 Results from the characterisation tests

Results from the characterisation tests highlighted many trends, one of which was the existence of pseudoplastic behaviour within the samples. As this is a common property of solder paste materials, this trend was one that was expected. By conducting the viscometry testing as a means of characterising the samples, the shear thinning classification became apparent. From Figure 4.21, it can be seen that each of the samples demonstrated a reduction in paste viscosity as an increase in shear was experienced. However, one significant observation, made through a comparison of each of the samples used within the study, was that a close correlation between results was demonstrated, with a slightly elevated viscosity observed for sample A.

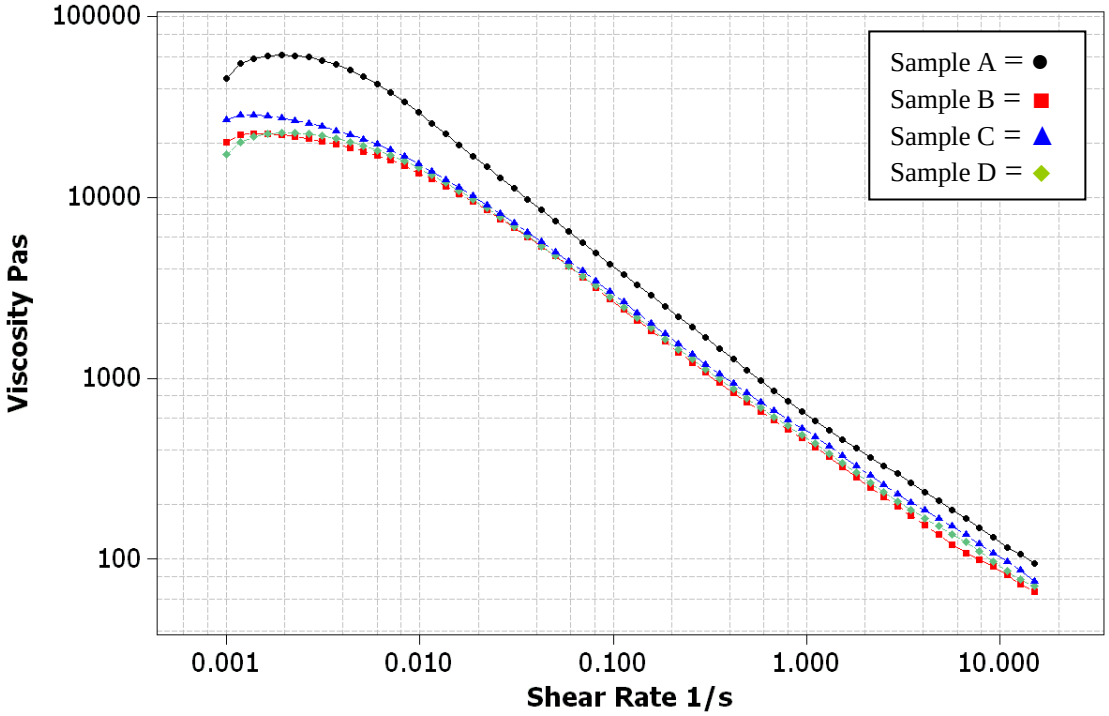

Figure 4.21: Results from the shear rate sweep characterisation test

This tendency for an increased viscosity – observed in each of the trials conducted – may be as a result of the increased PSD employed during the paste's manufacture. If this assumption is correct, the reasoning could also assist with providing an explanation for the elevated viscosity of sample C when compared with samples B and D (both of which were formulated using a reduced particle size distribution). The apparent influence of the PSD on viscosity may arise from the reduction in 'free space' for particle motion that is associated with an increase in PSD. As a consequence of this decrease in unoccupied space, the number of particle-to-particle collisions or interactions naturally increases, which results in an observed rise in viscosity as a result of the amplified internal friction.

With regard to the oscillatory characterisation tests, results further highlighted the similarity that existed between the paste samples, with common trends observed for each. Through investigating the LVR of the solder pastes, it was found that the upper limit for undertaking non-destructive research concluded between 5 Pa and 7 Pa for each of the samples. This result was complemented by an increase in phase angle, which reached a peak of between 40° and 45° during the testing period. Furthermore, the solid-like behaviour of the samples was emphasised, as the modulus of elasticity (G') remained dominant throughout the tests – as can be seen in Figure 4.22.

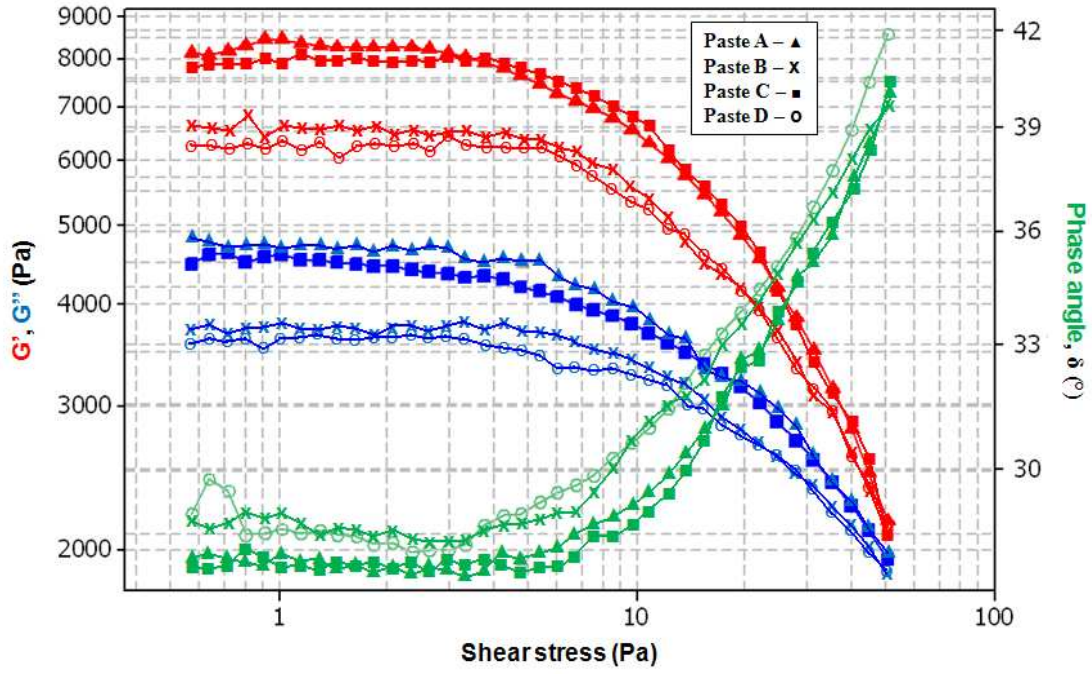

Figure 4.22: Results from the amplitude sweep characterisation test

Results from the frequency tests further highlighted that the paste samples demonstrate a predominant elastic component and therefore are naturally more solid-like in nature. This can also be seen from the values obtained for the phase angle, which remained below 45° throughout all measurements – where 90° represents purely viscous flow – with the exception of the final measurements for samples B and D. Additionally, the frequency sweep revealed that each of the pastes may be classified as time-dependent, which may be identified from the increase in measurements that follow an increase in frequency. The significance of this may be seen through the equation:

$$\text{Frequency} = \frac{1}{\text{Time}} \qquad \textbf{[4.1]}$$

Through application of equation [4.1], it is possible to identify that time is inversely proportional to frequency. Therefore, as the frequency is increased, the time decreases – in terms of the phase angle, this represents a decrease in viscous flow with increasing time. This relationship between phase angle and time demonstrates that during short passages of time, the samples behave elastically, whereas for long timeframes the pastes flow more viscously (Figures 4.23 and 4.24).

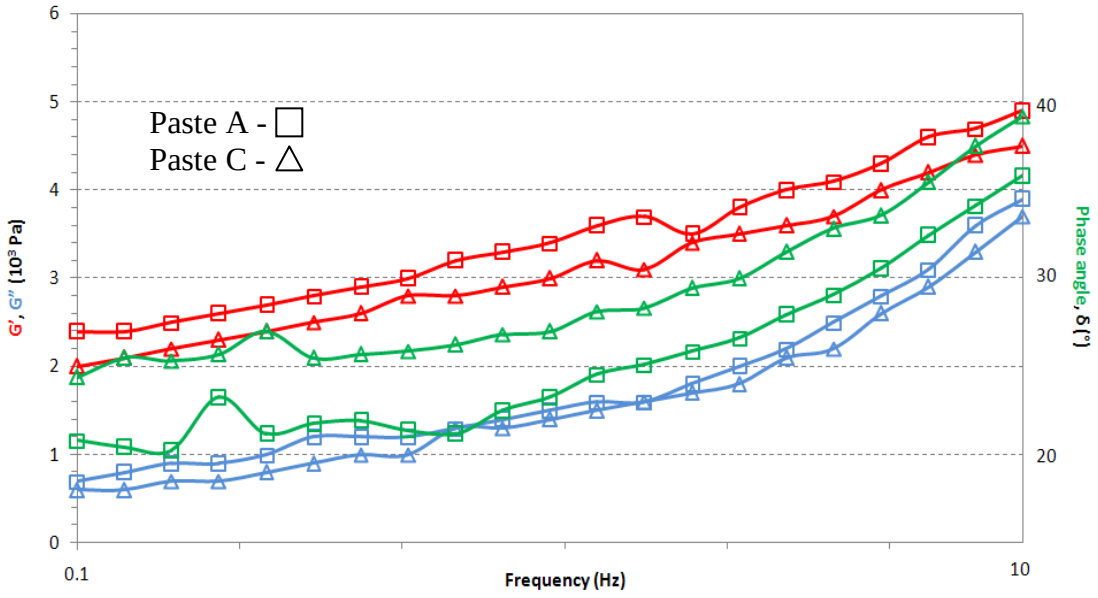

Figure 4.23: Results of the frequency sweep for pastes A and C

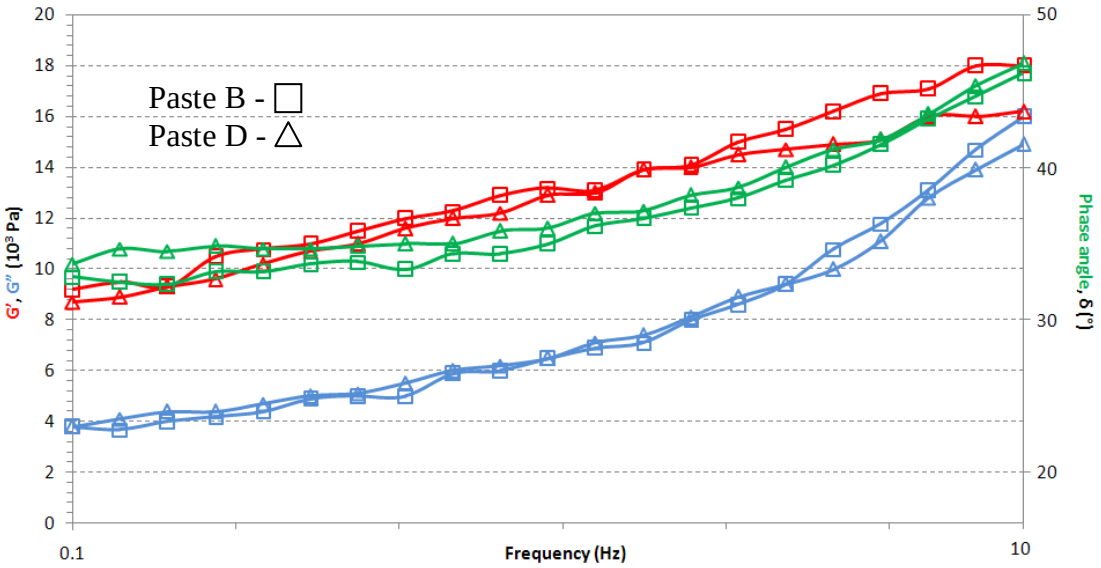

Figure 4.24: Results of the frequency sweep for pastes B and D

CHAPTER 5:
EFFECT OF FLUX COMPOSITION AND PSD ON THE CREEP RECOVERY PERFORMANCE OF LEAD-FREE SOLDER PASTES USED FOR FLIP-CHIP ASSEMBLY

5.1 Introduction

The focus of this chapter is the effect of flux composition and PSD on the creep recovery performance of Pb-free solder pastes. The aim of the study was to determine the extent to which the flux vehicle system and PSD can influence the creep recovery behaviour of paste materials. The tendency of a paste sample to flow after deposition leads to bridging and/or slumping defects in the paste printing process. With the flux medium dictating core properties such as viscosity, tack and flow behaviour, understanding its influence on the quality of print is essential. Further common defects encountered during the printing process include clogging of the apertures and skipping. Previous studies have related such issues to the PSD of the solder paste, suggesting that the solder powder should be of a ratio less than one-half the thickness of the stencil (Hwang, 1989).

Finding the correlation between stencil printing process parameters and rheological properties of pastes has been a long-standing challenge. By understanding how to improve the elastic response of an existing product (hence the 'recovery' of a material after removal of stress), it becomes possible to reduce print defects. In this case, improving a solder paste's capability to recover would increase its ability to retain deposit shape after removal of the stencil, effectively minimising the occurrence of slump.

The creep recovery method allows for an indication of the structural breakdown of a paste that is subjected to a constant stress – for example that exerted by a squeegee during printing – and the resultant elastic recovery of the paste upon removal of the

stress. The level of structural breakdown is an important characteristic to monitor; however, combining this result with the corresponding recovery highlights the ability of a paste deposit to retain shape after withdrawal from the aperture.

5.2 Creep recovery testing

With the challenge of finding correlations between paste rheology and printing performance; creep recovery testing offers an important understanding as to the ability of the paste to maintain deposit shape after removal of the stencil, and consequently the slumping tendency of a paste. As described in the previous chapter, solder paste combines both viscous and elastic components, each of which aid in determining the actual behaviour of the paste under an applied force. Therefore, it is possible that the structure of the material may be destroyed upon application of a sufficiently large stress. Creep recovery tests allow for characterisation of the elastic component by introducing a low stress to the material, which is held for a specific amount of time and removed once a purely viscous flow is observed. By monitoring the resultant strain, it is then possible to determine the degree to which the paste is able to regain its initial structure.

It is important to recognise that, when conducting creep recovery testing, compliance is generally displayed as opposed to strain (as shown in Figure 5.1). This is because the change of strain is dependent on the applied stress, thus making comparisons difficult between graphs with varied values for stress. Incorporating the compliance when analysing and producing graphs removes these difficulties, as this is simply a ratio of strain to applied stress.

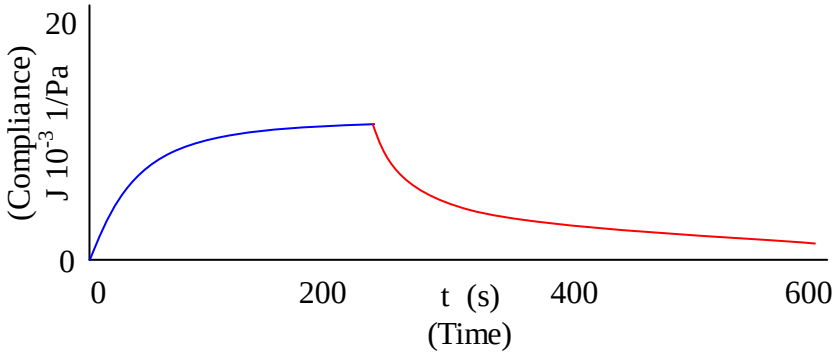

Figure 5.1: Typical creep recovery curve for a viscoelastic material

Initial tests in this study focused on the comparison of results between paste samples with variations in flux. During each test, 5 Pa of stress was applied to the sample for a period of 300 seconds, after which there was an allowed period of recovery of 600 seconds to monitor the elastic response of the sample. The value of 5 Pa was selected as Bao et al (1998) reported that testing should be conducted within the LVR of the material, with Durairaj et al (2009[a]) stating that for a paste with an LVR ranging up to 9.7 Pa, an applied stress of 5 Pa was selected during creep testing. The test was repeated on the paste with the same formulation as the initial sample, with the exception of the flux medium used. After having obtained the results, the tests were repeated on each paste a further six times to highlight any anomalous results and ensure reliability.

The subsequent phase of the study was testing the samples which varied due to PSD. Those parameters used previously were maintained for consistency reasons, ensuring that all results could be sensibly compared. Once again, an additional six trials were conducted on each paste to highlight anomalous results and further ensure consistency.

5.3 Creep recovery results and discussion

Results from this study's creep recovery testing have highlighted that, in order to achieve a successful recovery, a clear dependency exists on the formulation of the solder paste. Initial results highlighted that the flux medium selected during the paste manufacturing process can significantly influence the creep recovery behaviour of samples (see Figure 5.2). Upon comparing those results obtained for samples A and C with those obtained for samples B and D (those samples that had been formulated with a change in flux), this trend can be clearly observed in the graphs. In each instance, the results highlight that an alteration in the flux type can significantly improve paste recovery upon removal of applied stress. When continuing with the investigation, it became apparent that this trend may also be seen with a change in selected PSD.

By conducting a comparison between results for samples A and B, it becomes evident that paste recoverability (once an applied stress has been removed) can be almost fully eliminated through an alteration in PSD during the paste manufacturing process. The significance of these findings is relevant to consideration of the printing process, because a paste's inability to regain structure could lead to common defects such as slump and bridging becoming a concern. The correlation between PSD and an improved recovery may be due to the increase in viscosity that is associated with an increase in PSD – as reported in work conducted by Fletcher and Hill (2008). With the increased number of particle interactions – as a result of being more tightly packed – an increased resistance to flow ensues. Therefore, after concluding the stencil printing process the paste is able to retain a high viscosity and hence is more likely to maintain shape/structure, consequently demonstrating an improved ability to recover upon removal of stress.

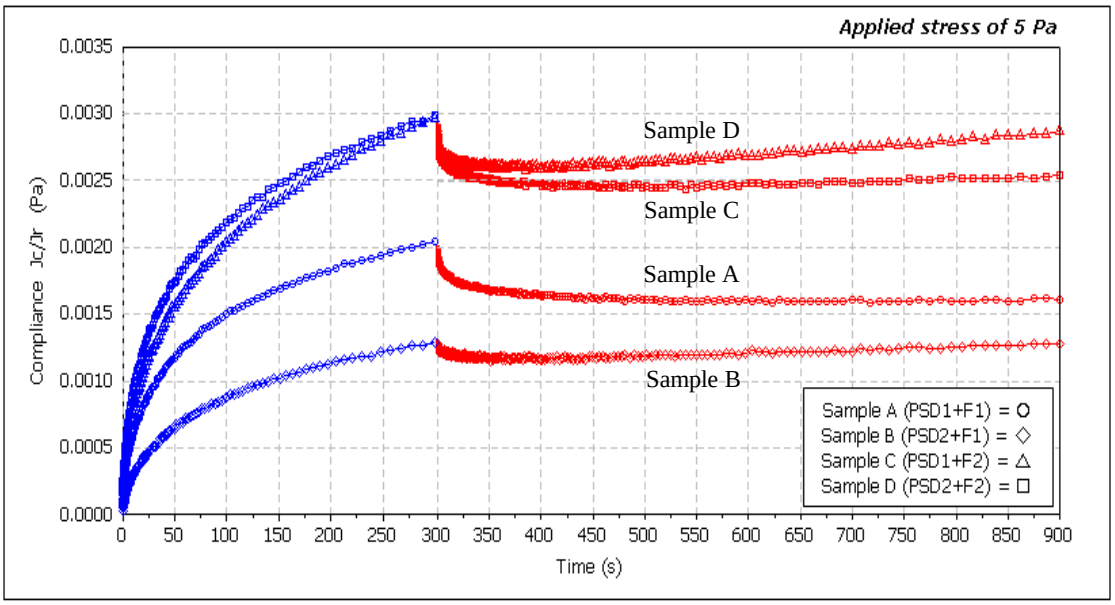

Figure 5.2: Graph showing the creep recovery performance of the paste samples

In order to understand these results further, the Marks equation for calculating recoverability was used [5.1], where J_1 is equal to the instantaneous strain (initial compliance), J_2 is the final creep compliance and J_3 is the final recovery compliance.

$$\text{Recovery Percentage (\%)} = \frac{J_2 - J_3}{J_2 - J_1} \times 100 \qquad \textbf{[5.1]}$$

Using this equation, it was observed that large variations in the recovery percentage were present, depending on the formulation of the solder pastes. This has been laid out in Table 5.1.

Solder Paste	J_1 (1/Pa)	J_2 (1/Pa)	J_3 (1/Pa)	Creep Recovery Index	Recovery Percentage (%)
Sample A	0.0000749	0.002045	0.001612	0.788264	21.98
Sample B	0.0000243	0.001287	0.001279	0.993784	0.63
Sample C	0.0001398	0.002992	0.002538	0.848262	15.92
Sample D	0.0001139	0.002971	0.002869	0.965681	3.57

Table 5.1: Details of compliance values for each of the paste samples

A further understanding of the influence of PSD and flux on the creep recovery performance of solder pastes can be gained through calculating the creep recovery index (Table 5.1). The creep recovery index (κ) is calculated using equation [5.2] as discussed in work by Nguty et al (1998), where a value tending towards 1 indicates a low level of recovery, and an exact value of 1 indicates no structural recovery.

$$\text{Creep-recovery index } (\kappa) = \frac{J_3}{J_2} \qquad \textbf{[5.2]}$$

Following these methods of quantifying the rheological results, it was possible to further analyse the results attained. Upon successful application of the Marks equation, it was found that in one instance the recovery percentage highlighted a variation of 6.06 percentage points between the paste samples as a result of flux variation. This was of significance, as this indicates that through appropriate selection of the flux during formulation, paste structure can possess the ability to rebuild to a greater extent, consequently leading to a lesser extent of paste flow upon removal of the stencil. Furthermore, results highlighted that PSD selection has a significant impact on creep recovery behaviour, with an observed variation in recovery

percentage of 21.35 percentage points in one instance. From these results, it becomes apparent that opportunities exist to further progress towards successfully discovering a correlation between paste rheology and the printing process through appropriate selection of paste constituents.

5.4 Printing results and discussion

During the course of the printing trials, preliminary findings highlighted significant variations between the samples, particularly pertaining to the level of bridging observed between deposits. Through consideration of those rheological findings from the study, this was a trend to be expected due to the recovery percentages calculated. That is, the paste samples clearly demonstrated significant variations in ability to recover from an applied stress, which could lead to differences in slump behaviour. In order to further understand these results, the VisionMaster equipment was utilised to determine the average heights of the solder paste deposits using equation [5.3]. In addition, using fundamental mathematical equations for calculating volumes, equation [5.4] was employed in an attempt to confirm the average height of the solder paste deposits as recorded by the VisionMaster apparatus. So we have:

$$\text{Average height} = \frac{\Sigma\,(h_i)}{(N \times (U_p - L_p))} \qquad \textbf{[5.3]}$$

where h is the height value at one pixel, N is the total number of height points, L_p is the lower sort cut-off percentage, U_p is the upper sort cut-off percentage and i is equal to the values of $(N \times L_p)$ up to $(N \times U_p)$ inclusive (for example, $(N \times L_p) + 1$, $(N \times L_p) + 2$, and so on). And we also have for average height:

$$\text{Average height of deposit } (\mu) = \frac{\text{Volume of Solder Paste}}{(\text{Length of Deposit x Breadth of Deposit})} \qquad \textbf{[5.4]}$$

By applying these equations, and hence calculating the average height of the solder paste deposits, it was intended to gain an indication of the slumping tendency after

completion of the printing process. As a result of having previously discovered rheological results for creep behaviour, these two methods of investigation can then be correlated in an attempt to confirm the influence of flux and particle size distribution on paste recoverability. During the investigation, samples A and B were subjected to six printing trials in order to identify print acceptability and quality for each, while allowing for anomalous results to be highlighted. Samples A and B were selected because they highlighted the greatest variation in recovery percentage from the rheological testing. From the results obtained, reliability of the findings was paramount and, as such, the highest and lowest volumes for the deposits were eliminated, with an average being taken from the remaining four results (Table 5.2).

Solder Paste	**Width (µm)**	**Length (µm)**	**Volume ($\mu m^3 \times 10^8$)**	**Average Height (µm)**	
				VisionMaster	**Manual calculation**
Sample A	642.857	2071.429	2.208	165.875	165.812
Recovery (Rheological)				21.979 %	
Sample B	642.857	1928.571	1.334	107.619	107.598
Recovery (Rheological)				0.634 %	

Table 5.2: Average height of print deposits compared with rheological results
(All results correct to three decimal places)

Results from the printing trials highlighted that correlations can be formed with those rheological results previously obtained. Upon review of the results shown in Table 5.2, it becomes apparent that sample B demonstrated a significantly reduced deposit height during the printing process, whilst also displaying a much lesser level of recoverability – through considering a deposit's ability to retain structural stability, the importance of this becomes evident. Rheological studies demonstrated that sample B was more susceptible to permanent structural breakdown, due to its inability to recover substantially after removal of stress, particularly when drawing comparisons with the results from sample A. When considering stencil printing, such

application of stress may be seen by forces rolling the paste into the apertures. From this observation, it may be possible to state that sample B had a greater tendency to display slumping characteristics due to its inability to recover structurally (see Figure 5.3), which could possibly account for the reduction in average paste deposit height between the two samples (58.256 microns). This could occur because an inability to recover structural integrity could lead to the incapability of retaining deposit shape, as once the flow behaviour has been initiated, the sample would be unable to prevent flow from continuing upon removal of stress. Although this could lead to the common defect of bridging, it may also present the possibility of reduced deposit height (as shown in Figures 5.4 and 5.5).

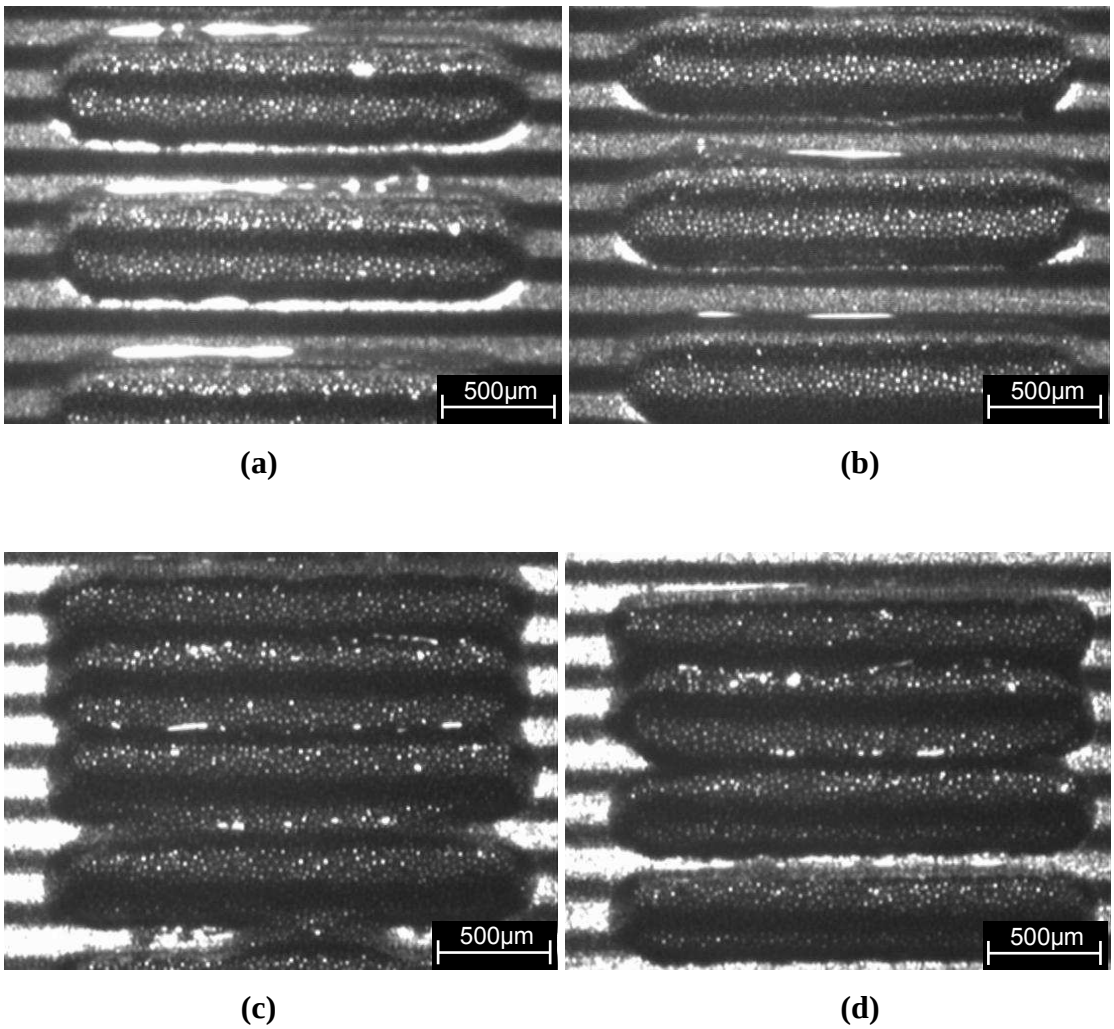

Figure 5.3: Sample prints for pastes A and B demonstrating slumping variations: (a) Paste B – 0.63 × 2.03 mm pads; (b) Paste A – 0.63 × 2.03 mm pads; (c) Paste B – 0.33 × 2.03 mm pads; (d) Paste A – 0.33 × 2.03 mm pads.

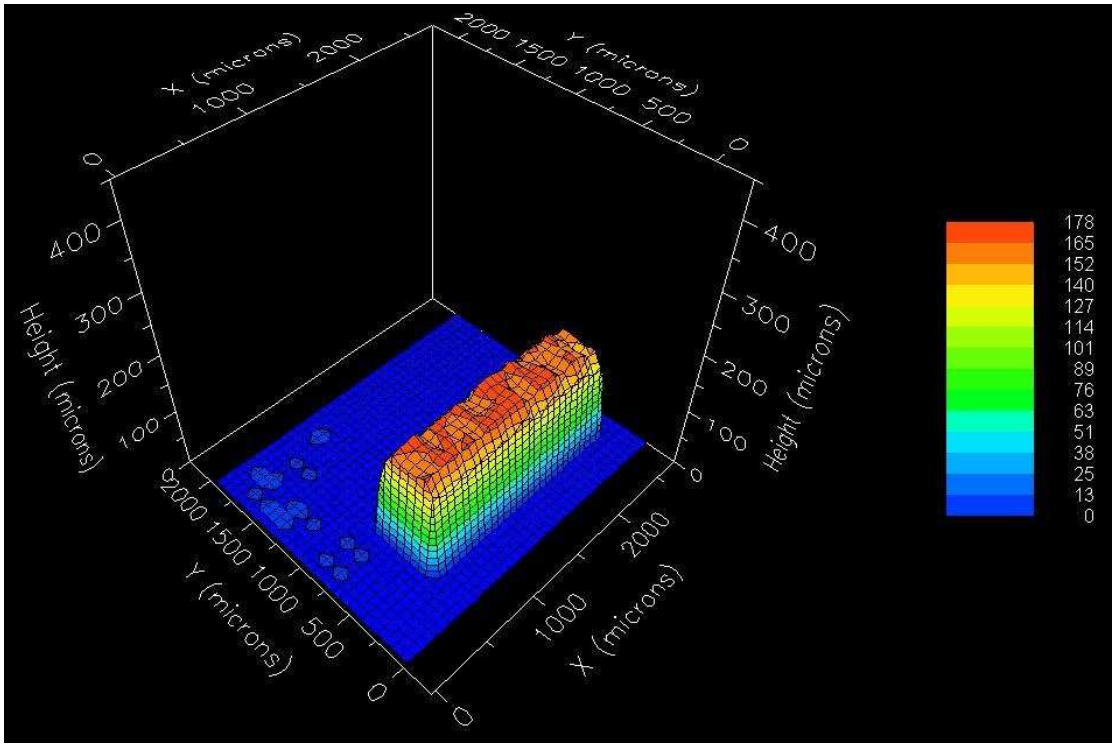

Figure 5.4: VisionMaster 3-D profile for paste A

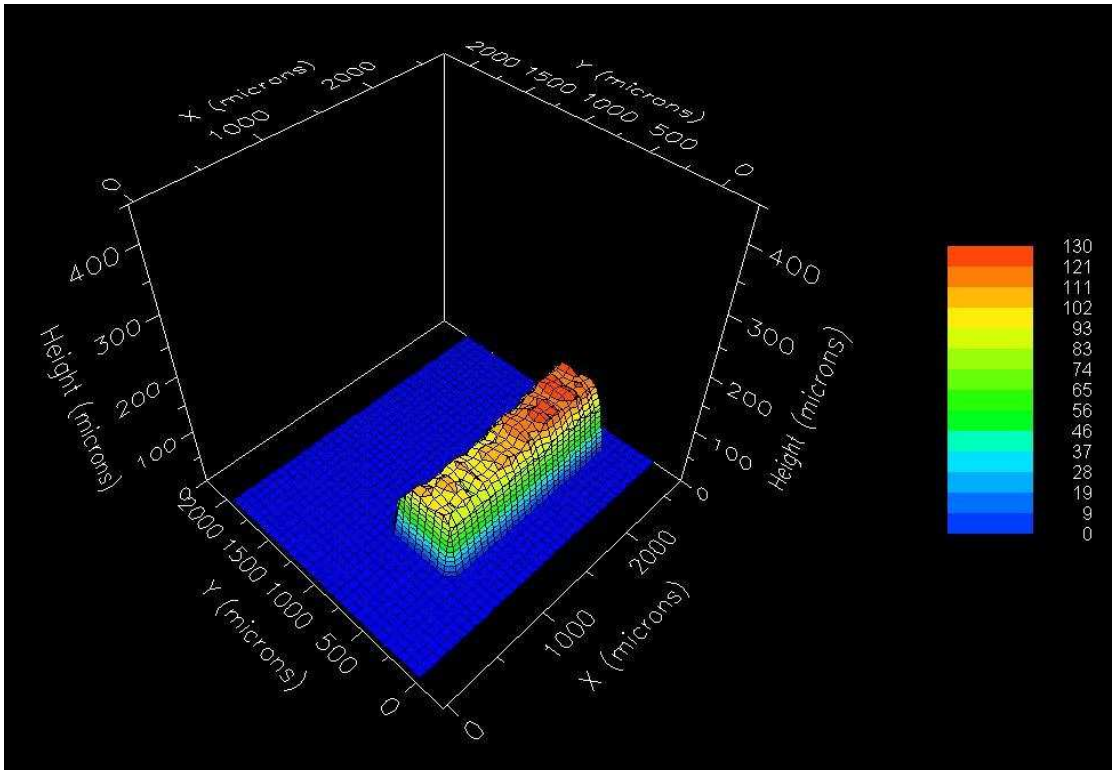

Figure 5.5: VisionMaster 3-D profile for paste B

5.5 Conclusions

The influence of flux and PSD on creep recovery performance has been investigated through conducting rheological measurements and printing trials on four Pb-free solder pastes. Initial research into rheological measurements of the samples highlighted the important role that the formulation of a solder paste can have on the quality of print. Results signify that a paste's ability to recover structurally upon removal of an applied stress is dependent on both the flux and PSD selected. This dependency was clearly highlighted, with one particular result demonstrating that an increase in PSD from a range of 20–38 microns (type 4) to a range of 25–45 microns (type 3) led to an increase in the recovery percentage from 0.63% to 21.98%. Further observations emphasised how an alteration in flux during the formulation process can negatively influence the recovery behaviour, with a decrease in recovery percentage from 21.98% to 15.98% being observed. The importance of these results was emphasised by conducting printing trials, which demonstrated that a significant increase in slumping behaviour was exhibited by those samples with a lower recovery percentage.

Upon concluding the printing trials, the printed deposits were then subjected to 3-D profiling studies, from which the results highlighted that paste sample A displayed a peak height of 178 microns after conducting the print process, whereas sample B displayed a peak height of only 130microns. Further to this, the average paste height after printing for sample A was 165.8 microns, whereas the average paste height for sample B was 107.7 microns. These findings are of significance, as this reduction in paste height could allow for correlations to be formed with slump behaviour observed during the printing trials and, furthermore, may provide an indication of the importance of paste recovery.

By correlating the results attained from both the printing trials and the rheological investigations, findings suggest that solder paste materials which demonstrate a reduced ability to recover structurally upon removal of stress will consequently exhibit an inability to retain deposit definition. By displaying such a characteristic,

this could therefore lead to increased slumping and consequentially bridging defects, which can be exacerbated even further through a subsequent reduction in paste height.

From those studies conducted, it becomes apparent that the flux and PSD play a pivotal role in the creep recovery behaviour of solder pastes. With regard to the stencil printing process, this is an important finding as creep behaviour can be contrasted with the stress applied to the solder paste during the print, whereas the recovery can be compared with the printed deposits at rest after removal of the stencil. Based on the findings from the study, it may be possible to develop samples that consistently exhibit high values of recoverability through introducing such an investigational method into the paste manufacturing process (possibly as a quality control tool). If this is possible, the potential exists for reducing and minimising the influence of defects on the reliability and quality of the printing process.

CHAPTER 6:
INFLUENCE OF LONG-TERM AGEING ON THE RHEOLOGY AND PRINT QUALITY OF LEAD-FREE SOLDER PASTES USED FOR FLIP-CHIP ASSEMBLY

6.1 Introduction

This chapter presents an investigation into the effect of long-term ageing on the rheology of Pb-free solder pastes and their print qualities. The shelf life of solder paste (as declared by the paste manufacturer) was studied to establish the shelf life at which the print quality was still of acceptable standard (usually six months is specified by the manufacturer). Three main paste characterisation techniques were used during the study: shear rate sweeps, amplitude sweeps and frequency sweeps. Additionally, three methods of storage were employed: a freezer environment, refrigeration, and storage at room temperature, all of which were applied for 24 months, with testing conducted on a monthly basis.

As mentioned above, current standards recommend a six-month lifespan for paste products; however, this is dependent on storage conditions and is merely an estimated shelf life. With the large quantity of solder paste produced by paste manufacturers, it is important to study shelf life in order to minimise waste caused by disposal of material that remains effective for SMA. Furthermore, by demonstrating that increases in paste life are possible, reductions in environmental effects and consumer costs become feasible.

Solder paste is a very complex material, and storage can greatly influence the long-term performance of a sample (ADTOOL, 2002; Coombs, 2008), with structural changes occurring in unsuitable environments. Atmospheric influences can cause the quality of a solder paste to deteriorate due to the formation of oxide layers; however, common storage methods present a possibility of sedimentation, which results in a

layer of flux forming on the surface of the sample. As a means of addressing such issues, it is advised that test materials are placed into storage at low temperature and exposure to typical atmospheric conditions is minimised.

An understanding of the effects of ageing on solder paste under different storage conditions will help to correlate the rheological characteristics of aged paste samples to printing performance. Consequently, opportunities exist to develop methodologies for benchmarking new formulations in terms of shelf life, rheological deterioration and print performance. Furthermore, the evaluation of such results can lead to the minimisation of environmental effects and create standards that can be implemented to retain paste quality.

6.2 Materials used and preparation

Throughout the duration of the study, two commercially available Pb-free paste formulations were used to investigate the shelf life property – both with a recommended shelf life of six months. In order to maintain as much consistency as possible (to ensure that variations in paste behaviour could not be attributed to several alternative variables), the only notable dissimilarity between the paste samples was that of the flux used during formulation.

The main part of the study commenced after segregation of the paste samples into monthly quantities to compare results over a period of 24 months. While preparing these monthly testing samples, specimens were further separated to allow for exposure to various storage temperatures. As general storage guidelines commonly dictate that paste should be stored between 0°C and 10°C, the first storage environment was that of a refrigerator maintained at 4°C. In addition, other samples were subjected to storage at room temperature (which deviated only between 23°C and 26°C throughout the course of the investigation), and finally in a freezer environment of –40°C in an attempt to understand whether the possibility of freezing paste exists, or whether guidelines dictating that paste must not be frozen are accurate.

The testing itself comprised printing trials and three rheological methods of study: (1) viscometry shear rate sweeps; (2) oscillatory amplitude sweeps; and (3) oscillatory

frequency sweeps. During the oscillatory and viscometry testing, the parameters were preserved as those from the preliminary rheological characterisation tests (as discussed within Chapter 4), while those parameters utilised for the creep recovery tests were taken from the study of creep behaviour as detailed within Chapter 5.

During the printing trials, the print quality was measured through regularly performing an assessment of specific characteristics, allowing comparisons to be made relating to the acceptability of the printing over a period of time. These included: paste roll, drop-off, bridging, skipping, shape of deposit, and cleanliness of the stencil and aperture after print. Table 6.1 highlights the sequence of testing that was undertaken during the investigation. Initially only six months of tests were intended, due to standard shelf-life properties, but this was increased to 24 months to highlight the point at which paste quality deteriorates.

Length of storage	**Paste Sample**	**Storage conditions**		
		Fridge (4°C)	**Ambient *(≈25°C)***	**Freezer (–40°C)**
1 month	A	Test 1	Test 3	Test 5
	B	Test 2	Test 4	Test 6
2 months	A	Test 7	Test 9	Test 11
	B	Test 8	Test 10	Test 12
3 months	A	Test 13	Test 15	Test 17
	B	Test 14	Test 16	Test 18
4 months	A	Test 19	Test 21	Test 23
	B	Test 20	Test 22	Test 24
5 months	A	Test 25	Test 27	Test 29
	B	Test 26	Test 28	Test 30
6 months	A	Test 31	Test 33	Test 35
	B	Test 32	Test 34	Test 36
12 months	A	Test 37	Test 39	Test 41
	B	Test 38	Test 40	Test 42
18 months	A	Test 43	Test 45	Test 47
	B	Test 44	Test 46	Test 48
24 months	A	Test 49	Test 51	Test 53
	B	Test 50	Test 52	Test 54

Table 6.1: Sequence of testing undertaken during the study

6.3 Results and discussion

The results from the study showed that after introducing an ageing period of six months (the shelf life recommended by the manufacturer), the solder paste samples that were investigated demonstrated an increase in viscosity – a trend that was expected and that is substantiated through work conducted by Nguty and Ekere (2000^{b}), at low shear values. This trend was seen to continue as the period of ageing was increased beyond six months to 12 months, 18 months and 24 months, and it was apparent regardless of the storage technique used (as seen in Figures 6.1 to 6.6 inclusive).

This observation, which may have been caused by evaporation of solvents from the paste material (consequently resulting in a 'drying-up' effect), flux separation or sedimentation, suggests very little justification for the disposal of solder paste after six months because, as can be seen in Figures 6.1 to 6.6, by simply applying an increased level of shear to a sample, its viscosity can once again converge with its initial viscosity. This was seen to be true for both samples (A and B), regardless of the storage system employed and, more importantly, regardless of the period of storage.

The possible explanations for the increased viscosity (e.g. flux separation or sedimentation) could also explain the convergence of the resultant viscosity after several months of ageing with the initial viscosity, as the application of shear would allow for the paste to regroup with its constituents. Taking paint as an example of this behavioural characteristic, upon being allowed to sit, the paint forms a skin-like growth on its surface; however, upon shearing the paint (by stirring etc.), this skin soon disappears and the paint once again displays its initial fluidity.

A further trend that was highlighted between the samples was that of the effect of the storage method on the viscosity of solder paste, where the variation in storage temperature dictated the increase in viscosity observed. With common guidelines stating that solder paste should optimally be stored between 0°C and 10°C, and some sources stating that paste materials should not be frozen (see Chapter 3, section 3.9.2),

it is believed that the observed result of a minimal increase in viscosity that was witnessed through applying freezer conditions was of great importance and value.

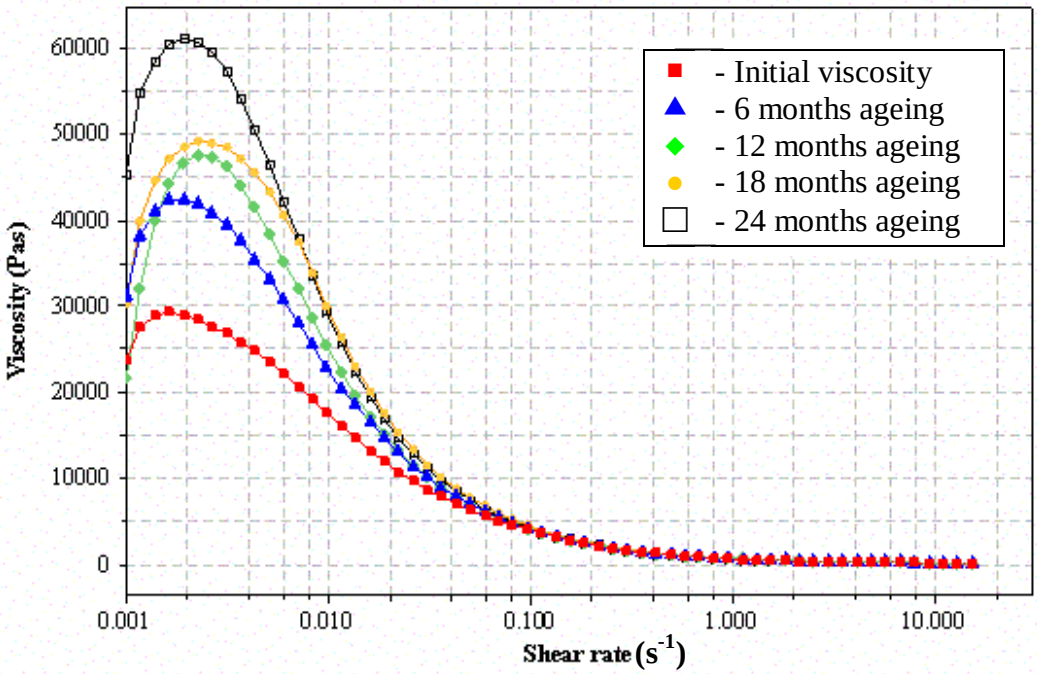

Figure 6.1: Viscosity ageing profile for paste A when stored at room temperature

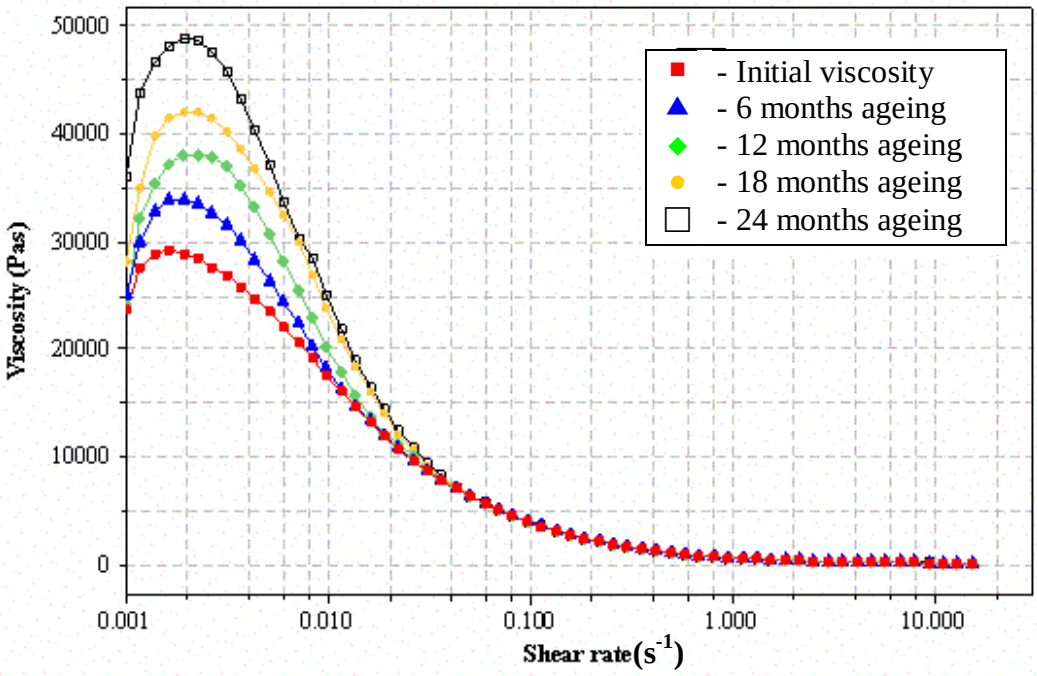

Figure 6.2: Viscosity ageing profile for paste A when refrigerated

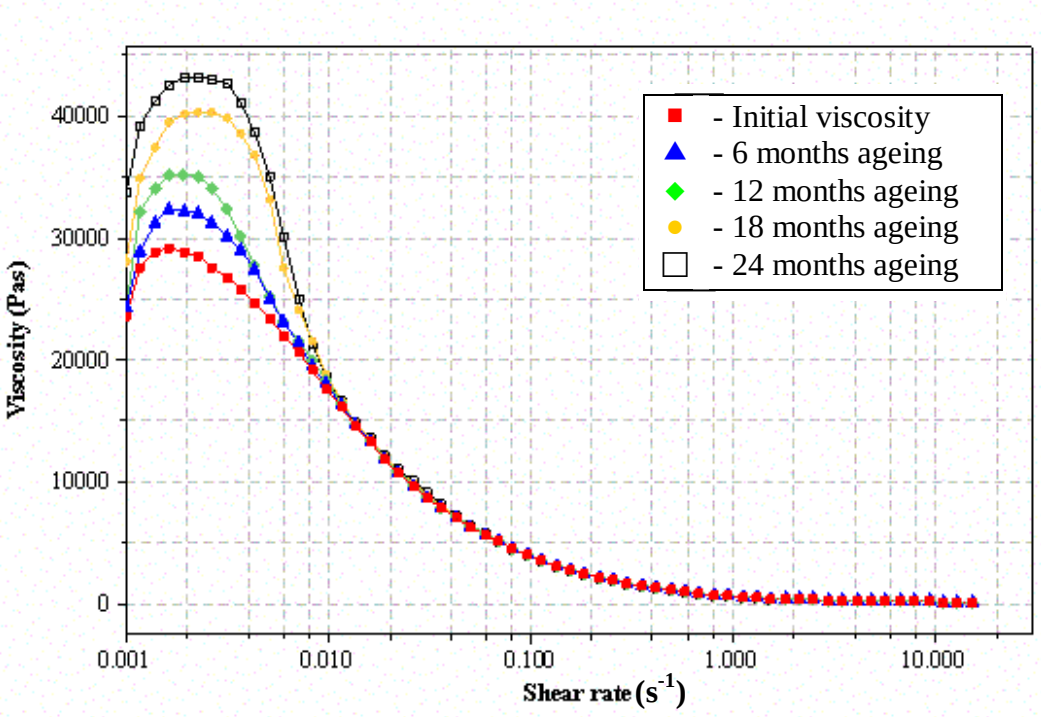

Figure 6.3: Viscosity ageing profile for paste A when in a freezer environment

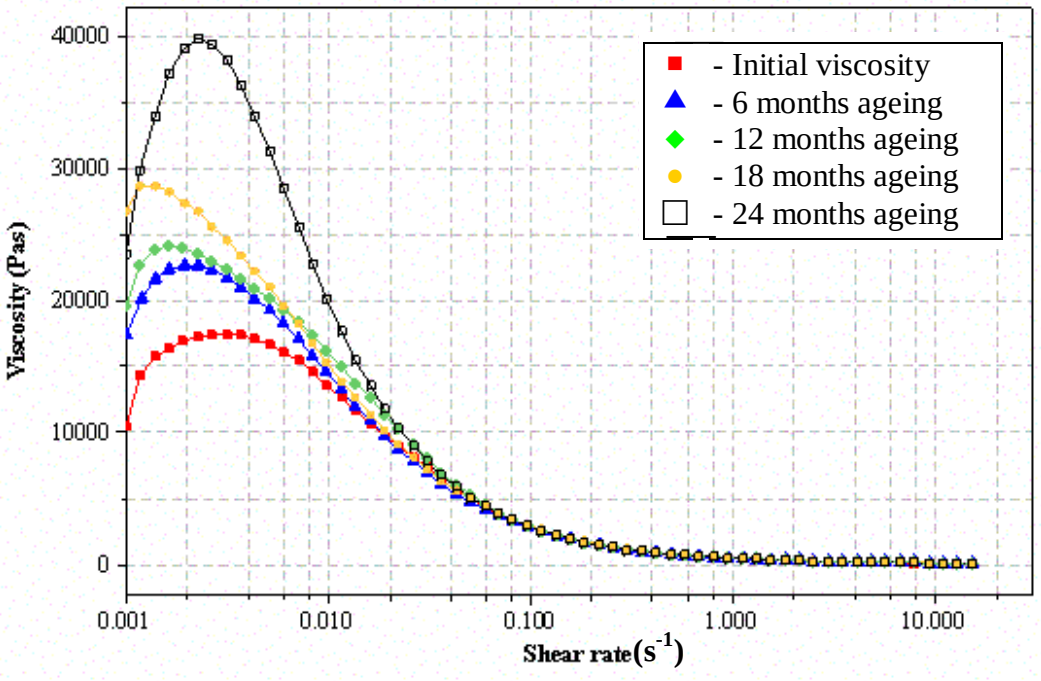

Figure 6.4: Viscosity ageing profile for paste B when stored at room temperature

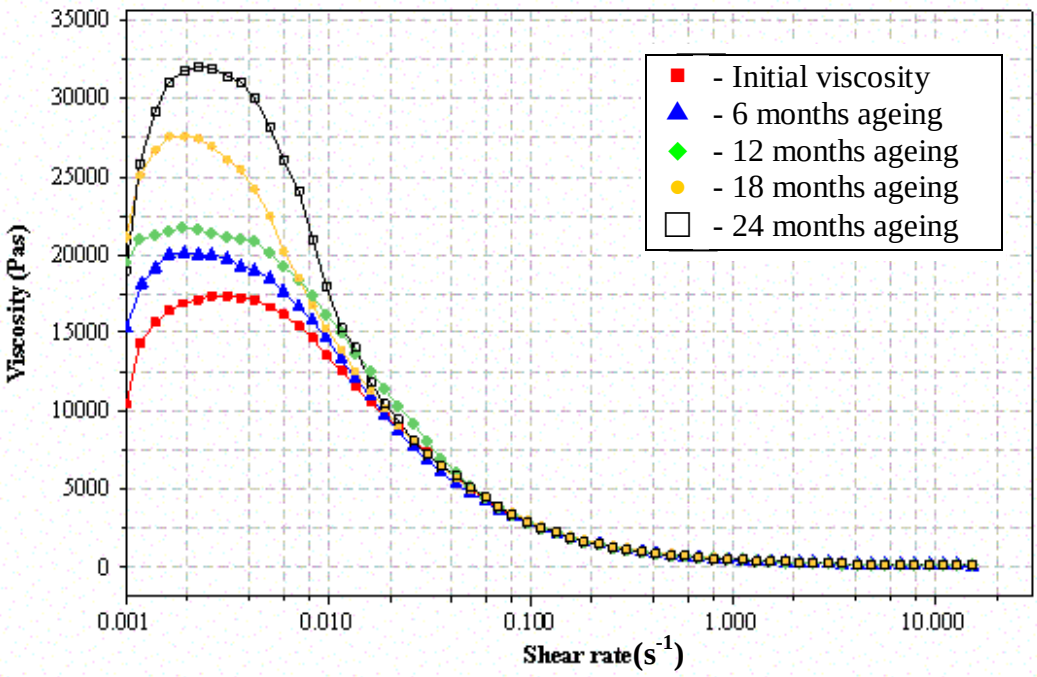

Figure 6.5: Viscosity ageing profile for paste B when refrigerated

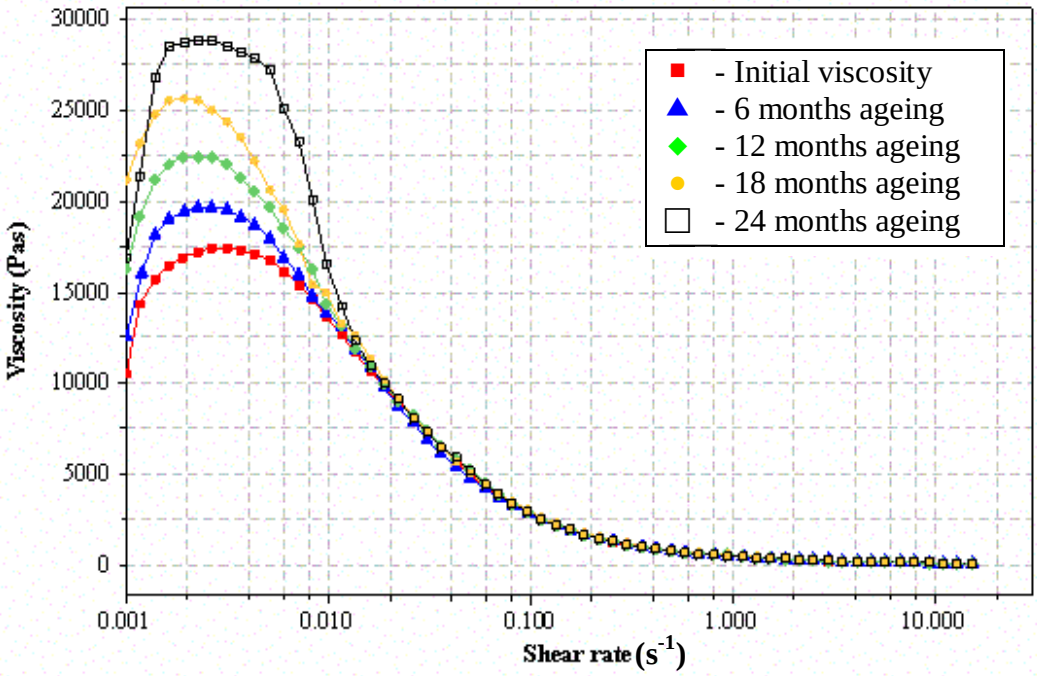

Figure 6.6: Viscosity ageing profile for paste B when in a freezer environment

By examining those results highlighted in Figures 6.7 and 6.8, the importance of the role of storage conditions becomes apparent. Thus it becomes evident that significant findings have been uncovered in relation to the length of ageing that a paste can undergo and in relation to the ability to apply freezer storage conditions. For those paste samples investigated, results clearly highlight that storage in a freezer environment significantly reduces the increase in viscosity observed, particularly when compared with the increase demonstrated upon storage at room conditions. Statistics from the rheological tests further highlight the significance of appropriate storage conditions but from a numerical viewpoint, highlighting that the peak viscosity observed reduced by approximately 17,000 Pas through storage in a freezer environment when compared with room conditions. By applying equation [6.1] it was then possible to determine the percentage increase in viscosity for each storage technique when compared with the initial viscosity measured (see also Table 6.2):

$$\frac{(\eta_s^{max} - \eta_i^{max})}{\eta_i^{max}} \times 100 = \%_{inc} \qquad \textbf{[6.1]}$$

where η_s^{max} is equal to the peak viscosity for the selected storage method, η_i^{max} is the peak viscosity for the initial characterisation test, and $\%_{inc}$ is the percentage increase in viscosity due to applying the storage technique.

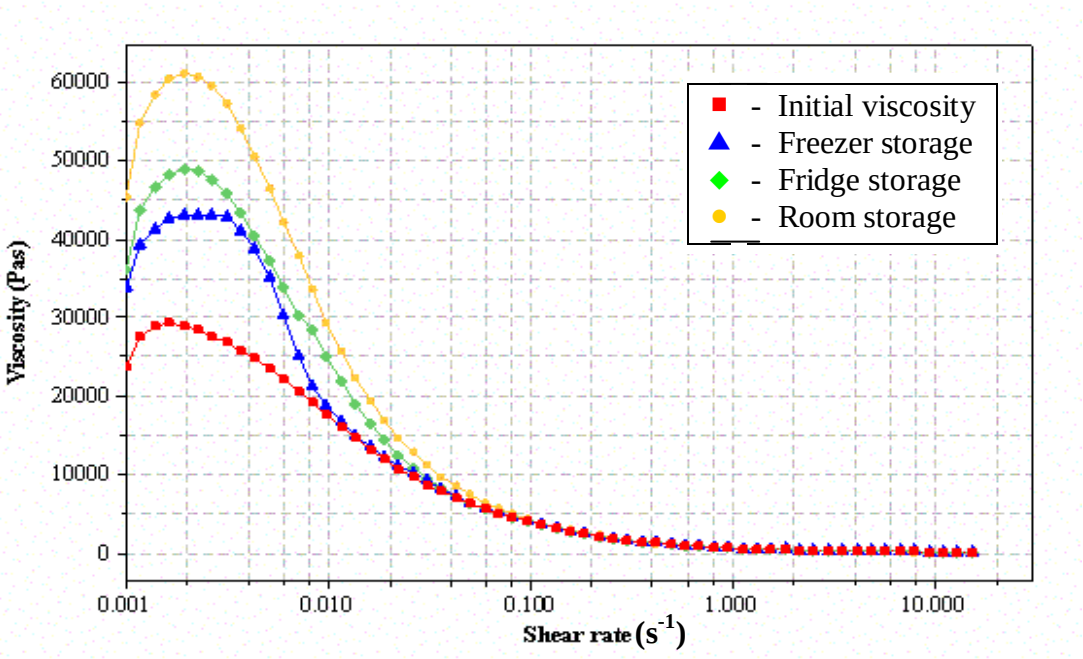

Figure 6.7: Comparison of viscosity profiles for paste A after 24 months of ageing

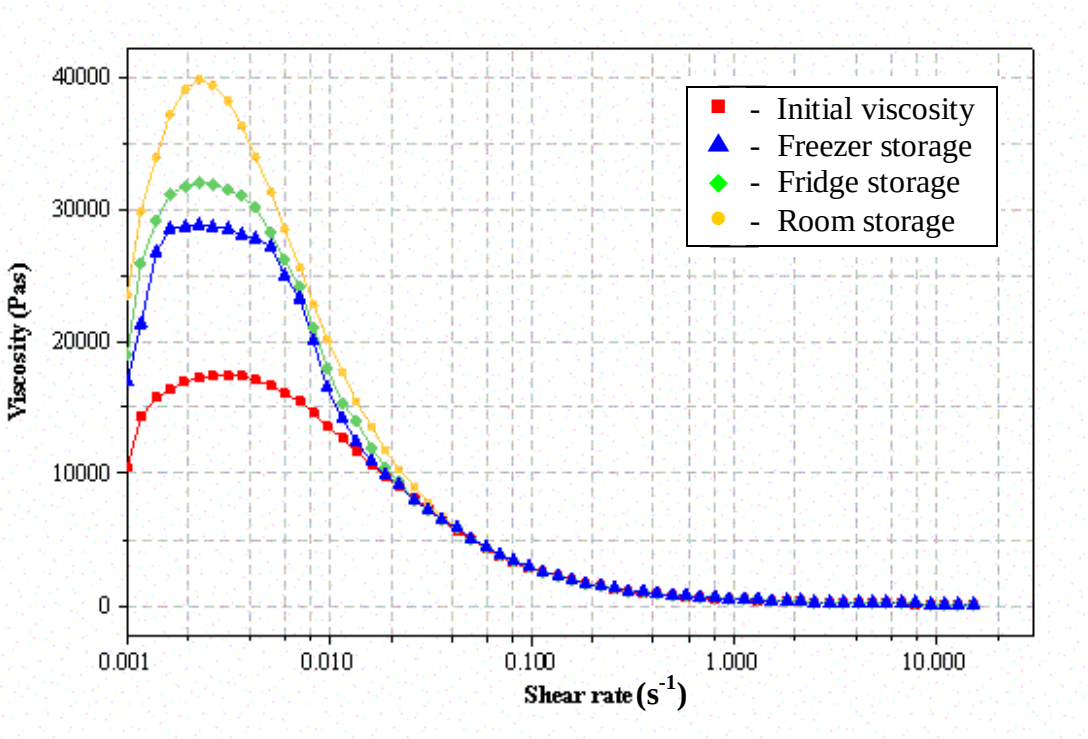

Figure 6.8: Comparison of viscosity profiles for paste B after 24 months of ageing

	Paste viscosity (Pas)	
	A	**B**
Initial viscosity	29180	17390
Room storage (≈25°C)	60980	39820
Total variance	31800	22430
Viscosity increase (%)	108.98	128.98
Initial viscosity	29180	17390
Fridge storage (4°C)	48800	32062
Total variance	19620	14672
Viscosity increase (%)	67.24	84.37
Initial viscosity	29180	17390
Freezer storage (–40°C)	43130	28796
Total variance	13950	11406
Viscosity increase (%)	47.81	65.59

Table 6.2: Comparison of peak viscosity for storage methods after 24 months' ageing

As shown in Table 6.2, when compared with the initial characterisation test, peak viscosity increased by 108.98% when sample A was stored at room conditions for a 24-month period; however, when stored in an environment below freezing point, this percentage increase reduced to 47.81% – a variation of 61.17% between storage techniques. This observed variation demonstrated that the freezer environment, when compared with room conditions, reduced the peak viscosity by 17850 Pas. With regard to sample B, upon application of storage at room conditions for 24 months the recorded viscosity increased by 128.98%, whereas within a freezer environment, although still significant, this was measured as only 65.59%, which demonstrates a variation between the two of 63.39% (11024 Pas).

Figure 6.9 highlights the results of viscosity increase as a percentage against the different storage methods. From the results, it can be seen that both paste samples A and B appear to follow a much-defined trend, with paste B only slightly elevated from those results demonstrated by paste A. This could be of great importance when attempting to understand the influence of storage temperature on solder pastes.

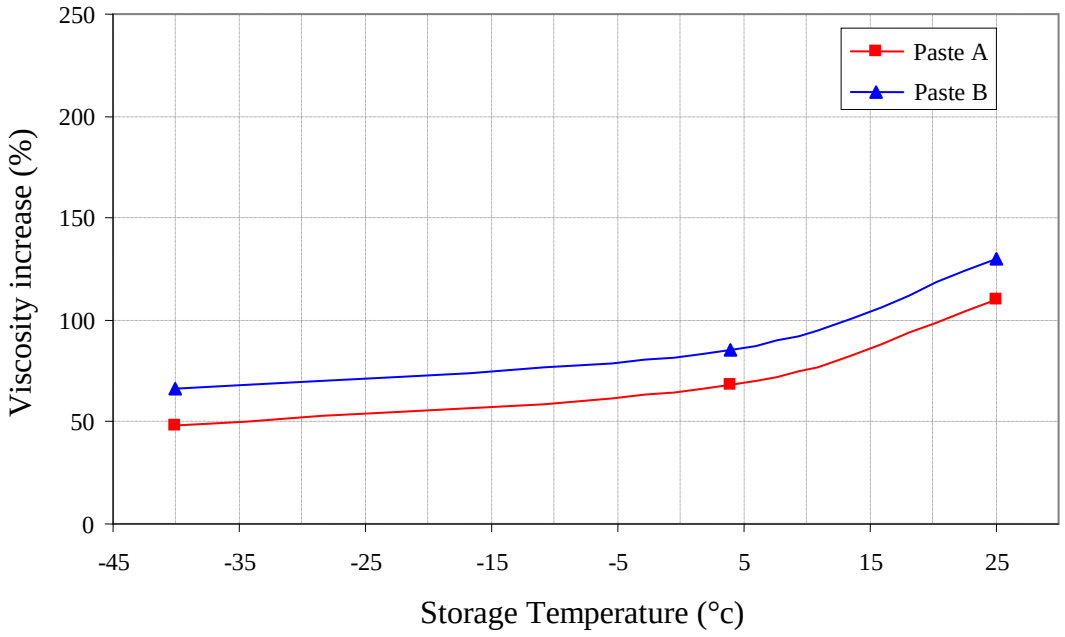

Figure 6.9: Comparison of percentage viscosity increase at different storage temperatures (after 24 months of ageing, and compared with the initial viscosity)

By conducting an investigation into how the Cross model (equation [6.2]) fits against the initial viscosity for both paste samples, it was found that a clear resemblance existed; furthermore, once a shear rate of between 0.01 and 0.03 s^{-1} was reached, the Cross model results overlapped those viscosity results recorded experimentally (see Figures 6.10 and 6.11).

With regard to paste A, it was found that a strong correlation also existed between the model analysis and the viscosity results from investigations conducted after ageing by 24 months. As can be seen in Figure 6.10, as shear rate was increased, the Cross analysis once again overlapped the results observed after the ageing process. So:

$$\eta = \eta_\infty + \frac{\eta_0 - \eta_\infty}{1 + (K \dot{\gamma}^n)} \qquad \textbf{[6.2]}$$

where η_0 is the zero shear viscosity, η_∞ is the infinite shear viscosity, K is the Cross time constant; and n is the Cross rate constant (see Chapter 3, section 3.9.2).

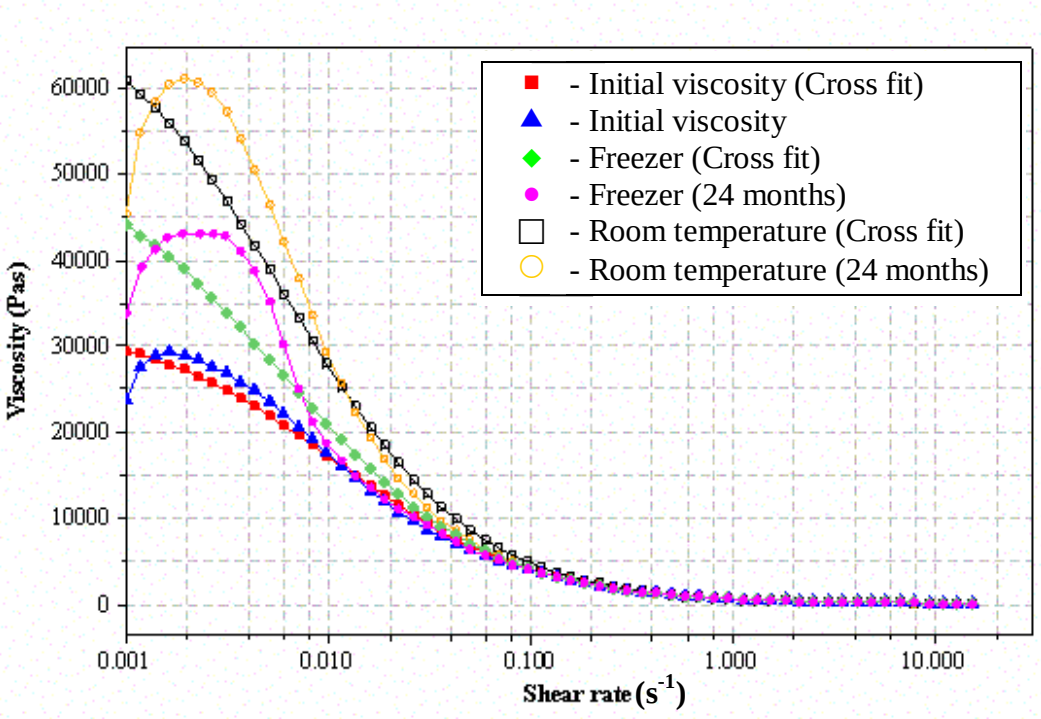

Figure 6.10: Cross model fit for paste A prior to and after 24 months of ageing

While conducting the process of modelling data through the use of the Cross model, the software identified a regression coefficient (r), which allowed for a recognition of the strength of fit between the model and the actual experimental data. General guidelines dictate that a strong fit exists with a value for r greater than 0.95; throughout the analysis process, this was seen to be true in each instance. For example, while analysing sample A, the Cross model fit of the initial viscosity returned a value for 'r' equal to 0.9947, and for the 24 months' ageing at room temperature this was equal to 0.9849. A further important aspect of analysis exists when acknowledging the value of the Cross time constant (K), where a high value is indicative of a relatively large structural breakdown (Cunningham, 2009[a]). In relation to the initial viscosity, the Cross model returned a value of 56.02, whereas for the room temperature data, which exhibited the greatest increase in viscosity, the value returned was 125.4. These results indicate that a significant variation exists between the two, which correlates to the necessity for the 'room-aged' paste structure to decay to a greater extent in order to allow for the expected viscosity to be achieved – as demonstrated by the initial viscosity tests.

While analysing the results of how the Cross model fitted for paste B, it was found that the trends observed for paste A continued to remain true. As can be seen in Figure 6.11, the model analysis also demonstrates a close resemblance to the measured viscosity values, again converging with an increase in applied shear rate albeit at a slightly reduced value of approximately 0.05 s^{-1} compared with the approximately 0.1 s^{-1} demonstrated by paste A. The coefficient constant (r) also demonstrated that a strong correlation existed between the modelled and actual data for sample B, with results exceeding the required value of 0.95. To illustrate this, modelling of the initial viscosity returned a value for r of 0.983, whereas for room temperature after 24 months of ageing this was equal to 0.9714. With regard to the Cross time constant (K), modelling the initial viscosity returned a value of 42.91, whereas for the room temperature data the value returned was equal to 97.18, once again linking to the necessity for a larger breakdown of structure to correspond to the initial viscosity.

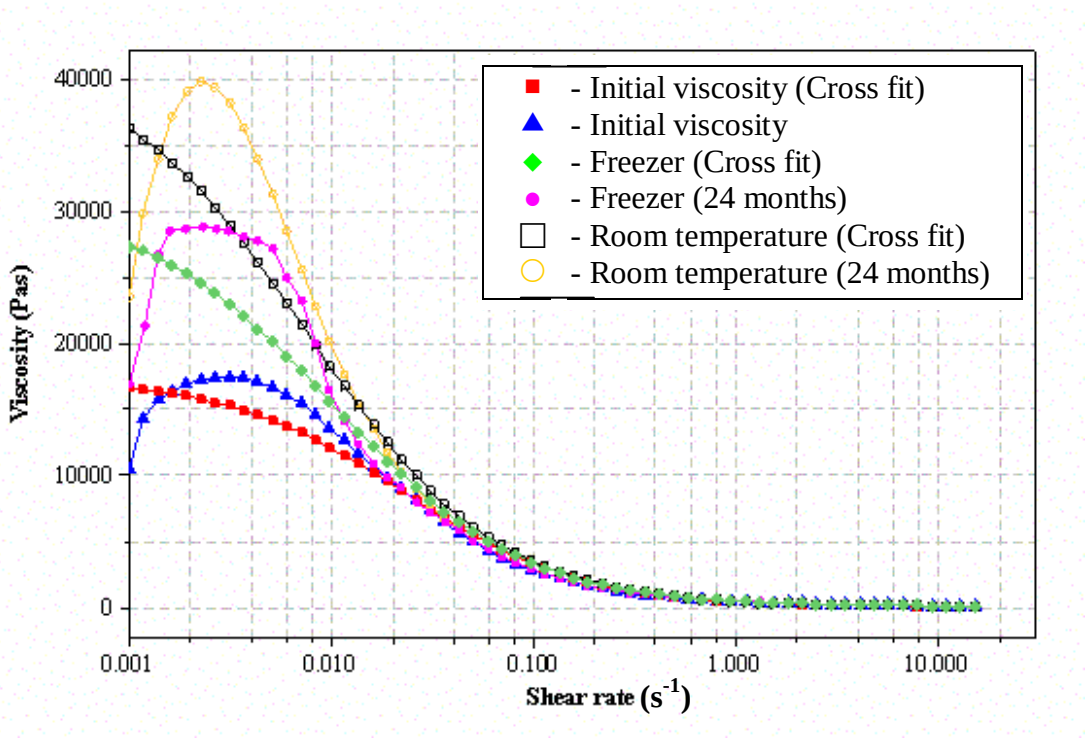

Figure 6.11: Cross model fit for paste B prior to and after 24 months of ageing

The results from the oscillatory tests confirm the findings from the previous viscometry investigations, which indicated that the paste initially becomes more solid as the period of ageing increases (prior to working the paste). This was observed as a trend shown by the increase in the storage (G') and loss (G") modulus recorded during the amplitude sweep, which represents the building of the paste structure (see Figures 6.12 and 6.13). Furthermore, the phase angle (δ) accentuates this increased viscosity by demonstrating a reduction in value with increased ageing (as 90° indicates purely viscous flow, while 0° indicates solid-like behaviour). Additionally, the results further illustrate the trend of convergence (by the aged sample) with the initial results recorded as the stress applied to the sample is increased; similarly, the results converged in the viscosity tests as the shear rate was increased. Figures 6.12 and 6.13 demonstrate the results of the amplitude sweep tests conducted for paste A and paste B respectively, allowing for a comparison to be made between initial results and those obtained after allowing for an ageing period of 24 months within a refrigerator (as this is the current standard method used for paste storage).

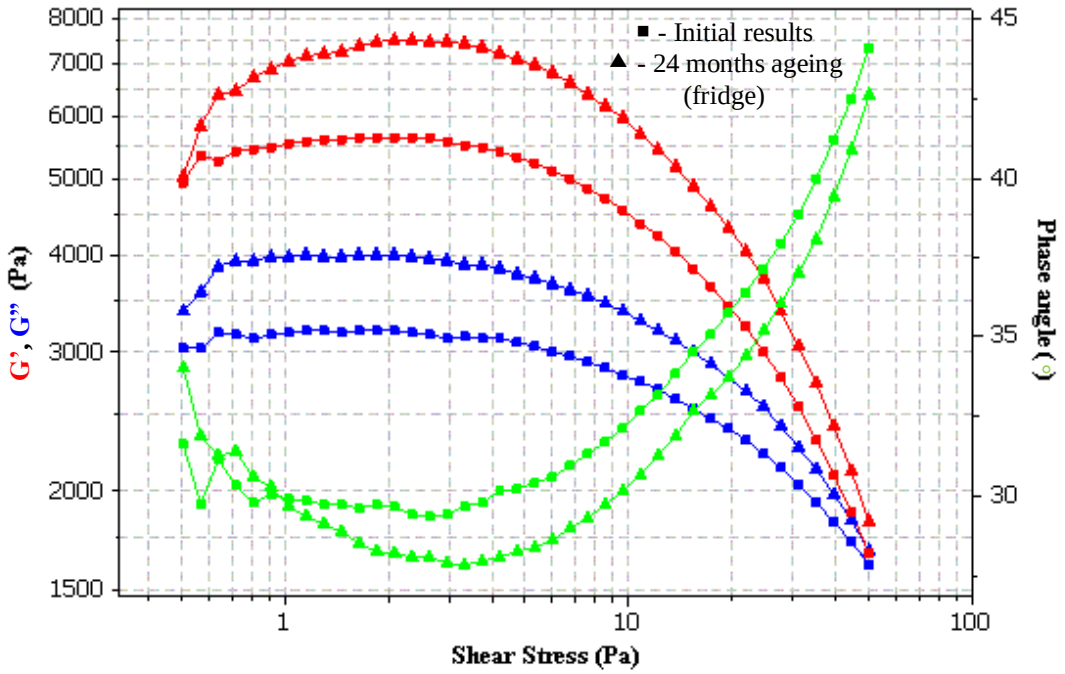

Figure 6.12: Amplitude sweep for paste A

(initial results compared with those after 24 months' ageing in a fridge environment)

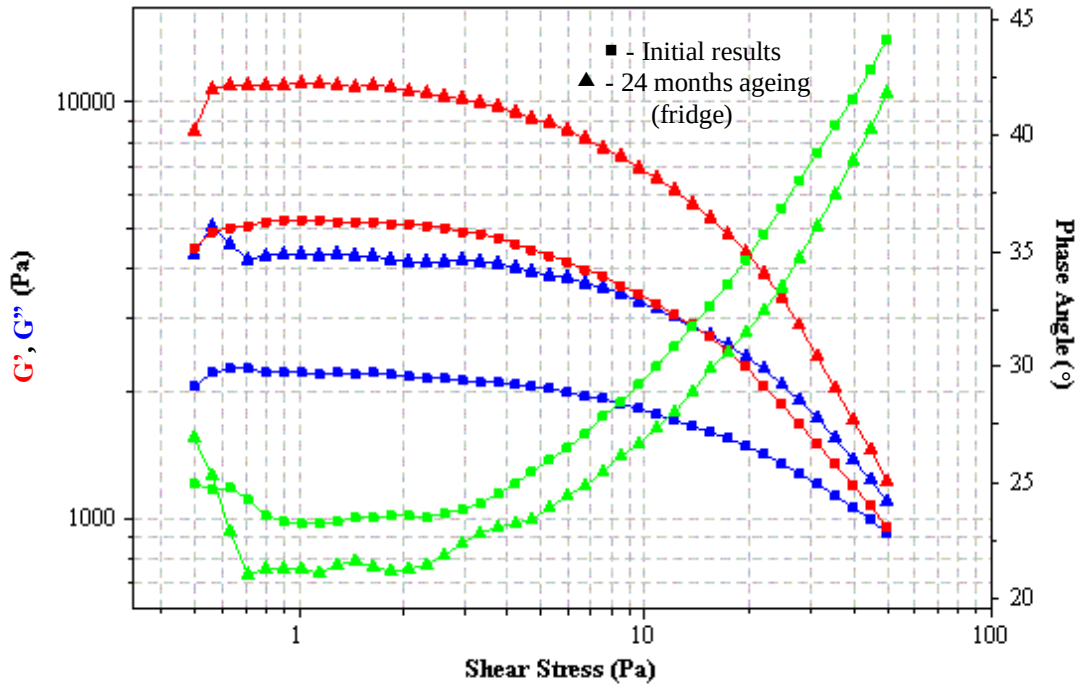

Figure 6.13: Amplitude sweep for paste B

(initial results compared with those after 24 months' ageing in a fridge environment)

This increase in paste structure also aids an understanding of the results from the printing trials conducted throughout the ageing study. By comparing the printing results observed both prior to and after the ageing process, a decrease in the level of bridging was noticed. Clearly, if the paste is more viscous or retains more structure, this would be evident as it should be less likely to flow to the extent initially recognised. This explanation could therefore be correlated with the occurrence of the skipping defect – explaining the finding of an increased level of skipping with a decrease in the bridging observed – because with an increase in paste structure or viscosity the paste samples will be less likely to perform aperture filling to the extent initially observed. Both pastes A and B also demonstrated an increase in the drop-off time from the squeegee after the print, which once again emphasises the presence of greater solidity that comes from an increased viscosity (see Table 6.3). After having successfully completed several printing trials, the print results for the aged sample closely resembled the initial printing results (pre-ageing) – indicating that subjecting a solder paste to a storage period beyond six months is feasible from a printing viewpoint.

Sample	Type of Storage applied	Bridging (0.33×2.03mm)[6.1]	Skipping	Drop-off (sec)	Stencil and Apertures (% clean)
A	Initial results	0.15 mm pitch	0	15–20	100
	Room temperature (24 months)	0.06 mm pitch	5	25–30	83
	Room temperature (after 5 prints)	0.1/0.15 mm pitch	1	20–25	95
	Fridge conditions (24 months)	0.1 mm pitch	3	20–25	93
	Fridge conditions (after 5 prints)	0.15 mm pitch	0	20–25	99
	Freezer conditions (24 months)	0.1 mm pitch	1	20–25	96
	Freezer conditions (after 5 prints)	0.15 mm pitch	0	15–20	100

[6.1] The same IPC slump stencil (0.33×2.03mm) pad size as demonstrated in Chapter 4, Figure 4.13.

Sample	Type of Storage applied	Bridging (0.33×2.03mm)	Skipping	Drop-off (sec)	Stencil and Apertures (% clean)
B	Initial results	0.1 mm pitch	0	15–20	100
	Room temperature (24 months)	0.06 mm pitch	2	25–30	92
	Room temperature (after 5 prints)	0.1 mm pitch	0	20–25	97
	Fridge conditions (24 months)	0.06/0.1 mm pitch	3	25–30	96
	Fridge conditions (after 5 prints)	0.1/0.15 mm pitch	1	15–20	100
	Freezer conditions (24 months)	0.1 mm pitch	0	20–25	98
	Freezer conditions (after 5 prints)	0.1 mm pitch	0	15–20	100

Table 6.3: Comparison of print observations for different storage techniques after allowing for 24 months of ageing

Within Table 6.3, bridging was recorded as the maximum pitch size that exhibited the presence of the defect, and the value for skipping was taken as the number of occurrences that were seen on the 36 vertical and horizontal 0.33 × 2.03 mm pads of the IPC stencil (as these were the smaller of the apertures and therefore more likely to demonstrate instances of skipping). The cleanliness of the apertures and stencil was recorded through overlapping a 10 × 10 translucent matrix (dimensions of 150 × 150 mm) over the stencil, with each sector (dimensions of 15 × 15 mm) that demonstrated a lower than 50% solder paste obscurity classified as 1% cleanliness.

As can be seen from the printing results set out in Table 6.3, a close resemblance exists between the results observed from testing ‘aged’ paste samples and those from the initial printing trials. This resemblance becomes closer still upon conducting several printing trials, with the results becoming near identical regardless of the storage condition applied. This tendency could possibly be correlated to the viscosity results, which demonstrated that with an increased shear rate, the aged samples descend from their elevated viscosity to converge once again with the viscosity initially recorded, i.e. pre-ageing. With regard to the stencil printing, with the shear

applied during the process, the paste viscosity should once again converge with the initial viscosity, therefore leading to a reduction in skipping, more likelihood of increased bridging, a faster paste drop-off time, and increased stencil cleanliness.

Additional visual observations of the printing demonstrated that paste roll was unaffected, with samples able to roll successfully and efficiently as opposed to being pushed along the surface of the stencil. Furthermore, aperture clogging was minimal (with only a few instances observed), and deposit definition was maintained consistently apart from a few instances of skipping and bridging. Overall, long-term paste storage influenced the quality of the printing to a minimal degree – and the actual print acceptability was seemingly unaffected.

6.4 Conclusions

As was expected from conducting an investigation into the ageing behaviour of solder paste materials, the viscosity of the samples was seen to increase as the period of ageing increased, which could occur due to those known issues such as sedimentation, separation, or drying out. Visual observations demonstrated the presence of a layer of flux on the surface of the solder paste, yet this was seen to be minimal and was remedied through 'mild stirring' of the paste with a plastic spatula. Regardless of this increase in viscosity, it was observed that by applying an increased shear rate the viscosity once again reduced to the optimal viscosity demonstrated by initial viscosity tests; therefore, despite ageing by 24 months, the viscosity of the samples was seen to be equivalent to that demonstrated by a newly manufactured solder paste material. Consequently, from a rheological point of view, the level of viscosity was seen to be acceptable, and further supported the indication that the shelf life of paste products could be extended beyond six months.

From an application viewpoint, the printing results further emphasised the acceptability of aged solder pastes. Initial printing trials of the aged samples demonstrated an elevated presence of the skipping defect and the drop-off time, for example; yet after conducting several print cycles, observed results actually replicated the initial printing trials very closely. As the initial printing trials were conducted using a paste that was recently manufactured (and therefore within the recommended

six-month shelf life period), it can be concluded that the possibility exists of conducting the printing process even using aged paste samples.

Theoretically, the Cross model provided an accurate opportunity to model the behaviour of the solder paste upon increase in shear rate applied. A close relation was seen between the results from this model and the actual results from the rheological testing process. As the results of the Cross model were also seen to converge with the initial viscosity data, there was further support for the view that the viscosity recorded after allowing ageing was accurate and hence acceptable. Consequently, additional evidence exists for the plausibility of increasing the shelf life of solder paste products beyond the currently recommended six-month period.

A valuable discovery revealed during the course of the testing related to the storage techniques that may be applied to the solder paste. Current standards generally dictate that solder paste should optimally be stored between 0°C and 10°C, with various sources (for example, ADTOOL (2002) and Radio Electronics (2007)) claiming that solder paste should not be stored within freezing conditions. Despite demonstrating a considerably improved performance when compared with extended storage at room conditions, the refrigerated paste was unable to perform to the same extent of similarity with the ‘pre-ageing' results when compared with the paste stored in the freezer. Therefore, by investigating the method/temperature of storage applied to a solder paste, it is believed that the use of a freezer environment offers the greatest opportunity to maintain the paste’s original properties with increased periods of ageing.

A further finding of interest that relates to the effect of storage on the viscosity of an aged paste was the similarity identified between paste samples. Upon analysing the results of aged paste viscosity, it was observed that both paste A and paste B performed nearly identically, with a reduced viscosity of 40–45% when comparing the room-conditioned paste with the refrigerated paste, and a 60–65% reduction when comparing the room-conditioned paste with paste from the freezer. The uniform percentage increase in viscosity with increasing storage temperature could allow for the possibility of predictions to be made as to paste viscosity at different storage temperatures with an applied period of ageing of 24 months.

By undertaking this investigation, results indicate an ability to elongate the shelf life of paste products, with rheological, theoretical and practical applications all correlating to suggest that the ability of maintaining paste quality and acceptability exists even after a storage period of 24 months. If this is to be true, a potential exists for the standard method of recommending a paste shelf life of six months can be relaxed, which could improve the efficiency of the manufacturing process from both an economical and environmental perspective. Further work would, however, be required to investigate 'post-print' behaviour before definitively extending the shelf life, because it was previously highlighted (within Chapter 3, at section 3.9.2) that the performance of aged pastes can demonstrate problems such as increased solder balling after the printing process. As such, it can be concluded that further studies must be conducted into reflow performance of aged samples, which will be addressed in the final chapter of this thesis. Therefore, at present, it may only be possible to state that the printing life of solder paste can be extended beyond six months.

CHAPTER 7:
RHEOLOGICAL SIMULATION OF SLUMPING BEHAVIOUR FOR LEAD-FREE SOLDER PASTE AS AN EFFECT OF VARIATION IN APPLIED TEMPERATURE

7.1 Introduction

The focus of this chapter is the rheological simulation of temperature influences on slumping behaviour of Pb-free pastes. The aim of the study was to investigate paste behaviour (particularly slumping behaviour) upon increasing the applied temperature to that experienced during the pre-heat stage of reflow. In order to determine rheological behaviour, visual investigations were conducted by means of stencil printing (to mimic industrial production lines) followed by simulation of the process on a rheometer.

The temperature applied to a paste can significantly influence its rheological properties and, with variations in temperature common during PCB assembly, understanding its effect on paste rheology and performance is essential. Typically, an increase in temperature will lead to a decrease in paste viscosity, consequently leading to slumping – a major defect of the assembly process that causes bridging. In order to consider a print as successful or otherwise, there are a number of quality assurance (QA) measures that must be passed. One such aspect is the degree of bridging observed. One of the main causes of failure at the QA stage is the presence of excessive bridging between solder deposits; hence this is an issue that requires some attention. The main topic for concern is the inability to accurately predict the amount of slump that will occur during and immediately after the stencil printing process.

Complications arise when attempting to predict paste slump due to the temperature gradients involved within the manufacturing process. Simply addressing the issue at room temperature is ineffective as aspects of the process will be overlooked. Within

laboratory conditions, SMA typically occurs within a temperature-controlled environment between 20°C and 25°C; however, temperature differences have been identified during the printing phase (in relation to those generated by the squeegee) and the reflow phase that alter the properties of the paste. As previously mentioned, an important property of a paste that is altered by the influence of temperature is its viscosity. With an increase in temperature applied to simple liquids, a decrease in apparent viscosity is measured – a result of the increasing Brownian motion of their constituent molecules (Barnes, 2000). With a significant reduction in print quality and the presence of temperature variations, understanding the relationship between slump and the temperature gradient is essential.

Standard test methods (as discussed by the IPC) dictate that, when studying slump, it is necessary to heat a printed sample to 150°C and then simply identify the pads on which the slump defect was present. Although this provides a valuable insight into the visible behaviour of paste samples, it fails to provide information as to why the solder pastes behave in this manner. Therefore, providing rheological reasoning for slumping behaviour offers valuable information. By analysing variations in bridging from print trials and the corresponding rheological measurements, a better understanding can be gained for the level of slump observed. Consequently, it is possible to identify which solder pastes offer greater acceptability from an industrial viewpoint, while presenting opportunities to correlate the printing process to the occurrence of slumping.

7.2 Slump testing method

In order to ensure the accuracy of results, pre-test investigations were required to discover the so-called ‘temperature intervals’ applying. Through conducting such a trial, it is possible to discover the amount of time needed for a printed board to reach a specific temperature (the time interval between applying heat to reaching the required temperature). As the slump study involves heating a board to a temperature of 150°C, it is necessary to understand how long upon application of increased temperature it takes for the board to reach a plateau of 150°C.

The identification of temperature intervals is a fundamental procedure when conducting any study that incorporates the use of a heating implement that requires

time to attain a specific temperature. Conversely, investigating the temperature intervals is essential when removing a test specimen from the source of heat and allowing it to cool to an ambient temperature, assuming that further tests will then be conducted. As an item of heating apparatus cannot instantaneously jump from 25°C to 150°C, the notion of temperature intervals becomes clear.

While conducting this investigation of temperature intervals, a thermocouple was utilised to monitor temperatures within the batch oven as well as the length of time taken to return to room temperature upon removal. This method was conducted six times – three times on two separate days – in an attempt to highlight any anomalous results and to take into consideration environmental influences.

Each sample was then printed onto two boards, one to remain at room temperature and the other to be heated to 150°C for 10 minutes (including the time to reach the desired temperature). The heated board was then removed from the batch oven and allowed to cool to ambient temperature. The print quality was checked on three separate occasions, immediately after printing, at the time that specimen 2 was removed from the batch oven, and once the second board had successfully returned to 25°C.

The next phase of the study required the use of the Bohlin rheometer in order to discover rheological reasons for the observed results. Initial tests were conducted into the rheological properties of the paste at a temperature of 25°C, which were conducted on six occasions. Further tests were then conducted in an attempt to replicate the process of manual heating using a batch oven. The testing process was then carried out as follows:

1. A print trial was conducted, with a sample of the worked paste taken for use on the rheometer for consistency.
2. Rheological characterisation tests were conducted on the paste.
3. Further print trials were conducted, with a sample taken once more for rheological investigations.
4. The temperature (applied to the sample on the rheometer) was increased to 150°C at a gradient that mimicked the result of the temperature interval test.

5. Further rheological characterisation tests were then conducted.
6. Steps 3 and 4 were repeated with the paste returning to 25°C before characterisation tests.
7. The process was repeated six times.

The temperature values used (25°C and 150°C) were selected as industrial standards, which are provided in the guidelines from the IPC for slump testing – where 150°C is still used for the pre-heat stage of reflow despite a move to Pb-free soldering. Despite being industrial standards, the appropriateness of such values was researched prior to the study, which provided a greater level of justification for employing these in the investigation.

The initial temperature of 25°C is commonly perceived to be the standard ambient temperature within experimental conditions. Numerous literature findings report the use of this ambient temperature, particularly during the rheological characterisation of solder paste and of alternative fluids such as conductive adhesives (Bao et al, 1998; Nguty et al, 1999; Billote et al, 2006; Zhang et al, 2010). The 150°C is not, however, a commonly applied temperature and therefore needs to be fully understood.

During the course of the testing period, a temperature of 150°C was used as the target temperature. As mentioned earlier, this is the industrial slump test standard, as defined in the IPC slump test guidelines. Through consideration of the whole PCB assembly process, selection of such a temperature becomes clear, because it is the minimum for the pre-heat stage of the reflow process. During the pre-heat stage, the assembly (including the board and components) is heated to prevent any damage to the components being mounted on the board through (for example) thermal shock or cracking. The pre-heat stage also acts as a means of initiating solvent evaporation from the solder paste, and if the temperature level is insufficient, the evaporation of flux volatiles will be incomplete. Through evaporation of these solvents, the paste is said to be 'conditioned' or prepared, which assists with improving the quality of the final interconnection. During this preparation and in addition to removal of the volatiles, the flux is activated, thus removing oxides from the metal surface which is to be soldered. Owing to the change in properties that are observed with application of an increased temperature (a reduction in viscosity due to evaporation, for example), it

is apparent that monitoring for slump defects at this value of 150°C is important in order to understand the behaviour, as printed boards are subjected to the reflow process.

The final stage of the testing involved the comparison and analysis of results. This included those results obtained from both the rheological software and the printing trials, with a final contrast being made between those results actually observed and those that were predicted (as detailed within Chapter 3, section 3.9.4), in order to attempt to highlight any relationships, correlations or similarities.

7.3 Results and discussion

7.3.1 Temperature interval pre-study investigation

The investigation into those temperature intervals presented during the slump investigation highlighted that the approximate time taken for the chosen equipment to reach a temperature of 150°C was five minutes (Table 7.1). With regard to the heated board returning to an ambient temperature (25°C in this instance), this was seen to be approximately nine minutes. Whilst conducting these investigations, several tests were carried out on different dates, to allow for clearer identification of anomalous results (possibly due to environmental influences). From Table 7.1 it is clear that there is no significant fluctuation between the recorded times, implying a degree of reliability in the results. It was predicted that any environmental effects should only influence the cooling period of the investigation, as the heating is conducted within the apparatus, and hence any cooling or additional heating would be negligible.

Test Number	Time taken to reach 150°C	Time taken to return to 25°C
1	4 Minutes 35.32 Seconds	6 minutes 58.29 seconds
2	5 minutes 10.29 seconds	9 minutes 37.41 seconds
3	4 minutes 48.33 seconds	8 minutes 12.10 seconds
4	4 minutes 59.61 seconds	9 minutes 53.21 seconds
5	5 minutes 26.33 seconds	9 minutes 19.58 seconds
6	5 minutes 13.17 seconds	10 minutes 33.65 seconds
Average	5 minutes 2.18 seconds	9 minutes 5.7 seconds

Table 7.1: Results from the temperature interval investigation

7.3.2 Main slumping investigation

Initial findings from the slumping study highlighted the predicted trend of a reduced viscosity upon increase of the applied temperature for the pastes. By taking the analogy of heating material such as chocolate, this was an obvious reaction to expect from the solder paste as the application of heat will cause the effect of melting. Owing to the nature of solder pastes and their intended use, once a specific temperature was achieved the viscosity of the pastes began to increase once more, which was another expected trend. This increase in viscosity was due to the evaporation of solvents from the test samples. As can be seen from the graph in Figure 7.1, it is possible to recognise that paste A began to demonstrate this increase in viscosity at a temperature of approximately 100°C, whereas for paste B, this was of a lesser temperature of approximately 80°C.

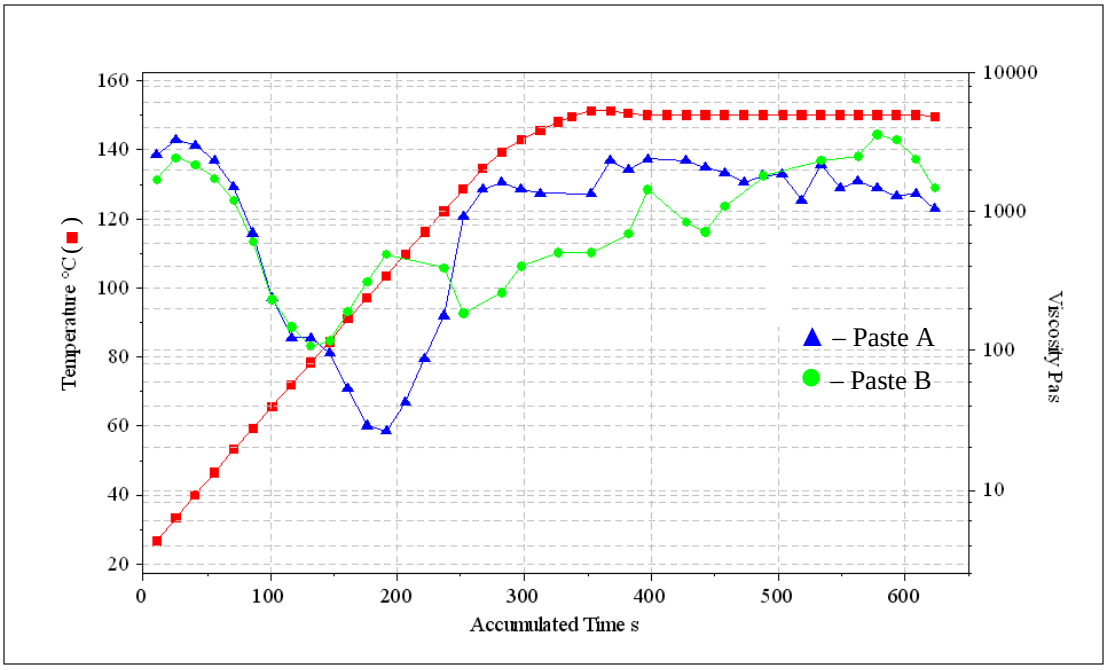

Figure 7.1: Viscosity results for pastes A and B upon applying a temperature profile.

From these results, it was expected that the quality of the print would be severely affected, with a large degree of slumping activity being demonstrated due to such a significant decrease in viscosity with the increase in temperature. This was indeed the case: for paste A, the level of bridging was seen to increase from a pitch of 0.1 mm to 0.3 mm (for a pad size of 0.33 × 2.03 mm), which corresponds to further bridging

across an additional four deposits; Paste B also demonstrated an increase in bridging (see Figures 7.2 and 7.3), but to a lesser extent, rising from a pitch of 0.15 mm to 0.25 mm (demonstrating bridging across an additional two paste deposits). Regarding a pad size of 0.63 × 2.03 mm, initial observations highlighted that no bridging was present; however, after applying a temperature profile, bridging was indeed experienced (Figure 7.4). The levels of bridging demonstrated by paste A after heating to 150°C were once again greater than those observed for paste B, covering a pitch size of 0.48 mm (whereas paste B bridged across a pitch size of 0.41 mm), as highlighted in Table 7.2.

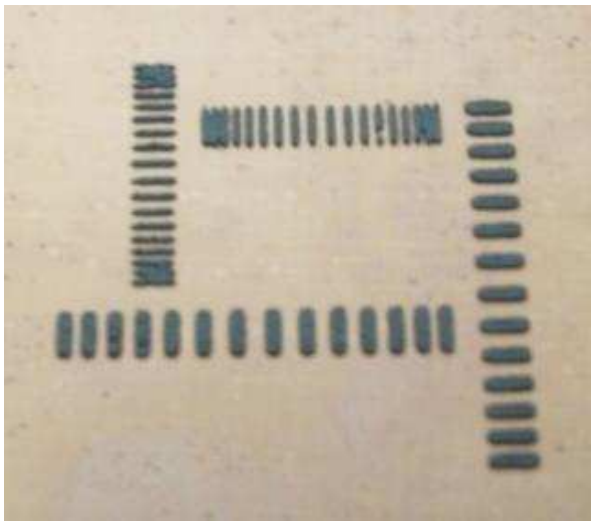

Figure 7.2: Example print from sample B prior to heating

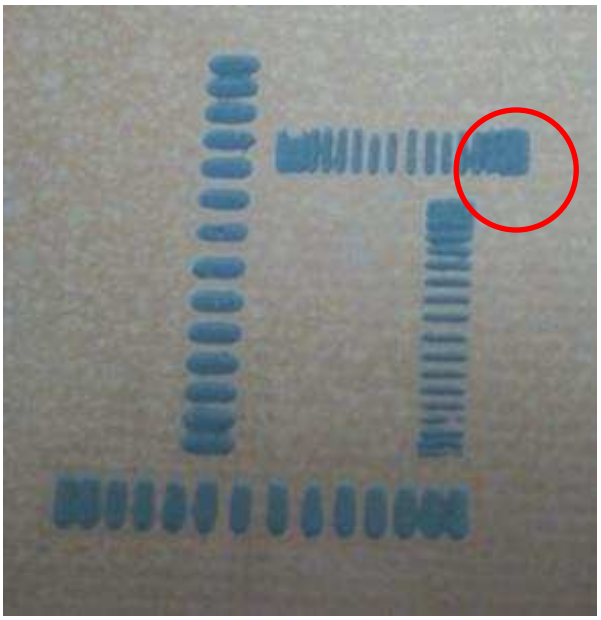

Figure 7.3: Example print from sample B after applying the temperature profile (0.33 × 2.03 mm pads highlighted)

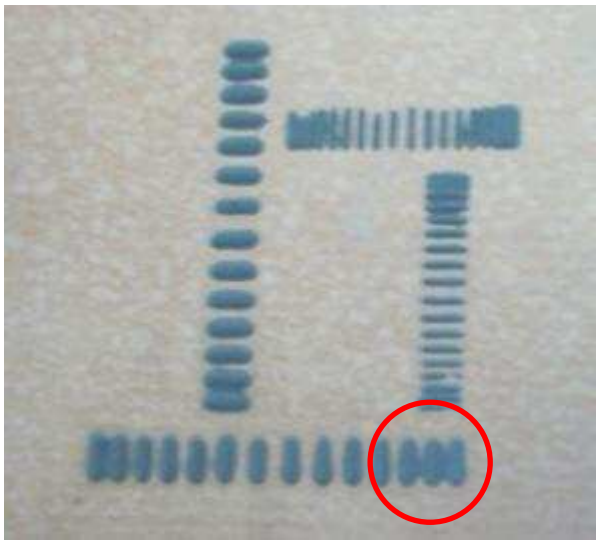

Figure 7.4: Example print from sample B after applying the temperature profile (0.63 × 2.03 mm pads highlighted)

Presence of slumping/bridging behaviour	Pad size 0.63 × 2.03 mm					Pad size 0.33 × 2.03 mm				
	Pitch size (mm)	Paste A		Paste B		Pitch size (mm)	Paste A		Paste B	
		Pre-heat	Post-heat	Pre-heat	Post-heat		Pre-heat	Post-heat	Pre-heat	Post-heat
	0.33		✓		✓	0.08	✓	✓	✓	✓
	0.41		✓		✓	0.10	✓	✓	✓	✓
	0.48		✓			0.15		✓	✓	✓
	0.56					0.20		✓		✓
	0.63					0.25		✓		✓
						0.30		✓		
						0.35				

Table 7.2: Observed bridging behaviour both before and after heating

Thus, the results of the study demonstrated the predicted trend of an increase in the level of bridging observed (resulting in a reduction in the printing quality achieved) upon heating to a temperature of 150°C. It is important to note that the use of 150°C for the applied temperature is the result of generic temperature profiles for the reflow process. These dictate that, within zone 1 (the 'pre-heat zone'), the board temperature

is increased rapidly from room temperature to a value of 150°C (Scheiner, 2003). Having acknowledged this information, the IPC devised a standard slump test that requires the heating of printed boards to 150°C for 10–15 minutes.

With such an increase in applied temperature, it was evident that the paste viscosity would reduce, allowing the sample to flow to a greater extent (Figure 7.5). However, an important discovery during the evaluation process was the variation in performance between samples – a result that may be related to the point at which evaporation of solvents of the material becomes prominent. As was mentioned previously, paste B was found to begin to display an increase in viscosity once a temperature of 80°C was reached, whereas paste A required an additional increase in temperature of around 20°C before it begins to become a soft-solid (Figure 7.6). Because of the temperature profile identified within the study (a linear increase in temperature from 25°C to 150°C over a time period of five minutes), this additional 20°C equates to an approximate timeframe of 50 seconds – so paste A was allowed an additional 50 seconds to flow, and hence lose print quality, when compared with paste B.

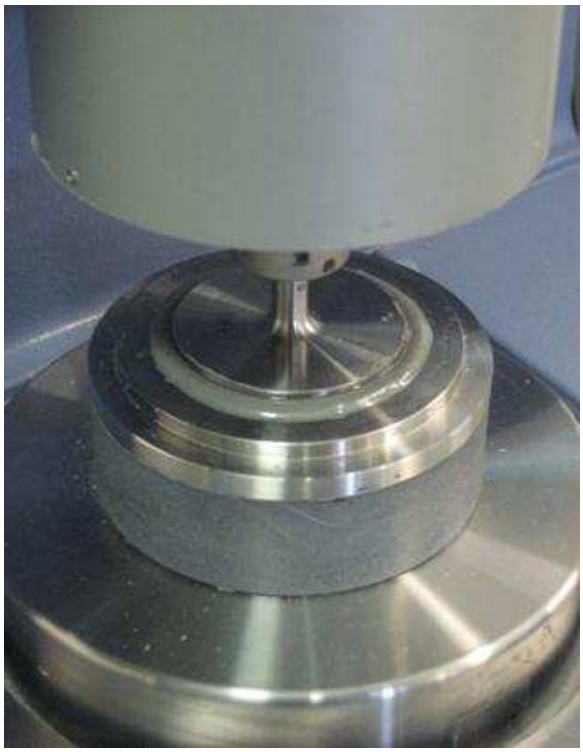

Figure 7.5: Image highlighting paste behaviour upon temperature increase to 150°C

Figure 7.6: Image highlighting the 'soft-solid' phase of the study

The importance of the results found during the study (relating to the 'soft-solid' phase) may also be beneficial within the development of new paste formulations. By assessment of the results obtained, it is believed that a solder paste that demonstrates an increase in viscosity at a lower temperature is more likely to exhibit a reduced level of bridging. It may therefore be possible to reduce the influence of defects in the manufacturing process by using this method of characterisation as a benchmark for future work, possibly by creating a certain target profile to achieve with new paste formulations. That is to say, by formulating a solder paste so that the viscosity will increase at a lower temperature, defects may be reduced. Further still, this process may allow optimal paste performance to be developed rather than simply identifying which of a selection of pastes may perform to a higher capability.

With respect to predicted viscosity results calculated theoretically (see Chapter 3, section 3.9.4), it was discovered that significant variations existed when compared with those results actually observed through the rheological tests (Table 7.3). For the

purpose of accurately analysing the similitude of these two sets of results, the viscosities from the theoretical section were recalculated using the same approach as previously employed, to correlate with those temperatures at which the rheometer recorded viscosity values.

Temperature (°C)	Viscosity of Sample A (Pas)		Temperature (°C)	Viscosity of Sample B (Pas)	
	Measured	Predicted		Measured	Predicted
26.8	2751.0	2349.489	27	2377.0	2279.075
33.4	2665.0	1453.821	33.7	2371.0	1786.375
40.1	2575.0	911.758	40.3	2031.0	1419.676
46.5	2348.0	594.644	46.8	1622.0	1142.729
53.2	1505.0	387.024	53.2	1096.0	930.715
59.5	698.9	262.549	59.5	546.0	766.362
65.8	240.6	180.697	66	225.1	631.917
72.1	123.0	126.071	72.3	151.6	527.805
78.3	122.9	89.585	78.6	120.7	443.699
84.6	97.1	64.082	84.8	136.5	376.263
91.1	52.84	45.908	91.3	239.8	318.455
97.3	28.88	33.765	97.6	331.5	272.432
103.6	26.26	24.969	103.8	393.7	234.832
109.9	42.31	18.648	110	602.7	203.397
116.1	88.41	14.122	116.3	1153.0	176.589
122.4	179.4	10.742	122.6	2122.0	154.005
128.8	923.0	8.208	129	605.4	134.608

Table 7.3: Comparison of actual and predicted viscosities upon temperature increase (predicted viscosities taken correct to three decimal places)

The significant variations between viscosities, as seen in Table 7.3, apply particularly with respect to the point at which the actual viscosity was seen to rise once more, whereas the predicted viscosity continued to decrease. This can be clearly identified in Figures 7.7 and 7.8.

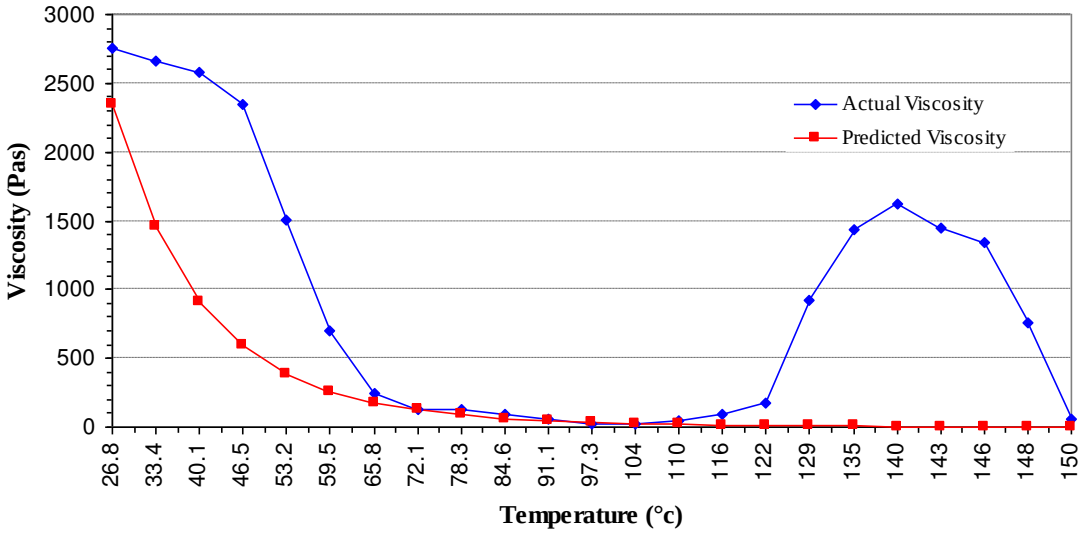

Figure 7.7: Comparison of predicted and actual viscosities for sample A

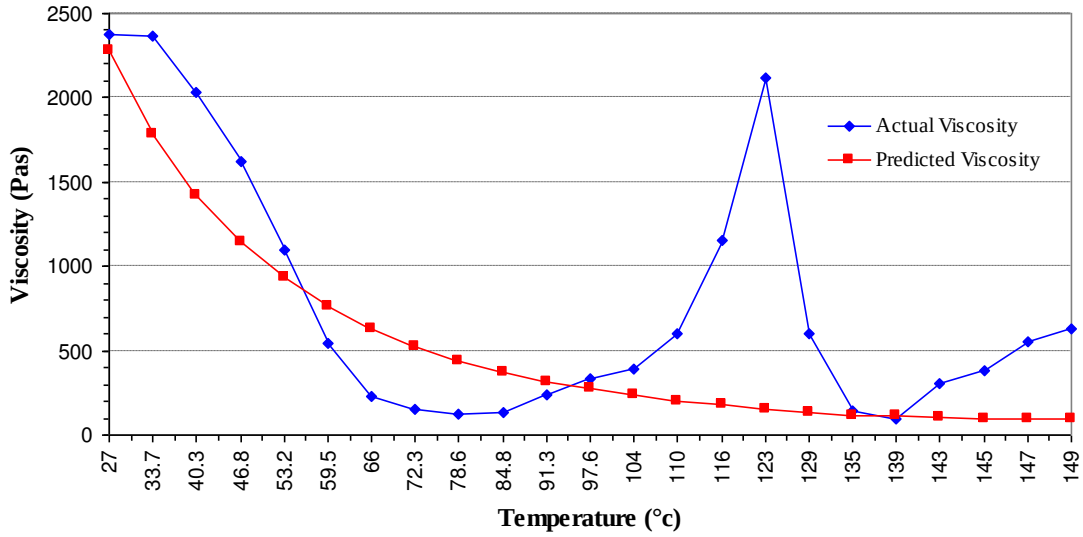

Figure 7.8: Comparison of predicted and actual viscosities for sample B

From these two graphs it can be seen that the predicted viscosity does loosely follow the trend displayed by the recorded viscosities from the rheometer. Indeed, for sample A (see Figure 7.7) the two viscosities actually appear to be nearly identical for a duration spanning a temperature range of around 40°C, from 65.8°C to 110°C.

Owing to the inability to accurately predict the point at which the temperature will raise viscosity again, a comparison of predicted and measured results was undertaken

where readings were limited to the point at which viscosity was seen to increase again (the start of the soft-solid phase). Results are shown in Figures 7.9 and 7.10.

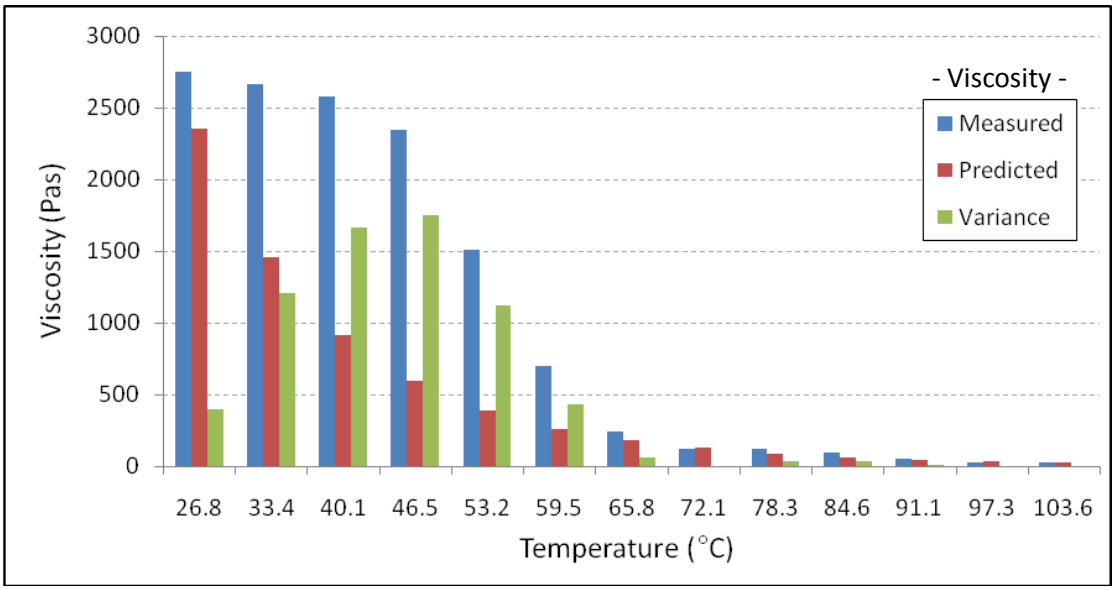

Figure 7.9: Variation of predicted and actual viscosity for paste A prior to viscosity increasing again

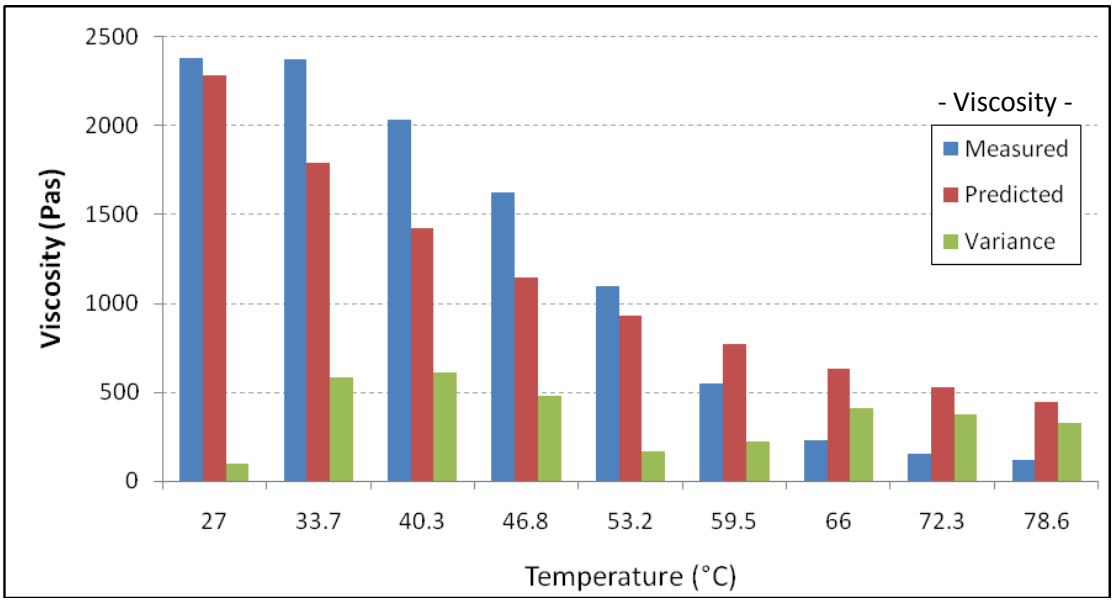

Figure 7.10: Variation of predicted and actual viscosity for paste B prior to viscosity increasing again

Results from limiting predictions – to the point at which the temperature causes viscosity of the paste to increase once more – demonstrate both the potential and failings of the method. From the viewpoint of paste B, Figure 7.10 exhibits a fairly consistent variation in viscosity, which could be implemented as a correction constant. Conversely, despite demonstrating good accuracy both initially and during later measurements, the predicted results for paste A (see Figure 7.9) failed to accurately compensate for the slow decrease in viscosity seen until approximately 50°C.

Whilst analysing the graphs, it was necessary to acknowledge visual observations from the rheometer itself, as the presence of the 'soft-solid' phase allowed the top plate to rotate freely on the surface of the solder paste. Consequently, the rheometer was unable to attain confidently valid results once the viscosity had increased to a point where the solid aspect of the solder paste was observed; this can be seen in Figure 7.11, in which an attempt was made to replicate a typical amplitude sweep test. The reason for such an unpredictable and inaccurate graph may be due to the inability of the rheometer to actually encounter resistance from the paste.

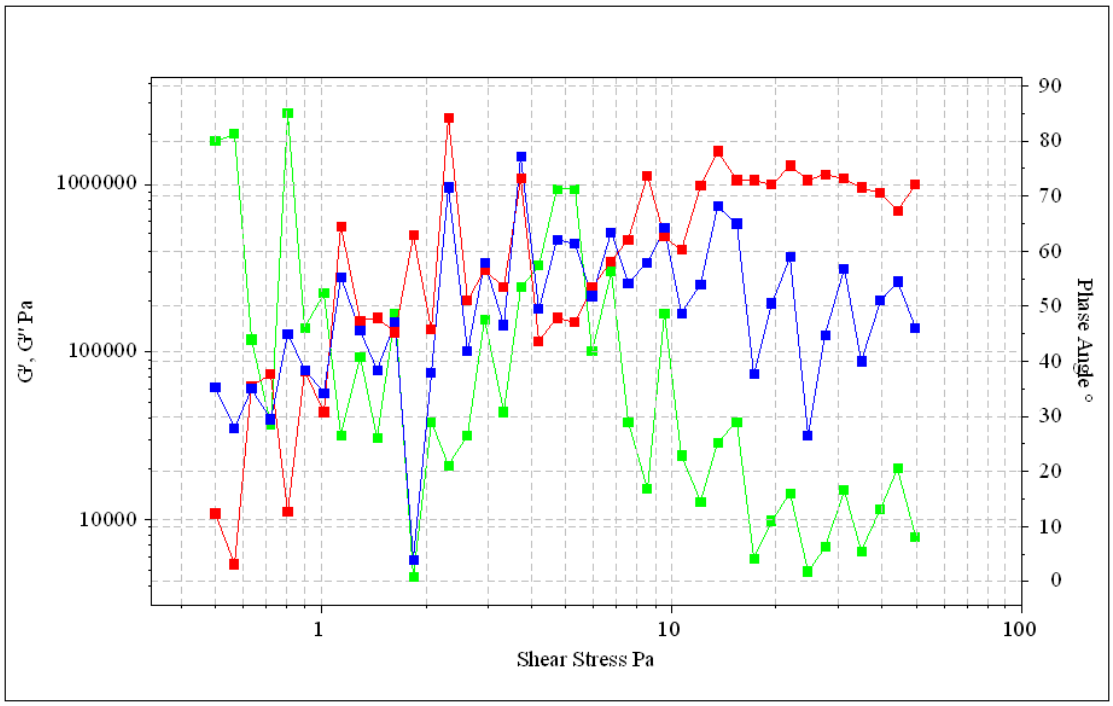

Figure 7.11: Example of amplitude sweep results during the 'soft-solid' phase

7.4 Conclusions

By studying the influence of temperature on the slumping behaviour of solder pastes, it became evident that the predicted trend of a reduction in viscosity upon increase in temperature was accurate. It was clearly observed that substantial temperature variations can have a highly significant influence on the viscosity of paste samples, with a strong tendency towards approaching a viscous phase. Results demonstrated that the solder paste begins to flow outwards from between the rheometer plates. Owing to this reduction in viscosity, it can only be expected that the occurrence of slumping behaviour will increase – a further result that was observed during the study.

With past works highlighting predicted trends for viscosity upon an increase in temperature of 1°C (Maiso and Bauer, 1990; Nguty and Ekere, 2000[a] and 2000[c]), and by manipulation of the Arrhenius equation to predict viscosity, it was anticipated that it may be possible to predict the viscosity of solder paste samples at elevated temperatures, which could therefore allow for a rapid indication as to slumping behaviour without the requirement for conducting numerous trials. Unfortunately, despite the comparability between those predicted viscosities (using equation [3.63]) and those from the assumptions made by Nguty and Ekere, accurately predicting exact viscosities was unachievable.

Furthermore, through conducting the trials it became apparent that the benefits of applying that method used for predicting viscosity were very limited. Firstly, as previously mentioned, the equation utilised (equation [3.63]) failed to offer precise values for the viscosity, and furthermore presents no indication of the point at which the viscosity will begin to increase once again (which is seen as a significant finding). Despite these negatives, it is believed that the method has potential in offering valuable information, particularly if new methods of interpretation are developed. This is important, as the paste sample itself offers many variables and complexities that could influence the outcome of the heating process (such as metal content and flux type to name but two) and that could have a significant impact on viscosity variations. The question as to whether predicting accurate viscosities is actually possible is then raised. Currently, however, the equation used for predicting viscosity is able to provide an indication into the representational trend that a solder paste

would follow upon an increase in temperature, and therefore it does offer a degree of potential.

From the study, it is believed that the key finding is that of the initiation of the 'soft-solid' phase of the solder pastes. This was seen during the rheological tests as a sudden increase in viscosity with a continued increase in temperature. This result was highly significant, as this can be directly correlated to the results from the printing trials, and could provide strong reasoning behind the differences observed relating to the occurrences of slump and bridging. Results obtained highlighted that, at a temperature of approximately 80°C, sample B begins to recover viscosity while sample A continues to demonstrate a decrease in viscosity. If this is then considered in terms of the actual printed board, it would indicate that the heated deposits from sample B will cease exhibiting a slumping behaviour once a temperature of 80°C is applied by the batch oven (or reflow oven in an industrial manufacturing context), whereas sample A should demonstrate a continued trend towards slumping for a further 50 seconds until a temperature of approximately 100° is attained. It is this substantial period of continued slumping behaviour that presents great opportunities for understanding, and possibly even reducing, slumping behaviour and its effect on the manufacturing process.

By successfully conducting an investigation into the rheological simulation of slumping behaviour as an effect of variation in applied temperature, it has become clear that the possibility of reducing print defects exists. Upon gaining an understanding of the 'soft-solid' phase, and pre-testing solder paste samples to discover the point at which the viscosity begins to increase (regardless of the continued elevation in temperature), paste selection may be appropriately performed to reduce the level of slump exhibited. With respect to theoretically predicting paste performance by calculating viscosities at various temperatures, further work is needed to allow accurate values to be achieved. This is on the assumption that it is actually possible to accurately predict viscosity, and that the complexities of the solder paste materials (which play a vital role in influencing viscosity) can be overcome. At present it may be necessary to concede merely a close resemblance of predicted results to the trend in actual viscosities.

CHAPTER 8:
RHEOLOGICAL CORRELATION BETWEEN PRINT PERFORMANCE AND ABANDON TIME FOR LEAD-FREE SOLDER PASTE USED FOR FLIP-CHIP ASSEMBLY

8.1 Introduction

The focus of this chapter is the investigation of the influence of abandon time on paste rheology and print performance. The aim was to investigate the abandon time capability of solder paste to establish the short-term ageing performance at room temperature, and the point at which print quality remains at an acceptable standard (typically within no more than four hours). In order to determine abandon time capability, four main paste characterisation techniques were used: shear rate sweeps, amplitude and frequency sweeps, and creep recovery testing. For each sample, regular measurements were recorded until a period of 50 hours of abandon time had been reached.

The abandon time characteristic is seen as a critical factor in reducing the number of defects observed during SMA, due to the need for achieving acceptable prints after an interruption on the production line. Gilbert (2001[a]) defines abandon time as the maximum period of delay that can be applied between successive printing cycles, while allowing for acceptable print results to be sustained without the necessity for stencil cleaning or reconditioning the solder paste. Consequently, studying the abandon time can assist with determining the plausible length of delay in processing whilst still maintaining acceptable prints.

The abandon time can also play a significant role in the actual stencil life of a solder paste. Diepstraten and Wu (2009) define this as the length of time a paste sample may be left idle on the surface of the stencil before it becomes redundant as a result of drying out. The importance of this is emphasised by Almit Technologies Ltd, which states (2006) that a short stencil life is the largest defect with Pb-free pastes. However,

unless employing continuous printing cycles, the stencil life becomes secondary to the abandon time; hence an understanding of abandon time capability is essential.

Data sheets offer some insight into the abandon time capability of solder pastes, and Henkel Technologies (as detailed in these data sheets) suggest interruptions of four hours are possible. However, at present, the technique for mass stencil printing is to apply a large quantity of paste to the printer, which is replaced halfway through the working day. Owing to the amount of paste being discarded upon replacement of the sample, doubts as to the efficiency of the process arise; furthermore, as paste printing is typically an everyday task within industry, this is a matter that needs addressing urgently. As paste is frequently replenished during printing to meet demands for large quantities of PCBs, questions relating to efficiency are raised because some paste disposed of may still be classified as 'fresh' and usable. Industry's aim is to maintain deposits of an acceptable standard such that the complete replacement of paste for a 'fresh batch' is redundant. By increasing this degree of paste usage, effects can be seen for manufacturers and users at a financial, environmental and efficiency level.

8.2 Abandon time testing method

For the purpose of this study, two paste samples were utilised, both of which were developed for long printer abandon times, with the abandon time capability of paste A detailed as up to four hours, and the capability of paste B as greater than 75 minutes on a 0.4 mm pitch (as a result of changing simply the flux during formulation).

With regard to the general method of investigation, industrial standards are in place addressing the method that should be followed for abandon time studies. The standard testing method from Henkel Technologies (Gregoire, 2003) states the procedure for testing abandon time capability comprises several steps. First, after having defined appropriate printing parameters, two prints must be carried out to ensure that the paste is of good condition (with regards to printability; see 3.5.1) – with repetition where any anomalous results appear. Assuming that the paste falls from the squeegee and that the remainder is to the other side of the stencil, the second step is to introduce an idle period of 30 minutes, after which an additional two prints are made. The third step is to increment the delay between print cycles to 60, 90, 120 and 240 minutes

until print quality deteriorates. The final step is to record observations of the printing trials, with the pastes required to demonstrate good roll, drop-off, deposit definition, consistent paste volume, resistance to bridging and repeat printability on 0.4 mm pitch footprints. Additional to the requirements stated within the standard testing method, observations were also conducted to identify the occurrence of skipping and also the cleanliness of both the stencil and the apertures after the print cycle was concluded.

Work conducted by Toleno (2005) details that tests have shown abandon times of up to four hours are possible during which 'optimal' results are still achievable; however, a major reduction in print quality was identified with paste volume recorded beyond an abandon time of just one hour. For this reason, it was evident that the abandon time implemented in the current study needed to exceed the standard maximum of 240 minutes in order to gauge longer-term effects. Therefore, the printing trials were also conducted after an abandon time of 27 hours and again after 50 hours, indicating print quality after abandonment spanning two days. Although the industrial standard for conducting an abandon time study recommends conducting print trials simply at intervals of 60, 90, 120 and 240 minutes, it was believed there was a necessity for the study to move beyond the limitations of these standards. It was for this reason that the length of experimental time was increased, from the 'strictness' of industrial standards limiting the investigation to 4 hours, to a new duration of 50 hours.

In an attempt to understand paste behaviour rheologically, further steps in the test method were included. After each print, a sample of the 'worked' paste was taken from the stencil printer and placed onto the rheometer for typical characterisation tests (which included oscillatory, viscometry and creep-recovery testing). These then allowed for an understanding to be gained relating to viscosity changes and structural differences between prints, and correlations to be made with the print process. In order to maintain consistency, the rheological tests that were carried out used the previously defined variables from the preceding studies.

8.3 Results and discussion

Initial observations from the printing trials demonstrated that paste B presented a high level of paste transfer consistency (with respect to deposit shape in particular) after an

abandon time of 50 hours on both the 0.63 × 2.03 mm pads and the 0.33 × 2.03 mm pads. With the close resemblance in deposit definition displayed between the initial printing and what was achieved after an abandon time of 50 hours, it may be plausible (in the case of paste B particularly) to state that these primary findings suggest an abandon time of 50 hours is acceptable. This is based merely on deposit definition, and further issues such as the occurrence of slumping, bridging and the volume of paste transferred play a significant role in the acceptability of the print; yet the ability of the paste to retain its shape after the final print signifies good potential. With regard to the performance of paste A, this was observed to behave significantly below the standard demonstrated by paste B. The reduction in performance was highlighted through severe deformities of the print, particularly due to skipping and bridging, that were demonstrated after an abandon time of 50 hours (see figures 8.1 through 8.4).

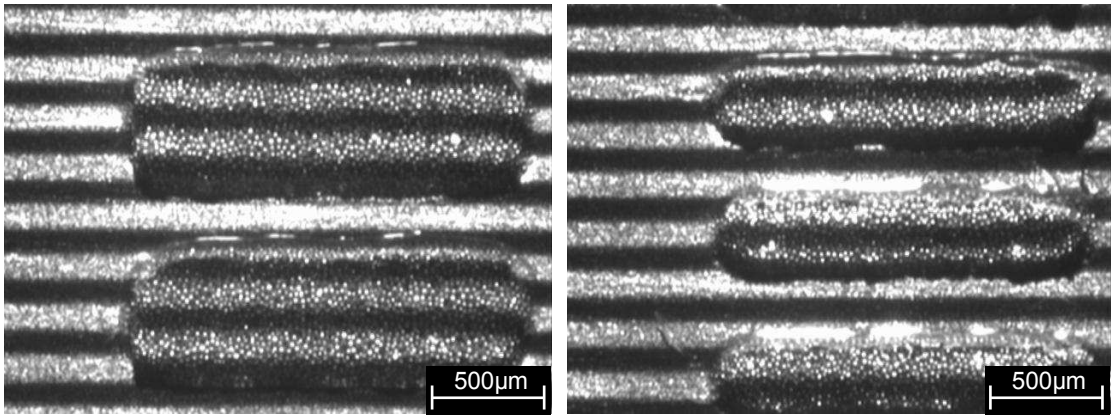

Figure 8.1: Examples of the initial print results for paste A

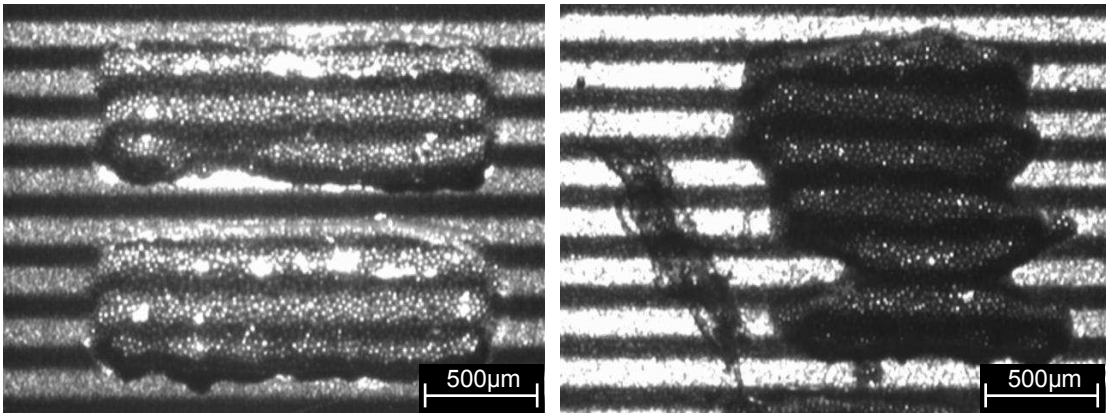

Figure 8.2: Example print results for paste A after an abandon time of 50 hours

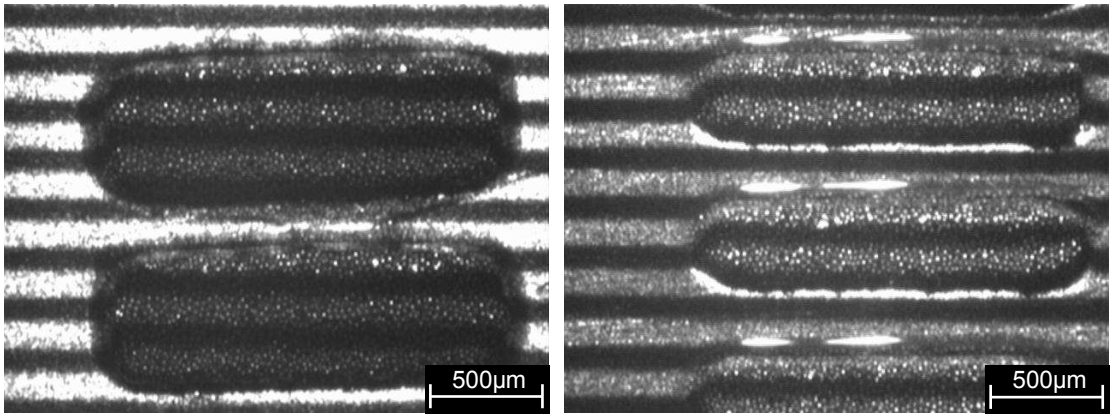

Figure 8.3: Examples of the initial print results for paste B

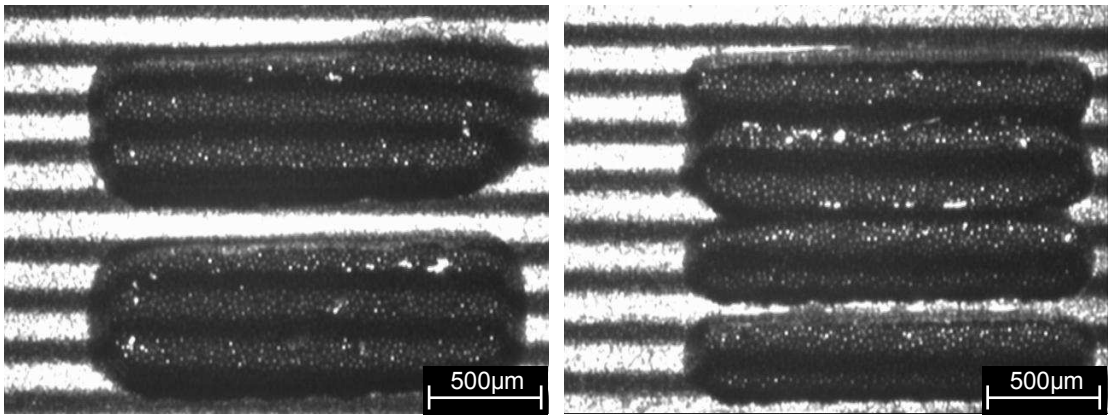

Figure 8.4: Example print results for paste B after an abandon time of 50 hours

To quantify the actual print results, it was observed that after an abandon time of 50 hours, the level of bridging increased for both pastes by a pitch size of 0.1 mm. Initial printing cycles (pre-abandon time) demonstrated a level of bridging for both pastes that extended across a pitch size of 0.1 mm (the equivalent of three bridged paste deposits using the IPC-A-21 stencil). After having been exposed to an abandon time period of 50 hours, this increased to 0.2 mm (an additional two bridged deposits, making the total five). Aside from the increased levels of bridging observed, additional observations that were made all appeared to deliver acceptable results. Both the stencil surface and the apertures were left clean after the print stroke, there was a continuing presence of a genuine paste roll as opposed to the paste being forced along the stencil in a 'pushing' motion, and the paste drop-off from the squeegee maintained an acceptable speed. Thus, the key variation exhibited was the quality of the print

deposit after subjecting the samples to an abandon time. This was consistent for paste B, yet paste A failed to perform to as high a standard.

As detailed in section 3.9.5 of Chapter 3, Lee (2002) reported that paste viscosity should theoretically increase with increased exposure time to environmental influences (unless hygroscopic in nature). With the cleanliness of both stencil and aperture being maintained, the continuing presence of a good paste roll and the slightly elevated speed of paste drop-off, observations appeared to suggest that the viscosity of the paste was actually reducing. With an increase in levels of bridging exhibited after introducing an abandon time of 50 hours (although only a 0.1 mm increase in pitch), the concept of an actually decreasing paste viscosity was substantiated.

Results from the printing trials demonstrated that the 0.63 × 2.03 mm apertures allowed for paste transfer to the board with an absence of bridging or any significant defects such as skipping. Therefore, further evaluations were focused around the 0.33 × 2.03 mm apertures, as these demonstrated the presence of defects and thus are worthy of a more detailed evaluation of the print process. With importance placed on identifying paste height and volume measurements for analysis, the initial requirement was to calculate the theoretical volume (the actual volume of the aperture) that should be exhibited by the printed paste. As the dimensions of the apertures were 0.63 × 2.03 × 0.2 mm, the calculated volume was equal to 1.3398 × 10^8 microns^3. It is important to note that the volume was derived with units of microns as this is the standard measurement used within solder paste technology and therefore is the principal measurement offered by the VisionMaster equipment.

During the actual investigation process, tests into the influence of abandon time were repeated on six different occasions, with the upper and lower recordings dismissed as anomalous results and an average taken of the remaining four readings in an attempt to maximise the chance of obtaining truly representative data. Table 8.1 details the solder paste height and volume results obtained (correct to 3 decimal places) from the printing trials after introducing abandon times of 1, 2, 3, 4, 27 and 50 hours.

Abandon time (mins)	Average paste height (µm)		Solder paste volume (µm^3 × 10^8)	
	Paste A	Paste B	Paste A	Paste B
0	187.619	183.486	1.199	1.215
60	182.192	183.105	1.102	1.211
120	179.268	182.710	1.013	1.208
180	178.148	182.169	1.009	1.201
240	175.713	180.915	0.989	1.199
1620	171.138	178.121	0.971	1.176
3000	165.226	176.768	0.969	1.159

.

Table 8.1: Paste height and volume measurements after exposure to abandon times

Through graphical representation of the results shown in Table 8.1 (see Figures 8.5 and 8.6), it becomes evident that the solder paste height demonstrated by paste A decreases fairly significantly as the abandon time increases. With regard to paste B, despite demonstrating a reduction in paste height the overall decrease is fairly insignificant, especially when compared with the decline demonstrated by paste A (Figure 8.5). Solder paste volumes appear to show high levels of stability, particularly with the results demonstrated by paste A (which exhibits a near-constant volume). Paste B, after an initial decrease in paste volume, demonstrates an almost constant paste volume after abandon times ranging from 2 to 50 hours (Figure 8.6).

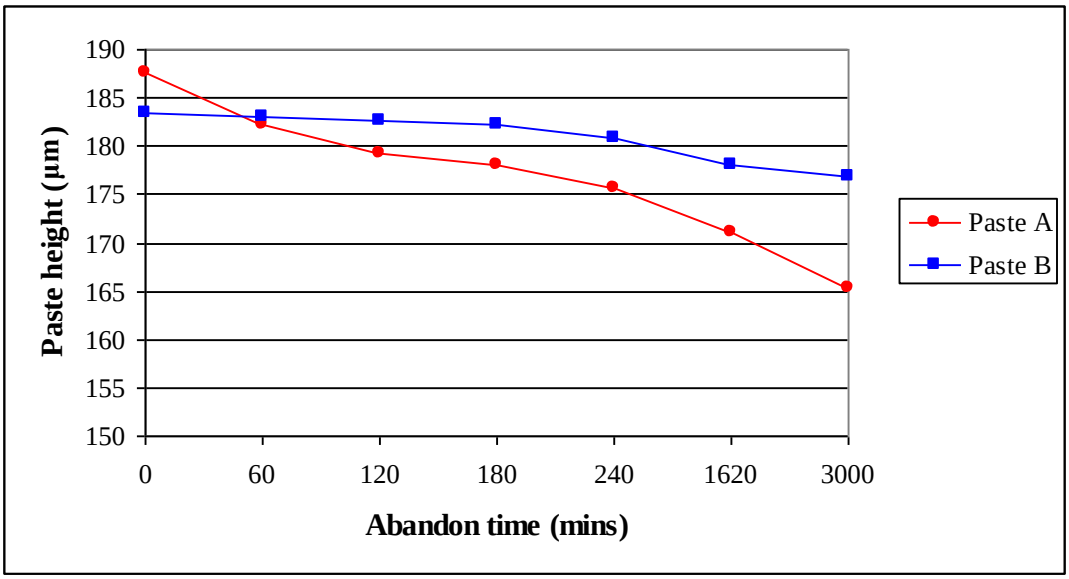

Figure 8.5: Response of observed paste height to increased abandon time

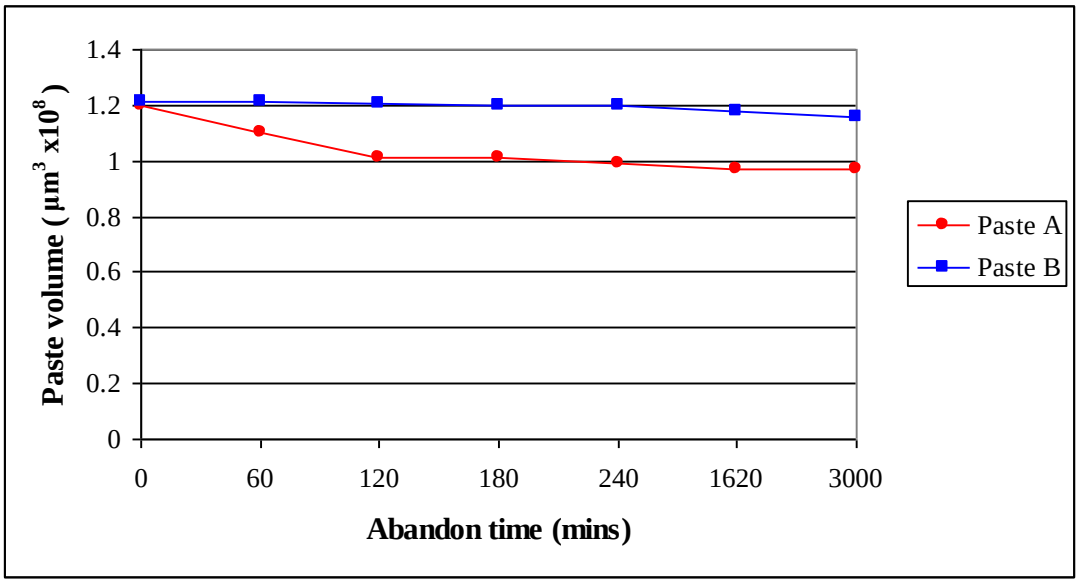

Figure 8.6: Response of observed paste volume to increased abandon time

By using the equation for transfer efficiency (equation [3.65]), it was then possible to discover the acceptability of the print from an industrial point of view (regardless of common printing defects such as bridging, slumping and skipping). As was previously mentioned (chapter 3, section 3.9.5), Heraeus (2005) discusses how generally a 15% or more reduction in measurements is considered as a failure, and therefore in order to be classed as an acceptable print 85% of the 'theoretical' measurements should be observed as a minimum. Initial calculations, prior to introducing an abandon time, were as set out in Table 8.2.

	Length (µm)	**Width (µm)**	**Height (µm)**	**Volume (μm^3)**
Aperture	2030	330	200	1.340×10^8
Paste A	1978.571	322.857	187.619	1.199×10^8
Transfer Efficiency				89.454%
Paste B	2013.841	328.416	183.486	1.215×10^8
Transfer Efficiency				90.712%

Table 8.2: Transfer efficiency prior to paste exposure to an abandon time

From these initial results, it can be observed that, on the basis of the information provided by Heraeus (2005), both the prints from paste A and paste B would be of an acceptable quality. However, from the viewpoint of ITW Kester (2007) – which states that a minimal paste deposition of 95% is required to consider a print as a pass (or as successful) – both of the solder pastes would fail before an abandon time is even applied. Continuing with the premise that a pass is anything exceeding 85% (as detailed by Heraeus), Table 8.3 details the results of investigating the transfer efficiency after having applied abandon times of up to 50 hours.

Abandon time (minutes)	**Average paste height (µm)**		**Solder paste volume ($\mu m^3 \times 10^8$)**	
	Paste A	**Paste B**	**Paste A**	**Paste B**
0	93.81%	91.74%	89.49%	90.69%
60	91.10%	91.55%	82.25%	90.39%
120	89.63%	91.36%	75.61%	90.16%
180	89.07%	91.08%	75.31%	89.64%
240	87.86%	90.46%	73.82%	89.49%
1620	85.57%	89.06%	72.47%	87.77%
3000	82.61%	88.38%	72.32%	86.51%

Table 8.3: Transfer efficiency calculated in relation to aperture dimensions

From Table 8.3, it can be seen that paste B continued to demonstrate a transfer efficiency exceeding 85% even after an applied abandon time of 50 hours. In the case of Paste A, despite acceptability with regard to paste height (bar the result observed after 50 hours, which fell short by a mere 2.39%), all results pertaining to volumetric measurements were classified as failures once an abandon time was involved. However, due to the low paste volumes observed prior to introducing an abandon time, it was believed that the transfer efficiency should be based on the initial paste-height measurements recorded as opposed to the theoretical measurements derived from the aperture dimensions. Table 8.4 highlights the results of transfer efficiency obtained by substituting the aperture measurements with those measurements recorded after the initial print.

Abandon time (minutes)	Average paste height (µm)		Solder paste volume ($\mu m^3 \times 10^8$)	
	Paste A	Paste B	Paste A	Paste B
0	187.619	183.486	1.199	1.215
60	97.11%	99.79%	91.91%	99.67%
120	95.55%	99.58%	84.49%	99.42%
180	94.95%	99.28%	84.15%	98.85%
240	93.65%	98.60%	82.49%	98.68%
1620	91.22%	97.08%	80.98%	96.79%
3000	88.07%	96.34%	80.82%	95.39%

Table 8.4: Transfer efficiency calculated in relation to initial paste dimensions

As can be seen in Figure 8.7, throughout the course of these investigations paste B demonstrated a significantly increased transfer efficiency percentage to that recorded for paste A regardless of establishing results based on the theoretical (or actual aperture) volume or the initial volume recorded prior to an abandon time. Furthermore, results from paste B demonstrated a transfer efficiency that was maintained at approximately 90%, whereas results recorded for paste A highlighted how transfer efficiency ranged from more than 90% to approximately 70%.

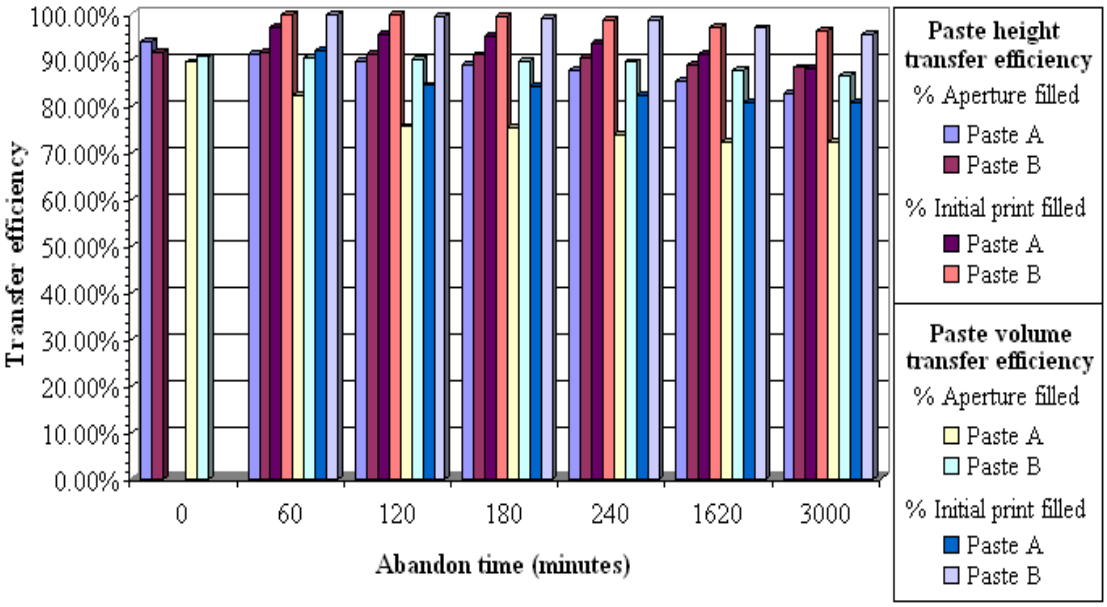

Figure 8.7: Comparison of paste transfer efficiency due to aperture dimensions and dimensions of the initial prints

From the results shown in Tables 8.3 and 8.4, and the graph shown in Figure 8.7, it becomes apparent that a trend of reduced transfer efficiency is demonstrated as the abandon time is increased. This loss of efficiency may be linked to the reduction in viscosity detailed previously, because a reduced viscosity will naturally promote the onset of slumping, which would consequently result in the recording of diminished paste heights. Furthermore, an observation of reduced paste height would result in the expectation of a lesser paste volume. The reduced transfer efficiency could therefore be accurately related to the increased levels of bridging observed.

Regardless of the reduced viscosity and transfer efficiency of the solder pastes, the quality of the print after each abandon time was maintained to an acceptable standard. This was of particular importance, as the two measurements of viscosity and transfer efficiency correlate with levels of bridging and paste volume, both of which are commonly linked to the failure of joints – and paste deposits in general – within PCB assembly and quality assurance. With bridging being the major defect observed during the printing trials (as paste roll, print definition and paste drop-off were all seen as acceptable), this factor determined the acceptability of the paste samples with regard to the abandon times applied during the investigation.

Standard testing procedures suggest that an acceptable print will demonstrate an absence of bridging across a 0.4 mm pitch, and it was observed that during the printing trials the levels of bridging merely reached 0.2 mm. With abandon time acceptability depending on the quality of the first print after stencil downtime, from a printing point of view, applying a 50-hour abandon time (and potentially a downtime in excess of this) is possible. Furthermore, the 'predicted' results (see Figure 3.28 in section 3.9.5) were seen to be inaccurate, as the quality attained from the printing cycles ensured that a 'first-pass' successful result was achieved and therefore the predicted 11.3 printing cycles were unnecessary.

Results from the rheological tests confirmed the observation of a reduced viscosity from the printing trials for both pastes A and B. However, of interest was the significant variation in viscosity that was exhibited through comparing the two pastes. Paste A demonstrated a variation in peak viscosity ranging from 1.995×10^4 Pas to 4.37×10^4 Pas (Figure 8.8), whereas paste B demonstrated a variation of 3.124×10^4

Pas to 3.669 × 10^4 Pas (Figure 8.9). From these results, paste B exhibits a much greater level of stability with regard to paste viscosity (after an abandon time) when compared with paste A. Furthermore, this consistency could be responsible for the maintenance of print quality because the significant reduction demonstrated by paste A could account for increased levels of slumping and hence the reduced transfer efficiency observed.

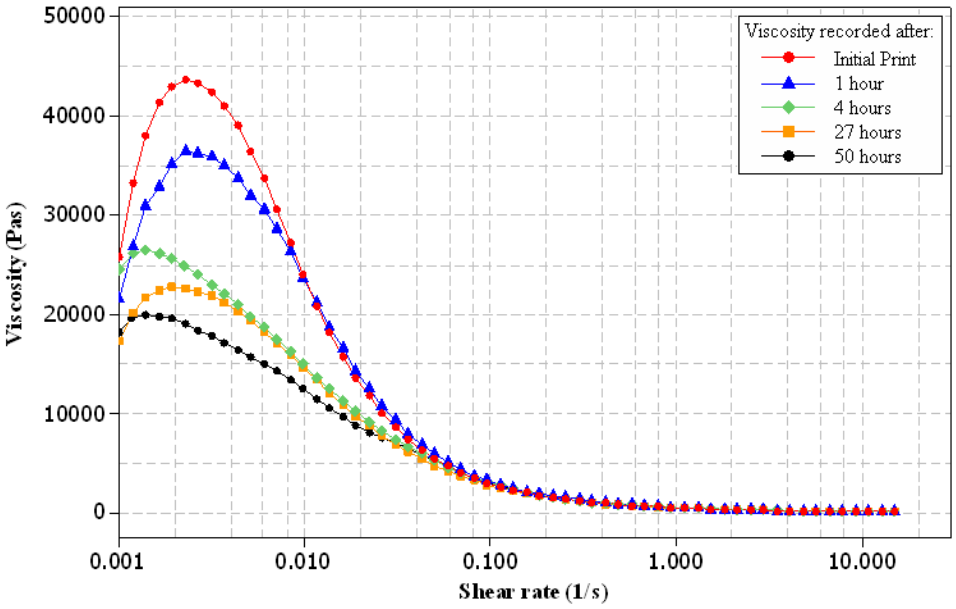

Figure 8.8: Viscosity measurements for paste A

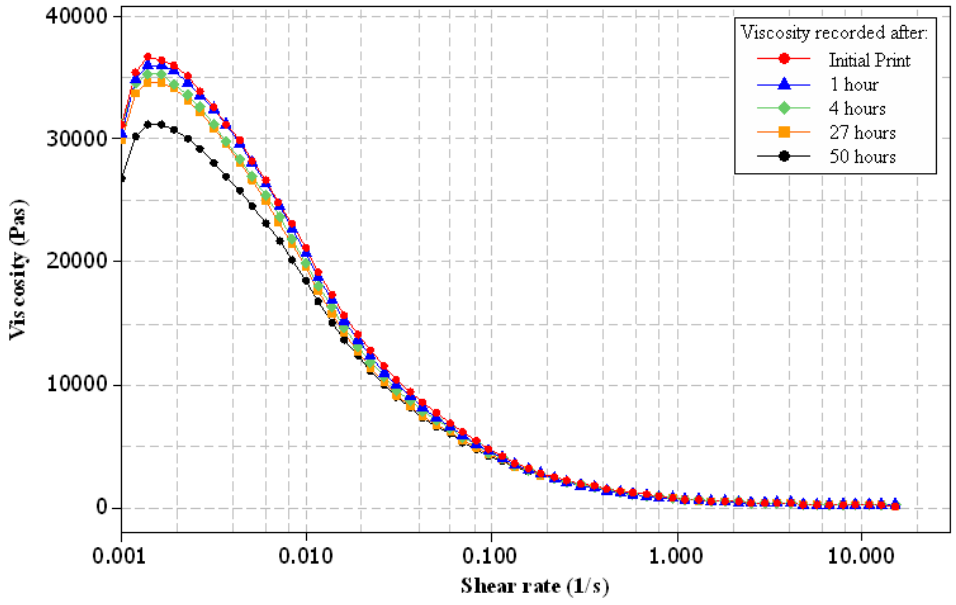

Figure 8.9: Viscosity measurements for paste B

As the viscometry tests demonstrate a reduction in the viscosity of the pastes after incorporation of an abandon time, it follows that the paste is more likely to flow after removal of the stencil (losing ability to maintain print shape), which would lead to an increase in bridging. In addition, the reduction in viscosity could also provide an explanation for the increase in the speed of drop-off witnessed after printing 50 hours after the initial print (Table 8.5).

Observation	**Paste A**		**Paste B**	
	Initial Print	**After 50 hours**	**Initial Print**	**After 50 hours**
Bridging (0.33 pads)	Across a 0.1 mm pitch	Across a 0.2 mm pitch	Across a 0.1 mm pitch	Across a 0.2 mm pitch
Skipping (%)	5	5	5	5
Drop-Off (s)	15–20	10–15	15–20	10–15
Additional notes	Clean stencil and apertures and good paste roll	Clean stencil and apertures and good paste roll	Clean stencil and apertures and good paste roll	Clean stencil and apertures and good paste roll

Table 8.5: Initial print observations compared with those after 50 hours' abandon time

The results attained through the viscometry testing (highlighting that an increased abandon time leads to a decrease in the viscosity) may also be correlated with the oscillatory data, which demonstrated a breakdown of paste structure. Results observed through conducting the oscillatory tests showed that both the elastic and viscous modulus decreased with an increased abandon time. This indicates that during these periods of abandoned printing time, the structure of the paste was breaking down – a trend that was also depicted by the increase in phase angle (Figures 8.10 and 8.11). This observation may be due to separation of the solder particles from the flux medium, which could create the impression of reduced viscosity because the rheometer would incorporate readings from the separated flux medium during the characterisation tests. If this were true, the amount of paste resistance encountered by the rheometer would be reduced, due to the presence of a layer of separated flux medium between the solder particles and the top plate; consequently, the amount of force required to move the paste would be reduced, which would result in a viscosity reduction and a breakdown in paste structure from the oscillatory tests.

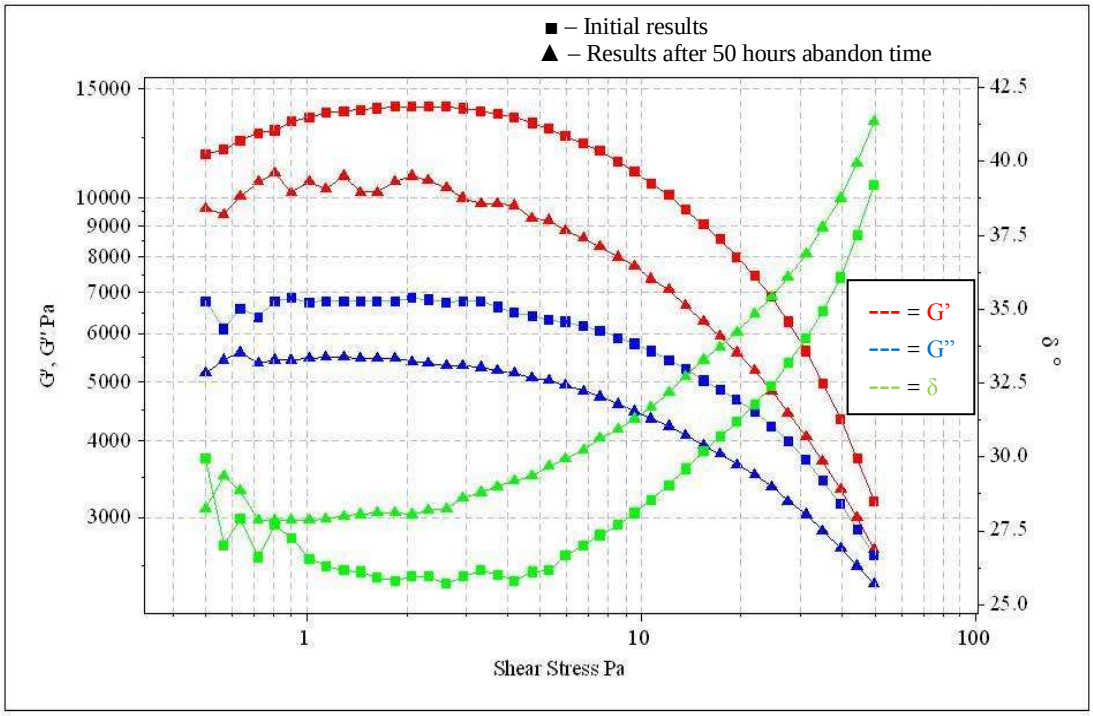

Figure 8.10: Oscillatory results for paste A before and after a 50-hour abandon time

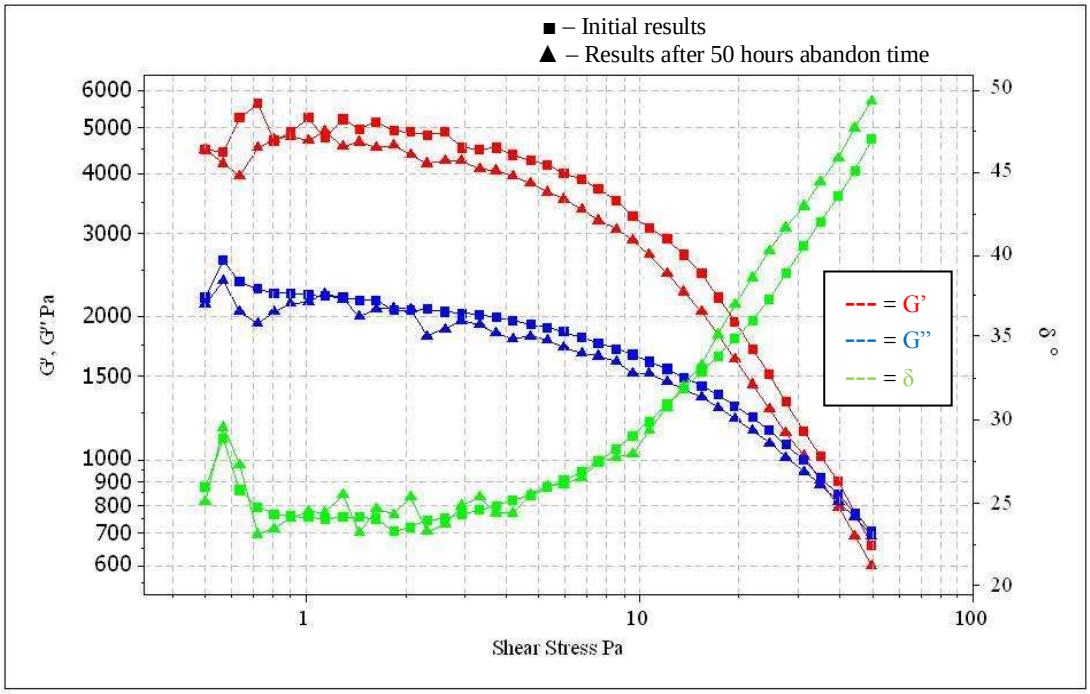

Figure 8.11: Oscillatory results for paste B before and after a 50-hour abandon time

Throughout all the investigations conducted in this part of the study, the rheology of paste B was observed to remain highly consistent, particularly in relation to the observations made through studying paste A. This would certainly influence the

transfer efficiency, which can ultimately dictate the pass/fail rate (acceptability) of printing trials after an abandon time period (as discussed by industrial manufacturers such as Heraeus). One additional significant result observed through both the viscosity and oscillatory tests was the convergence of the graphs (those after the initial print and those after an abandon time of 50 hours). This trend indicates that upon working the paste after an abandon time, once a certain number of printing cycles have been conducted, the print results achieved may closely resemble those attained from a sample that had not been subjected to the influence of an abandon time.

After having successfully attained results from the abandon time study relating to both a rheological and stencil-printing viewpoint, it became apparent that paste transfer quality could be maintained even after a 50-hour downtime. However, because of print acceptability commonly depending on a successful 'first-pass' basis (Jensen, 2004; Qualitek, 2008; Koorithodi, 2010), it was believed that further investigations were required in order to understand the effect an abandon time can present when the printing cycles are resumed. From an industrial viewpoint, in the event of the printing process becoming interrupted for a period of one hour a solitary print is unlikely to follow the downtime – a typical production line would be printing more than one board every hour. Therefore, it was believed that the number of prints that directly follow an abandon time should also be investigated. Literature findings support this proposal, with work by Lee (2002) reporting how initial print quality may be acceptable yet this quality tends to degrade with an increase in the number of prints – with common defects of skipping and aperture clogging being encountered. Conversely, in some instances the paste may demonstrate smearing and flux bleeding as a result of 'thinning' with increased printing time. It was for this reason that the study was extended and an investigation was conducted into the influence of 'print frequency' in order to conclude this aspect of the study.

8.4 The influence of abandon time and print frequency on the quality of print

8.4.1 Introduction

Current industrial techniques raise questions as to the efficiency of the printing process, due to an inability to appropriately correlate paste properties with the printing

process and hence predict the quality of the final joint/interconnection produced. As a result of this current lack of knowledge, further investigation is necessary in order to accurately state whether a solder paste can plausibly be used beyond the time frames currently employed. By further advancing those results previously attained from the abandon time investigation (by introducing an element of multiplicity into the print cycle), the possibility exists of discovering the extent to which the number of prints completed in a specific time frame affects the print quality.

The importance of studying the abandon time was clearly highlighted as being of significance because it emphasised the additional extent of time that the paste can plausibly be left on the stencil printer before the quality of the paste diminishes. However, industrial standards involve almost continuous application of the printing process in order to mass-produce PCBs. By introducing a print frequency aspect into the previous abandon time investigation, it is possible to build on the validity of those results, significantly increasing the importance of the findings from an industrial viewpoint. The paste printing process is typically an everyday task within industry, and so if studies can show that a paste may be used for a whole day – possibly even two days – before the need for replacement arises (regardless of the number of prints being undertaken), it may be possible to greatly increase the efficiency of the SMA process.

8.4.2 Test method

As a result of the investigation into print frequency being an extension of the previous abandon time study, the materials and apparatus used remained the same to ensure that consistency was maintained. Furthermore, the fundamental method of investigation remained the same, with the only variation being the number of print cycles conducted. Therefore, in order to complete such an investigation, the paste was worked a number of times within the space of one hour before introducing an abandon time into the process.

Initial studies focused on print trials using a five-minute interval between successive prints. Thus, the paste had been worked twelve times within the first hour of printing before an abandon time of one hour was introduced. The process was then repeated

for print trials conducted with a four-minute interval between prints prior to commencing an abandon time, and then with three-minute and two-minute intervals. In each instance, rheological tests were conducted using paste samples taken from the stencil after concluding the first print cycle that directly followed an observed abandon time.

8.4.3 Results and discussion

Initial results from the study highlighted that, despite the introduction of an increased number of prints between abandon times, the quality of the final deposition was maintained at a consistently acceptable standard. As has been mentioned previously, bridging and slump are two of the most common defects observed in the solder paste printing process. After the initial printing trials, where print cycles were conducted every five minutes, results indicated that the level of bridging increases by a mere 50 µm (0.05 mm), which consequently indicates that the industrial acceptability standard is still achieved. This result therefore signifies that with an increased level of print frequency it is still plausible to introduce an abandon time into the printing process without a significant degradation to the quality of deposition.

Test (pm)	Print shape	Skipping	Bridging (0.33 pads)	Paste roll	Drop off (sec)	Stencil/ Apertures
12:00	95%	5%	0.20 mm pitch	Yes	15–20	Clean
12:05	90%	5%	0.20 mm pitch	Yes	15–20	Clean
12:10	85%	10%	0.25 mm pitch	Yes	15–20	Clean
12:15	85%	10%	0.25 mm pitch	Yes	15–20	Clean
12:20	85%	15%	0.25 mm pitch	Yes	15–20	Clean
12:25	85%	15%	0.25 mm pitch	Yes	15–20	Clean
12:30	90%	5%	0.25 mm pitch	Yes	15–20	Clean
12:35	85%	5%	0.25 mm pitch	Yes	15–20	Clean
12:40	85%	15%	0.25 mm pitch	Yes	15–20	Clean
12:45	80%	10%	0.30 mm pitch	Yes	15–20	Clean
12:50	80%	10%	0.30 mm pitch	Yes	15–20	Clean
12:55	85%	10%	0.25 mm pitch	Yes	15–20	Clean

Table 8.6: 5-minute print frequency results for paste B after a 1-hour abandon time

Details within tables 8.6 – 8.8 highlight the key observations that were made during the stencil printing to identify paste performance, with varying print-cycle and abandon times. With regard to print shape, this relates to the definition of deposit shape, which is given a percentage value depending on the degree to which it fills a rectangular view using the VisionMaster solder paste height-measuring equipment. Skipping relates to the percentage of instances where gaps are observed within the deposit in relation to the percentage of deposit as a whole. Bridging in this instance is related to the level of bridging across specific pitch sizes for the smaller 0.33 × 2.03 pads. The paste roll relates to whether the observation was of an actual roll of the solder paste on the stencil or whether the paste was simply 'pushed' along the surface of the stencil. Drop-off relates to the amount of time taken for the solder paste to fall away from the squeegee once it has been lifted away from the stencil surface. Finally, stencil/aperture relates to the observation detailing whether there were any obvious deposits of paste remaining on the surface after the print cycle, and also whether there were any noticeable remnants of solder paste within the apertures after removal of the board.

Table 8.6 gives the observations made with a five-minute print frequency and one-hour abandon time. Table 8.7 gives the observations under the same printing conditions but after a 50-hour abandon time. By increasing the length of abandon time (but maintaining the same print frequency after the delay), it was found that the quality of the print remained at a high standard that almost replicated the results achieved after a single hour of abandon time. Although the paste deposits exhibited some bridging, the extent was insufficient to reach a pitch size of 0.4 mm, which would therefore classify the print as successful. From the results, it appears plausible that conducting printing cycles once every five minutes and attaining acceptable prints is possible, even after an abandon time of 50 hours.

Test (pm)	Print shape	Skipping	Bridging (0.33 pads)	Paste roll	Drop off (sec)	Stencil/ Apertures
13:00	95%	5%	0.2 mm pitch	Yes	15-20	Clean
13:05	95%	5%	0.25 mm pitch	Yes	15-20	Clean
13:10	85%	10%	0.2 mm pitch	Yes	15-20	Clean
13:15	80%	15%	0.25 mm pitch	Yes	15-20	Clean
13:20	85%	10%	0.25 mm pitch	Yes	15-20	Clean
13:25	90%	10%	0.2 mm pitch	Yes	15-20	Clean
13:30	90%	5%	0.25 mm pitch	Yes	15-20	Clean
13:35	85%	10%	0.25 mm pitch	Yes	15-20	Clean
13:40	85%	10%	0.3 mm pitch	Yes	15-20	Clean
13:45	85%	15%	0.3 mm pitch	Yes	15-20	Clean
13:50	80%	15%	0.25 mm pitch	Yes	15-20	Clean
13:55	80%	15%	0.3 mm pitch	Yes	15-20	Clean

Table 8.7: 5-minute print frequency results for paste B after a 50-hour abandon time

A comparison of those results detailed within Tables 8.6 and 8.7 suggests a close resemblance between the two sets of paste performances, regardless of the abandon time applied. Figure 8.12 highlights this similarity between results.

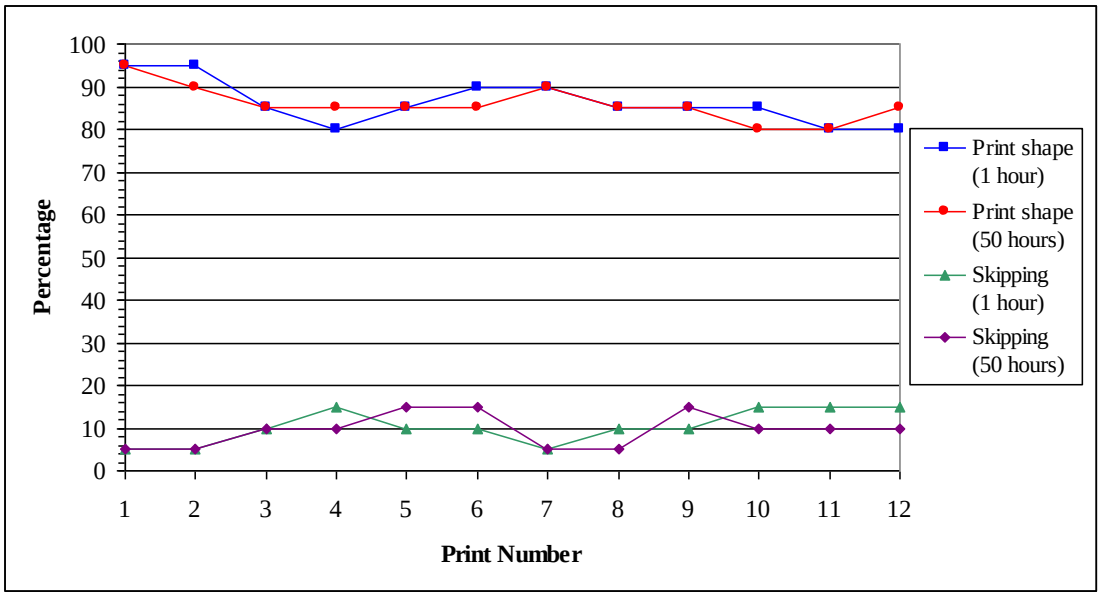

Figure 8.12: Comparison of print shape and skipping for 1-hour and 50-hour abandon times with a 5-minute print frequency thereafter

With results from introducing a 5-minute print frequency demonstrating a high level of consistency for all abandon times, further investigations were conducted into paste response to four-, three- and two-minute print frequencies. Table 8.8 details the results of the print observations taken from the two-minute print frequency investigation, as this represented the harshest conditions (and closest resembling conditions to industrial practice) applied to the paste samples. As can be seen from the results shown in Table 8.8, the acceptability of the print remained intact after introducing both a 50-hour abandon time and a two-minute print frequency standard. Despite the level of bridging increasing by 0.15 mm, the maximum level observed only reached a 0.35 mm pitch size, therefore remaining within the limits of the 0.4 mm fail boundary.

Test (pm)	Print shape	Skipping	Bridging (0.33 pads)	Paste roll	Drop off (sec)	Stencil/ Apertures
14:00	95%	0%	0.20 mm pitch	Yes	15–20	Clean
14:02	95%	5%	0.20 mm pitch	Yes	15–20	Clean
14:04	95%	5%	0.25 mm pitch	Yes	15–20	Clean
14:06	95%	5%	0.25 mm pitch	Yes	15–20	Clean
14:08	95%	5%	0.25 mm pitch	Yes	15–20	Clean
14:10	90%	10%	0.20 mm pitch	Yes	15–20	Clean
14:12	90%	5%	0.15 mm pitch	Yes	15–20	Clean
14:14	85%	10%	0.25 mm pitch	Yes	15–20	Clean
14:16	85%	15%	0.25 mm pitch	Yes	15–20	Clean
14:18	90%	5%	0.20 mm pitch	Yes	15–20	Clean
14:20	85%	10%	0.20 mm pitch	Yes	15–20	Clean
14:40	80%	15%	0.20 mm pitch	Yes	10–15	Clean
14:42	75%	15%	0.15 mm pitch	Yes	10–15	Clean
14:44	75%	15%	0.25 mm pitch	Yes	10–15	Clean
14:46	75%	20%	0.30 mm pitch	Yes	5–10	Clean
14:48	85%	10%	0.20 mm pitch	Yes	15–20	Clean
14:50	80%	15%	0.30 mm pitch	Yes	10–15	Clean
14:52	75%	15%	0.25 mm pitch	Yes	10–15	Clean
14:54	80%	15%	0.30 mm pitch	Yes	10–15	Clean
14:56	75%	15%	0.35 mm pitch	Yes	10–15	Clean
14:58	85%	10%	0.35 mm pitch	Yes	15–20	Clean

Table 8.8: 2-minute print frequency results for paste B after a 50-hour abandon time

During the course of the printing trials, it was found that both pastes A and B performed to an equally high standard, although after the introduction of the element of print frequency, paste A actually demonstrated the greater level of consistency. As the print frequency was increased, the performance of paste A was nearly identical to initial tests conducted, and therefore results focused primarily on paste B as this demonstrated the greatest variation (although this variation was also very minimal).

Rheological results further confirmed the stability of both pastes, with viscosity tests demonstrating that the print frequency, although appearing to instigate a reduction in viscosity, fails to significantly influence the measurements attained. From the results displayed in Figure 8.13, it can be seen that, for a print frequency of 5 minutes and an abandon time of 50 hours, the viscosity of paste B reduced from 3.81×10^4 Pas to 3.632×10^4 Pas. Conversely, for a print frequency of 2 minutes, the viscosity was seen to decrease from 3.608×10^4 Pas to 3.124×10^4 Pas.

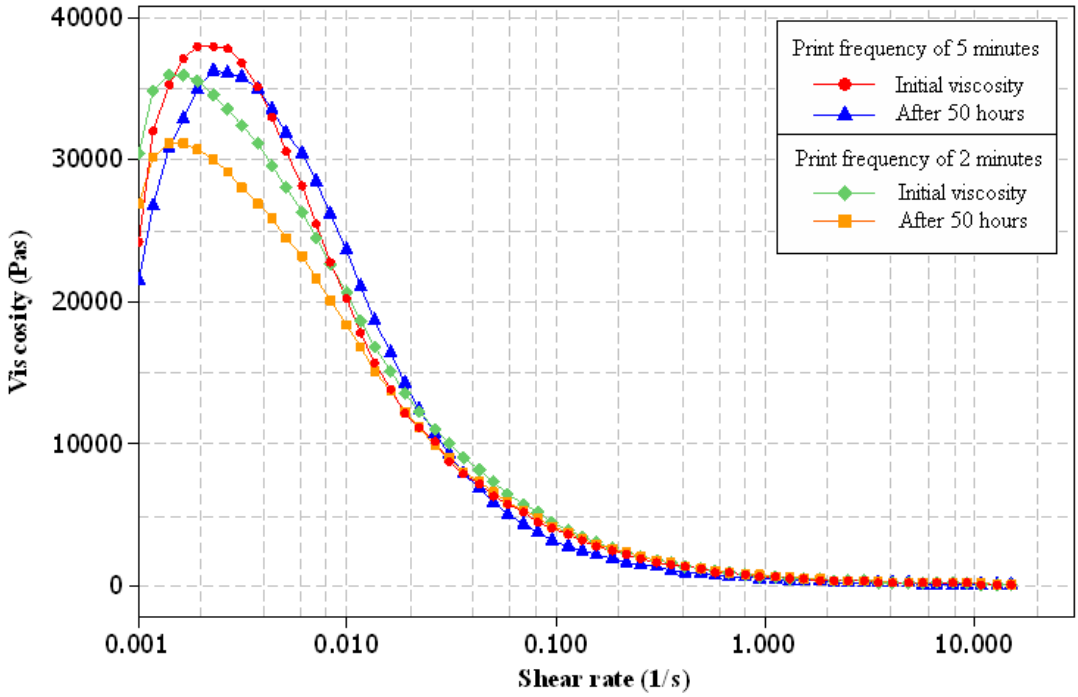

Figure 8.13: Comparison of results for varied print frequency and abandon time for paste B

These results demonstrate that even after an abandon time of 50 hours, the print frequency can be maintained at an industrial standard without paste deterioration or the presence of a significant reduction in print quality.

8.5 Conclusions

By initially investigating the influence of abandon time on the print quality and rheological behaviour of solder pastes, observations highlighted that as the period of printer downtime was increased, the viscosity of the samples decreased. This trend was observed throughout each of the tests conducted (relating to print observations themselves and the various rheological tests undertaken) and could be a result of separation of the flux (which would appear to increase flow behaviour) or moisture pick-up from the unenclosed printer environment. Regardless of this reduction in viscosity, the quality and repeatability of the print was seen to remain at a consistent and high standard, which allowed for a successful pass to be achieved in relation to those print guidelines dictated by various paste manufacturers such as Henkel Technologies and Heraeus.

Owing to successfully retaining high-quality prints, it appears that the potential exists to allow for an abandon time of 50 hours and above to be incorporated into industrial operations. This is a substantial difference to the one-hour maximum standard mentioned within the literature (or four hours as a ‘possible’ time limit in the case of Henkel Technologies). With these indications that print quality is conceivably acceptable after such a postponement within the assembly line, questions are posed relating to the current process employed, where a single hour of abandon time is overlooked for fear of unacceptable deposits. With this in mind, it may also be possible to utilise this method as a means of benchmarking, in order to estimate possible abandon times for other pastes.

While investigating the influence of abandon time, it was also concluded that current specifications for determining a successful print must be revised. The reasoning for this was due, first, to the conflicting requirements specified between guidelines: in the case of ITW Kester (2007) an acceptable print is achieved with a paste deposition of at least 95%, whereas information from Heraeus (2005) details that only 85% is

necessary to achieve a ‘pass’. As was seen from the results obtained, these differing specifications led to the print outcome demonstrating acceptability in one instance but failure in the second. Secondly (relating to the criteria stated from Heraeus and ITW Kester), the pass/fail specifications neglect to acknowledge the actual printing observations themselves. For example (using the aforementioned parameters), a print result that has a solder paste volume of 95% would automatically be classified as a ‘pass’, but this fails to take into consideration any elements of bridging or skipping. As has been discussed in technical papers by Henkel Technologies (Gregoire, 2003), in order to achieve a ‘pass’ classification a solder paste must be able to demonstrate repeat printability on a 0.4 mm pitch. It is for this reason that it has been concluded that definitive guidelines must be developed.

Through introducing an element of print frequency into the investigation, a trend of reducing viscosity was once again observed. This viscosity drop was expected as a result of the shear-thinning nature of the solder pastes, yet (much like the principal investigation into abandon time) it was deemed insignificant. The decrease in viscosity arising from increased print frequency was nonetheless seen to result in an increase in the level of bridging observed. Even so, observations from the printing trials continued to exhibit acceptable prints.

In addition to the acceptable results attained, it was also observed that through conducting rheological investigations the paste viscosity after an abandon time of 50 hours converged with the initial paste viscosity determined prior to applying any printer idle time (regardless of the print frequency). The significance of this finding lies within the industrial method for PCB assembly, where numerous boards may be printed within the space of one hour. With the convergence of viscosity levels over time, an abandon time of 50 hours could well be applied within current industrial manufacturing procedures without adverse effect. Furthermore, as the viscosity demonstrates convergence after applying a shear to the sample, by simply conducting ‘pre-print’ printing cycles to work the paste it may be possible to replicate those results that were attained prior to any abandon times (while conducting the actual printing process). This would therefore signify that an abandon time of 50 hours plays no significant role in print deterioration.

The value of the findings from the study may demonstrate considerable importance, as an increase in abandon time limits could have a huge significance for both paste manufacturers and users in terms of both cost savings and reduced impact on the environment (less waste disposal). With regard to disposal, the WEEE directive dictates that electronic waste must be disposed of appropriately: BLT Circuit Services Ltd (2009) states that redundant paste materials should be forwarded to licensed contractors for metal recovery whenever possible. This arises as solder paste is viewed within electronics manufacturing as presenting significant environmental and health risks (Keely, 2000). Therefore, through using a paste formulation that allows for an abandon time of up to 50 hours (two days), the level of waste would be reduced as the paste would no longer be discarded each half-day or at the end of each eight-hour shift as is typically the situation. The reduction in waste would consequently lessen the cost encountered during PCB assembly, while potentially increasing marketability for the paste manufacturer, as products with longer abandon times may be more desirable to customers and users.

CHAPTER 9:

THE INFLUENCE OF APPLIED STRESS, APPLICATION TIME AND RECURRENCE ON THE RHEOLOGICAL CREEP RECOVERY BEHAVIOUR OF LEAD-FREE SOLDER PASTES

9.1 Introduction

The focus of this chapter is the investigation of the creep recovery behaviour of Pb-free solders subjected to variations in applied stress, stress application time and repeated applications of stress. The aim of the study was to investigate typical stencil printing procedures to determine paste behaviour in relation to printing cycles. In order to understand paste response, various aspects of the stencil printing process were replicated on a rheometer, which were then combined to imitate the actual print cycle rheologically. The areas investigated included the amount of stress applied, the length of time the stress was applied, and repeated cycles of creep recovery behaviour.

After removal of an applied stress, samples exhibiting higher levels of recovery should demonstrate a superior structural stability in order to resist slump to a greater extent. Therefore, by identifying the elastic response of solder paste (from the recovery behaviour of the creep recovery method), strides can be made in reducing the severity of printing defects. This is achievable because, with a greater ability to retain structure, a lesser opportunity for paste flow exists. Previous studies relating to creep recovery investigations have highlighted the trend of reducing levels of slump with increased values of recovery (Bao et al, 1998). This understanding underlines the importance of the test method when attempting to discover correlations between the print process and rheological characteristics.

Literature findings demonstrate that creep recovery results are typically correlated with the printing process through observations relating to performance and rheological behaviour. However, as generally the printing process is not accurately

represented during these rheological tests (see section 9.2), questions arise as to the accuracy of these results. Hence, investigating parameters such as the duration of an applied stress and the actual value of the applied stress become important. Furthermore (as previously discussed in Chapter 8), industrial practices do not simply involve printing single boards but, rather, mass production. This consequently raises the need for repeated cycles of the creep recovery test, in order to gauge the true behaviour of the paste during the stencil printing process. Therefore, as creep recovery testing offers great potential with understanding and minimising slump and bridging defects, it is necessary to incorporate elements of the printing process into these investigations. For this reason, three individual investigations are considered necessary:

- **Effect of creep application time on the recovery performance of lead-free pastes:** Correlating the printing process with rheological properties of solder paste is an essential step in the reduction of assembly defects in industry, and hence is of particular importance within the project. In order to conduct appropriate investigations for such an evaluation, understanding the industrial printing process is essential. Common creep-recovery tests are conducted by applying a constant stress until a purely viscous flow is achieved – in order to ensure that structural breakdown has reached a plateau. This typical period for the creep aspect of the test may last in excess of several minutes, yet the complete process of depositing paste onto a board for an industrial production line takes a matter of seconds. Therefore, to correspond with the industrial process it is apparent that the sample should not be subjected to an applied stress for more than a few seconds. The purpose of this part of the study was therefore to replicate this aspect of the industrial printing process through applying stress to the sample for a short period of time (for example, 10 seconds). The relaxation period was then applied to monitor the extent of recovery achieved, indicating the ability of the sample to withstand slump by retaining structure and hence limiting paste flow.
- **Creep recovery behaviour of lead-free pastes as a function of applied stress:** When determining the stress applied to a test sample, the common trend is to apply a value taken from within the linear viscoelastic region

(LVR) in an attempt to prevent permanent structural breakdown. By conducting basic amplitude sweep testing, a range of up to 10 Pa is often identified as the LVR. Assuming this to be a universal standard, the printing process must not exert a stress greater than 10 Pa for correlations to be drawn between the rheological results and the printing process. As this is not the case, it is essential to increase the applied stress beyond the LVR in an attempt to understand the recoverability of paste during the printing process. Testing consisted of the application of a high stress value for the duration of the investigation, with the resultant elastic response or recovery monitored. The extent of recovery was then contrasted between varying samples, yielding an understanding of paste response to applied stress, with a further correlation between rheological properties and the printing process.

- **The influence of recurrent applications of creep recovery on paste rheology:** One additional element that requires addressing is that of multiple print cycles within the assembly process. Because industrial manufacturers employ the concept of mass production, the procedure of depositing solder paste during SMA is one that is consistently repeated without paste replacement. Typical creep-recovery testing involves performing one cycle of the investigation, which is followed by replacing the material with a fresh sample. This not only removes the element of 'worked paste' (seen in industrial practices) but also introduces a delay into the application time. Although it may be possible to achieve valuable results from such testing, this method fails to incorporate a link to the process that will evidently be practised.

During the course of these investigations, the testing focused on subjecting a single sample of solder paste to repeated cycles of the creep recovery method. Through conducting such an investigation, it was possible to identify paste recovery behaviour based upon multiple applications of stress and relaxation periods. Simply by ensuring that the paste was worked and then allowed to rest, on a repetitive cycle, it was possible to discover an accurate correlation of the results observed with the stencil printing process.

9.2 Background theory

With the significant contribution towards print failure attributed to the presence of slumping and consequently bridging defects, the creep recovery method of investigation offers substantial potential in understanding methods to minimise their influence. Work by Bradley et al (2007) supports this theory, reporting that structural recovery is inversely proportional to the number of print defects, which indicates that with an increase in recovery, a decrease in print defects would be observed. This is a trend that would be expected, as an improvement in recovery behaviour would point towards an increased ability to retain structural stability upon removal of stress, subsequently limiting the slumping behaviour of the paste sample.

Efforts have been previously made to investigate the creep recovery behaviour of solder materials (Girdwood and Evans, 1996; Mostafa et al, 2003; El-Khalek, 2009), yet literature findings commonly highlight that the parameters typically employed during these investigations are not representative of the actual stencil printing process (particularly pertaining to the length of application time and the stress applied), and thus correlations of the recovery behaviour to the print achieved are questionable. One such example is that of the work conducted by Durairaj et al (2009[b]), in which it is discussed that within the LVR – the maximum deformation recorded prior to structural breakdown – the particles remain closely packed together, demonstrating a strong elastic recovery to any deformation and subsequently solid-like behaviour. Once this upper threshold is surpassed, the structure begins to break down, which is indicated by an increase in the viscosity characteristic. After having acknowledged that the LVR represents the stress that can be applied without instigating structural breakdown, Durairaj et al continue to discuss how the samples investigated demonstrate an LVR of up to 9.7 Pa. During the creep recovery period, however, the stress applied to the sample was equal to 5 Pa, which is clearly within the observed LVR. If this is to be truly representative of the stencil printing process, this would indicate that throughout the printing cycles the paste is not subjected to stresses exceeding 5 Pa.

The work conducted by Durairaj and colleagues is also supported by Cunningham (2009[b]), in which the method for selecting an appropriate stress for application during

creep recovery testing is detailed. Initially Cunningham discusses how a simple oscillatory stress sweep provides a straightforward opportunity to identify a suitable value, after which values of 0.001 Pa and 100 Pa are given as limits. The guideline then continues to describe the existence of the LVR, identifying the yield point at which the modulus of elasticity drops rapidly (Figure 9.1). Cunningham then states that an ideal stress for incorporation within creep testing can be taken from the point immediately following the 'noisy data' – significantly less than the upper limit of the LVR.

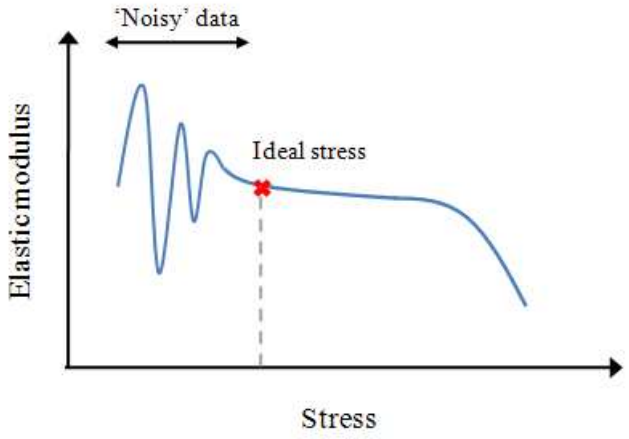

Figure 9.1: Typical method used for stress selection during creep recovery testing (Cunningham, 2009[b])

As can be seen in the work conducted by Durairaj et al and Cunningham, typical values for incorporation within creep recovery testing are taken from within the LVR. However, in work conducted by Costello (1997) it was reported that samples were pre-sheared in an attempt to reproduce typical stencil printing conditions, with typical values for the printing process recorded as 10 s^{-1} as an estimate. Furthermore, in work conducted by Trease and Dietz (1972), it was discovered that during the printing of solder pastes a range of shear rates from 0.01 s^{-1} to above 1000 s^{-1} are experienced. Thus, by using the standard equation [3.13] for the viscosity of a material, it is possible to state that:

$$\text{Shear Stress } (\sigma) = \text{Viscosity } (\eta) \times \text{Shear Rate } (\dot{\gamma}) \qquad \textbf{[9.1]}$$

Therefore, through combining this fundamental equation with those findings from Trease and Dietz (1972), it is possible to state that the shear stress experienced during the stencil printing process comprises the range given by:

$$\sigma = \eta \times 0.01\ s^{-1} \longrightarrow \sigma = \eta \times 1000\ s^{-1} \qquad \textbf{[9.2]}$$

Utilising the information attained previously (see Chapter 6, Figure 6.1), it can be shown that, for these particular shear rates, the viscosity for the experimental pastes can range from approximately 30,000 Pas to 10 Pas. By using this information, it can be stated that the stress encountered by the solder paste during the stencil printing process may fall in the range of:

$$\sigma = 30{,}000\ \text{Pas} \times 0.01\ s^{-1} \longrightarrow \sigma = 10\ \text{Pas} \times 1000\ s^{-1} \qquad \textbf{[9.3]}$$

so $\sigma = 300$ Pa $\longrightarrow$ 10,000 Pa

If these are to be correct or accurate estimations of the stress values experienced by the solder paste during the stencil printing process, then those values (or methods for selecting values) previously discussed in the works by Durairaj et al and Cunningham clearly do not represent the actual print process. This observation is further supported in work by Kay et al (2003), who utilised computational fluid dynamics to simulate the motion of adhesive paste ahead of a moving squeegee blade during the stencil printing process (Figure 9.2).

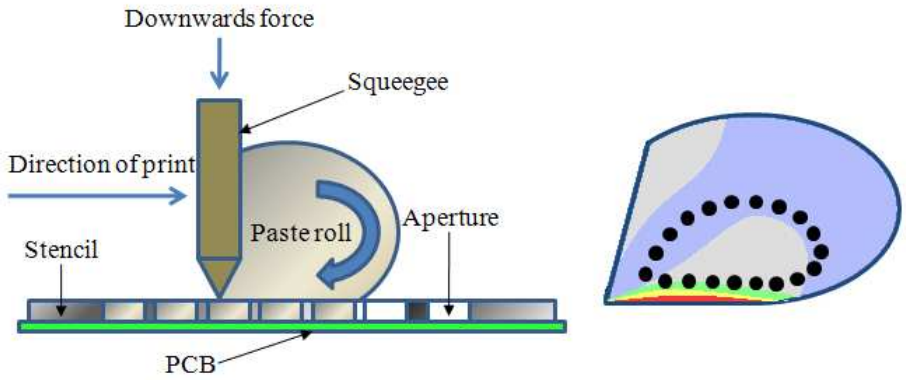

Figure 9.2: Simulated motion of solder paste during stencil printing (Kay et al, 2003)

During the investigation, attempts were made to highlight the predicted trend of pressure distribution in paste materials while using a squeegee with a forward print speed of 10, 20, 30 and 40 mm/s and an angle of 60° with the stencil surface. Results from the investigation highlighted that the solder paste was exposed to stress values ranging from approximately 2,000–10,000 Pa during the stencil print (Figure 9.3), which further emphasises the necessity for undertaking creep recovery testing 'outside' the LVR in order to accurately form correlations.

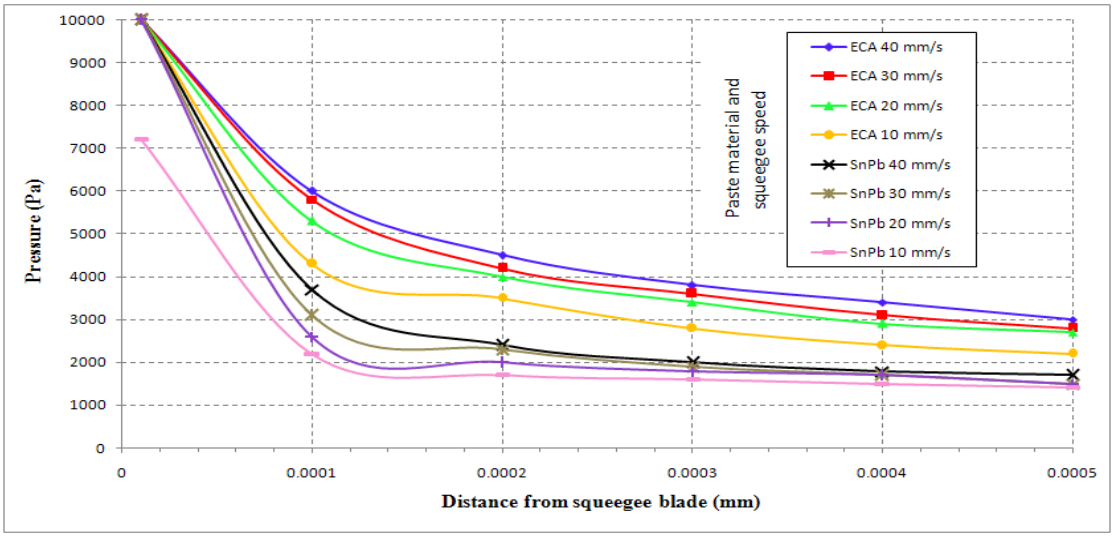

Figure 9.3: Pressure in paste at different distances from the blade tip (Kay et al, 2003)

In addition to the stress applied during creep testing, the typical period of time during which the stress is applied is misleading (or inaccurate of values encountered) when attempting to form correlations with the stencil printing process. That is, a standard stencil print may be completed within seconds, whereas typical application times for creep recovery testing commonly last for minutes. In his work, Tadros (2008) details a method for conducting creep testing, suggesting that a constant stress be applied to the material for a period of two minutes, during which the strain is measured to define the severity of deformation – with compliance determined as the ratio between strain and stress. Tadros then states that the stress should be removed from the sample, and the strain monitored for an additional two minutes to measure the resultant recovery.

Additional examples of this extended period of creep can be identified within work by:

- Lokhande et al (2011), who state that upon conducting creep testing, a stress value from within the LVR should be applied consistently for 100 seconds, with a recovery period following that lasts 200 seconds
- Durairaj et al (2009[a]), in which the stress applied to the samples was maintained at a constant level for 120 seconds, with a recovery of 120 seconds
- Nguty and Ekere (2000[a]), who actually state that simulation of the stencil printing process was undertaken by initially applying a pre-shear of 10 s^{-1} followed by the application of stress for two minutes and a subsequent recovery period that also lasted for two minutes.

The two-minute recovery period that follows the removal of stress (as discussed by Tadros, Durairaj et al, and Nguty and Ekere) can justifiably be related to the recovery of the solder paste once the board has been successfully printed; yet a stress application time of two minutes during the printing process would be highly irregular. The Benchmarker 2 test board (which is commonly used within industry for investigatory purposes) has dimensions of 127 × 190.5 × 1.5 mm, and therefore – assuming a print stroke length of 200 mm and a squeegee speed of 20 mm/s (as specified in section 4.5.1.2 in the results of the speed step test) – the maximum length of time that the solder paste is subjected to stress from the squeegee would be 10 seconds. This is obviously significantly less than the 120 seconds applied by authors recommending a two-minute application of stress. In fact, at a processing speed of 20 mm/s (which in some industrial practices is particularly slow), in order to constantly apply stress to the sample for 120 seconds, the length of the print stroke would be equivalent to 2,400 mm (240 cm or almost 8 foot). Therefore, there appears to be a significant void in the knowledge pertaining to creep recovery behaviour in respect of representing the actual printing process to allow comparisons to be drawn.

In order to assist with analysing results attained from the investigations, Nguty et al (1999) detail how numerical estimations of sample deformation can be obtained by using the four-parameter Burger viscoelastic model [3.40] or alternatively the Bohlin cooperative theory [3.41]. In addition to these two equations, the oscillatory model [9.4] also exists, which can be used to determine structural changes that can occur within a sample due to viscoelastic behaviour:

$$\sigma = \sigma(t) = \sigma_0 \text{ Sin } (\omega t) \quad \textbf{[9.4]}$$

where σ_0 represents the sinusoidal applied stress and ω represents the frequency of oscillations. However, because the creep recovery test measures the compliance response of a sample (where compliance is a measure of the strain in a sample to the stress applied), the Bohlin cooperative theory appears to be of higher significance due to incorporating compliance measurements within the calculation. Despite this greater potential, as a result of current standards of conducting creep-recovery tests while applying a stress from within the LVR the Bohlin equation was set aside in favour of equation [9.5]. This equation was selected because it was specifically designed for instances where the imposed stress is too insignificant to create permanent deformation. As such, this model allows for the prediction of theoretical deformation behaviour of the pastes that would be expected assuming that current standards are followed. This may therefore provide valuable emphasis regarding the variation in deformation observed while applying values that are representative of the actual stencil printing process. We have

$$\gamma (S_0, t) = S_0 \, J(t) \quad \textbf{[9.5]}$$

where γ (S_0, t) is the deformation as a function of time, S_0 represents the constant shear stress applied and J (t) is the creep compliance of the material. Through utilising equation [9.5] and previously attained results regarding the creep behaviour of paste materials upon an applied stress within the LVR (see section 5.3), theoretical estimations were made on the deformation values of paste materials (Table 9.1).

	Paste A	**Paste B**	**Paste C**	**Paste D**
Applied Stress (Pa)	5	5	5	5
Creep compliance (1/Pa)	0.002045	0.001287	0.002971	0.002992
Deformation	0.010225	0.006435	0.014855	0.01496
Applied Stress (Pa)	300	300	300	300
Creep compliance (1/Pa)	0.002045	0.001287	0.002971	0.002992
Deformation	0.6135	0.3861	0.8913	0.8976
Variation between deformations	**0.603275**	**0.379665**	**0.876445**	**0.88264**

Table 9.1: Estimations of paste deformation behaviour
(for applied stress values within and outside the LVR)

Although the total variation exhibited between deformations (when increasing the applied stress to 300 Pa) appears to be of an insignificant value, this may not necessarily be true. Results shown in Chapter 5 demonstrate that the variation in recovery percentage between samples A and B was 21.35 percentage points; yet by comparison of the values for deformation between these results (for a 5-Pa applied stress), it can be observed that this 21.35% increase in recoverability corresponds to a mere 0.000758 variation in deformation. This therefore signifies that (for instance in the case of sample D) the 0.88264 variation in deformation value may play a significant role in the recovery behaviour exhibited by the sample, and hence may greatly influence the slumping nature exhibited.

9.3 Creep recovery testing methods

9.3.1 Creep recovery behaviour as a function of applied stress

Initial steps of the testing method included the appropriate selection of parameters to apply during the study. Throughout the stencil printing trials, the squeegee speed and pressure were maintained at 20 mm/s and 8 kg respectively – remaining consistent with those results detailed within Chapter 4. As was highlighted in Chapter 3 and restated above, for a squeegee (with blade angle of 60°) travelling at 20 mm/s, the stress encountered by the solder paste ranges from approximately 2,000 Pa to 10,000 Pa (according to work conducted by Kay et al, 2003). However, as the standard viscosity equation highlights that the stress during stencil printing ranges from 300 Pa to 10,000 Pa (assuming the shear rate experienced ranges from 0.01 s^{-1} to 1000 s^{-1}), as shown in section 9.2, the applied stress for use during the creep testing was selected as 300 Pa.

In order to identify the influence that the applied stress alone has on the solder paste during creep testing, the application time was maintained at 120 seconds, consistent with the works conducted by Durairaj et al (2009[a]) and Nguty and Ekere (2000[c]). Once the two minutes had passed, the 300 Pa stress was removed, and a recovery period of 120 seconds was then initiated. After that, the solder paste was removed

from the top plate of the rheometer and replaced with a fresh sample. The whole cycle was then repeated a minimum of six times to highlight any anomalous results.

9.3.2 Effect of stress application time on recovery performance

With regard to conducting an investigation into application time, initial steps required the appropriate selection of the length of time to apply the stress to the sample. As the squeegee speed during the printing trials was maintained at 20 mm/s, and the length of the print stroke was approximated to 20 cm, together they indicate that the maximum length of time the stress is applied to the sample is 10 seconds. Therefore, during the testing period the paste samples were subjected to an applied stress of 5 Pa for a period of 10 seconds followed by a recovery period of 120 seconds.

An applied stress of 5 Pa was selected to maintain consistency with previous investigations into creep testing and current standards, whereby a stress is selected from within the LVR. The 120-second recovery period was applied to acknowledge the full amount of recovery that would typically be experienced according to current standards for creep testing (because within an industrial environment there may not necessarily be a time limit for the recovery).

9.3.3 Influence of recurrent applications of creep recovery

In order to investigate the influence of recurrent applications of the creep recovery test method on solder paste behaviour, the variables were required to represent typical standards for the testing. Therefore, a stress of 5 Pa was applied to the sample for a period of 120 seconds, which was then followed by a period of rest of 120 seconds. Once the recovery period was concluded, the test was re-initiated without replacing the solder paste on the rheometer. This would therefore give an indication of the behaviour of the paste on the stencil assuming that the print cycles continued. Once the creep-recovery behaviour periods had been repeated three times, the solder paste was replaced with a fresh sample, and that cycle was then repeated. In order to allow for comparisons to be drawn with the printing process, print trials were extended to replicate the investigation, with repeat cycles conducted three times before the quality of the print was inspected.

9.3.4 Combining the three investigations

The final stage for this method of investigation was to combine the separate tests to allow for the influence of combining all three to be identified. During the investigation, the rheometer was programmed to apply a stress of 300 Pa to the sample for a creep application time of 10 seconds. The recovery period was then reduced to 10 seconds, after which the 300 Pa stress was reapplied. This cycle was repeated three times prior to replacing the solder paste with a fresh sample. By combining all three of the previous investigations, the test method aimed to replicate fully the stencil printing process through creep recovery testing (where recurrent applications of a high stress occur for a short period of time).

9.4 Results and discussion

By conducting rheological investigations into the creep recovery behaviour of solder paste (while attempting to replicate aspects of the printing process), it was discovered that the efficiency of predicting the printing process, utilising current standards, is questionable. This was observed through comparing typical results (using standard techniques) with those attained from the study. Figure 9.4 highlights an example of a standard creep-recovery investigation (used as a benchmark), where an applied creep time of 300 seconds (which, as with 120 seconds, is a commonly applied creep period) and recovery time of 600 seconds were utilised – common guidelines dictate that the recovery period is often twice the length of the creep time. Assuming results such as those exhibited in Figure 9.4 are typically accepted as indicative of print performance (in terms of resistance to slump, for example), the accuracy of this interpretation was determined through assessing results from the study.

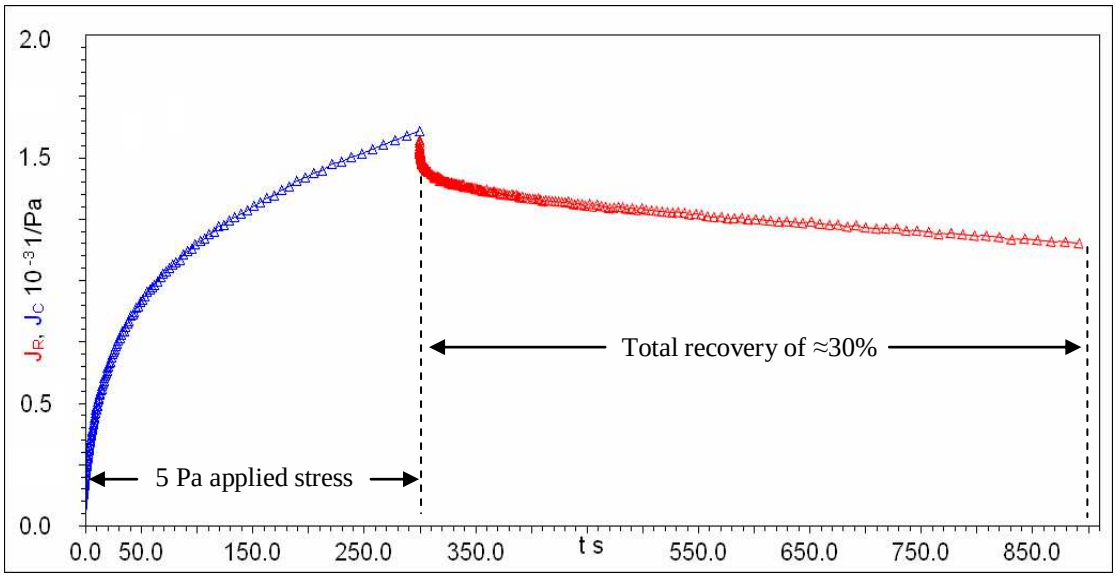

Figure 9.4: Typical expected creep recovery response using standard test methods

9.4.1 Results due to variations in applied stress

As was discussed within theoretical section 9.2 above, the stress experienced by the solder paste during the stencil printing process is far greater than the upper limit for the linear viscoelastic region (with standard techniques for creep recovery testing recommending that stress values within the LVR are applied) and therefore, in order to replicate the printing process through rheometry, the applied stress was increased to 300 Pa. The resultant outcome of increasing the applied stress within the test from 5 Pa (as demonstrated within Figure 9.4) to 300 Pa can be seen within Figure 9.5.

Initial observations from the creep recovery results highlight an apparent increase in the level of structural breakdown exhibited by the four solder pastes when compared with the example graph in Figure 9.4. This can be seen through the significant increase in the measurement of creep compliance (particularly with regard to paste D) as highlighted in Table 9.2 by the initial compliance value (J_1), which in one instance was doubled. Furthermore, the graphical results demonstrate that by increasing to 300 Pa the variable of applied stress within the test, a significant reduction in paste recoverability can be observed (Table 9.2). In the example of an increase in initial compliance from 1.2 to 2.42 × 10^{-4}, this corresponded to a decrease in recovery from 30.14% to 7.8% (a variation of 22.34 percentage points), which could account for the

presence of printing defects such as bridging. With such a substantial variation, questions can be raised as to the ability of current standards to appropriately model paste behaviour during the printing process.

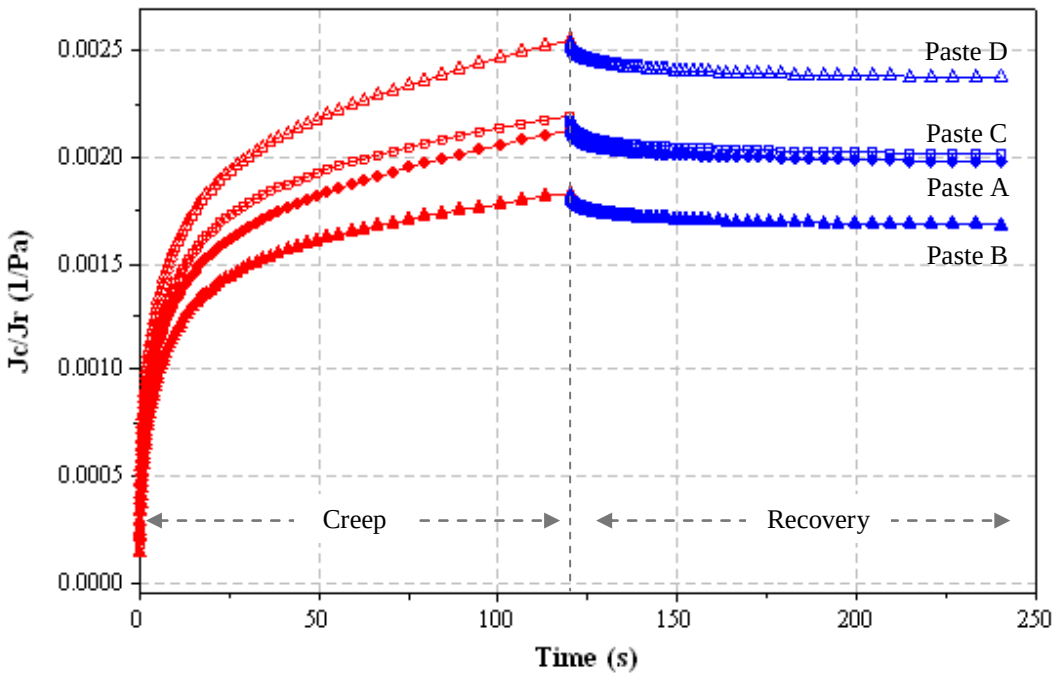

Figure 9.5: Creep recovery results on applying a stress of 300 Pa to the sample

Solder Paste	J_1 (1/Pa) ($\times 10^{-4}$)	J_2 (1/Pa) ($\times 10^{-3}$)	J_3 (1/Pa) ($\times 10^{-3}$)	Creep Recovery Index	Recovery Percentage (%)
Benchmark	1.20	1.58	1.14	0.72	30.14
Sample A	2.02	2.13	1.98	0.93	7.78
Sample B	1.48	1.83	1.68	0.92	8.92
Sample C	1.77	2.19	2.02	0.92	8.45
Sample D	2.42	2.55	2.37	0.93	7.80

Table 9.2: Comparison of results for an applied stress of 300 Pa and benchmark 5 Pa (all results correct to 2 decimal places)

The recovery percentage of the samples was determined utilising the Marks equation for calculating recoverability [5.1], where J_1 is the instantaneous strain (initial compliance), J_2 is the final creep compliance and J_3 is the final recovery compliance.

By comparing the recovery results with the benchmark data (from Figure 9.4), it becomes evident that an increase in applied stress can lead to a significant reduction in recoverability. Table 9.2 highlights that during this investigation, such an increase in stress led to a minimum drop in recovery percentage of 21.22 percentage points (from comparing the benchmark data to that of paste sample B). And since slumping (one of the most common defects) may directly result from such a reduction in recoverability, this becomes an important observation.

Of further interest is the similarity between the recovery percentages for each of the pastes. The results documented in Chapter 5 indicate that the flux and particle size distribution (PSD) play a significant role in the creep performance of solder paste material, with the recovery percentage varying by 21.35% in one instance. By attempting to replicate the stencil printing process as opposed to following standard guidelines, this variation due to flux and PSD (although still present) is reduced significantly to 1.14 percentage points, which demonstrates a far greater level of stability with results. Therefore, with the similarity of recoverability between paste samples and the significant drop in recovery percentage itself, increasing the applied stress during investigations (in order to replicate the stencil printing process) further questions the accuracy of current standards.

9.4.2 Results due to variations in application time

Increasing the applied stress during creep recovery testing highlighted that significant variations in paste performance may be recorded; furthermore, revising current standards to replicate the application time encountered by samples during the stencil printing process was also seen to notably influence paste behaviour (Figure 9.6).

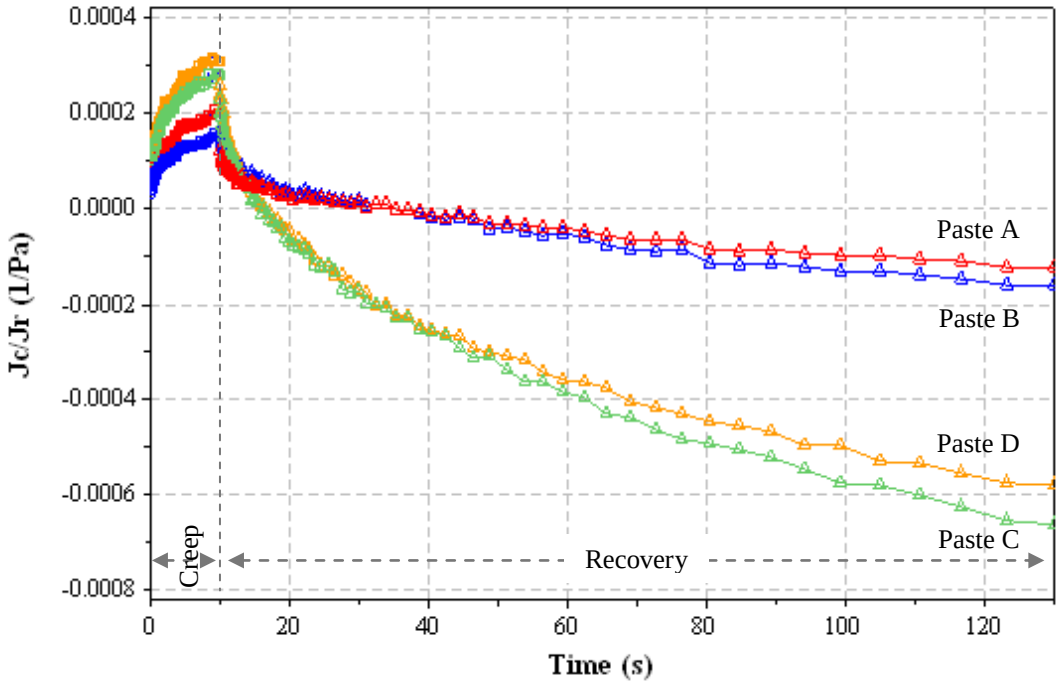

Figure 9.6: Creep recovery results after a stress application time of 10 seconds

The results shown in Figure 9.6 clearly demonstrate that by reducing the creep application time from the standard 120 or 300 seconds to a far shorter 10 seconds, paste structure may exhibit a 100% recovery ($J_1 = J_3$). Furthermore, upon applying a period of creep to the sample lasting 10 seconds, the recovery period may be reduced substantially without affecting this 100% recovery (Table 9.3).

Solder Paste	Recovery (%)	$J_1 \geq J_3$ (s)
Benchmark	30.14	–
Sample A	100	8.23
Sample B	100	8.23
Sample C	100	3.07
Sample D	100	4.14

Table 9.3: Time taken for 100% recovery after stress application time of 10 seconds

By identifying the point at which the initial creep compliance (J_1) is equal to or greater than the final recovery compliance (J_3), it was observed that a full structural recovery may be achieved after only 3.07 seconds, assuming that the creep time is

reduced to 10 seconds and an applied stress from within the LVR is employed. Furthermore, the longest time observed for attaining a 100% recovery was 8.23 seconds, which itself can be seen as a short length of time. Therefore, results from the investigation highlight that the stress application time can have a profound effect on the recoverability of solder paste.

By comparing the results with those from the benchmark data, it can be seen that a variation in recoverability exists of 69.86 percentage points (100% v 30.14%). The importance of this is further emphasised by highlighting that the 30.14% recovery demonstrated by the benchmark data was achieved after a recovery period of 600 seconds (10 minutes). By reducing the creep application time to replicate the duration of the stencil printing process, not only was a full recovery demonstrated, but this was achieved by sample C (for example) 596.93 seconds faster than the 30.14% recovery attained from the benchmark data. Therefore, the effectiveness of current standards can once again be questioned.

9.4.3 Results due to recurrent applications of creep recovery

While attempting to replicate the repeated printing cycles encountered by solder paste in a typical industrial environment, rheological tests highlighted that the level of structural breakdown demonstrated by the paste reduces with an increase in the number of recurrent applications of creep recovery. From results attained, this appears to be a direct result of the level of recovery demonstrated during each cycle. For example, with only a 50% recovery after completion of the first cycle, a loss of structure has already been demonstrated; therefore, there is a lesser structure available for undergoing further breakdown on any additional applications of creep (see Figures 9.7 through 9.10). In contrast, with a full 100% recovery it would be expected that the structural breakdown observed for the second cycle would closely resemble that of the recorded data from the initial creep recovery test.

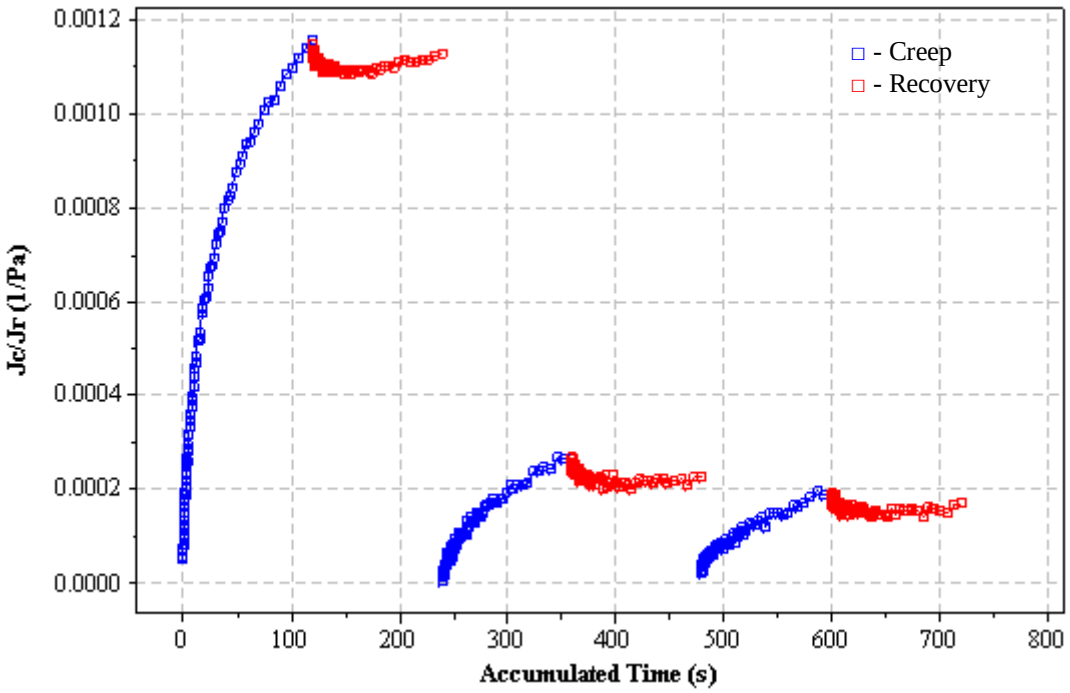

Figure 9.7: Results of recurrent applications of creep recovery cycles for paste A

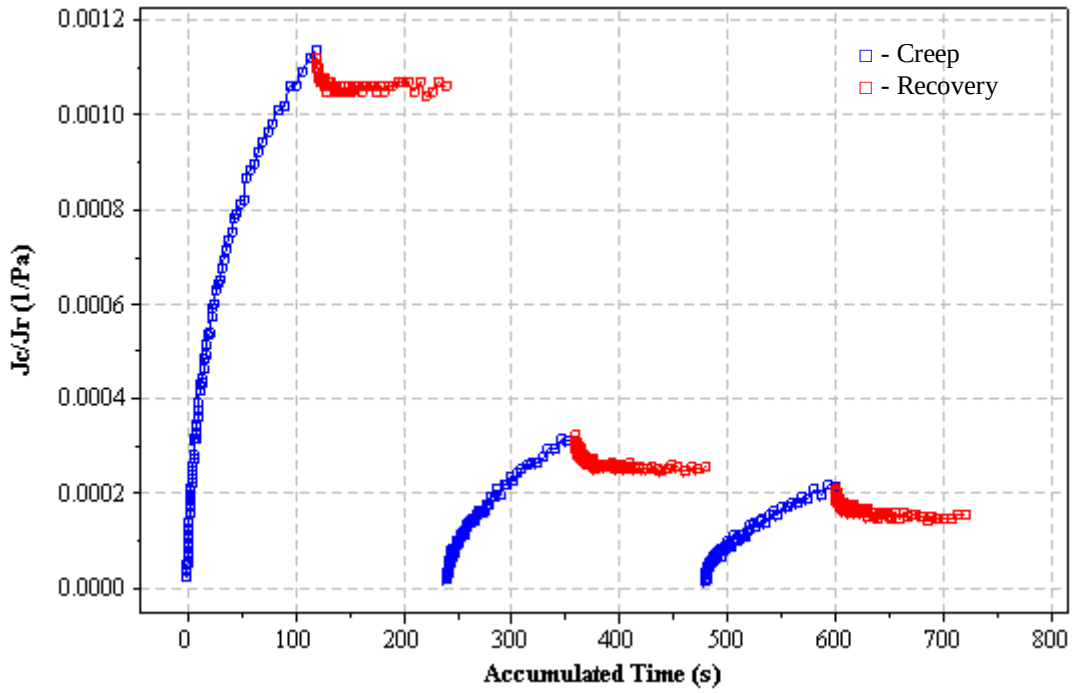

Figure 9.8: Results of recurrent applications of creep recovery cycles for paste B

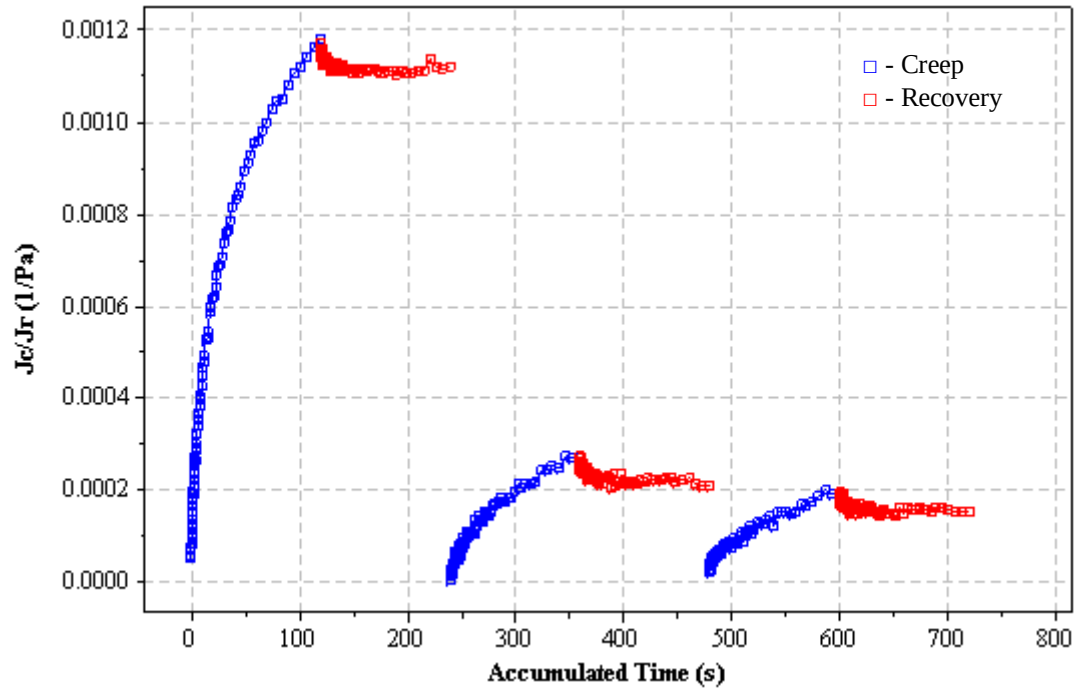

Figure 9.9: Results of recurrent applications of creep recovery cycles for paste C

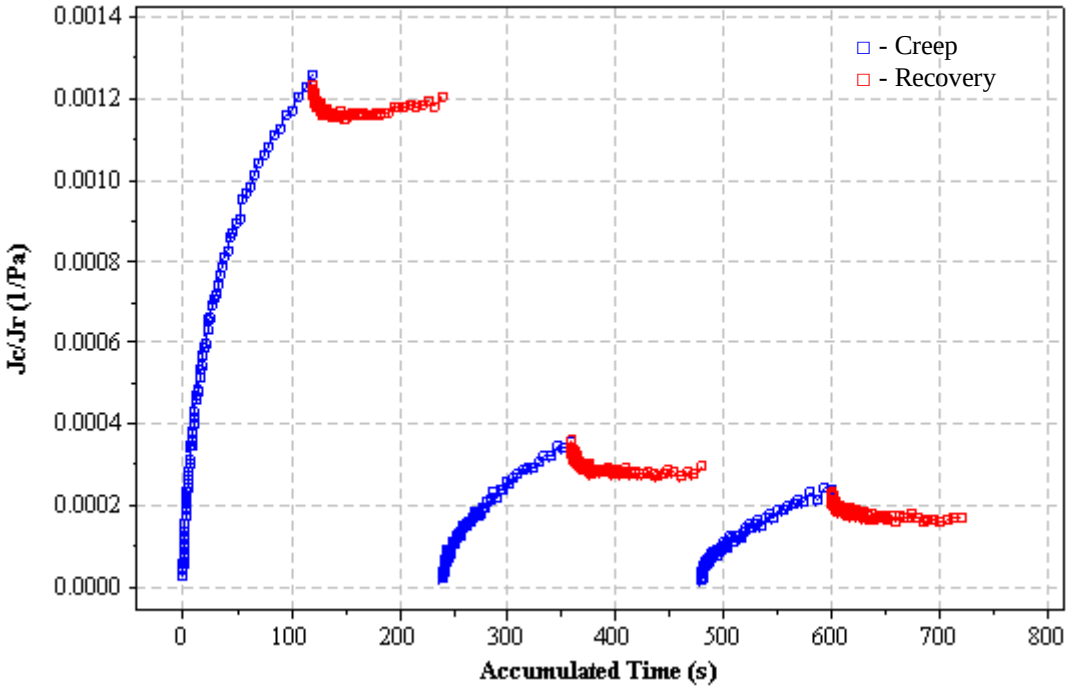

Figure 9.10: Results of recurrent applications of creep recovery cycles for paste D

From those results shown within Figures 9.7 to 9.10, it can be seen that a fairly strong consistency has been maintained regardless of paste sample investigated, with the initial value of J_2 approximately 0.0012, after which values of approximately 0.0003 and 0.0002 are seen from consecutive cycles. This finding suggests that the process of repeating creep recovery cycles can significantly influence the quality of the print, as a lesser level of structural breakdown (as demonstrated by the reduced values of J_2) could correspond to a reduced ability to slump and consequently bridge.

By extending the Marks equation for recoverability [5.1], it is possible to calculate using equation [9.6] the total recovery percentage demonstrated by the samples as a result of the number of repeat cycles applied during testing:

$$\text{Total Recovery Percentage} = J_{r1} \times J_{r2} \times J_{r3} \quad \ldots \quad \times J_{r\,n} \times 100\% \qquad \textbf{[9.6]}$$

where J_{r1} is equal to the initial recovery, J_{r2} is equal to the recovery from the second cycle, J_{r3} is the recovery from the third creep-recovery cycle, etc and J_{rn} is the recovery from the n^{th} cycle. In each instance, the recovery is calculated using equation [9.7] thus

$$\text{Recovery} = \frac{J_2 - J_3}{J_2 - J_1} \qquad \textbf{[9.7]}$$

where J_1 is the instantaneous strain (initial compliance), J_2 is the final creep compliance and J_3 is the final recovery compliance.

From those results displayed within Table 9.4, it becomes apparent that the number of print cycles conducted can affect the paste rheology (with regard to recoverability) to a high level. With current creep recovery techniques incorporating a single application of applied stress, it is ineffective to draw comparisons between results obtained by this method and those from typical stencil printing procedures. This can be highlighted through the significant drop in recovery percentage recorded, which when comparing current techniques to those that replicate repeated printing cycles was equal to approximately 30 percentage points. One example in particular (for paste A) demonstrated that, by introducing merely three stress applications (the equivalent of

printing three circuit boards), the drop in total recovery percentage was equal to 30.09 percentage points (30.14% v 0.05%).

	Benchmark	**Paste A**	**Paste B**	**Paste C**	**Paste D**
First application of creep recovery testing					
J_1 (1/Pa $\times 10^{-3}$)	0.12	0.05	0.03	0.05	0.03
J_2 (1/Pa $\times 10^{-3}$)	1.58	1.15	1.14	1.18	1.26
J_3 (1/Pa $\times 10^{-3}$)	1.14	1.13	1.06	1.12	1.20
J_{r1} ($\times 10^{-2}$)	**30.14**	**2.45**	**7.18**	**5.32**	**4.32**
Second application of creep recovery testing					
J_1 (1/Pa $\times 10^{-4}$)	-	0.05	0.29	0.05	0.32
J_2 (1/Pa $\times 10^{-4}$)	-	2.64	3.24	2.69	3.56
J_3 (1/Pa $\times 10^{-4}$)	-	2.26	25.40	2.07	2.93
J_{r2} ($\times 10^{-1}$)	**-**	**1.45**	**2.38**	**2.35**	**1.94**
Third application of creep recovery testing					
J_1 (1/Pa $\times 10^{-4}$)	-	0.20	0.15	0.21	0.17
J_2 (1/Pa $\times 10^{-4}$)	-	1.91	2.15	1.95	2.37
J_3 (1/Pa $\times 10^{-4}$)	-	1.68	1.54	1.50	1.69
J_{r3} ($\times 10^{-1}$)	**-**	**1.37**	**3.06**	**2.58**	**3.07**
Total Recovery (%)	**30.14**	**0.05**	**0.52**	**0.32**	**0.26**

Table 9.4: Total recovery percentages after three recurrent cycles of creep recovery testing (all values correct to two decimal places)

Of further significance were the particularly low levels of recovery demonstrated by the paste samples, with paste A exhibiting a total recovery percentage of 0.05% (the lowest recorded from the investigation) and paste B (which demonstrated the highest ability to recover) only 0.52%. These are of particular importance, as a drop of 30

percentage points in recovery may be viewed as acceptable assuming the upper value was (say) 90%; however, this reduction actually resulted in a total recovery that was below 1%, which would generally be perceived as exceptionally poor. The reduction in recovery percentage can be seen to affect the slumping behaviour of the solder pastes, which directly affects the quality of the print (as highlighted in Figures 9.11 and 9.12).

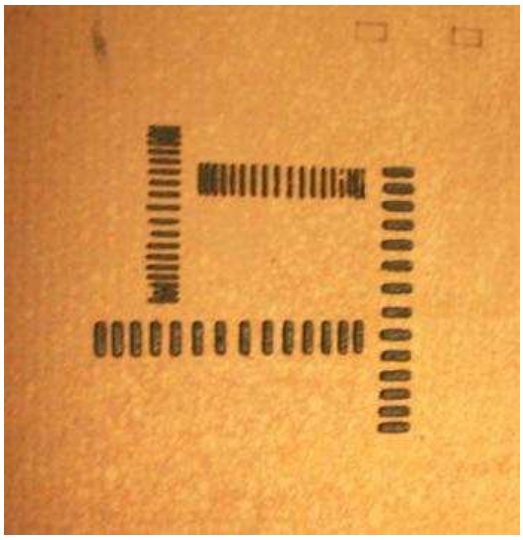

Figure 9.11: Example print result after a solitary stencil printing cycle

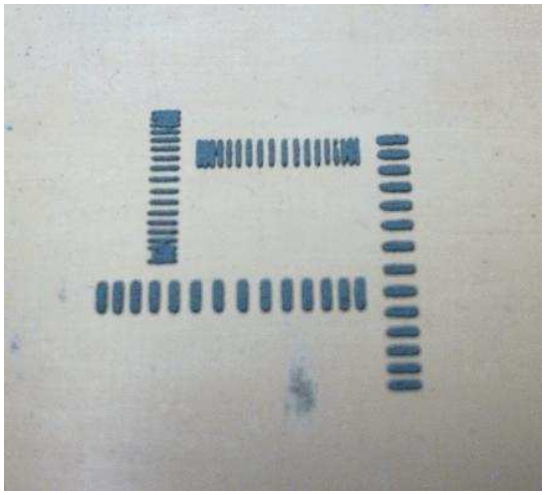

Figure 9.12: Example print result after three stencil printing cycles

Despite the presence of skipping seen within Figure 9.11, the print definition after a single cycle was seen to be of a high standard. However, by introducing an additional two printing cycles, the deposits tended towards a more rounded shape with increased levels of bridging, which could be a direct result of the reduced capability of the pastes to recover.

9.4.4 Results of combining the three previous variations

Results from attempting to replicate within the creep recovery behaviour of solder paste various aspects of the printing process through rheological investigations have demonstrated that the applied stress, application time and number of creep applications can significantly impact the results attained. By investigation of the effect of combining all three variations, attempts were made to replicate stencil printing as a whole process. Results from investigating the combination of the three previously detailed variables highlighted that the structural breakdown once more reduced upon increasing the number of applications of creep recovery cycles. When a fourth application was introduced, it was observed that the level of structural breakdown exhibited was actually appearing to tend towards a plateau value as the number of cycles increases (Figures 9.13 to 9.16).

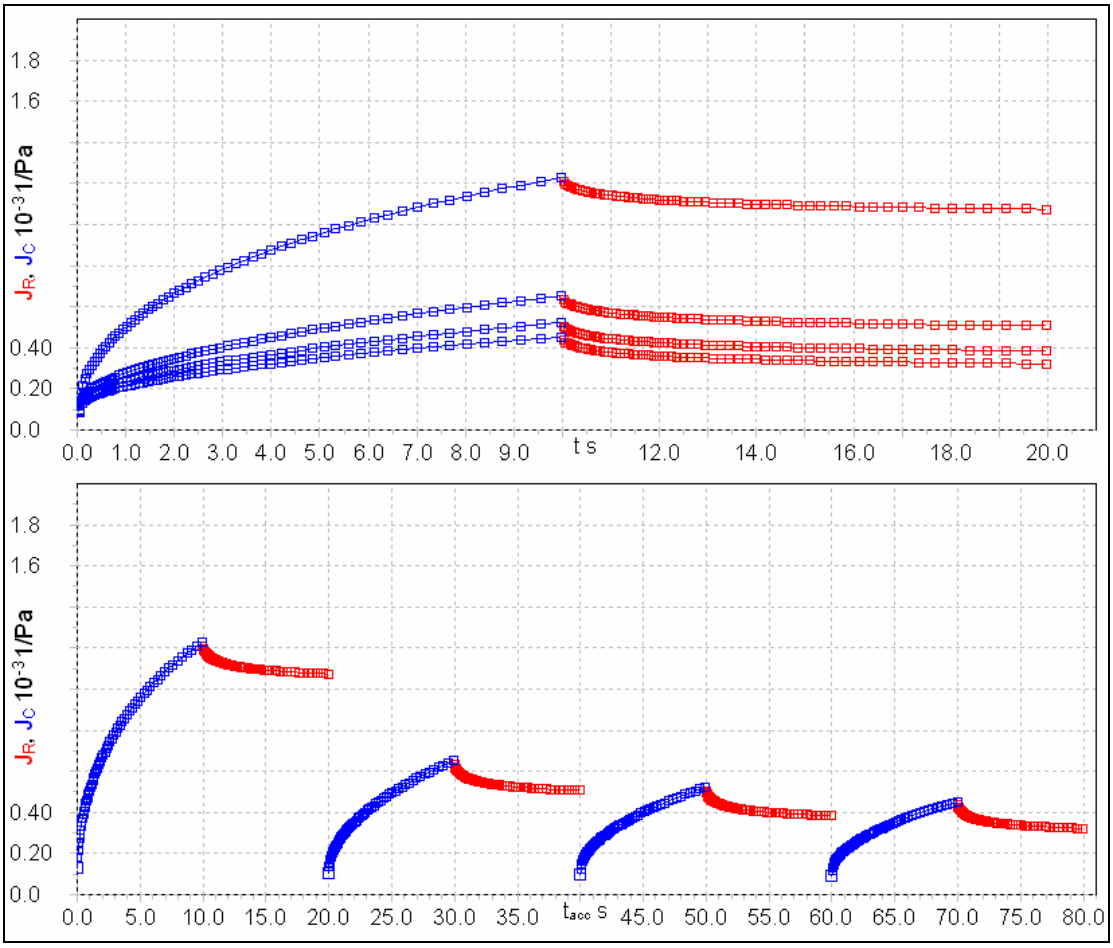

Figure 9.13: Creep recovery results for paste A upon combining the three previous investigations (shown for accumulated time and standard test time)

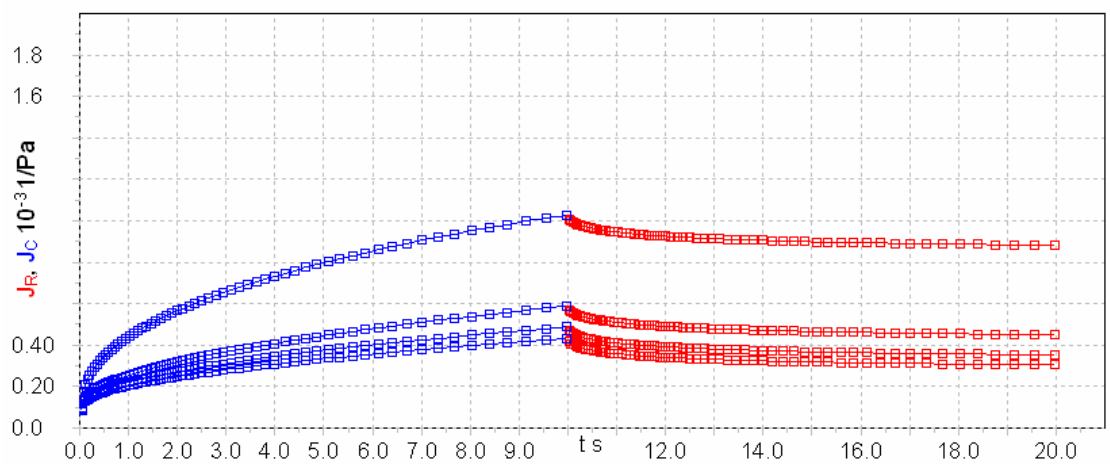

Figure 9.14: Creep recovery results for paste B upon combining the three previous investigations

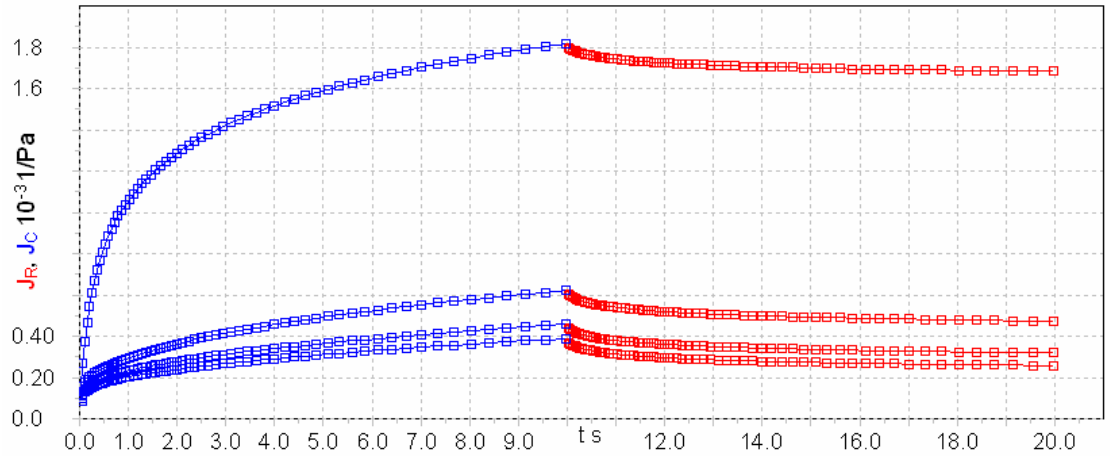

Figure 9.15: Creep recovery results for paste C upon combining the three previous investigations

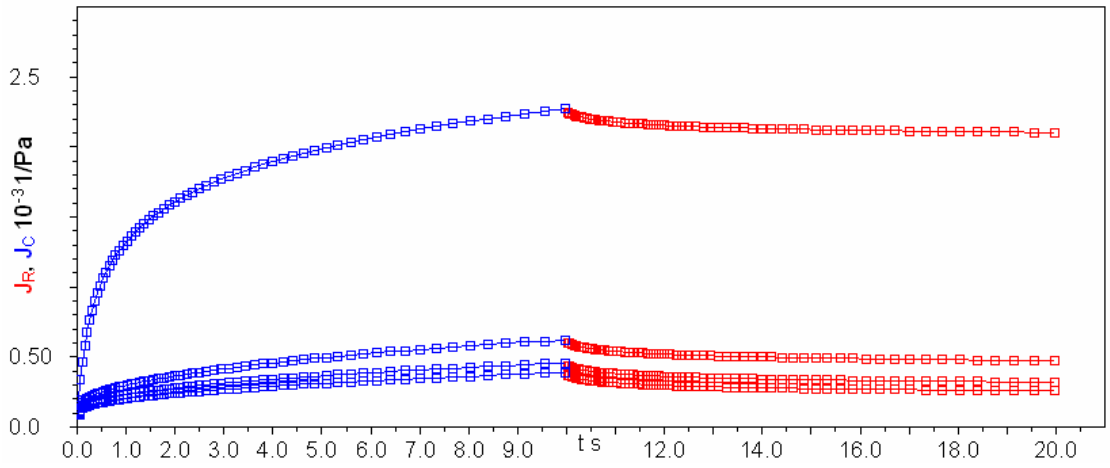

Figure 9.16: Creep recovery results for paste D upon combining the previous investigations

With regard to the recovery percentage, this was once again seen to be lower than that of the 30.14% attained from the benchmark test, which was representative of current test standards. Initial observations from the first application of creep appeared to demonstrate an approximate recovery of 10%, which itself is considerably less than 30%; yet this value fails to even consider the influence of the recurrent applications of creep recovery (see Table 9.5).

	Benchmark	**Paste A**	**Paste B**	**Paste C**	**Paste D**
First application of creep recovery testing					
J_1 (1/Pa $\times 10^{-4}$)	1.20	1.25	1.26	1.45	1.81
J_2 (1/Pa $\times 10^{-3}$)	1.58	1.23	1.03	1.81	2.27
J_3 (1/Pa $\times 10^{-3}$)	1.14	1.07	0.88	1.68	2.10
J_{r1} ($\times 10^{-1}$)	**3.01**	**1.40**	**1.64**	**0.78**	**0.81**
Second application of creep recovery testing					
J_1 (1/Pa $\times 10^{-4}$)	-	1.02	0.99	0.93	1.16
J_2 (1/Pa $\times 10^{-4}$)	-	6.49	5.86	4.95	6.18
J_3 (1/Pa $\times 10^{-4}$)	-	5.03	4.46	3.76	4.70
J_{r2} ($\times 10^{-1}$)	**-**	**2.67**	**2.87**	**2.96**	**2.96**
Third application of creep recovery testing					
J_1 (1/Pa $\times 10^{-5}$)	-	9.53	9.20	7.94	9.92
J_2 (1/Pa $\times 10^{-4}$)	-	5.19	4.85	3.62	4.53
J_3 (1/Pa $\times 10^{-4}$)	-	3.81	3.49	2.53	3.16
J_{r3} ($\times 10^{-1}$)	**-**	**3.26**	**3.45**	**3.86**	**3.82**
Fourth application of creep recovery testing					
J_1 (1/Pa $\times 10^{-5}$)	-	8.95	8.87	7.23	9.03
J_2 (1/Pa $\times 10^{-4}$)	-	4.51	4.31	3.08	3.85
J_3 (1/Pa $\times 10^{-4}$)	-	3.19	3.01	2.03	2.54
J_{r3} ($\times 10^{-1}$)	**-**	**3.64**	**3.80**	**4.46**	**4.44**
Total Recovery (%)	**30.14**	**0.44**	**0.62**	**0.41**	**0.40**

Table 9.5: Total recovery percentages after four recurrent cycles of creep-recovery testing at 300 Pa for 10 seconds (all values correct to two decimal places)

By combining the previous investigations to fully replicate the stencil printing process from a rheological perspective, results once again demonstrate that the 30.14% recovery demonstrated by the benchmark test are not indicative of paste behaviour during stencil printing. As can be seen from those results detailed in Table 9.5, the recovery percentage was seen to drop by between 29.52 and 29.74 percentage points, which led to a total paste recovery of between 0.4% and 0.62%. These substantial variations could significantly impact the quality of the print, with a lesser ability to recover paste structure upon removal of stress leading to increased levels of slumping and bridging. Therefore, current test methods that demonstrate a 30.14% recovery may be misleading when attempting to predict slumping behaviour from solder pastes.

9.4.5 Results of paste deformation behaviour

Theoretical estimations of paste deformation behaviour highlight the expected trend of an increase in deformation with an increase in applied stress to a sample. Results from the investigation (Table 9.6) demonstrated this expected trend to be accurate.

		Paste A	Paste B	Paste C	Paste D
Benchmark deformations (applied stress of 5 Pa)					
Creep compliance (1/Pa)		0.002045	0.001287	0.002971	0.002992
Deformation		0.010225	0.006435	0.014855	0.01496
Predicted deformations (applied stress of 300 Pa)					
Creep compliance (1/Pa)		0.002045	0.001287	0.002971	0.002992
Deformation		0.6135	0.3861	0.8913	0.8976
Deformations from first creep cycle					
Applied Stress (Pa)		300	300	300	300
Creep compliance (1/Pa)		0.00123	0.00103	0.00181	0.00227
Deformation		0.369	0.309	0.543	0.681
Variation to	**benchmark**	**0.358775**	**0.302565**	**0.528145**	**0.66604**
	predicted	**0.2445**	**0.0771**	**0.3483**	**0.2166**
Deformations from fourth creep cycle					
Applied Stress (Pa)		300	300	300	300
Creep compliance (1/Pa)		0.000451	0.000431	0.000308	0.000385
Deformation		0.1353	0.1293	0.0924	0.1155
Variation to	**benchmark**	**0.125075**	**0.122865**	**0.077545**	**0.10054**
	predicted	**0.4782**	**0.2568**	**0.7989**	**0.7821**

Table 9.6: Variations in recorded deformation with predicted and benchmark data

From those results detailed within Table 9.6 it becomes apparent that the deformation behaviour does indeed increase with increasing stress. However, of interest is the finding that as the number of applications of creep cycles increases, the deformation begins to closer resemble the results recorded from the benchmark data (recorded upon application of a stress of 5 Pa). This trend can be clearly observed within Figure 9.17, in which the recorded deformation after a single creep-recovery application closely resembles the predicted deformation, whereas the recorded deformation after a fourth application of creep recovery closely resembles the benchmark data.

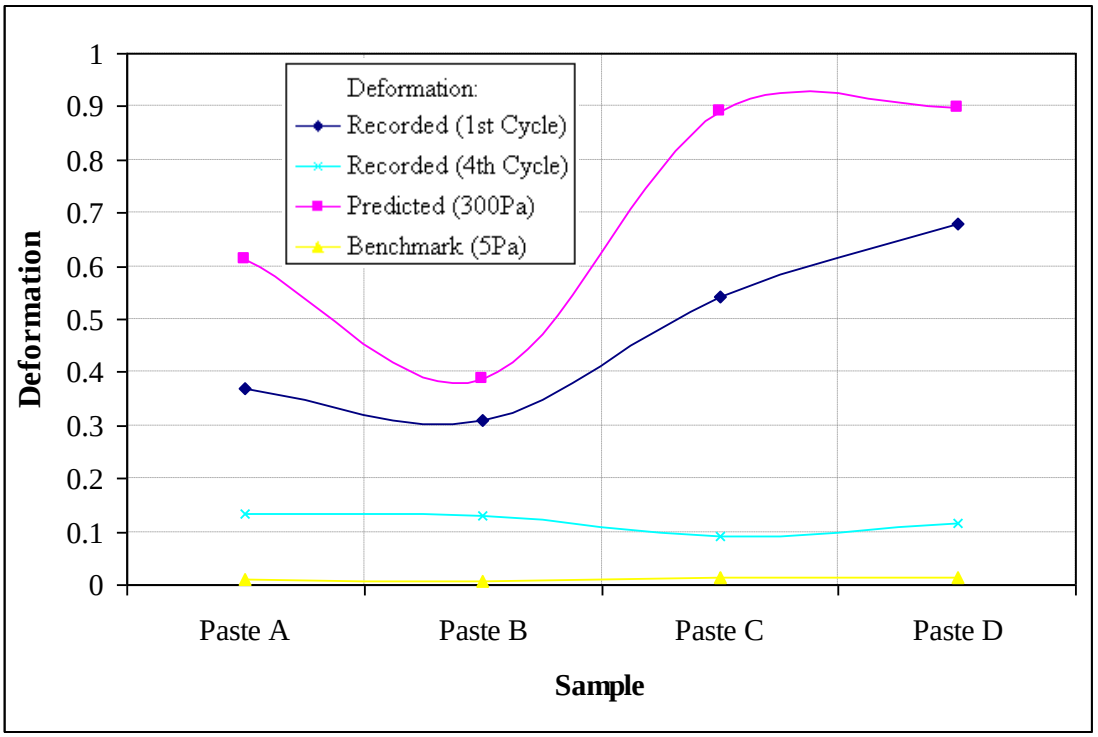

Figure 9.17: Recorded deformation behaviour compared with both predicted and benchmarked data

The results of investigating the deformation behaviour of the solder pastes therefore appear to suggest that, by use of current standards for creep testing to calculate compliance values for use within the deformation equation [9.5], an estimation may be gained as to the deformation behaviour of paste materials after several applications of applied stress of around 300 Pa (in other words, an indication of paste response to several stencil printing cycles). Furthermore, the resemblance between the predicted deformation and the recorded data from the initial cycle demonstrate that equation [9.5] may be used as a good method for predicting initial paste deformation behaviour, but the equation requires further revision to allow for predicting behaviour after several applications of stress.

Upon comparing results of the recorded deformation with increasing numbers of creep recovery cycles, an interesting trend was discovered relating to the similarity between results after excluding the data from the initial cycle (Figure 9.18). From the results, it can be observed that a strong correlation exists between those results attained after 2, 3 and 4 applications of creep testing, which further adds potential to developing or

revising the equation(s) for predicting print performance after a variable number of print trials. Furthermore, as the number of creep recovery applications increases, the variation in level of deformation is seen to reduce (and is particularly highlighted between the results for cycles 3 and 4), indicating the possibility that after a number of cycles have been conducted, the deformation may actually become consistent.

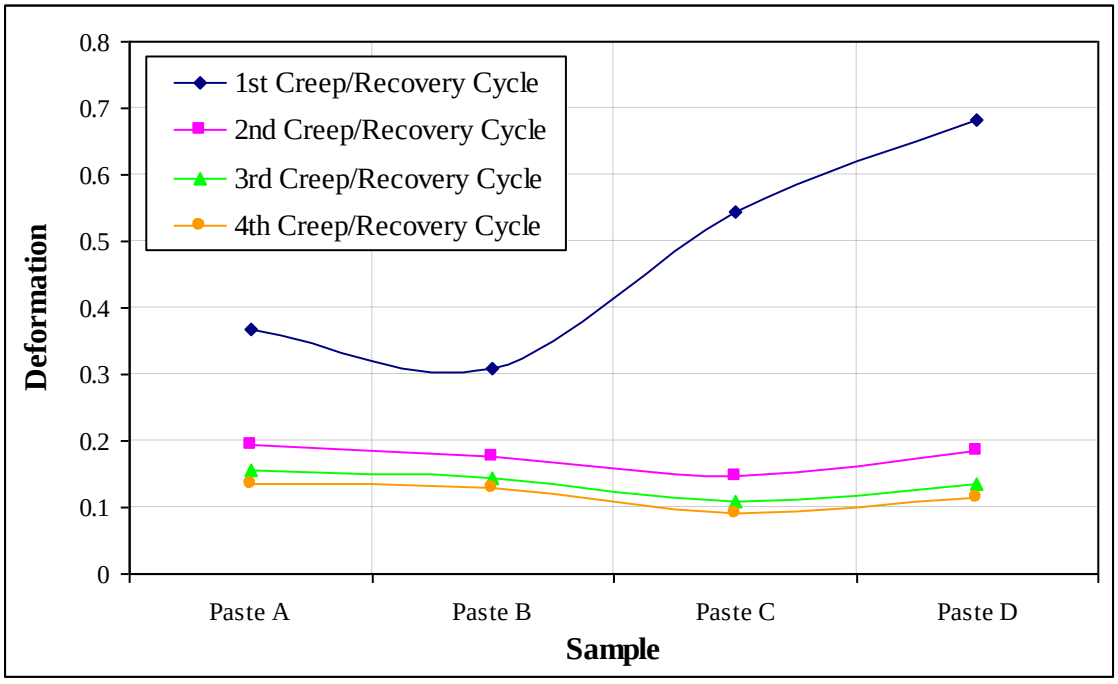

Figure 9.18: Deformation behaviour as a result of repeated creep recovery applications

9.5 Conclusions

By conducting investigations into the applied stress, application time and number of repeat applications of creep-recovery testing, it has become apparent that current standards are unable to accurately determine paste behaviour after stencil printing with regard to recoverability. Current standards dictate that when undertaking creep testing, it is necessary to apply a stress from within the linear viscoelastic region for a lengthy period (commonly 120 or 300 seconds); however, results from the study highlight that these are not true representatives of the printing process.

A comparison between results for benchmark data (conducted using current methods) and those achieved by replicating rheologically the stencil printing process

demonstrated that a drop in recovery percentage was observed of approximately 30 percentage points. More importantly, however, this drop demonstrated that recovery percentages were maintained below 1% when applying 'realistic' values for variables (in terms of those encountered from the printer) of time and stress and incorporating repeat cycles. This significant reduction in recoverability demonstrates that current techniques for creep recovery testing must be revised in order to accurately correlate paste behaviour data with the stencil printing process.

The significant drop in recoverability observed whilst attempting to replicate the stencil printing process is likely to be due to the increase in applied stress leading to a greater level of structural breakdown. This is because the paste retains a lesser ability to recover a greater deformation, which then becomes 'permanent'. By combining this increased permanent deformation with a lesser time for recovery before consecutive applications of stress, the amalgamation of the two effects could be held responsible for the significant reduction in paste recoverability. It should, however, be noted that despite results (from investigating recurrent applications of applied stress) appearing to demonstrate an increased level of recovery percentage with an increasing number of cycles, these are representative of the level of recovery from an already deformed sample. With paste A for example, using the Marks equation on that data in table 9.5, the recoverability was recorded as 14%, 26.7%, 32.6% and 36.4% for cycles 1 through 4 respectively. However, the importance of this result is that the 26.7% recovery is in relation to the 14% recovery observed previously and therefore equates to a total recovery percentage of only 3.74% (equation [9.8]).

$$\text{Actual recovery (\%)} = \frac{\text{Initial recovery (\%)}}{100} \times \text{Subsequent recovery (\%)} \qquad \textbf{[9.8]}$$

This apparent increase in recoverability may be a result of the previous 'permanent' or 'irreversible' structural breakdown, as successive creep-recovery cycles will have a 'lesser structure' available for further breakdown, which would consequently correspond to an increased ability to recover to the initial integrity of the creep cycle.

When investigating the deformation behaviour of the solder pastes, it was discovered that the level of deformation measured decreases with increased activity (or increased

number of creep cycles), which could be correlated to the 'apparent' increase in recovery measured with the increasing number of creep applications. This might be possible because the reduction in deformation recorded may once more be due to the deformation already demonstrated by the sample. That is, while recording data for the second application of applied stress, the sample has previously undergone a degree of permanent deformation and therefore consecutive applications should only measure a fraction of the initial deformation recorded. This was particularly seen with the deformation recorded after the third and fourth creep recovery cycles, where results demonstrated that the level of deformation was appearing to tend towards a consistent value. This can be seen as a significant finding, as this may indicate that after some (variable) number of cycles ≥ 3, the observed deformation may become consistent, and hence print quality may become possible to predict.

Results of the study highlighted that the paste samples are highly susceptible to variations in the design of the creep recovery testing method, and hence an appropriate selection of variables for incorporation is essential. With regard to the recoverability of the pastes utilising standard methods, this was seen as ≈30%; however, alterations in standard variables highlighted significant variations:

- Increasing the applied stress to 300 Pa from within the LVR resulted in a decrease in recovery percentage from ≈30% to ≈10%.
- Reducing the stress application time to 10 seconds resulted in an increase in recovery percentage from ≈30% to 100%.
- Increasing the number of recurrent applications of creep recovery testing to three cycles reduced the recovery percentage from ≈30% to less than 1%.

Owing to the observed substantial differences in paste performance, it can clearly be seen that appropriate care must be taken when designing creep recovery investigations. More importantly, however, current standards must be updated to ensure that creep recovery testing can be successfully undertaken to indicate paste performance in relation to the stencil printing process (particularly as the level of paste recovery can be directly correlated with slumping behaviour).

CHAPTER 10:
CONCLUSIONS, AND RECOMMENDATIONS FOR FUTURE WORK

10.1 Introduction

Within the electronics manufacturing industry, attempting to understand the rheological behaviour of solder pastes (and how their properties can affect printing performance) has been a long standing challenge. With developments in the industry necessitating printability on reduced pitch sizes while implementing new Pb-free paste formulations (due to government directives), a growing need exists for reducing processing defects. With literature findings commonly stating that the printing process is responsible for approximately 60% of manufacturing defects, the work reported in this thesis was focused towards developing a greater understanding of the interaction between paste rheology and the printing performance.

Throughout the course of the project, the efficiency of current standards was also questioned in an attempt to achieve the key objectives previously determined for the studies:

1. To develop new techniques for characterising new paste formulations using the parallel-plate rheometer.
2. To investigate techniques for correlating specific paste material properties with print performance.
3. To develop a parallel-plate rheometry test for abandon time.
4. To develop a parallel-plate rheometry test for shelf life.
5. To assist with developing a greater understanding of printing for Pb-free soldering and to investigate the possibility of reducing printing defects, identifying methods that could assist with this.

Of those objectives established prior to the project commencing, it was believed that attempting to discover methods of reducing printing defects through rheological characterisation (objective 5) was the most significant. This was due to the rate of failure that is associated with the stencil printing process, and hence much emphasis has been placed on reduced defects throughout the course of the project. As such, the work discusses how rheological studies have been used to identify the ageing, abandon time, slumping and creep recovery behaviour of Pb-free paste formulations for understanding print performance and capability. The work also examines the influence of varying the flux and particle size distribution during paste formulation, the effect of varying print frequency and the importance of selecting appropriate print parameters.

10.2 Key contributions

Results from the investigations have demonstrated many significant findings, with a number of methods recommended for potentially reducing defect occurrence at the stencil printing stage of PCB assembly. From those results, several key contributions have been identified, as set out next.

10.2.1 Effect of flux and PSD on creep recovery performance

By investigating the effect of flux and PSD on creep recovery performance (see Chapter 5), two significant contributions have been made to the body of knowledge within the field of electronics manufacturing (see below). The investigations into creep recovery performance also demonstrated that a variation in the flux was seen to affect the recovery by as much as 15%, which can be seen as a significant finding.

10.2.1.1 Derivation of an equation for calculating recoverability percentage

From the work, an initial conclusion drawn was the inaccuracy of current techniques relating to the recoverability of solder pastes after removal of the applied stress. Past literature details how the recovery percentage is calculated as a ratio of J_3/J_1, where a ratio of 1 is a successful 100% recovery, whilst a ratio of 2 is equivalent to a 50% recovery. As revealed through an investigation of creep recovery performance, this

method of calculation appears to be inaccurate, and hence new guidelines have been proposed for assessing a paste's ability to retain the initial structure recorded, through utilising the Marks equation for calculating recoverability [10.1] (where J_1 is the instantaneous strain (initial compliance), J_2 is the final creep compliance and J_3 is the final recovery compliance):

$$\text{Recovery Percentage (\%)} = \frac{J_2 - J_3}{J_2 - J_1} \times 100 \qquad \textbf{[10.1]}$$

By development of this equation, paste behaviour upon stencil release can be rheologically simulated, allowing for an indication of slumping and bridging tendency to be gained through indicating the ability of a paste deposit to recover structurally after removal of an applied stress.

10.2.1.2 A significant opportunity for reducing printing defects

By conducting creep tests, it was identified that a simple alteration in PSD during the paste formulation process could affect the recovery behaviour by as much as 21 percentage points (rising from 0.63% to 21.98%). In this instance the mean particle size during paste development was increased from 31 to 36 microns, resulting in an increased ability to recover after removal of stress. Work by Hwang (2004) indicated that an increase in PSD should typically lead to an increase in viscosity; however, there have been no discussions regarding an increased ability to recover structurally (after a printing cycle) with an increase in mean particle size. Although it may not always be possible to increase the mean particle size (due to miniaturisation trends), it becomes evident that a minor variation can still drastically impact recoverability and hence minimise slumping and bridging defects, consequently improving print quality by retaining deposit definition.

10.2.2 Solder paste behaviour under different temperatures

The key result relating to flux was presented within the study focused on pre-heat reflow temperatures (Chapter 7), which also provided the two significant contributions to knowledge that are set out below.

10.2.2.1 Significance of solvent evaporation from flux

From investigating the influence of temperature on paste behaviour, results demonstrated that a variation in flux led to a noticeable change in solvent evaporation rate. This was seen through a more rapid occurrence of the 'soft solid' phase, in which the solder paste sample being examined increased in viscosity despite a continued increase in temperature. Therefore, through formulating the solder paste with a flux that allowed for evaporation of solvents at lower temperatures, an improved ability to resist slumping during the pre-heat stages of reflow was achieved, thus minimising bridging and hence one of the major causes of failure in SMA.

10.2.2.2 Rheological simulation of the reflow pre-heat stage

The work relating to paste behaviour at elevated temperatures also offered a new technique for investigating paste behaviour at pre-heat reflow temperatures. By use of a rheometer during the study, it was possible to demonstrate and offer a novel method for simulating the heating process rheologically (from ambient temperatures to 150°C). Through developing this method, indications of paste behaviour can be achieved without the necessity for undertaking the reflow process itself. Therefore, recommendations can be made for 'engineering solder pastes' for the future.

10.2.3 Other key contributions

Investigations into the ageing capability of solder paste (Chapter 6) demonstrated that, from a stencil printing point of view, a six-month shelf life can be dramatically increased – a finding that has been conveyed to the project partner (Henkel Technologies). Through conducting further studies relating to post-reflow acceptability, this could potentially lead to a definitive increase in shelf life, and not just from a stencil printing perspective.

Furthermore, despite many sources categorically dismissing paste storage at sub-zero temperatures, a significant finding from the study was that paste stored in freezer conditions demonstrated reduced variations in characteristics when compared with typical storage methods.

As with the ageing study, investigations into the abandon time capability of solder pastes (Chapter 8) demonstrated that current abandon times can be increased considerably from a printing perspective when compared with those standards currently employed. This is of particular significance when considering the hazardous classification of solder pastes, and the strict guidelines that have now been applied with regard to disposal of such materials (as described by the WEEE directive).

Finally, through utilising the work conducted by Mezger (2006); relating to the Arrhenius equation), a single formula for predicting viscosity was developed during the project. Through utilising this novel equation, it is possible to achieve some close approximations to viscosity at various temperatures. However, it is necessary for further investigations to be conducted into the accuracy of the equation for additional paste samples, and any correction constants that must be applied to increase accuracy of measurements.

10.3 Project conclusions

By undertaking the experimental procedures discussed within this thesis (using the limited range of samples given to test), it has been shown that steps can be taken to help minimise the influence of defects during the stencil printing process. Furthermore, by conducting rheological studies, correlations between paste properties and printing behaviour have been discovered which not only offer opportunities to improve stencil printing performance but also question current industrial standards relating to issues such as shelf life and acceptable periods of printer downtime.

10.3.1 Conclusions from experimental procedures

In addition to those key contributions originating from the investigations into creep recovery behaviour discussed in Chapter 5 and summarised above in section 10.2.1 (namely the derivation of the Marks equation and the significant impact of flux and PSD on recovery performance), it was also discovered that the ability of a paste to recover was directly correlated with the solder paste height demonstrated by the samples – with a reduced recovery percentage associated with a reduced deposit height. This was another significant finding of the investigation, as the height

measurement of paste deposits can be directly related to the 'pass/fail' rate as discussed in Chapter 8, while also being indicative of the levels of slumping present. Therefore, it was concluded that by using the experimental procedure during the paste development process, it may be possible to reduce printing defects through discovering which combination of flux and PSD presents the highest percentage of recoverability during creep testing, thus potentially reducing slumping and bridging.

By means of conducting studies regarding the ageing properties of solder pastes (Chapter 6), significant findings were made relating to the potential for exceeding a six-month shelf life and the impact of storage conditions (as discussed above in section 10.2.3). However, one further conclusion from the study was the potential possibility of predicting paste viscosity at specific temperatures after a period of storage lasting 24 months. Further work would, however, be required to understand the accuracy (and, indeed, the feasibility) of these predictions – yet it is believed that this approach could yield valuable information during quality control or experimental procedures where specific viscosities may be required over a period of time.

Results from investigating the influence of pre-heat reflow temperatures (Chapter 7) demonstrated the importance of the so called 'soft solid' phase experienced by the paste sample. Aside from offering an opportunity to reduce the impact of defects, the soft-solid phase may also provide a significant opportunity to predict paste behaviour through modelling the temperature at which the viscosity once again increases during quality control. Through pre-testing developmental solder pastes to determine the point at which the soft-solid phase in encountered, it may be possible to predict slumping behaviour and hence indicate performance during the reflow process. In addition to this finding; conclusions from the investigation also demonstrated that, at present and regardless of existing methods that allow for the modelling of paste viscosity as a function of applied temperature (such as the Arrhenius equation), it is not possible to predict accurately the viscosity of a solder paste at elevated temperatures. Moreover, once a specific temperature has been reached, paste viscosity demonstrates an increasing viscosity once more (due to the soft-solid phase and/or the evaporation of solvents). With current methods of modelling, the simple fact remains that as temperature increases viscosity decreases, and hence the demonstrated increase in viscosity is not catered for within current models.

Aside from the possibility (from a printing viewpoint) of introducing a 50-hour abandon time, which would significantly reduce levels of waste, conclusions from studying the correlation between print performance and abandon time (Chapter 8) highlighted that the print frequency (after an abandon time) had no significant detrimental effect on the quality of the print, with acceptable deposits once again observed. From this result, it was possible to conclude that typical industrial conditions (printing multiple boards within a set time frame) can be replicated after an abandon time of 50 hours, while retaining acceptable standards of print output. Further to this conclusion, it was also found that upon working the paste after an abandon time, the viscosity converges with the initial viscosity (pre-abandon time). Therefore, it may also be concluded that industrial practices may not even recognise any influence of an introduced abandon time, assuming that a pre-print stage is introduced to initially work the paste.

Results from the abandon time study also indicated that current standards need to be revised when considering the method of determining the 'pass/fail' classification. Industrial literature offers methods for establishing whether a print deposit can be classified as a pass or fail, with dependency solely placed on the paste height observed. Conclusions from the investigation highlight that these current standards are insufficient as they fail to incorporate defect elements such as bridging, smearing or skipping. Therefore, these guidelines should be revised to incorporate stricter methods of classifying a print as a pass or a fail. Additionally, it has been concluded that a universal guideline must be developed in order to declare whether a print is deemed acceptable. This is necessary because of the lack of consistency between sources determining specifications for pass/fail rates. For example, three different sources state (respectively) that a pass is classified as a paste height of 85%, a paste height of 95% or repeat printability on a 0.4 mm pitch. It might then be possible to grant a pass in accordance with one criterion, but a fail against another.

Investigations into the influence of applied stress, application time and recurrence on the rheological creep recovery behaviour of lead-free solder pastes (Chapter 9) further highlighted the need for reviewing current investigation standards. In the conducting

of a benchmark test (utilising current techniques) to allow for comparisons to be drawn, several key findings were discovered:

- Increasing the applied stress from within the LVR to 300 Pa resulted in a decrease in recovery percentage from ≈30% to ≈10% for the test samples.
- Reducing the stress application time to 10 seconds resulted in an increase in recovery percentage from ≈30% to 100%.
- Increasing the number of recurrent applications of creep recovery testing to merely three cycles reduced the recovery percentage from ≈30% to less than 1%.

In each of these three situations, attempting to replicate aspects of the printing process (through rheological investigations into creep recovery behaviour) emphasised the inaccuracy or inability of current standards to determine paste behaviour during stencil printing.

Results from the study also suggested that the deformation behaviour of solder paste (which is inversely linked to the recovery percentage, from Chapter 5) reduces upon increase in the number of individual applications of stress. This is of interest, as it signifies that while the number of printing trials increases, the total level of deformation observed will decrease, tending towards a point at which the recorded deformation becomes a constant. It might then be possible to determine that, once this 'constant deformation' is reached, the quality of the print observed will also become consistent. Therefore, it may be possible to rheologically determine the quality of the print by forming correlations between the paste deformation behaviour and the recoverability.

From investigating the current techniques for creep recovery testing, it was concluded that the major failing of existing methods is the exclusion of repeated applications of stress (or creep recovery cycles). Results from the study highlighted that the application time and stress that were applied, despite varying substantially from those values commonly applied, continually allowed for a successful recovery response to be attained. It was through introducing an element of repeated creep-recovery cycles

that this recoverability faltered unacceptably, dropping to below a 1% recovery percentage. This was concluded to be a result of the permanent structural deformation/breakdown of the paste after the initial application of stress, which resulted in further creep cycles allowing for only a recovery of the previously recovered portion of the structure. This continual process of allowing for a 'recovery of a recovery' leads to a total recoverability value which continues to reduce in acceptability.

From concluding the investigations, a significant stride towards understanding the rheological behaviour of solder pastes and their correlation with the stencil printing process has been achieved. Upon review of current procedures within industry and within the published articles researched, it is evident that the project possesses a considerable potential to greatly improve knowledge relating to paste behaviour. Results seen have uncovered new trends that can influence industrial manufacturers considerably, allowing for early identification of paste performance during the printing process. Furthermore, observed tendencies of the samples to exceed expectations for performance (relating to shelf life and abandon time) signify strong possibilities for developing characterisation techniques, and have assisted with specifying confident new standards for paste life. With the possibility of a reduction of defects during stencil printing, which has been documented throughout this thesis, great strides can be made to reduce the significant level of SMT failure attributed to the stencil printing process.

10.3.2 Success of the project aims and objectives

In referring back to Chapter 1, it was discussed that the project was "aimed at providing guidelines for industry and paste manufacturers (such as Henkel Technology, the project partner) relating to the paste stencilling process and the use of rheological measures for predicting performance". By assessing the findings of the project, it can be concluded that this was achieved successfully; and methods have been developed that can assist with predicting printing performance, while importantly offering techniques to minimise printing defects (which is seen as the major reason for PCB failure). This success can be seen throughout the course of the thesis:

1. Within Chapter 5, it has been discussed how an appropriate selection of paste formulation (with respect to combinations of flux and particle size distribution) can improve the quality of PCB printing and greatly reduce print defects. The rheological method utilised can also be employed as a tool for predicting paste performance based on creep recovery data.
2. Within Chapter 6, methods for increasing the shelf life of solder paste have been discussed, with the potential existing to predict how solder paste will behave after a period of storage lasting two years at various temperatures. Furthermore, it was highlighted that the storage method used can influence the quality of the print achieved.
3. Within Chapter 7, the discovery of a 'soft solid' point during the heating of solder paste allows for a prediction to be made as to the level of slumping and bridging to be expected during periods of elevated temperature (such as during the reflow process).
4. Within Chapter 8, it was highlighted that the abandon time capability of solder pastes can be extended beyond industrial standards, whilst still retaining prints of acceptable quality. Rheological tests used during the investigation allow for an indication and potential prediction of paste behaviour to be attained through contrasting and comparing viscosity results.
5. Within Chapter 9, current standards for creep recovery testing were revised to attempt to replicate the stencil printing process, with results highlighting that current creep techniques fail to adequately determine paste behaviour during the process. The rheological tests conducted may be utilised during prediction to estimate how a solder paste will respond to the stencil printing process, and the level of decay in print quality that might occur with an increasing number of print trials.

In each of the experimental chapters, the test method that was conducted may be used within industrial settings as a guideline tool for investigating further solder paste materials (in an attempt to predict stencil printing performance). Furthermore, the documented results may act as a benchmark for industrial manufacturers, allowing for pastes to be developed that perform to a higher standard, thus reducing printing defects.

With the aim of the project being achieved, it was also important to address each of the project objectives. Once again, through acknowledging the findings of each of the chapters, it is believed that each of the objectives has also been accomplished:

1. **To develop new techniques for characterising new paste formulations using the parallel-plate rheometer:** Particular evidence of achieving this objective can be seen through the development of a novel method for rheologically simulating the pre-heat stage of the reflow process and, consequently, the discovery of the 'soft solid' phase of solder paste during heating, as well as discussion of the importance of this characteristic within the SMT industry.
2. **To investigate techniques for correlating specific paste material properties to print performance:** Particular evidence of achieving this objective can be seen through the many results that offer methods for reducing the occurrence of printing defects, such as the combination of flux and PSD used during paste formulation and the influence of temperature on solvent evaporation.
3. **To develop a parallel-plate rheometry test for predicting abandon time:** Particular evidence of achieving this objective can be seen through the investigation into abandon time capability of solder pastes, in which the method utilised assisted with highlighting that abandon time need not be limited (from a printing point of view) to one hour, but can actually exceed 50 hours.
4. **To develop a parallel-plate rheometry test for post-production ageing:** Particular evidence of achieving this objective can be seen through the investigation into the shelf life capability of solder pastes, in which the method used helped to highlight that restrictions on paste life need not be limited to six months from the date of production, but can acceptably be declared as two years (from a printing point of view).
5. **To assist with developing a greater understanding of Pb-free soldering and to investigate the possibility of reducing printing defects, identifying methods that could assist with this:** Particular evidence of achieving this objective can be seen from each of the key contributions mentioned earlier in this chapter. One particular example is the derivation of the Marks equation, which allows for an understanding of paste response both to the printing process and to the

presence of defects. Furthermore, by following the methods described in the chapters, it has become clear that the possibility exists of reducing printing defects, with several novel techniques developed that could greatly assist with reducing printing defects (such as using the Marks equation to predict paste response to a print cycle).

10.4 Recommendations for future work

After conducting investigations into the rheological characterisation of solder pastes and correlating certain properties of the pastes with the stencil printing process, it became apparent that several further investigations would be beneficial, and hence recommended for future work. These are set out next.

10.4.1 Investigations into rheological characterisation of paste materials correlated with the reflow and pick-and-place operations

With the focus of the project on the rheological characterisation of solder paste materials and the stencil printing process, the remaining aspects of the manufacturing production line were not looked into. As was discussed within Chapter 1, the stencil printing process accounts for approximately 64% of SMT defects and, furthermore, it is said that 87% of defects during reflow originate from stencil printing. For this reason, it becomes clear that minimising defects during stencil printing is essential. However, component pick-and-place, as well as the reflow process, still account for a combined 30% of defects and therefore it is believed that these are important to investigate also.

10.4.2 Investigations into the reliability of solder joints post-reflow

In addition to a proposed investigation regarding reflow and ‘pick and place’, the significance of incorporating investigations into post-reflow observations is recommended as an extension of the work reported in this thesis. Literature findings during the project work (relating to abandon time capability) highlighted that paste material is classified to ‘pass’ an abandon time assuming that the quality of the print is maintained without the requirement for further kneading of the paste. However,

although the print may be acceptable, it is recommended that attempts should be made to investigate how this 'abandon time' can affect the quality of the solder joint formed after the reflow process (for, at present, standards for acceptability rely solely on rheological characteristics and print trials); questions still remain as to the acceptability of the solder joint and, moreover, the estimated life of the joint (or product lifecycle). This recommendation is believed to be of major importance, and it can also be related to the shelf life investigation.

From a shelf life viewpoint, one particular investigation that would be of importance includes printing a small sample of paste onto a bare substrate (such as one of ceramic or copper) and then undertaking the reflow process. In doing this, observation of a single solder ball in a clear pool of residue will indicate that the flux has remained active enough to remove oxides from the surface of the solder, indicating acceptability from a post-reflow perspective, whereas a large number of balls may signify that the sample is unfit for use.

10.4.3 Rheological investigation of type 6 and type 7 solder pastes

With trends towards miniaturisation continuing within electronics manufacturing, the requirement for printing on smaller pitch sizes is constantly increasing, and hence solder particle sizes are also reducing accordingly. Throughout the course of the project, the solder paste samples used were classified as types 3 and 4, which is the equivalent of a particle size distribution of 25–45 microns and 20–38 microns respectively. However, in order to understand paste performance in respect to current trends towards miniaturisation, it is believed that investigating the performance of type 6 (5–15-micron) and type 7 (2–12-micron) pastes should be undertaken (following the test parameters detailed within this thesis) as a valuable extension to the project.

10.4.4 Investigations into the effect of specific temperatures applied during storage

Through conducting the investigation detailed within Chapter 6 (regarding the ageing of solder paste), it was concluded that a potential exists to predict paste viscosity after

a two-year period of storage. The tests that were conducted monitored the rheological properties of material stored at ≈25°C, 4°C and –40°C, with viscosity trends identified. Even so, it is recommended that further work should be conducted that builds on those results detailed within Chapter 6, highlighting viscosity trends over a two-year period for a range of temperatures. By conducting such an investigation, it may be possible to confirm this as a feasible prediction method for forecasting paste behaviour during its storage in various conditions.

10.4.5 Further investigations into the 'soft solid' phase of solder pastes demonstrated at specific temperatures

Investigations into the rheological simulation of slumping behaviour for lead-free solder paste as a result of variations in applied temperature (see Chapter 7) demonstrated that the temperature at which a solder paste becomes a 'soft solid' could have significant potential in attempting to reduce the influence of defects (primarily slumping and bridging). It is therefore recommended that further investigations are conducted into the temperature dependency of this 'soft solid' phase, where various materials should be studied that display a range of different 'transition temperatures' (i.e. those points where viscosity begins to rise once again). This investigation could be regarded as highly important, as not only could this assist with minimising the occurrence of defects, but it could also link into the experiments discussed earlier in the chapter where the rheology of paste materials could be correlated with the reflow process (due to the elevated temperatures experienced during reflow).

This recommendation for future work could also investigate the use of DSC/TGA (differential scanning calorimetry/thermo-gravimetric analysis) analysis to determine the response of the flux vehicle to the temperature profile that was applied. This would provide an indication of what happens to the flux during the pre-heat stage of reflow as opposed to the solder paste as a whole. From this perspective, a further understanding of paste behaviour during the reflow process may be attained.

PUBLICATIONS

Durairaj, R., Mallik, S., Marks, A., Winter, M., Bauer, R., Ekere, N.N. (2006) "Rheological Characterisation of New Lead-Free Solder Paste Formulations for Flip-Chip Assembly". 1st Electronics System Integration Technology Conference. Dresden, Germany. pp. 995–1000

Durairaj, R., Mallik, S., Seman, A., Marks, A.E., Ekere, N.N. (2008) "Viscoelastic Properties of Solder Pastes and Isotropic Conductive Adhesives used for Flip-Chip". 33rd International Electronics Manufacturing Technology Symposium (IEMT 2008). Malaysia. pp. 1–8

Durairaj, R., Mallik, S., Seman, A., Marks, A., Ekere, N.N. (2008) "Investigation of Wall-Slip Effect on Paste Release Characteristic in Flip Chip Stencil Printing Process". 10th Electronic Packaging Technology Conference (EPTC 2008), Singapore. pp. 1328–1333

Durairaj, R., Mallik, S., Seman, A., Marks, A., Ekere, N.N. (2009) "Rheological Characterisation of Solder Pastes and Isotropic Conductive Adhesives used for Flip-Chip Assembly". Journal of Material Processing Technology, Volume 209, Issue 8. pp. 3923–3930

Durairaj, R., Ramesh, S., Mallik, S., Seman, A., Marks, A., Ekere, N.N. (2009) "Rheological Characterisation of Sn/Ag/Cu Solder Pastes". Journal of Materials and Design, Volume 30, Issue 9. pp. 3812–3818

Mallik, S., Ekere, N.N., Durairaj, R., Marks, A. (2007) "A Study of the Rheological Properties of Lead Free Solder Paste Formulations used for Flip-Chip Interconnection". 32nd International Electronics Manufacturing Technology Symposium (IEMT 2007). California, USA. pp. 165–171

Mallik, S., Ekere, N.N., Durairaj, R., Marks, A.E. (2008) “An Investigation into the Rheological Properties of Different Lead-Free Solder Pastes for Surface Mount Applications”. Journal of Soldering and Surface Mount Technology, Volume 20, Number 2. pp. 3–10

Mallik, S., Ekere, N.N., Marks, A.E., Seman, A., Durairaj, R. (2008) “Modelling of the Time-Dependent Flow Behaviour of Lead-Free Solder Pastes used for Flip-Chip Assembly Applications”. 2nd Electronics System Integration Technology Conference. London, UK. pp. 1219–1223

Mallik, S, Ekere, N.N., Durairaj, R., Seman, A., Marks, A.E. (2009) “Wall-Slip Effects in SnAgCu Solder Pastes used in Electronics Assembly Applications”. Journal of Materials & Design, Volume 30. pp. 4502–4506

Mallik, S., Ekere, N.N., Marks, A.E., Seman, A., Durairaj, R. (2010) “Modeling the Structural Breakdown of Solder Paste using the Structural Kinetic Model”. Journal of Materials Engineering and Performance, Volume 19, Number 1. pp. 40–45

Marks, A., Mallik, S., Durairaj, R., Ekere, N.N. (2007) “Effect of Abandon Time on Print Quality and Rheological Characteristics for Lead-Free Solder Pastes used for Flip-Chip Assembly”. 32nd International Electronics Manufacturing Technology Symposium (IEMT 2007). California, USA. pp. 14–19

Marks, A.E., Ekere, N.N., Mallik, S., Durairaj, R. (2008) “Effect of Long-Term Ageing on the Rheological Characteristics and Printing Performance of Lead-Free Solder Pastes used for Flip-Chip Assembly”. The Second International Symposium on Smart Processing Technology (SPT 07), Published in Smart Coating Technology, Volume 2. pp. 131–134

Marks, A.E., Mallik, S, Ekere, N.N., Seman, A. (2008) “Effect of Temperature on Slumping Behaviour of Lead-Free Solder Paste and its Rheological Simulation”. 2nd Electronics System Integration Technology Conference. London, UK. pp. 829–832

Marks, A.E., Ekere, N.N., Mallik, S., Bhatti, R. (2011) “Effect of Particle Size Distribution (PSD) and Flux Medium on the Creep Recovery Performance of Lead-Free Solder Pastes”. Journal of Soldering and Surface Mount Technology, Volume 23, Number 2. pp. 75–84

Seman, A., Ekere, N.N., Ashenden, S.J., Mallik, S., Marks, A.E., Durairaj, R. (2008) “Development of an In-Situ, Non-Destructive Ultrasonic Monitoring Technique for Solder Pastes”. 2nd Electronics System Integration Technology Conference. London, UK. pp. 209–214

Seman, A., Ekere, N.N., Ashenden, S.J., Mallik, S., Marks, A.E., Durairaj, R. (2008) “In-Situ Non-Destructive Ultrasonic Rheology Technique for Monitoring Different Lead-Free Solder Pastes for Surface Mount Applications”. 10th Electronic Packaging Technology Conference (EPTC 2008), Singapore. pp. 1448–1454

REFERENCES

Adams, T. (2009) "A Walk-Through of the Reflow Process". EE Times India, Global Sources, Manufacturing/Packaging. Available at: http://www.eetindia.co.in/ART_8800564399_1800007_TA_2c238108.HTM (Accessed 18th August 2010)

ADTOOL (2002) "Solder Paste Handling Guidelines" ADTOOL Electronics Corporation, Koki Company Ltd. Available at: http://www.adtool.ca/images/paste%20handling%20guidelines%20Nov02.pdf (accessed 20th March 2009)

Afrouz, A., Harvey, J.M. (1974) "Rheology of Rocks within the Soft to Medium Strength Range". International Journal of Rock Mechanics and Mining Science and Geomechanics Abstracts, Volume 11, Issue 7. pp. 281–290

AIM (2003) "Lead Free Soldering Guide". Available at: http://www.psma.com/ul-files/forums/leadfree/aim_lead_free_guide.pdf (Accessed last 16th March 2011) pp. 11–22

Alger, M.S.M. (1997) Polymer Science Dictionary, 2nd Revised Edition, Chapman & Hall, London, U.K. p. 108

Almit Technologies Ltd (2006) "Almit Pb-Free Solder Paste LFM-48 TM-HP". Almit Technologies Ltd. Available at: http://www.almit.com/dloads/Agents/LFM-48TM-HP%20Solder%20Paste.pdf (Accessed last 24th January 2011)

Ancey, C. (2005) "Notebook Introduction to Fluid Rheology", Laboratoire Hydraulique Environnementale (LHE). Lausanne, Switzerland

Aravamudhan, S., Santos, D. Pham-Van-Diep, G., Andres, F. (2002) "A Study of Solder Paste Release from Small Stencil Apertures of Different Geometries with Constant Volumes". Proceedings of the 27th Annual IEEE/SEMI International Electronics Manufacturing Technology Symposium (IEMT). San Jose, California, U.S.A. pp. 159–165

Armelin, E., Martí, M., Rudé, E., Labanda, J., Llorens, J., Alemán, C. (2006) "A Simple Model to Describe the Thixotropic Behavior of Paints". Progress in Organic Coatings, Volume 57, Issue 3. pp. 229–235

Baluch, D., Minogue, G. (2007) "Fundamentals of Solder Paste Technology". Global SMT and Packaging, Volume 7.12. pp. 14–22

Bao, X., Lee, N.C., Raj, R.B., Rangen, K.P., Maria, A. (1998) "Engineering Solder Paste Performance through Controlled Stress Rheology Analysis". Journal of Soldering and Surface Mount Technology, Volume 10, Issue 2. pp. 26–35

Barnes, H.A., Hutton, J.F., Walters, K. (1989) An Introduction to Rheology: Volume 3 of Rheology Series. Edition 7, Elselvier Publishers, Oxford, UK. pp. 11–25

Barnes, H.A. (2000) A Handbook of Elementary Rheology. Institute of Non-Newtonian Fluid Mechanics, University of Wales, UK. pp. 2–21

Barnes, J. (2002) The Presocratic Philosophers: The Arguments of the Philosophers. Routledge, New York, USA. p. 49

Bath, J.S. (2007) Lead-Free Soldering. Springer Publishing, New York, USA. pp 76–77

Bentzen, B.S. (2000) "Solder Paste Printing". SMT in Focus, Technical Papers: Solder Paste and Printing. November 28th 2000

Billote, C., Carreau, P.J., Heuzey, M.C. (2006) “Rheological characterisation of a Solder Paste for Surface Mount Applications”. Rheologica Acta, Volume 45. pp. 374–386

Blair, G.W.S. (1958) “Rheology in Food Research”. Advances in Food Research, Volume 8. pp. 1–61

BLT Circuit Services Ltd (2009) “Lead Free Solder Paste LFS-UFP-ZQ” Safety Data Sheet. Available from BLT Circuit Services, Suffolk, UK

Boger, D.V. (1977) “Demonstration of Upper and Lower Newtonian Fluid Behaviour in a Pseudoplastic Fluid”. Nature Journal, Issue 265. pp. 126–128

Bohloli, B., de Pater, C.J. (2006) “Experimental Study on Hydraulic Fracturing of Soft Rocks: Influence of Fluid Rheology and Confining Stress”. Journal of Petroleum Science and Engineering, Volume 53, Issues 1–2. pp. 1–12

Boitnott, G.N. (1997) “Experimental Characterization of the Nonlinear Rheology of Rock”. International Journal of Rock Mechanics and Mining Sciences, Volume 34, Issues 3–4. pp. 379–388

Boyes, W. (2008) Instrumentation Reference Book. Fourth Edition, Butterworth-Heinemann, Oxford, UK. p. 70

Bradley, E., Handwerker, C.A., Bath, J., Parker, R.D., Gedney, R.W. (2007) “Lead-Free Electronics: iNEMI Projects Lead to Successful Manufacturing”. Institute of Electrical and Electronics Engineers, John Wiley and Sons, New Jersey, USA. pp. 139–171

Braun, D.B., Rosen, M.R. (2000) “Rheology Modifiers Handbook: Practical Use and Application”. William Andrew Publishing, New York, USA. pp. 30–45

Bremmell, K.E., Evans, A., Prestidge, C.A. (2006) “Deformation and Nano-Rheology of Red Blood Cells: An AFM Investigation”. Colloids and Surfaces B: Biointerfaces, Volume 50, Issue 1. pp. 43–48

Brookfield Engineering Laboratories (1985) “More Solutions to Sticky Problems – A Guide to Getting More from your Brookfield Viscometer”. Literature of Brookfield Engineering Laboratories, Inc., AG6000, 20 M, 5/85

Bursell, E. (1960) “The Effect of Temperature on the Consumption of Fat During Pupal Development in Glossina”. Bulletin of Entomological Research 1960, Volume 51, Issue 3. pp. 583–598

Cambridge Polymer Group, Inc. (2002) “The Cambridge Polymer Group Silly Putty™ Egg”. Available at: http://www.campoly.com/documents/appnotes/sillyputty.pdf (accessed last 24th November 2010)

Carpenter, B., Pearsall, K., Raines, R. (1994) “Predicting Printability of WSPs through Rheological Characterization”. Proceedings of the 44th Electronic Components and Technology Conference, Washington, USA. pp. 1082–1088

Carrington, S., Langridge, J. (2005) “Viscometer or Rheometer? Making the Decision”, Laboratory News, Particle Analysis. August 2005 Issue

Cha, D.H., Kim, H-J., Park, H.S., Hwang, Y., Kim, J-H., Hong, J-H., Lee, K-S. (2010) “Effect of Temperature on the Molding of Chalcogenide Glass Lenses for Infrared Imaging Applications”. Applied Optics, Vol. 49, Issue 9. pp. 1607–1613

ChemSec (2010) “Reach and RoHS – Complementary Regulations”. ChemSec: The International Chemical Secretariat Available at: http://www.chemsec.org/rohs/review-of-rohs-directive/reach-and-rohs (Accessed last 11th November 2010)

Chen, X., Wang, X., Liu, B.Y. (2009) “Effect of Temperature on Elastic Properties of Single-Walled Carbon Nanotubes”. Journal of Reinforced Plastics and Composites, Volume 28, Issue 5. pp. 551–569

Chhabra, R.P., Richardson, J.F. (1999) Non-Newtonian Flow in the Process Industries: Fundamentals and Engineering Applications. Butterworth-Heinemann, Oxford, UK. pp. 9–16

Connors, K.A. (1990) Chemical Kinetics: The Study of Reaction Rates in Solution. VCH Publishers, Cambridge, UK. p. 245

Coombs, C.F.Jr. (2008) Printed Circuits Handbook. Sixth Edition, McGraw Hill Companies, New York, USA. p. 44.6

Costello, B. (1997) "The use of Creep tests after Preshear to Predict the Sagging and Slumping Properties of Multicore Solders". TA Instruments (Thermal Analysis and Rheology) Industrial Report for Multicore Solders Ltd, June 1997. p. 2

Cramer, S.D. (1968) "Momentum Transfer in Simple Fluids for Viscometric Flows" PhD Thesis, University of Maryland, USA

Cross, M.M. (1965) "Rheology of Non-Newtonian Fluids: A New Flow Equation for Pseudoplastic Systems". Journal of Colloid Science, Volume 20, Issue 5. pp. 417–437

Cunningham, N. (2007) "Practical Rheology for Chemists". Available at: http://www.rheologyschool.com/practical_rheology_training_course.html (accessed last 15th June 2010)

Cunningham, N. (2009[a]) "Making Use of Models: The Cross Model". Rheology School: Rheology Tips. Available at: http://www.rheologyschool.com/id46.html (accessed 13th December 2009)

Cunningham, N. (2009[b]) "Getting the Stress right in a Creep Test". The Rheology School: Rheology Tips. Available at: http://www.rheologyschool.com/creep_test.html (Accessed last 3rd September 2009)

Cunningham, N. (2010) “What is Yield Stress and Why Does it Matter?”. Rheology School, 2010 Brookfield Engineering Rheology Papers. Available at: http://www.brookfieldengineering.com/education/rheology_papers_yield_stress.asp (accessed last 28th November 2010)

Danielsson, H. (1995) Surface Mount Technology with Fine Pitch Components: The Manufacturing Issues. Chapman and Hall, London, U.K. pp. 70–82

DEK (1995) “DEK 260 Series”. 260 Series Printer: Installation Guide, Operator’s Manual and Technical Reference Manual. pp. 3-31 – 3-53

DEK (2004) “DEK Europa Brochure”. Scanditron Products. Available at: http://www.etalgroup.com/Screen_printers.aspx (Accessed 10th September 2010)

DEK (2007) “DEK Europa”. Dek Screen Printing Range. Available at: http://www.dek.com/web.nsf/us/product_europa (Accessed 10th September 2010)

Di Cola, E., Moussaid, A., Sztucki, M., Narayanan, T., Zaccarelli, E. (2009) “Correlation between Structure and Rheology of a Model Colloidal Glass”. The Journal of Chemical Physics, Volume 131, Issue 14. pp. 144903-144903-9

Diepstraten, G., Wu, D. (2009) “Estimating Stencil Life and Ideal Heating Profile of Solder Paste Using Advanced Thermo-Gravimetric Analysis”. Presented Paper at: IPC: Association Connecting Electronics Industries APEX Exposition 2009, Las Vegas, USA. pp.1–18

Dintenfass, L. (1969) “Blood Rheology in Pathogenesis of the Coronary Heart Diseases”. American Heart Journal, Volume 77, Issue 1. pp. 139–147

Doraiswamy, D. (2002) “The Origins of Rheology: A Short Historical Excursion”. The Society of Rheology: Rheology Bulletin, Volume 71, Number 1. p. 1

DTI (2006) RoHS Regulations: June 2006. Department for Trade and Industry, Government Guidance Notes. p. 5

Durairaj, R. (2006) “Rheological Characterisation of Solder Pastes and Isotropic Conductive Adhesives (ICAS) for Microsystems Assembly Technology”. PhD Thesis, Electronics Manufacturing Engineering Research Group, University of Greenwich, UK. 2006

Durairaj, R. Jackson, G.J. Ekere, N.N. Glinski, G. Bailey, C. (2002) “Correlation of Solder Paste Rheology with Computational Simulations of the Stencil Printing Process”. Journal of Soldering and Surface Mount Technology, Volume 14, Issue 1. pp. 11–17

Durairaj, R., Mallik, S., Seman, A., Marks, A., Ekere, N.N. (2009[a]) “Rheological Characterisation of Solder Pastes and Isotropic Conductive Adhesives used for Flip-Chip Assembly”. Journal of Materials Processing Technology, Volume 209, Issue 8. pp. 3923–3930

Durairaj, R., Ramesh, S., Mallik, S., Seman, A., Ekere, N.N. (2009[b]) “Rheological Characterisation and Printing Performance of Sn/Ag/Cu Solder Pastes”. Journal of Materials and Design, Volume 30, Issue 9. pp. 3812–3818

Dusek, M., Zou, L., Hunt, C. (2002) “Rheology Testing of Solder Pastes and Conductive Adhesives – A Guide”. NPL Report MATC(A) 109. Centre for Materials Measurement and Technology, National Physical Laboratory, Teddington, Middlesex. ISSN 1473-2734

Dutt, N.V.K., Prasad, D.H.L. (1993) “Relationships between Rheological Properties and Paint Performance”. Journal of Pigment and Resin Technology, Volume 14, Issue 1. pp. 10–18

Einstein, A. (1906) “Eine neue bestimmung der molekuldimension”. Annalen der Physik, Volume 19. pp. 289–306 (Translated as: “A New Determination of Molecule Dimensions”)

Einstein, A. (1911) “Berichtigung zu meiner arbeit: Eine neue bestimmung der molekuldimension”. Annalen der Physik, Volume 34. pp. 591–592 (Translated as: “Correction to my work: A New Determination of Molecule Dimensions”)

Ekere, N.N., Lo, K. (1991) “New Challenges in Solder-Paste Printing”. Journal of Electronics Manufacturing, Volume 1, Number 1. pp. 29–40

Ekere, N.N., Lo, E.K., Mannan, S.H. (1994) “Process Modeling Maps for Solder Paste Printing”. Journal of Soldering and Surface Mount Technology, Number 17. pp. 4–11

El-Khalek, A.M.A. (2009) “Steady State Creep and Creep Recovery Behaviours of Pre-aging Al–Si Alloys”. Journal of Materials Science and Engineering A: Structural Materials Properties, Microstructure and Processing, Volume 500, Issues 1–2. pp. 176–181

Electronics Yorkshire, TWI, ECO^3 (2005) “Lead-Free Workbench Guide”. Electronics Yorkshire Publication, Yorkshire, UK. pp. 4–19

EM Asia (2010) “Electronics Manufacturing Asia: May 2010 Edition”. Electronics Manufacturing Asia. Available at: http://www.emasiamag.com (Accessed last 10th November 2010)

Emerson & Cuming (2000) “Understanding Rheology”. Emerson & Cuming: A National Starch and Chemical Company, Technical Data Sheet. Available at: http://www.kitpackers.com/PDFs/TT-UnderstandingRheology.pdf (accessed last 2nd December 2010)

Evans, J., Beddow, J. (1987) “Characterization of Particle Morphology and Rheological Behavior in Solder Pastes”. IEEE Transactions: Components, Hybrids and Manufacturing Technology, Volume 10, Issue 2. pp. 224–231.

Ferguson, J., Kemblowski, Z. (1991) Applied Fluid Rheology. Elsevier Applied Science, London, U.K. pp. 47–133

Fischer, E.K. (1950) “Rheological Properties of Commercial Paints”. Journal of Colloid Science, Volume 5, Issue 3. pp. 271–281

Fisher, R.A (1926) “The Arrangement of Field Experiments”. Journal of the Ministry of Agriculture of Great Britain, Volume 33. pp. 503–513

Fisher, R.A. (1935) The Design of Experiments. Hafner Press, New York, USA. pp. 2–79

Fletcher, J., Hill, A. (2008) “Making the Connection - Particle Size, Size Distribution and Rheology”. ChemEurope.com: Electronic Articles. Available at: http://www.chemeurope.com/articles/e/61207/ (accessed last 8th December 2010)

Franco, J.M., Delgado, M.A., Valencia, C., Sanchez, M.C., Gallegos, C. (2005) “Mixing Rheometry for Studying the Manufacture of Lubricating Greases”. Chemical Engineering Science, Volume 60, Issues 8-9. pp. 2409–2418

Freeman, G. (1990) “The Fine-Pitch Screen-Printing Process”. Circuits Manufacturing, Volume 30, Number 1. pp. 50–55

Galdi, G.P., Rannacher, R., Robertson, A.M., Turek, S. (2008) Hemodynamical Flows: Modeling, Analysis and Simulation. Birkhäuser, Berlin, Germany. p. 25

Ganesan, S., Pecht, M. (2006) Lead-Free Electronics. John Wiley and Sons, New Jersey, USA. p. 128

Gastel, S-V. (2011) “Improve margins by reducing rework – a benchmark comparison” Available at: http://www.smtnet.com/library/files/upload/reducing-rework.pdf (Accessed last 19th July 2012)

Geraghty, R., Butler, F. (1999) “Viscosity Characterisation of a Commercial Yoghurt at 5c using a Cup in Bob and a Vane Geometry over a Wide Shear Rate Range ($10^{-5}s^{-1}$-$10^{3}s^{-1}$)”. Journal of Food Process Engineering, Volume 22, Issue 1. pp. 1–10

Gere, J.M., Goodno, B.J. (2009) Mechanics of Materials. Seventh Edition. Cengage Learning, Toronto, Canada. pp. 27–28

Gilbert, B. (2001[a]) "Surface Mount Technology, Step 7 – Soldering". Available at: http://smt.pennnet.com/Articles/Article_Display.cfm?Section=Archives&Subsection=Display&ARTICLE_ID=109071&KEYWORD=flux (Accessed last 6th March 2007)

Gilbert, B. (2001[b]) "Step by Step SMT Soldering: Reducing Soldering Defects". Loctite Corporation: Technical Papers. Available at: http://www.xs4all.nl/~tersted/PDF_files/Loctite/Step_by_Step_Soldering_0801.pdf (Accessed last 24th January 2011)

Gilleo, K. (1996) Polymer Thick Film. Van Nostrand Reinhold, A Division of International Thompson Publishing, New York, USA. p. 173

Girdwood, R.B., Evans, R.W. (1996) "Recovery of Creep Properties of the Nickel-Base Superalloy Nimonic 105". International Journal of Pressure Vessels and Piping, Volume 66, Issues 1-3. pp. 141–153

Goldman, J.C., Carpenter, E.J. (1974) "A Kinetic Approach to the Effect of Temperature on Algal Growth". Journal of Limnology and Oceanography. Volume 19, Issue 5. pp. 756–766

Gregoire, M. (2003) "Printing Abandon Time Capability of Solder Paste Products". Henkel Loctite Technologies (Multicore): Standard Test Method, 28th March 2003.

Han, M., Shi, L., Ye, M., Guo, Q. (1996) "Characterization of Viscoelastic Properties of Polyacrylamide/Cr(III) Hydrogels". Polymer Bulletin, Volume 36, Number 4. pp. 483–487

Harper, C.A. (2000) "High Performance Printed Circuit Boards". McGraw-Hill, New York, U.S.A. p. 7.26

Harper, C.A. (2005) “Electronic Packaging and Interconnection Handbook”. Fourth Edition, McGraw-Hill, New York, U.S.A. p. 5.27

Haslehurst, L., Ekere, N.N. (1996) “Parameter Interactions in Stencil Printing of Solder Pastes”. Journal of Electronics Manufacturing, Volume 6, Number 4. pp. 307–316

Heraeus (2005) “Solder Paste Series F 640”. Application Recommendation Sheet for Heraeus Lead Free Solder Paste. p. 9

Herh, P., Tkachuk, J., Wu, S., Bernzen, M., Rudolph, B. (1998) “The Rheology of Pharmaceutical and Cosmetic Semisolids”. Rheologica Instruments Application Note, July 1998. pp. 12–14

Hillman, S.R., Mannan, S.H., Durairaj, R., Seman, A., Ekere, N.N., Dusek, M., Hunt, C. (2005) “Correlation Between Jamming and Skipping during Solder Paste Printing”. Journal of Soldering and Surface Mount Technology, Volume 17, Issue 4. pp. 17–36

Hooke, R.J. (1678) “Lectures De Potentia Restitutiva” (Of Spring; Explaining the Power of Springing Bodies). J. Martyn, London, UK.

Hughes, W.F., Brighton, J.A. (1999) *Schaum’s Outline of Theory and Problems of:* Fluid Dynamics. Third Edition. McGraw-Hill Professional, New York, USA. p. 303

Humpston, G. (2004) Principles of Soldering. ASM International Publishing, Ohio, U.S.A. p. 116

Hwang, J.S. (1989) Solder Paste in Electronics Packaging: Technology and Applications in Surface Mount, Hybrid Circuits, and Component Assembly. Van Nostrand Reinhold, New York, USA. pp. 169

Hwang, J.S. (1994) “Solder / Screen Printing”. Surface Mount Technology, March 1994 Issue. pp. 44–50

Hwang, J.S. (2004) Implementing Lead-Free Electronics. McGraw Hill Companies, New York, USA. pp. 136–139

Indium Corporation (2008) "Gold Alloy Assembly Materials", Indalloy 182 Gold-Tin Solder Paste Product Data Sheet. Available at: http://www.indium.com/gold/ (Accessed 31st August 2010)

IPC (1995) "IPC-TM-650 Test Methods Manual". The Institute for Interconnecting and Packaging Electronic Circuits, Illinois, USA. p. 3

Itoh, M. (2002) "General Information on Solder Paste". Koki Company Limited Technical Documents, pp. 6–12. Available at: http://www.koki.org/Files/pdf/Tech/Solder%20paste%20general%20info.pdf (Accessed last 10th March 2010)

ITW Kester (2007) "EnviroMark 919G No-Clean Lead-Free Solder Paste". Product Data Package, ITW Kester Research and Development Group, Illinois, U.S.A. p. 27

ITW Kester (2009) "NXG1 No-Clean Lead-Free Solder Paste". Supplemental Data Package, ITW Kester, Illinois, U.S.A. p. 16

Jackson, G.J., Hendriksen, M.W., Kay, R.W., Desmulliez, M., Durairaj, R.K., Ekere, N.N. (2005) "Sub Process Challenges in Ultra Fine Pitch Stencil Printing of Type-6 and Type-7 Pb-Free Solder Pastes for Flip Chip Assembly Applications". Journal of Soldering and Surface Mount Technology, Volume 17, Issue 1. pp. 24–32

Jensen, T. (2004) "Solder Paste Evaluation Techniques to Simplify the Transition to Pb-Free". Indium Corporation: Technical Documents, Soldering White Papers. pp. 2–3

Jinescu, V.V. (1974) "The Rheology of Suspensions". Journal of International Chemical Engineering, Volume 143. pp. 397–420

Jirinec, M.J. (1984) “Characterisation of Solder Paste for Surface Mount Attachment”. Proceedings of Circuit Exposition 1984. pp. 43–48

Johnson, C.C., Kevra, J. (1989) Solder Paste Technology: Principles and Applications. TAB Professional and Reference Books, Michigan, U.S.A. pp. 73–122

Jones, S.P., Tyson, J.K. (1952) “The Rheology of a Lubricating Oil at Temperatures below the Pour Point”. Journal of Colloid Science, Volume 7, Issue 3. pp. 272–283

Kay, R., Desmulliez, M., Stoyanov, S., Bailey, C., Durariaj, R., Ekere, N., Hendrikson, M., Frimpong, F., Smith, B., Price, D., Roberts, A., Whitmore, M., Ongley, P., Gourlay, J. (2003) “Low Temperature Flip-Chip Packaging based on Stencil Printing Technology”. MicroTech 2003, IMAPS UK, Stratford-upon-Avon, UK.

Keely, C.M. (2000) “Container Cap Cover for the Environmental Recovery and Recycling of Solder Paste”. Motorola Technical Developments, January 2000. p. 118

Kelessidis, V.C. (2008) “Investigations on the Thixotropy of Bentonite Suspensions”. Energy Sources, Part A: Recovery, Utilization, and Environmental Effects, Volume 30, Issue 18. pp. 1729–1746

Khadom, A.A., Yaro, A.S., Kadum. A.A.H., AlTaie, A.S., Musa, A.Y. (2009) “The Effect of Temperature and Acid Concentration on Corrosion of Low Carbon Steel in Hydrochloric Acid Media”. American Journal of Applied Sciences. Volume 6, Issue 7. pp. 1403–1409

Kim, J.H., Satoh, M., Iwasaki, T. (2005) “Rheological Properties of Particle–Flux Suspension Paste”. Advanced Powder Technology, Volume 16, Number 1. pp. 61–71

Koorithodi, L (2010) “Modern Solder Paste Technology”. Electronics Manufacturing Asia Magazine, November 2010 Print Edition. Available at: http://www.emasiamag.com/article-7755-modernsolderpastetechnology-Asia.html (Accessed last 6th January 2011)

Koszkul, J., Nabialek, J. (2004) “Viscosity Models in Simulation of the Filling Stage of the Injection Molding Process”. Journal of Materials Processing Technology, Volumes 157–158. pp. 183–187

Kotz, J.C., Treichel, P., Townsend, J.R. (2009) Chemistry and Chemical Reactivity: Volume 2. Seventh Edition. Cengage Learning, USA. pp. 696–697

Lapasin, R., Sirtori, V., Casati, D. (1994) “Rheological Characterisation of Solder Pastes”. Journal of Electronic Materials, Volume 23, Number 6. pp. 525–532

Laser Vision Technologies (2005) “VisionMaster”. Solder Paste Inspection Systems. Available at: http://www.lvtechnologies.com/visionmaster.html (Accessed 14th September 2010)

Lee, K.W. (2006) Asphalt Mix Design and Construction: Past, Present, and Future. ASCE Publications (American Society of Civil Engineers), Virginia, USA. p. 142

Lee, N-C. (2002) Reflow Soldering Processes and Troubleshooting: SMT, BGA, CSP, and Flip Chip Technologies. Newnes (an imprint of Elsevier), Massachusetts, USA. pp. 3/43–5/92 (Newnes Publishing, Oxford, UK. pp. 5/91–5/103)

Lee, H.S., Kim, J. (2009) “Determination of Viscoelastic Poisson's Ratio and Creep Compliance from the Indirect Tension Test”. Journal of Materials in Civil Engineering, Volume 21, Issue 8. pp. 416–425

Lewandowski, R., Chorazyczewski, B. (2010) “Identification of the Parameters of the Kelvin–Voigt and the Maxwell Fractional Models, used to Modeling of Viscoelastic Dampers”. Journal of Computers and Structures, Volume 88, Issues 1–2. pp. 1–17

Licari, J.J., Swanson, D.W. (2005) Adhesives Technology for Electronic Applications: Materials, Processes, Reliability. William Andrew, New York, USA. p. 399

Lieberman, N.P., Lieberman, E.T. (2008) A Working Guide to Process Equipment. Third Edition, McGraw Hill, USA. pp. 503–510

Lofti, A., Howarth, M. (1998) "Industrial Application of Fuzzy Systems: Adaptive Fuzzy Control of Solder Paste Stencil Printing". Journal of Information Sciences, Volume 107, Issues 1–4. pp. 273–285

Lokhande, A., Biradar, S., Paradkar, A., Mahadik, K. (2011) "In Vitro Evaluation of Topical Gel prepared using Silk Fibroin at Different Concentration of Gel Accelerating Agent – Glycerol". International Journal of Pharmaceutics and Bio Sciences, Volume 2, Issue 1. pp. 646–660

LPKF Laser and Electronics USA (2010) Lead-Free Solder Paste – SN100C NL900 Technical Data Sheet. Available at: http://www.lpkfusa.com/SMTAssembly/leadfreesolderpaste.htm (Accessed 31st August 2010)

Ma, L., Barbosa-Cánovas, G.V. (1995) "Rheological Characterization of Mayonnaise. Part II: Flow and Viscoelastic Properties at Different Oil and Xanthan Gum Concentrations". Journal of Food Engineering, Volume 25, Issue 3. pp. 409–425

Mackie, A. (2009) "How Much Metal is in Solder Paste?". Indium Corporation Web Log. Available at: http://blogs.indium.com/blog/semiconductor-and-power-semi-assembly/0/0/how-much-metal-is-in-solder-paste (accessed last 8th December 2010)

Macosko, C.W. (1994) Rheology: Principles, Measurements and Applications. Advances in Interfacial Engineering Series. Wiley-VCH, New York, U.S.A.

Maiso, P.S., Bauer, B. (1990) "Statistical Process Control in Solder Paste Manufacture and Use". IPC Technical Review, September. pp. 20–26

Mallik, S., Ekere, N.N., Durairaj, R., Marks, A.E. (2008) "An Investigation into the Rheological Properties of different Lead-Free Solder Pastes for Surface Mount

Applications". Journal of Soldering and Surface Mount Technology, Volume 20, Issue 2. pp. 3–10

Mallik, S. (2009) "Study of the Time-dependent Rheological Behaviour of Lead-free Solder Pastes and Flux Mediums used for Flip-Chip Assembly Applications". PhD Thesis, Electronics Manufacturing Engineering Research Group, University of Greenwich, UK. January 2009

Malvern Instruments (2004) "Rheology Introduction". Rheology Training and Principles of Viscoelasticity Presentation courtesy of Malvern Instruments, Worcestershire, UK.

Manko, H.H. (1995) Soldering Handbook for Printed Circuits and Surface Mounting. Second Edition, Kluwer Academic Publishers, USA. pp. 223–226

Manko, H.H. (2001) Solders and Soldering: Materials, Design, Production, and Analysis for Reliable Bonding. Fourth Edition, McGraw Hill Companies, New York, USA. pp. 432–440

Mannan, S.H., Ekere, N.N., Lo, E.K., Ismail, I. (1993) "Predicting Scooping and Skipping in Solder Paste Printing for Reflow Soldering of SMT Devices". Journal of Soldering and Surface Mount Technology, Volume 5, Issue 3. pp. 14–17

Mannan, S.H., Ekere, N.N., Ismail, I., Lo, E.K. (1994) "Squeegee Deformation Study in the Stencil Printing of Solder Pastes". IEEE Transactions on Components, Packaging, and Manufacturing Technology, Part A, Volume 17, Issue 3. pp. 470–476

Mannan, S.H., Ekere, N.N., Ismail, I., Currie, M.A. (1995). "Flow Processes in Solder Paste during Stencil Printing for SMT Assembly". Journal of Materials Science: Materials in Electronics, Volume 6, Number 1. pp. 34–42

Marin, A., Simion-Zanescu, D. (2005) "Rheology of Solder Pastes for SMT Applications". Hidraulica: Magazine of Hydraulics, Pneumatics, Tribology, Ecology, Senzorics, Mechatronics. Number 1-2 (17) August 2005. pp. 7–16

Marks, A.E., Ekere, N.N., Mallik, S., Bhatti, R. (2011) “Effect of Particle Size Distribution (PSD) and Flux Medium on the Creep Recovery Performance of Lead-Free Solder Pastes”. Journal of Soldering and Surface Mount Technology, Volume 23, Number 2. pp. 75–84

Matveenko, V.N., Kirsanov, E.A., Remizov, S.V. (1995) “Rheology of Highly Paraffinaceous Crude Oil”. Colloids and Surfaces A: Physicochemical and Engineering Aspects, Volume 101, Issue 1. pp. 1–7

McCrum, N.G., Buckley, C.P., Bucknell, C.B. (1997) Principles of Polymer Engineering. 2nd Edition, Oxford University Press, Oxford Science Publications, U.K. pp. 117–176

Metzner, A.B. (1985) “Rheology of Suspensions in Polymeric Liquids”. Journal of Rheology, Volume 29. pp. 739–775

Mezger, T.G. (2006) The Rheology Handbook: For Users of Rotational and Oscillatory Rheometers. Second Edition. Vincentz Network GmbH and Co KG, Hannover, Germany. pp. 53–100

Morris, J.R., Wojcik, T. (1991) “Stencil Printing of Solder Paste for Fine-Pitch Surface Mount Assembly”. IEEE Transactions on Components, Hybrids and Manufacturing Technology, Volume 14, Number 3. pp. 560–566

Morrison, F.A. (2004) “What is Rheology Anyway?”. The Industrial Physicist, American Institute of Physics, Volume 10, Issue 2, pp. 29–31

Mostafa, M.M., Al-Ganainy, G.S., El-Khalek, A.M.A., Nada, R.H. (2003) “Steady-State Creep and Creep Recovery during Transformation in Al-Zn Alloys”. Physica B: Condensed Matter, Volume 336, Issues 3–4. pp. 402–409

Naguib, W., Mirmiran, A. (2003) "Creep Analysis of Axially Loaded Fiber Reinforced Polymer-Confined Concrete Columns". Journal of Engineering Mechanics, Volume 129, Number 11. pp. 1308–1319

National Electronics Manufacturing Centre of Excellence (2000) "The Science of Stencil Printing". Empfasis: A Publication of the National Electronics Manufacturing Centre of Excellence, Philadelphia, USA. pp. 1–2

Navarrette, H.E. (1969) "The Rheology of Glass Filled Polystyrene". Published by the University of Connecticut, Connecticut, USA.

Navarro, F.J., Partal, P., Boza, F.M., Gallegos, C. (2005) "Influence of Crumb Rubber Concentration on the Rheological Behaviour of a Crumb Rubber Modified Bitumen". Journal of Energy Fuels, Volume 19, Issue 5. pp. 1984–1990

Newton, Sir I. (1687) Philosophiae Naturalis Principia Mathematica. First Edition, Bk2, Section IX, Royal Society, London, U.K.

Nguty, T.A., Riedlin, M.H.A., Ekere, N.N. (1998) "Evaluation of Process Parameters for Flip Chip Stencil Printing". IEEE/CPMT International Electronics Manufacturing Technology Symposium. Austin, Texas, U.S.A. pp. 206–215

Nguty, T.A., Ekere, N.N., Adebayo, A. (1999) "Correlating Solder Paste Composition with Stencil Printing Performance". Twenty Fourth IEEE/CPMT International Electronics Manufacturing Technology Symposium Proceedings. pp. 304–312

Nguty, T.A., Ekere, N.N. (2000[a]) "Modelling the Effects of Temperature on the Rheology of Solder Pastes and Flux System". Journal of Materials Science: Materials in Electronics, Volume 11. pp. 39–43

Nguty, T.A., Ekere, N.N. (2000[b]) "Monitoring the Effects of Storage on the Rheological Properties of Solder Paste". Journal of Materials Science: Materials in Electronics, Volume 11. pp. 433–437

Nguty, T.A., Ekere, N.N. (2000[c]) "The Rheological Properties of Solder and Solar Pastes and the Effect on Stencil Printing". Rheologica Acta, Volume 39. pp. 607–612

Nordson EFD (2007) "Complete Solder Solutions: Choosing the Right Solder Paste". Nordson Engineered Fluid Dispensing (EFD), Available at: http://www.infopromi.com/pdf_tech/SSL610a%20Choosing%20the%20Right%20Solder%20Paste.pdf (accessed last 21st October 2010)

Okuru, T., Kanai, M., Ogata, S., Takei, T., Takakusagi, H. (1993) "Optimisation of Solder Paste Printability with Laser Inspection Technique". Proceedings of IEEE/CPMT International Electronics Manufacturing Symposium. pp. 157–161

Osswald, T.A. (1998) Polymer Processing Fundamentals. Hanser-Verlag, München, Germany. pp. 48–49

Owczarek, J.A., Howland, F.L. (1990[a]) "A Study of the Off-Contact Screen Printing Process. I. Model of the Printing Process and some Results Derived from Experiment". IEEE Transactions on Components, Hybrids, and Manufacturing Technology, Volume 13, Issue 2. pp. 358–367

Owczarek, J.A., Howland, F.L. (1990[b]) "A Study of the Off-Contact Screen Printing Process. II. Analysis of the Model of the Printing Process". IEEE Transactions on Components, Hybrids, and Manufacturing Technology, Volume 13, Issue 2. pp. 368–375

Owens, R.G., Phillips, T.N. (2002) Computational Rheology. Imperial College Press, London, U.K. pp. 77–81

Pal, R. (2000) "Slippage during the Flow of Emulsions in Rheometers". Colloids and Surfaces A: Physicochemical and Engineering Aspects, Volume 162, Issues 1–3. pp. 55–66

Pan, J., Tonkay, G.L. (1999) "A Study of the Aperture Filling Process in Solder Paste Stencil Printing". In: Sahay, C., American Society of Mechanical Engineers. Design

Engineering Division (1999) “Electronics Manufacturing Issues”. ASME International Mechanical Engineering Congress and Exposition, Nashville, Tennessee. p. 75

Pan, J., Tonkay, G.L., Storer, R.H., Sallade, R.M., Leandri, D.J. (2004) “Critical Variables of Solder Paste Stencil Printing for Micro-BGA and Fine-Pitch QFP”. IEEE Transactions on Electronics Packaging Manufacturing, Volume 27, Issue 2. pp. 125–132

Pandy, B.P., Saraf, D.N. (1982) “An Experimental Investigation in Rheological Behaviour of Glass-Water Suspensions”. The Chemical Engineering Journal, Volume 24, Issue 1. pp. 61–69

Pecht, M.G. (1993) Soldering Processes and Equipment. John Wiley and Sons Inc, New York, USA. pp. 22–37

Planche, J.P., Claudy, P.M., Létoffé, J.M., Martin, D. (1998) “Using Thermal Analysis Methods to Better Understand Asphalt Rheology”. Thermochimica Acta, Volume 324, Issues 1–2. pp. 223–227

Polacco, G., Stastna, J., Biondi, D., Antonelli, F., Vlachovicova, Z., Zanzotto, L. (2004) “Rheology of Asphalts Modified with Glycidylmethacrylate Functionalized Polymers”. Journal of Colloid and Interface Science, Volume 280, Issue 2. pp. 366–373

Prasad, R.P. (1997) Surface Mount Technology: Principles and Practice. Second Edition, Kluwer Academic Publishers, Massachusetts, USA. pp. 401–429

Prasad, P.S.R.K., Reddy, A.V., Rajesh, P.K., Ponnambalam, P., Prakasan, K. (2006) “Studies on Rheology of Ceramic Inks and Spread of Ink Droplets for Direct Ceramic Ink Jet Printing”. Journal of Materials Processing Technology, Volume 176, Issues 1–3. pp. 222–229

Price, P. (2005) “Lead-Free Soldering Means Changes”. Electronics Weekly articles. 3rd March 2005. Available at: www.electronicsweekly.com/Articles/2005/03/03/134529/lead-free-soldering-means-changes.htm (Accessed last 21st January 2008)

Puttlitz, K.J., Stalter, K.A. (2004) Handbook of Lead-Free Solder Technology for Microelectronic Assemblies. Marcel Dekker Inc, New York, USA. pp. 499–531

Qualitek (2007) “DSP 878 Lead Free No Clean Solder Paste”. Qualitek Group of Companies Sn/Ag/Cu Technical Data Sheet, Wirral, UK. p. 6

Qualitek (2008) “DSP XP799 Water Soluble (OA) Solder Paste”. Qualitek Group of Companies: Technical Data Sheet. Available at: http://www.qualitek.com/XP799%2520(Sn63Pb37).pdf (Accessed last 26th January 2011)

Radio Electronics (2007) “How to use Solder Paste”. Resources and Analysis for Electronics Engineers. Available at: http://www.radio-electronics.com/info/manufacture/soldering/solder_paste/how-to-use-solder-paste.php (accessed 16th February 2009)

Radler, F. (1965) “The Effect of Temperature on the Ripening of Sultana Grapes”. American Journal of Enology and Viticulture, Volume 16, Issue 1. pp. 38–41

Rahn, A. (2006) “Pastes, Stencils, and Process Control”. Surface Mount Technology, February 2006 Issue. pp. 28–34

Rajkumar, D., Nguty, T., Ekere, N.N. (2000) “Optimising Process Parameters for Flip Chip Stencil Printing using Taguchi’s Method”. Twenty-Sixth Electronics Manufacturing Technology Symposium, IEEE/CPMT International, California, USA. pp. 382–388

Rao, M.A. (2007) Rheology of Fluid and Semisolid Foods: Principles and Applications. Second Edition, Springer Publishing, New York, USA. pp. 30–37

Remington (2005) Remington: The Science and Practice of Pharmacy. Twenty-First Edition, Lippincott Williams & Wilkins, Philadelphia, USA. pp. 342–345

Riande, E., Diaz-Calleja, R., Prolongo, M.G., Masegosa, R.M., Salom, C. (1999) Chapter 10 ("Viscoelastic Models") in Polymer Viscoelasticity: Stress and Strain in Practice (ed E. Riande), Marcel Dekker, New York, USA. p. 400

Riedlin, M.H.A., Ekere, N.N. (1999) "How Heat Generation in Stencil Printing Affects Solder Joint Quality". Surface Mount Technology, 1st August 1999. I-Connect 007 Publications.

Romberg, J.W., Traxler, R.N. (1947) "Rheology of Asphalt". Journal of Colloid Science, Volume 2, Issue 1. pp. 33–47

Rowland, R. (2006) The SMT Step-By-Step Collection 2006. Penwell Books, Oklahoma, USA. p. 19

Schantz, B., Rohm, H. (2005) "Influence of Lecithin–PGPR Blends on the Rheological Properties of Chocolate". Lebensmittel-Wissenschaft und-Technologie, Volume 38, Issue 1. pp. 41–45

Scheiner, D. (2003) "Reflow Profile Optimization". Surface Mount Technology, Volume 17, Issue 9, September 2003. Available at: http://smt.pennnet.com/Articles/Article_Display.cfm?Article_ID=186600 (accessed 21st November 2007)

SEED (2009) "Viscosity: What causes viscosity?". Schlumberger Excellence in Educational Development. Available at: http://www.seed.slb.com/v2/FAQView.cfm?ID=555 (accessed last 30th August 2009)

Seman, A. (2010) "On-Line Non-Destructive Ultrasonic Rheology Measurement of Solder Pastes". PhD Thesis, Electronics Manufacturing Engineering Research Group, University of Greenwich, UK

Shangguan, D. (2005) Lead-Free Solder Interconnect Reliability. ASM International Publishing, Ohio, USA. pp. 2–7

Suganuma, K. (2003) Lead-free Soldering in Electronics: Science, Technology and Environmental Impact. Marcel Dekker, Inc., New York, USA. pp. 1–48

Sybilski, D. (1993) "Non-Newtonian Viscosity of Polymer-Modified Bitumens". Journal of Materials and Structures, Volume 26, Issue 1. pp. 15–23

Tadros, T.F. (2008) Colloids in Cosmetics and Personal Care. Volume 4, Colloids and Interface Science Series. Wiley-VCH, Weinheim, Germany. p. 132

Tarr, M. (2007) "Solder Paste Characteristics". University of Bolton, Online Postgraduate Courses for the Electronics Industry: Soldering Course. Available at: http://www.ami.ac.uk/courses/topics/0246_spc/index.html (accessed last 7th December 2010)

Toleno, B. (2005) "Case Study – Implementation of Pb-free Solder Paste in a Real Manufacturing Environment". EMSNow (Electronic Manufacturing Services), EMSNow Media White Papers. October 2005.

Trease, R.E., Dietz, R.L. (1972) "Rheology of Pastes in Thick-Film Printing". Solid State Technology, Volume 15, Number 1. pp. 39–43

Tsai, T-N., Yang, T. (2005) "A Neuro-Computing Approach to the Thermal Profile Control of the Second-Side Reflow Process in Surface Mount Assembly". Journal of Manufacturing Technology Management, Volume 16, Issue 3. pp. 343–359

Tsai, T-N. (2008) "Modeling and Optimization of Stencil Printing Operations: A comparison Study". Journal of Computers and Industrial Engineering, Volume 54, Issue 3. pp. 374–389

Van Acker, K., Xiang, D.Z., Rillaerts, E., Van Gaal, L., De Leeuw, I. (1989) "Blood Rheology during an Intensified Conventional Insulin Treatment (ICIT) in Insulin-

Dependent Diabetes". Diabetes Research and Clinical Practice, Volume 6, Issue 4. pp. 259–264

Wan Nik, W.B., Ani, F.N., Masjuki, H.H., Eng Giap, S.G. (2005) "Rheology of Bio-Edible Oils According to Several Rheological Models and its Potential as Hydraulic Fluid". Industrial Crops and Products, Volume 22, Issue 3. pp. 249–255

Wang, Z., Lu, H., Shen, Z., Liu, H., Bouillard, J. (2007) "Prediction of Flow Behaviour of Micro-Particles in Risers in the Presence of Van Der Waals Forces". Journal of Chemical Engineering, Volume 132. pp. 137–149

Wang, Y., Zhang, D. (2009) "Creep-Effect on Mechanical Behavior of Concrete Confined by FRP under Axial Compression". Journal of Engineering Mechanics, Volume 135, Number 11. pp. 1315–1322.

Westerlaken, E. (2000) "The Characterization of Printing Properties of Solder Pastes". Cobar Europe BV Marketing Papers. pp. 1–5

Whitfield, G.W. (1965) "Rheology of Printing Ink (Letterpress and Litho)" Rheologica Acta, Volume 4, Number 4. pp. 276–278

Whitmore, M., Mackay, C., Hobby, A. (1997) "Plastic Stencils for Bottom-Side Chip Attach". Journal of Electronic Packaging and Production, Volume 37, Issue 13. pp. 68–72

Wiese, J., Goedecke, A., Audiger, S., Grebner, S., Schmitt, W., Scheikowski, M. (2005) "Development of a Lead Free Solder Paste during the IMECAT Project". 15th European Microelectronics and Packaging Conference (EMPC), Brugge, Belgium. pp. 423–426

Williamson, R.V. (1929) "The Flow of Pseudoplastic Materials". Industrial and Engineering Chemistry, Volume 21, Issue 11. pp. 1108–1111

Yang, T., Tsai, T-N. (2004) “A Neurofuzzy-Based Quality-Control System for Fine Pitch Stencil Printing Process in Surface Mount Assembly”. Journal of Intelligent Manufacturing, Volume 15, Number 5. pp. 711–721

Yang, T., Tsai, T-N., Yeh, J. (2005) “A Neural Network-Based Prediction Model for Fine Pitch Stencil-Printing Quality in Surface Mount Assembly”. Engineering Applications of Artificial Intelligence, Volume 18, Issue 3. pp. 335–341

Zeghal, M. (2008) “Modeling the Creep Compliance of Asphalt Concrete Using the Artificial Neural Network Technique” GeoCongress 2008: Characterization, Monitoring, and Modeling of GeoSystems (GSP 179) Proceedings of sessions of GeoCongress 2008. pp. 910–916

Zettlemoyer, A.C., Lower, G.W. (1955) “The Rheology of Printing Inks. III. Studies of Simple Dispersions”. Journal of Colloid Science, Volume 10, Issue 1. pp. 29–45

Zeus Industrial Products (2005) “RoHS and WEEE – The Essentials”. Zeus Industrial Products, Technical White Paper. Available at: http://www.zeusinc.com/UserFiles/zeusinc/Documents/Zeus_RoHS_and_WEEE.pdf (Accessed 5th November 2010)

Zhang, S.S., Zhang, Y.J., Wang, H.W. (2010) “Effect of Particle Size Distributions on the Rheology of Sn/Ag/Cu Lead-Free Solder Pastes”. Journal of Materials and Design, Volume 31. pp. 594–598

Zou, B., Dusek, M., Wickham, M., Hunt, C. (2001) “The Effect of Solder Alloy, Metal Particle Size and Substrate Resist on Fine Pitch Stencil Printing Performance”. NPL Report MATC(A) 18. Centre for Materials Measurement and Technology, National Physical Laboratory, Teddington, Middlesex. ISSN 1473-2734

Zou, C., Gao, Y., Yang, B., Zhai, Q. (2010) “Melting and Solidification Properties of the Nanoparticles of Sn3.0Ag0.5Cu Lead-Free Solder Alloy”. Journal of Materials Characterisation, Volume 61, Issue 4. pp. 474–480